ARCTIC '98: The Expedition ARK-XIV/1a of RV "Polarstern" in 1998

Edited by Wilfried Jokat
with contributions of the participants

Ber. Polarforsch. 308 (1999)
ISSN 0176 - 5027

Contents

I ARCTIC '98: ARK XIV/1a BREMERHAVEN - TIKSI
27.06.98 - 27.07.98

I ARCTIC '98: ARK XIV/1a Bremerhaven - Tiksi (27. Juni - 28. Juli 1998)

Summary

The expedition ARK XIV/1a of RV POLARSTERN and the Russian nuclear ice breaker ARKTIKA was the first attempt to reach the Alpha Ridge in the central Arctic Ocean directly with surface ships in order to sample the area with geoscientific, biological and geophysical methods. The Alpha Ridge is a submarine mountain chain discovered almost 40 years ago by American ice drift station Alpha. While the surrounding deep sea basin shows a water depth of more than 3000 m, the Alpha Ridge has water depths up to 1200 m only.

The available scientific information from this region is at least 20 years old. Geophysical measurements and geological sampling were performed from drifting ice station operated by American and Canadian institutions. Four short cores contained material documenting the environment of the Amerasian Basin in its early phase of development. One of the objectives was to try to reach this positions again to retrieve longer cores in the area with the more modern equipment available on POLARSTERN. Although there will be only a maximum of 5 days available for any science on the ridge, all scientific groups were ready to go for retrieving new and exciting material from this area.

At the 27th of June 1998 POLARSTERN left Bremerhaven to meet the Russian nuclear ice breaker ARKTIKA at the boundary of the Norwegian-Russian exclusive economic zone (EEZ) at 79°N 35°E. After 6 days of steaming we met the Russian ship in the morning of the 4th July. From this position on both ships operated in a convoy till we reached the Laptev Sea at 80°N 143°E. At 81°N we tried to start the seismic measurements but had to stop the investigations after the ship was caught in pressed ice conditions. Here we lost one third of the streamer. POLARSTERN needed more than 4 hours after it could move again in the ice. Extensive support from ARKTIKA was necessary to continue. During the whole transit towards the Lomonosov Ridge no seismic profiling was possible because the ice conditions remain difficult especially the pressed ice conditions. Open leads were almost not present. However, with the support of the nuclear ice breaker we were able to move with a mean velocity of 6 - 8 ktns (table 1). After passing the Lomonosov Ridge at the 10th of July the ice conditions became favourable again to collect seismic data. After less than half a day the seismic gear was again caught in pressed ice and could only be retrieved with severe damages of the streamer stretch sections. Approximately 100 NM south of Alpha Ridge the ships hit extremely difficult ice conditions, so that even ARKTIKA could not move anymore. Satellite images and a helicopter reconnaissence flight showed that the primary research area could not be reached within the given time frame because the difficult ice conditions remained along the proposed track. However, the images suggested that ice conditions became easier towards the west. Here

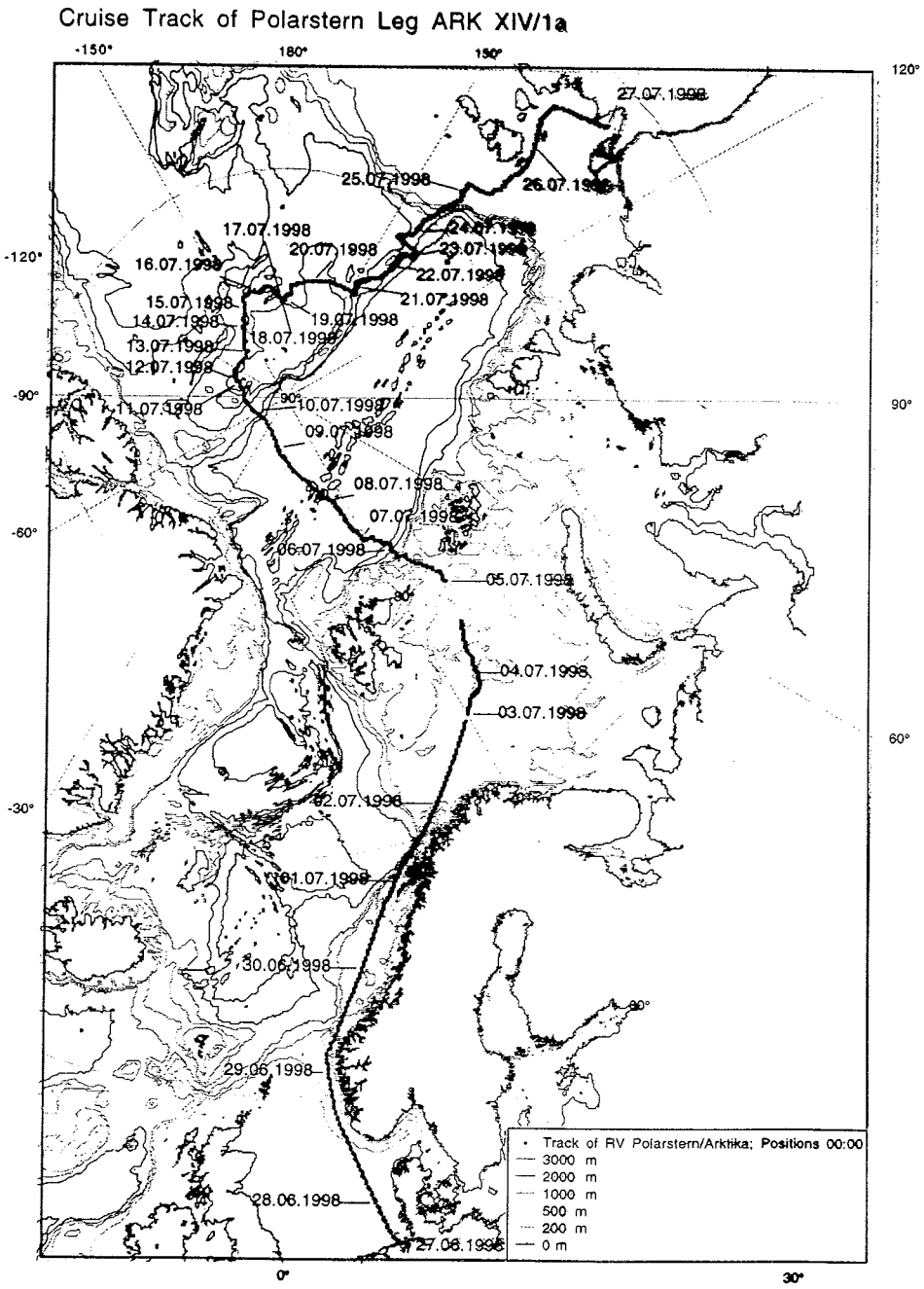

Fig.: Cruise Track of POLARSTERN during leg ARK-XIV/1a (Arctic '98)

Tab. 1: Summary of daily 12:00 positions and mean ships speed from the POLARSTERN logbook

Date	Time	Position		Distance per day (NM)	Total NM	Mean Speed (ktns)
27.06.98	15:00	B-haven Depart.				
28.06.98	12:00	57°48'N	05°18'E	253	253	14.9
29.06.98	12:00	63°07'N	05°36'E	332	585	13.9
30.06.98	12:00	66°30'N	09°46'E	231	816	10.0
01.07.98	12:00	69°34'N	15°40'E	228	1044	09.5
02.07.98	12:00	72°14'N	23°39'E	224	1268	09.7
03.07.98	12:00	74°48'N	33°52'E	235	1503	09.8
04.07.98	12:00	76°44'N	36°01'E	163	163	05.4
05.07.98	12:00	80°42'N	38°56'E	277	440	11.5
06.07.98	12:00	82°11'N	35°11'E	131	571	05.5
07.07.98	12:00	83°39'N	26°48'E	148	719	06.2
08.07.98	12:00	86°06'N	15°01'E	190	909	07.9
09.07.98	12:00	87°57'N	12°41'W	173	1082	07.2
10.07.98	12:00	88.11'N	88°04'W	158	1240	06.6
11.07.98	12:00	87°44'N	108.05'W	059	1358	02.5
12.07.98	12:00	87°40'N	110°35'W	000	1363	00.2
13.07.98	12:00	86°57'N	144°09'W	126	1489	05.3
14.07.98	12:00	86°23'N	148°03'W	043	1532	01.8
15.07.98	12:00	85°22'N	155°24'W	079	1611	03.3
16.07.98	12:00	85°06'N	171°24'W	101	1712	04.2
17.07.98	12:00	85°35'N	174°56'W	075	1787	03.1
18.07.98	12:00	85°45'N	177°00'W	041	1828	01.7
19.07.98	12:00	85°24'N	177°31'E	039	1867	01.6
20.07.98	12:00	84°35'N	158°42'E	144	2011	06.0
21.07.98	12:00	83°37'N	145°12'E	150	2161	05.0
22.07.98	12:00	81°38'N	141°50'E	121	2282	05.0
23.07.98	12:00	81°30'N	142°38'E	145	2427	06.0
24.07.98	12:00	80°00'N	142°27'E	152	2581	06.4
25.07.98	12:00	77°35'N	136°20'E	229	2810	09.5
26.07.98	12:00	72°58'N	138°01'E	313	3123	13.0
27.07.98	12:00	71°50'N	130°40'E	161	3284	14.0

also core positions were known where Late Mastrichtian sediments were recovered. After one day of steaming at the foot of the Alpha Ridge it became clear, that POLARSTERN will not be able to operate in the proposed area even with the support of ARKTIKA. Again we shifted our research area towards the west. After one day the ships were able to move southward onto the Alpha

Ridge. As ice conditions did not permit any seismic investigations, geological sampling had to be performed without this information. Although, the bathymetric and PARASOUND sensors suffered from the ice conditions, they provided enough information for choosing sampling sites. When we reached the top of the western prolongation of the Alpha Ridge the wind calmed down significantly and allowed to acquire a 190 km long seismic profile at the crest of the ridge. The line terminated on top of the Lyons Seamount to perform a full geological and biological station. As wind and ice conditions remained favourable a seismic line could be collected perpendicular to the ridge. It showed some promising sampling sites. The primary target was an escarpment where the seismic data clearly showed some outcropping sediments. Although the wind increased, the ships could reach the area again without major difficulties. In total 6 gravity core samples were recovered. One of them contained a strongly weathered basalt sample. No evidence for a recovery of old sediments could be found so far.

At this time, 18th of July, POLARSTERN was not able to operate in the ice conditions despite the support of ARKTIKA. Pressed ice conditions and large floes prevented to reposition the ship to the known escarpment. Ice thickness of more than 6 m were determined from electromagnetic profiling on the floes. For the route to the Laptev Sea the satellite images showed favourable ice conditions along the Lomonosov Ridge. A decision was made together with the masters of ARKTIKA, who confirmed our interpretation, to choose the route along the Lomonosov Ridge to reach the Laptev Sea. A final station on the northern end of Alpha Ridge was carried out before we steamed towards Lomonosov Ridge along 84°30'N. However, the difficult ice conditions remained till we reached the foot of Lomonosov Ridge. The seismic profiles collected across the ridge show a different tectonic style than that was found during the ODEN'96 cruise some 100 km more north. Instead of a flat topped ridge, large basement highs in the central part of the ridge can be identified on the records. Two more crossings closer to the Laptev Sea suggest that this kind of structure is characteristic for the Lomonosov Ridge south of 85°N. Finally two more sampling sites were chosen at the eastern margin of the ridge based on the seismic recordings. Both sites looked promising to recover older sediments. Again, at the moment it cannot be decided if such material could be recovered. At 24th of July all scientific activities were terminated north of the Russian EEZ. ARKTIKA left POLARSTERN at 23:00 of the 25th of July 1998. POLARSTERN arrived 30 NM east of Tiksi at 23:30 of the 26th of July. After several unsuccessful trials the ship was able to make contact to the Russian ship *DUNAI*, which transfered approximately 40 scientists from Tiksi to POLARSTERN for the leg ARK XIV/1b. The ship arrived at 17:22 on 27th of July. With the change of the scientific crew the leg ARK XIV/1a ended at the 27th July 1998 off Tiksi. The cruise track is shown in fig.1, while the positions of the ships at 12:00 are summarized in table 1.

In brief some remarks on the scientific results and technical problems of leg ARK XIV/1a:

- The expedition demonstrated that it is possible to reach the Alpha Ridge with surface ships. For performing any reasonable research the support of a strong ice breaker is definitely needed. Although the expedition was quite early in the season I believe that the pressed ice conditions north of Alpha Ridge are typical for the region, and can only be handled by the support of an icebreaker of the ARKTIKA class. The co-operation with the Russian icebreaker was excellent and critical to the success of the cruise.

- In several situations it was obvious that POLARSTERN operated at its limits while ARKTIKA could still move freely in the ice. A lot of time was needed to free POLARSTERN from such difficult situations. In case of a new expedition into this area it is highly recommended that POLARSTERN can be taken in tow. For this it might be necessary to strengthen certain constructions on the bow of the ship to allow such operations.

- At the moment it is not known, if the severe ice conditions we hit close to the Alpha Ridge are a) normal, b) due to a heavy ice year or c) just a consequence of being in the region middle of July. In addition, bad visibility made navigation difficult. A new attempt to reach Alpha Ridge should be scheduled for end of July for arriving in the research area as it was originally planned. Anyhow, the ice conditions cannot be predicted.

- While the seismic transects across the Nansen and Amundsen basins could not be acquired, first high quality seismic profiles could be collected along the Alpha Ridge. They show a more or less constant sediment thickness of 800 to almost more than 1000 m. In total, 1250 km of seismic data could be acquired, 300 km of the lines are located on Alpha Ridge itself. On the way to the Laptev Sea the Lomonosov Ridge between 85°N and 80°N could be mapped with MCS data. The lines across and along the Lomonosov Ridge reveal a spectacular topography south of 85°N which is in strong contrast to what has been known so far from seismic data more in the north.

- Although the expedition did not collect Cretaceous sediments because we could not reach the planned research area, new information on the environment of the last 2 - 3 Mio. years could be collected. Here, the cores from the Lyons Seamount are the key to this information. Furthermore a basalt sample could be cored. Although heavily weathered, there is little doubt, that it is an in situ sample of the old Alpha Ridge basement and does not represent ice rafted material. As older samples from the ridge could not be dated so far, the sample will be one of the most promising possibilities to determine the age of the Alpha Ridge, which is so far only inferred from plate tectonic considerations and from vague dating of dredged samples.

- The biological sampling showed that the Alpha Ridge is a benthic desert. All investigated parameters reveal low productivity. This is in strong contrast with the results from Lomonosov Ridge.

- Almost along the whole ships route ice sampling and ice thickness measurements were carried out. Especially dirty ice was sampled to determine the source areas of the floes. In addition, on the few long stations a sediment trap was deployed close to the ship for 4 - 5 hours to measure the current sediment flux.

- HYDROSWEEP and PARASOUND data were collected along the whole track. However, the quality is highly variable. The data quality was bad to poor in heavy ice conditions. Currently it is not known if some acoustic windows of the HYDROSWEEP system are damaged due to collision with ice floes.

1 Meteorological conditions (L. Kaufeld, H. Sonnabend)

During the first five days of the cruise, the general atmospheric circulation was characterized by high pressure over the north polar basin and several cyclones south of about 65°N. The wind over the Arctic Basin blew in a clockwise sense, the coasts of Sibiria, the Norwegian Sea, northern Greenland and the North Canadian Islands observed northeasterly winds.

This situation changed in the first days of July. Since then a more or less strong cyclone near the North Pole controlled the wind regime in the Arctic with westerly winds. The counterpart to this low was formed by an anticyclone which mainly stayed in the Kara Sea region. - Wind speed and wind direction during the whole cruise are shown in figures 2 and 3.

In the beginning of our voyage, June 27th to 28th, POLARSTERN moved into a cyclone which was nearly stationary over the northern North Sea and the southern Norwegian Sea. During this time we had weak or moderate southerly to westerly winds. We passed the low's center at 29 June, 06 UTC.

Afterwards the wind turned to northeast and increased to speeds of 14 to 22 knots (kts). Sailing along the northwestern Norwegian coast, the wind slowly turned to north. The first two July days it blew with forces 3 to 5 bft. Air temperatures dropped from 15 °C (29.06.21 UTC) to 5 °C (02.07.00 UTC) and remained at this level until we reached the ice edge at July 3rd, 15 UTC.

At this time a weak anticyclonic ridge passed us with weak variable winds. The sea surface temperature dropped from 5.1 °C to 0.7 °C, the air temperature from 4 to 0 °C. In the early morning of July 4th, at a position of 75.5°N, 35.0°E, POLARSTERN met with ARCTICA. At this time, the cold front of an Arctic low, centered north of Franz Joseph Land passed us, accompanied by a little frezzing drizzle and snow. At 06 UTC, the air temperature dropped to -2.4 °C, the dew point to -3.7 °C. These were the lowest values of the whole cruise! The winds were light (2 to 9 kts) from southwesterly directions, veering to west.

During July 5th and 6th, POLARSTERN was hampered by severe ice conditions near 81 to 82°N. - The cyclone north of Franz Joseph Land moved exactly to the North Pole while a weak anticyclone formed over Spitzbergen and the northern Barents sea. Between both systems the wind blew with 9 to 12 kts from the west at July 5th and increased from 12 to 20 kts during the next day. It came from southwest or west. At this time, westerly winds covered the whole Arctic Basin.

With backing from WNW to SW, the wind weakened during July 7th from 18 to about 10 kts. The passage of an occlusion brought rain at July 8th, accompanied by a short increase of wind speed to 22 kts. - The strengthening of an anticyclone over the

Kara Sea resulted in another increase of wind speed to about 20 kts during the next day.

The shift of wind direction from south over east to north during July 8th to 10th, as seen in figure 4, was caused by the close passage of the North Pole, not due to a real shift of wind direction over the whole area.

The polar cyclone had weakened and moved to northern Greenland so that the wind in our cruise area was weak (8 to 10 kts) during the first half of July 10th, but the anticyclone near Svernaja Zemlja was strong (1033 hPa). At the same time an intense low (990 hPa) approached from northwestern Greenland. Between both these systems the wind over the whole central Arctic increased. In the evening of July and during July 11th - when POLARSTERN was fixed within the ice at 87.7°N, 109°W - it blew with 17 to 20 kts from the Spitzbergen and the Barents Sea area. During the next day the wind weakened to about 14 kts and POLARSTERN could continue her cruise.

The following four days until July 16th brought sunshine but also fog, clouds, drizzle and a little snow. The wind speed decreased to near zero, the direction was north to northeast which means that the air approached from the Barents Sea and Spitzbergen area. Within this period the anticyclone near Svernaja Zemlja and the cyclone over northern Greenland weakened.

The air pressure over the central Arctic rose and at July 18th, 09 UTC, POLARSTERN measured 1021.8 hPa, the highest air pressure of the whole cruise. An anticyclone with weak pressure gradients covered nearly the whole Arctic Basin. Afterwards, the wind direction changed to southeast, the speeds remained low.

With the approach of a weak low from the Kara Sea, the air pressure dropped to 1010 hPa until July 20th but the winds remained weak; they veered from south over west to north.

During the next four days the air pressure rose again; the weak to moderate winds backed from north over west and south to southeast. The air was relatively cold with about -1 °C. An anticyclone over the Kara Sea had intensified since the 20th and the weak low which had passed POLARSTERN at that day, moved to the North Pole and became stationary there.

The last two days of our cruise saw a change of the general weather situation: A strong cyclone had formed near the Khatanga river during July 24th and wandered under intensification to the central Laptev Sea. In the early morning of July 25th, it passed our route 300 km west of POLARSTERN while moving northward, bringing strong winds up to 33 kts and a squall of 41 kts. The cold front passed us at 09 UTC with moderate rain and a wind shift from 170 to 270 degrees.

During the next day the wind calmed down to 4 kts but increased again to about 20 kts in the night from July 26th to 27th. Southerly winds advected warm air while waiting for the crew change off Tiksi. Air temperature rose to 8 °C, the highest value since we had left the Norwegian Sea. The depression over the Tajmyr Peninsula which caused this warm air advection moved northeastward and merged with the old cyclone near 84°N, 130°E and formed the new steering central polar cyclone.

The most frequent wind directions during the cruise ARK 14/1a were W, N and S, the least frequent one E (see fig. 4). Wind forces 3 and 4 occured most frequently; 7 bft was the highest mean wind force (fig. 5). About 27 % of fog and another 11 % of poor visibility below 4 kms were calculated from the three-hourly observations.

Wind, temperature and weather conditions including visibility have been quite normal for the arctic summer.

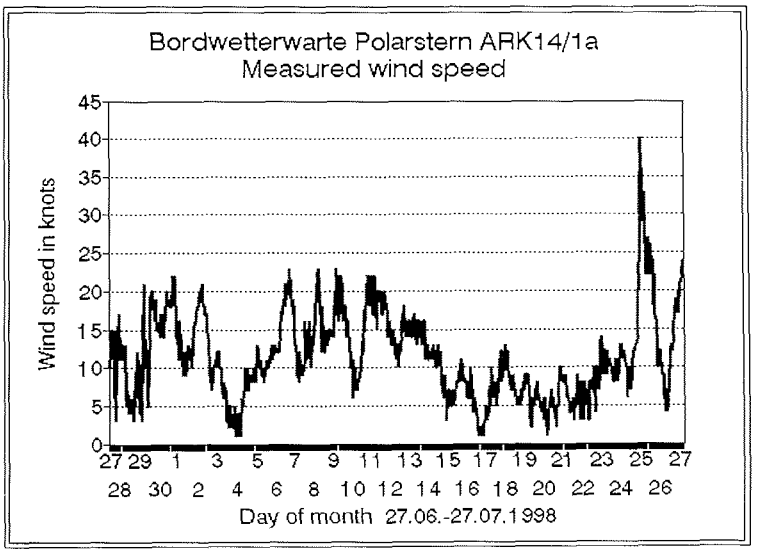

Fig. 2: Wind speed 27.06.-27.07.1998

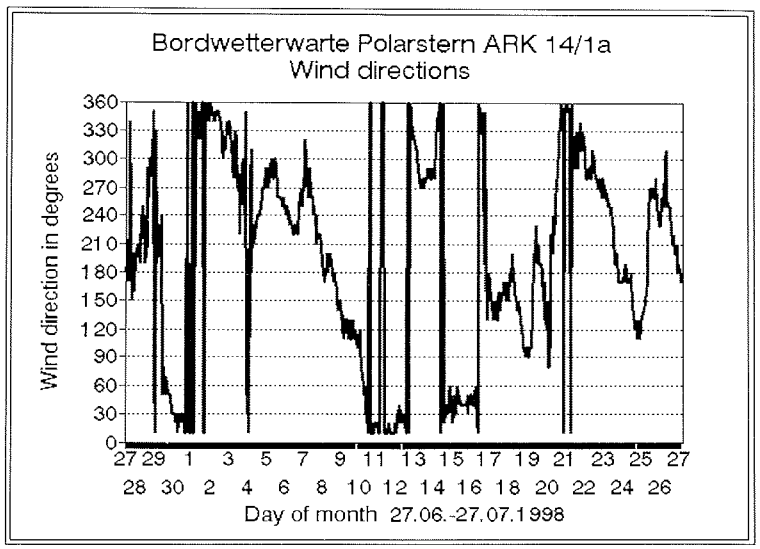

Fig. 3: Wind directions 27.06.-27.07.1998

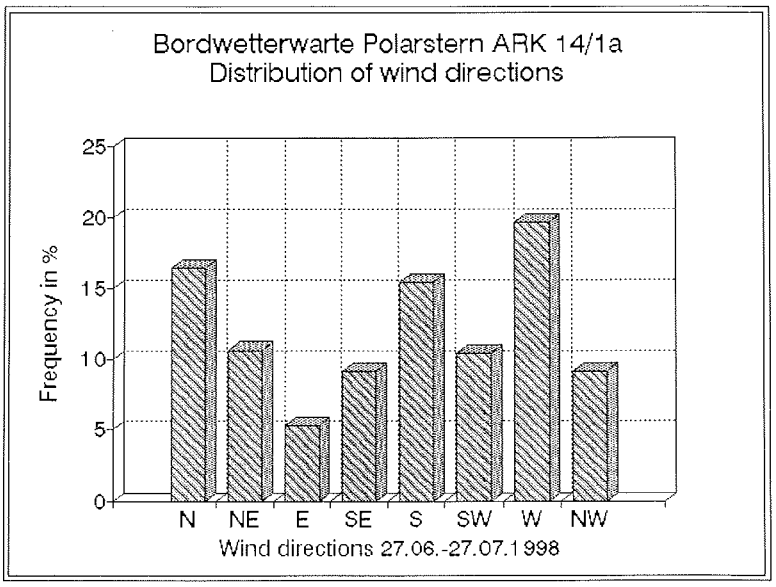

Fig. 4: Distribution of wind directions

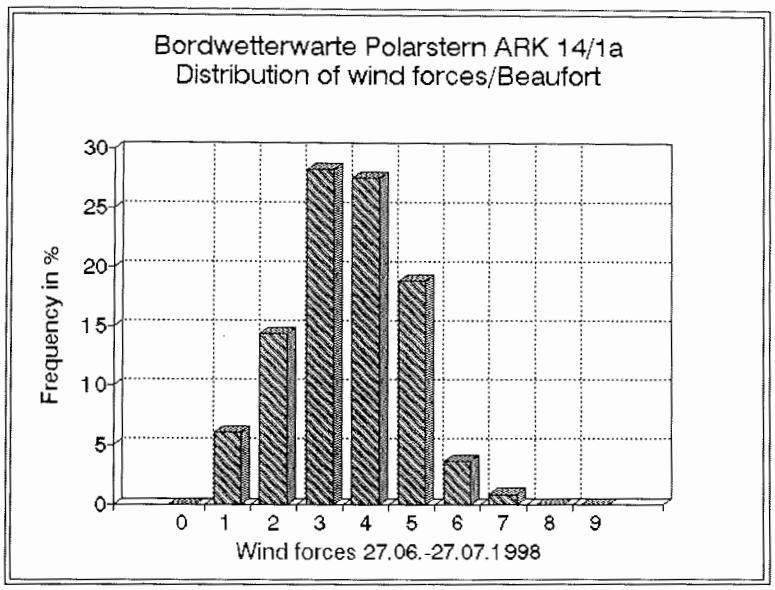

Fig. 5: Distribution of wind forces

2 Marine Geophysics

(W. Jokat, V. Butzenko, A. Duerr, R. Jackson, G. Jentzsch, M. Koenig, N. Lensch, H. Martens, V. Poselov, E. Schmidt, K. Schüler, S. Stephanov, K. Thalmann, E. Weigelt, M-K. Yoon)

2.1 Introduction

While the Cenozoic spreading at the Gakkel Ridge explains the opening of the eastern Arctic and the shapes of the continental margins between the Eurasian continental margin and Lomonosov Ridge, the nature of the Alpha-Mendeleev Ridge in the Amerasian Basin as well as the age of the deep sea basins are virtually unknown. As far as we can tell, the earliest Arctic deep-sea basin (Canada Basin) evolved in Jurassic times, seafloor spreading opened the southern Canada Basin mainly in the Cretaceous and the Arctic Ocean for most of the Mesozoic consisted of an isolated deep-sea area with no major deep-water connection to the world ocean. The main reason for this lack of data is the more or less dense ice cover in the Arctic Ocean. Especially the use of towed systems means a high risk to damage or loose the equipment.

However, in the last years some high quality data have been collected in the Amundsen Basin and across the Lomonosov Ridge. During the Arctic '98 cruise one objective was to complement these measurements on the way to the Alpha Ridge, which was the main scientific target and to minor extend the Mendeleev Ridge. Here, no new geophysical data with modern research platforms could be collected since the CESAR expedition. In brief, the objectives of the geophysical programmes should be:

- Is the Alpha Ridge-Mendeleev Ridge complex a single geologic structure or does it have a different origin?
- What is the nature of the crust forming the Alpha Ridge-Mendeleev Ridge?
- What is the subsidence history of the ridges relative to the basins?
- How do the Lomonosov and Alpha Ridge relate to the origin of the adjacent ocean basins especially the Makarov Basin?

2.2. Geoscientific Knowledge

Alpha-Mendeleev Ridge Complex

The Alpha-Mendeleev Ridge is the largest single submarine feature in the Arctic Ocean. In areal extent it exceeds the Alps and large portions are buried beneath the Canada Abyssal Plain. The ridge is the key to the understanding of the genesis of the Amerasian Basin. Investigators have suggested that this blocky ridge may be: (1) of continental origin; (2) a former spreading centre; (3) result of "hot spot" activity; and (4) a former region of subduction or compression.

Physically Alpha Ridge is covered in the most part by a sedimentary sequence which can reach up to 1 km in thickness and has yielded Cretaceous sediment. The basement material on which the sedimentary cover was deposited has a velocity of 5.3 km/s. This velocity is typical of oceanic layer 2 and also indurated sedimentary rock. The seismic velocity of the layer below ranged from 6.45 to 6.8 km/s and at a depth of 20 km a velocity of 7.3 km/s was measured. This velocity structure is similar to oceanic plateaus. The measured depth of the crust mantle boundary is 38 km. Dredged material recovered by the Canadian CESAR expedition from exposed basement of the ridge yielded a fragmented and weathered alkaline volcanic rock.

The magnetic anomaly pattern of Alpha Ridge is extremely variable with peak to trough anomalies of up to 1500 n T and wave lengths of 20 - 75 km.

Lomonosov Ridge

Although Lomonosov Ridge - a transpolar feature rising over 3 km above the adjacent abyssal plains - was discovered in 1948 by the Soviet "High Latitude Air Expeditions". The presence of a deep bathymetric barrier across the Arctic Ocean has been inferred from tidal measurements in 1904 and 1936 and also from deep water temperature differences in 1953. Ever since Heezen and Ewing in their 1961 paper recognised that the mid-oceanic rift system extended from the North Atlantic into the Arctic Ocean, it has been assumed that Lomonosov Ridge was a continental fragment originally split from the Barents-Kara Sea margin. Aeromagnetic surveys of the Eurasia Basin have since mapped a remarkably simple pattern of magnetic lineations which can be interpreted in terms of seafloor spreading along the Gakkel Ridge since chron 24. If we compensate for that motion, the Lomonosov Ridge was indeed brought into juxtaposition with the Barents-Kara Sea margin in the early Cenozoic. During expeditions in 1991 (POLARSTERN) and 1996 (ODEN) first high quality geophysical data were collected confirming the hypothesis of a continental origin of the ridge.

Makarov Basin

Russian and Canadian seismic refraction results from Makarov Basin indicate a crustal structure similar to Alpha Ridge but thinner. Crustal velocities range from 4.3 km/s to an upper mantle velocity of 8.3 km/s. Moho is observed at a depth of 14 km versus 38 km for Alpha Ridge. Magnetic profiles across the basin suggest an episode of sea floor spreading from magnetic anomaly 21 (53 Ma) to magnetic anomaly 34 (80 Ma). These dates would indicate that this basin was opening from the Late Cretaceous through the Palaeocene. These correlations, however, are very tenuous and may well reflect basement topography rather than sea floor spreading anomalies.

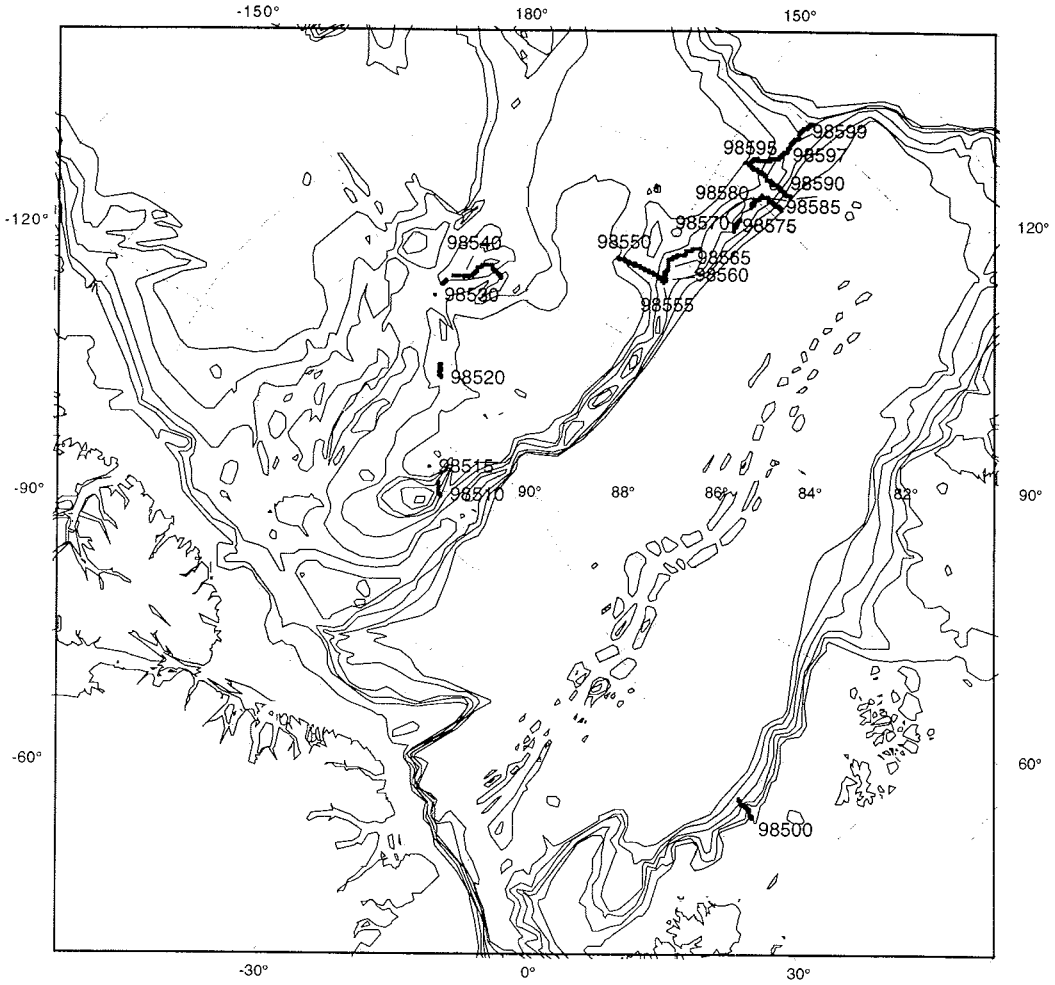

Fig. 6: Location of seismic profile acquired during Arctic '98

Tab. 2: Recording parameters and locations of the seismic profiles shown in Fig. 6

Shot Statistics ARK XIV/1a

Profile	Start		End		Source	Streamer	Sonobuoys	Number	Length	Start		End	
Number	Date /	Time	Date /	Time		(Active Length [m])		of Shots	(km)	Lat	Lon	Lat	Lon
98500	05.07.1998	18:30:00	05.07.1998	23:47:00	VLF	Prakla 300	None	1276	61,8	81.4862 N	34.7450 E	81.9617 N	34.7246 E
98510	10.07.1998	07:37:45	10.07.1998	10:31:00	VLF	Prakla 200	None	694	35,3	88.1861 N	87.0393 W	88.1558 N	96.3331 W
98511	10.07.1998	11:28:00	10.07.1998	14:14:00	VLF	Prakla 200	None	662	31,8	88.1222 N	99.1796 W	87.9447 N	102.6535 W
98515	10.07.1998	20:06:15	10.07.1998	20:21:15	VLF	Prakla 200	None	61	1,7	87.9257 N	104.0373 W	87.9223 N	104.3757 W
98520	13.07.1998	07:34:15	13.07.1998	11:34:40	VLF	Prakla 200	None	960	46,5	86.9748 N	143.5109 W	86.7003 N	146.3503 W
98530	15.07.1998	15:07:30	16.07.1998	07:48:00	VLF	Prakla 200	9801-03	3993	192,2	85.3782 N	155.4891 W	85.1202 N	171.3642 W
98540	16.07.1998	15:52:45	16.07.1998	23:14:00	VLF	Prakla 200	9804-05	1885	87,7	85.1429 N	171.5667 W	85.6742 N	177.0767 W
98550	20.07.1998	08:26:30	20.07.1998	20:00:00	VLF	Prakla 200	9806-07	2767	145,0	84.5937 N	158.6291 E	84.6013 N	146.9872 E
98555	20.07.1998	20:00:00	20.07.1998	20:40:00	VLF	Prakla 200	None	160	9,0	84.5535 N	146.6837 E	84.2980 N	147.7609 E
98560	20.07.1998	20:40:00	20.07.1998	23:30:00	VLF	Prakla 200	None	677	38,3	84.5535 N	146.6837 E	84.2980 N	147.7609 E
98565	20.07.1998	23:30:00	21.07.1998	08:40:00	VLF	Prakla 200	9808-09	2014	97,8	84.2235 N	147.9930 E	83.5712 N	144.9424 E
98570	21.07.1998	21:51:00	21.07.1998	23:18:45	VLF	Prakla 200	9810	351	17,0	82.8509 N	141.6656 E	82.7356 N	142.0553 E
98575	22.07.1998	00:51:45	22.07.1998	02:09:45	VLF	Prakla 200	9811	310	11,0	82.6231 N	142.1238 E	82.5349 N	142.0796 E
98580	22.07.1998	05:10:45	22.07.1998	09:05:00	VLF	Prakla 200	9812	931	43,4	82.1912 N	141.8863 E	81.8599 N	141.6963 E
98585	22.07.1998	09:05:00	22.07.1998	14:00:00	VLF	Prakla 200	None	1177	64,5	81.8599 N	141.6943 E	81.8220 N	137.9968 E
98590	23.07.1998	01:09:30	23.07.1998	13:41:00	VLF	Prakla 200	9813-15	2999	147,6	81.4945 N	138.1554 E	81.4849 N	146.5475 E
98595	23.07.1998	13:45:00	23.07.1998	21:44:00	VLF	Prakla 200	9816-17	1910	90,5	81.4777 N	146.5322 E	81.0038 N	143.0174 E
98597	23.07.1998	21:51:30	24.07.1998	02:04:30	VLF	Prakla 200	None	1009	53,1	80.9923 N	142.9676 E	80.5591 N	142.9924 E
98599	24.07.1998	02:48:30	24.07.1998	08:47:00	GI	Prakla 200	9818	1428	74,1	80.5134 N	142.8607 E	79.9548 N	142.2258 E

Total length of Profiles (km) : 1248,3

2.3 Data Acquisition - set-up and problems -

At the beginning we used a 500 m streamer with an active length of 300 m (48 channels). After it got caught in pressed ice conditions close to the Barents Shelf, we lost 2 streamer sections and shortened the total length of the streamer to 400 and later to 350 m (32 channels). Problems only arose in pressed ice conditions, which happened several times during this leg. As seismic source we used almost during the whole leg a 24 l airgun cluster as described by Jokat et al. (1995). Although the airgum frame was dragged several times over ice floes only minor damages occured. The most dangerous situations happened when one or both of the steel cables broke, which towed the array. This happened in total three times. Only when two of the cables broke the array was close to be lost. The data were recorded with a ES2420 seismograph. Time control was supplied by an external GPS clock. In parallel to the seismic reflection data acquisition sonobouys were deployed to record more accurate velocity information from the sedimentary sub surface. Fig. 6 and Tab. 2 show the locations and recording parameters of the seismic profile acquired during this leg.

2.4 Seismic data processing

For the seismic data processing a CONVEX 3410EX vector computer and three SUN workstations were available. On the computers commercial seismic processing software (FOCUS) was installed. While the main frame computer processed seismic jobs with heavy input/output operations, analyses of the seismic data were done on the workstation, e. g. velocity analyses and filter tests. All computers were networked and shared their discs. Most of the processing could be finished during the leg ARK XIV/1b (Tab. 3). This included demultiplexing, velocity analyses, filter tests and CDP sorting. In addition, all 18 sonobuoys were analysed and raytraced during both legs. The locations of the buoys can be found in table 4 .

2.5 Preliminary Results - Seismics -

Nansen/Amundsen/Makarov basins

Due to the difficult ice conditions it was only possible to collect seismic reflection data close to the Barents Shelf. Pressed ice conditions prevented any acquisition of seismic data up to 82°N 34°40'E (98500, Fig. 6). The line was terminated at the slope of the Barents Shelf. After we lost 100 m of the streamer, an attempt to collect seismic lines in the Makarov Basin close to Lomonosov Ridge (98510, Fig. 6) failed again as the pressed ice conditions still occurred. Here one of the stretch sections of the streamer were heavily damaged.

Tab. 3: Summary on the onboard seismic data processing during the legs ARK XIV/ 1a - b

Seismic Processing ARK XIV/1a

Profile	Lead-in (m)	Offset to 1st Hydrophone (m)	Chan.	Group (m)	RL (s)	SR (ms)	SI (s)	Field-Cartridge No.	Demultiplex	Cartridge No.	Sorting	Cartridge No.	Velocity Anal.	Brutestack Plot/Mute	Final Stack	Sonobuoys
98500	30	180	48+4	6,25	12	2	15	F 02813 - 02818	06.07.1998	C 15200 - 15206	11.08.1998	C 15207 - 15212	18.08.1998	18.08.1998		None
98510	60	110	32+4	6,25	12	2	15	F 02819 - 02821	10./11.07.1998	C 15213 - 15215	17.08.1998	C 15220 - 15222	18.08.1998	18.08.1998		None
98511	60	110	32+4	6,25	12	2	15	F 02821 - 02823	11.07.1998	C 15216 - 15218	17.08.1998	C 15223 - 15225	18.08.1998	18.08.1998		None
98515	60	110	32+4	6,25	12	2	15	F 02824	11.07.1998	C 15219	17.08.1998	C 15226	19.08.1998	19.08.1998		None
98520	60	110	32+4	6,25	12	2	15	F 02825 - 02827	13.07.1998	C 15227 - 15230	17.08.1998	C 15231 - 15233	18.08.1998	18.08.1998		None
98530	60	110	32+4	6,25	12	2	15	F 02828 - 02839	16.07.1998	C 15234 - 15247	16.08.1998	C 15255 - 15267	18.08.1998	18.08.1998		None
98540	60	110	32+4	6,25	12	2	15	F 02842 - 02847	17.07.1998	C 15248 - 15254	16.08.1998	C 15965 - 15970	18.08.1998	18.08.1998		13.08.1998
98550	60	110	32+4	6,25	12	2	15	F 02848 - 02856	23.07.1998	C 15268 - 15277	16.08.1998	C 15971 - 15979	18.08.1998	18.08.1998		13.08.1998
98555	60	110	32+4	6,25	12	2	15	F 02856	23.07.1998	C 15278	16.08.1998	C 15991	18.08.1998	18.08.1998		None
98560	60	110	32+4	6,25	12	2	15	F 02856 - 02859	23.07.1998	C 15279 - 15282	16.08.1998	C 15980 - 15982	18.08.1998	19.08.1998		None
98565	60	110	32+4	6,25	12	2	15	F 02859 - 02864	23.07.1998	C 15283 - 15289	16.08.1998	C 15983 - 15988	18.08.1998	19.08.1998		16.08.1998
98570	60	110	32+4	6,25	12	2	15	F 02865 - 02866	23.07.1998	C 15290 - 15292	17.08.1998	C 15989 - 15990	18.08.1998	16.08.1998		16.08.1998
98575	70	120	32+4	6,25	12	2	15	F 02867	23.07.1998	C 15293 - 15294	17.08.1998	C 15992	18.08.1998	16.08.1998		16.08.1998
98580	60	110	32+4	6,25	12	2	15	F 02868 - 02870	23.07.1998	C 15295 - 15298	30.07.1998	C 15403 - 15405	11.08.1998	12.08.1998		12.08.1998
98585	60	110	32+4	6,25	12	2	15	F 02870 - 02874	23.07.1998	C 15299 - 15302	30.07.1998	C 15406 - 15409	11.08.1998	12.08.1998		12.08.1998
98590	60	110	32+4	6,25	12	2	15	F 02875 - 02883	23.07.1998	C 15303 - 15313	30.07.1998	C 15410 - 15419	11.08.1998	12.08.1998		12.08.1998
98595	60	110	32+4	6,25	12	2	15	F 02883 - 02889	24.07.1998	C 15314 - 15321	30.07.1998	C 15420 - 15425	11.08.1998	12.08.1998		12.08.1998
98597	60	110	32+4	6,25	12	2	15	F 02889 - 02892	23./24.07.1998	C 15322 - 15325	30.07.1998	C 15426 - 15429	11.08.1998	12.08.1998		None
98599	60	110	32+4	6,25	12	2	15	F 02893 - 02899	24.07.1998	C 15326 - 15335	17.08.1998	C 15993- 16001	18.08.1998	19.08.1998		13.08.1998

Tab. 4: Locations of the deployed sonobuoys during Arctic '98. Furthermore, the distance range is given in which seismic signals can be idintified

Sonobuoys ARK XIV/1a

Profile	Sonobuoy	Type	Start		End		Start		End		Shot Range	Rec Distance	Signal Range
Number	Number		Date	Time	Date	Time	Lat	Lon	Lat	Lon		(km)	(km)
98530	9801	30L+	15.07.1998	15:39:00	15.07.1998	17:19:30	85.3314 N	155.7502 W	85.2145 N	156.9993 W	129 - 530	0-18	0-18
	9802	10L+	15.07.1998	17:29:45	15.07.1998	23:00:30	85.2077 N	157.1721 W	85.1566 N	162.8789 W	571 - 1890	0-30	0-26
	9803	30L+	16.07.1998	00:15:00	16.07.1998	02:23:30	85.2000 N	164.0368 W	85.1857 N	166.3716 W	2187 - 2700	0-15	0-15
98540	9804	30L+	16.07.1998	16:43:15	16.07.1998	17:41:00	85.2148 N	171.9055 W	85.2766 N	172.6000 W	207 - 437	0-1	0-1
	9805	10L+	16.07.1998	17:41:45	16.07.1998	20:33:00	85.2766 N	172.6000 W	85.4992 N	174.2032 W	438 - 1120	0-28	0-28
98550	9806	10L+	20.07.1998	10:45:15	20.07.1998	13:27:00	84.5765 N	156.2772 E	84.5791 N	153.3751 E	557 - 1200	0-30	0-12
	9807	30L+	20.07.1998	16:36:15	20.07.1998	20:00:00	84.5540 N	149.8815 E	84.6013 N	146.9872 E	1954 - 2767	0-18	0-18
98565	9808	10L+	21.07.1998	01:29:30	21.07.1998	04:18:00	84.1611 N	148.5648 E	83.9314 N	146.9684 E	188 - 870	0-30	0-18
	9809	30L+	21.07.1998	07:27:30	21.07.1998	08:40:30	83.6919 N	145.8080 E	83.5712 N	144.9424 E	1612 - 1910	0-13	0-13
98570	9810	10L+	21.07.1998	22:31:30	21.07.1998	23:18:00	82.7862 N	141.8237 E	82.7356 N	142.0553 E	166 - 351	0-8	0-8
98575	9811	10L+	22.07.1998	01:34:15	22.07.1998	02:09:45	82.5562 N	142.0942 E	82.6231 N	142.1238 E	172 - 310	0-3	0-3
98580	9812	30L+	22.07.1998	05:32:00	22.07.1998	08:37:00	82.1495 N	142.1510 E	81.9088 N	141.7538 E	163 - 821	0-28	0-20
98590	9813	10L+	23.07.1998	04:10:00	23.07.1998	07:46:00	81.4811 N	140.2369 E	81.5036 N	142.4556 E	724 - 1576	0-30	0-30
	9814	30L+	23.07.1998	08:50:00	23.07.1998	11:15:00	81.4735 N	143.1718 E	81.4808 N	144.8187 E	1840 - 2417	0-24	0-24
	9815	10L+	23.07.1998	11:35:00	23.07.1998	13:41:00	81.4863 N	145.0554 E	81.4849 N	146.5475 E	2500 - 2999	0-25	0-18
98595	9816	30L+	23.07.1998	16:27:00	23.07.1998	20:15:00	81.3080 N	145.5939 E	81.2933 N	145.4270 E	650 - 1556	0-24	0-21
	9817	10L+	23.07.1998	20:19:15	23.07.1998	21:44:00	81.1044 N	143.8150 E	81.0038 N	143.0174 E	1573 - 1910	0-18	0-18
98599	9818	10L+	24.07.1998	04:47:15	24.07.1998	07:25:30	80.3275 N	142.7277 E	80.0774 N	149.5972 E	479 - 1103	0-30	0-30

Alpha Ridge - Lyons Seamount

As we could not reach the primary target area on the Alpha Ridge both ships steamed along the foot of Alpha Ridge westwards. Here, we were able to acquire one profile (Fig. 6; 98520). It shows only a thin sedimentary cover of approximately 500 m. The basement is not imaged well along the whole line. While the south western part of the ridge was not accessible with the ships during the given time frame, we were able to collect 190 km multichannel seismic (MCS) data along the westernmost part of the ridge. Three sonobuoys were deployed which provided signals up to a distance of 30 km (table, 4). The sediment thickness along the ridge varies between 1000 m (SB9803) and approximately 800 m (SB9801, SB9802; Fig. 7). The basement of the ridge is imaged along most parts of the two profiles. It is characterized by seismic velocities of 4.5 to 4.7 km/s (Fig. 7). At deeper levels we identified on two sonobuoys seismic velocities of 5.0, 5.1, 5.4 to 5.7 km/s, which can be interpreted as the uppermost basaltic layer of oceanic crust. On line 98540 which runs almost perpendicular to the ridge, the sediments are thinning towards the north. An escarpment of 800 m was found at approximately 85°30'N 175°W (Fig. 8). Geological coring (s. Chapter 3) recovered several basalt samples from the slope of the structure. North the escarpment the basement became more rugged. As the lines could not be continued towards the Makarov Basin we only can speculate that the rugged basement is representing the flank of the Alpha Ridge being strongly affected by extension tectonics during the formation of the Makarov Basin. In total 320 km of MCS profiles could be collected in the area of the Alpha Ridge.

Makarov Basin/Lomonosov Ridge

While the ships sailed towards the Laptev Sea we tried to acquire MCS data along the track. Unfortunately the ice conditions allowed seismic profiling only from 85°N 158°E onwards. The profile 98550 just started at the southern flank of the Lomonosov Ridge. In contrast to its structure at 88°N, the ridge topography shows variations up to 1000 m in its central part. These might be caused by basement structure which were formed during the rifting of either the Makarov Basin or the Eurasian Basin. The seismic data show the absence of a ridge wide erosional unconformities as it has been found more towards the north. Line 98590 at 81°30'N shows similar basement structure although more pronounced. Based on velocities from three sonobouys we calculate a sediment thickness of 600 to 800 m along this profile. At greater depths seismic velocities between 4.1 and 4.8 km/s are found. It is not clear at the moment if these velocities are representing compacted sediments or indicate basement rocks. Our assumption is that the velocities of 4.1 to 4.8 km/s are sediments while the transition to basement rocks is indicated by velocities of 5.4 km/s. On SB9814 and SB9815 crustal velocities of 6.5/6.6 km/s could be identified. Raytracing of the traveltime curves provided a depth of 6 km for the top of this crustal unit.

Two more lines (98597, 98599) in the strike of the central part of the Lomonosov Ridge towards the Siberian Shelf allow to distinguish between Cenozoic and Mesozoic sediments (Fig. 9):

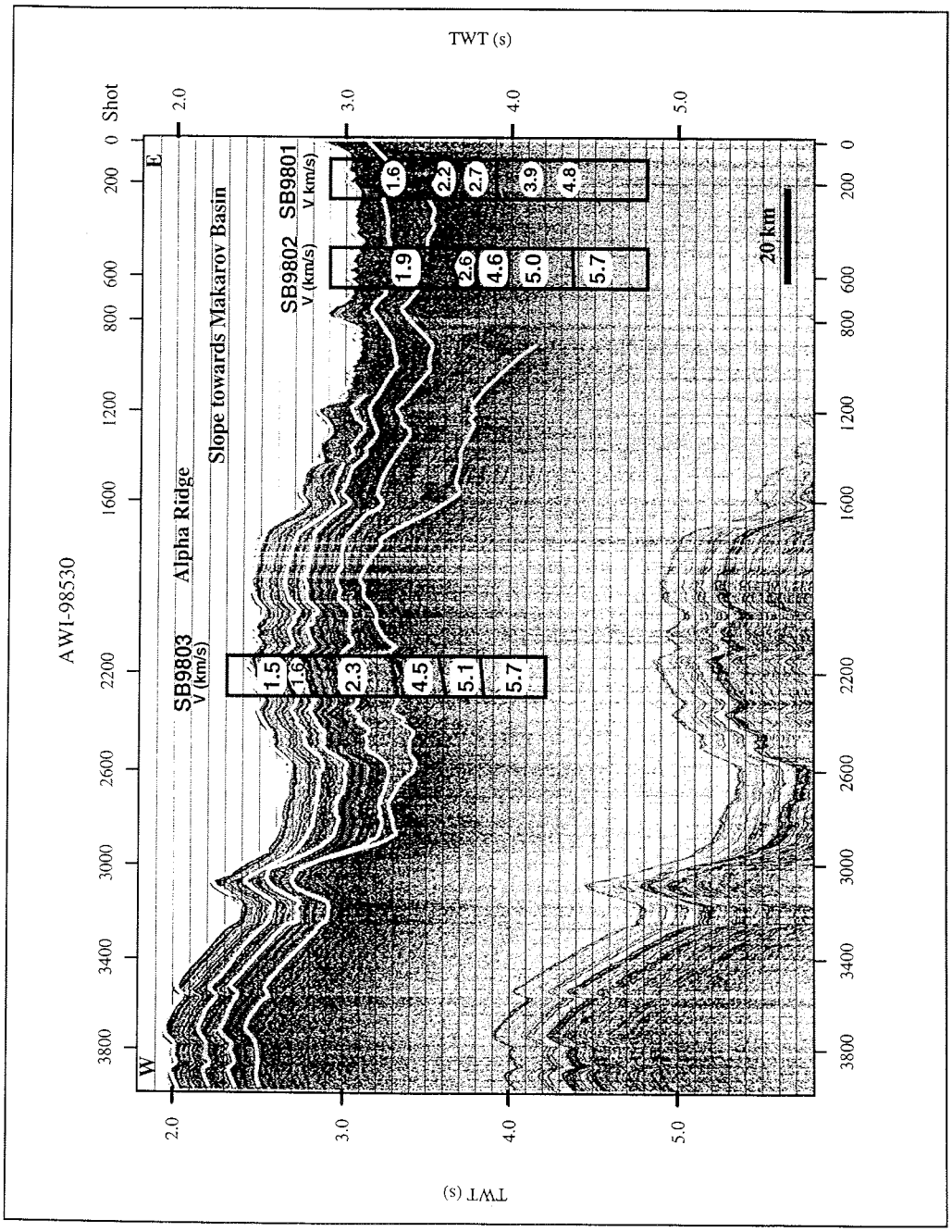

Fig. 7: Seismic profile 98530 along the strike of the westerwest part of Alpha Ridge. The grey lines represent the main reflectors identified in the section by interpretation of three sonobuoys. The 2D interpretation of the sonobuoys are overlain.

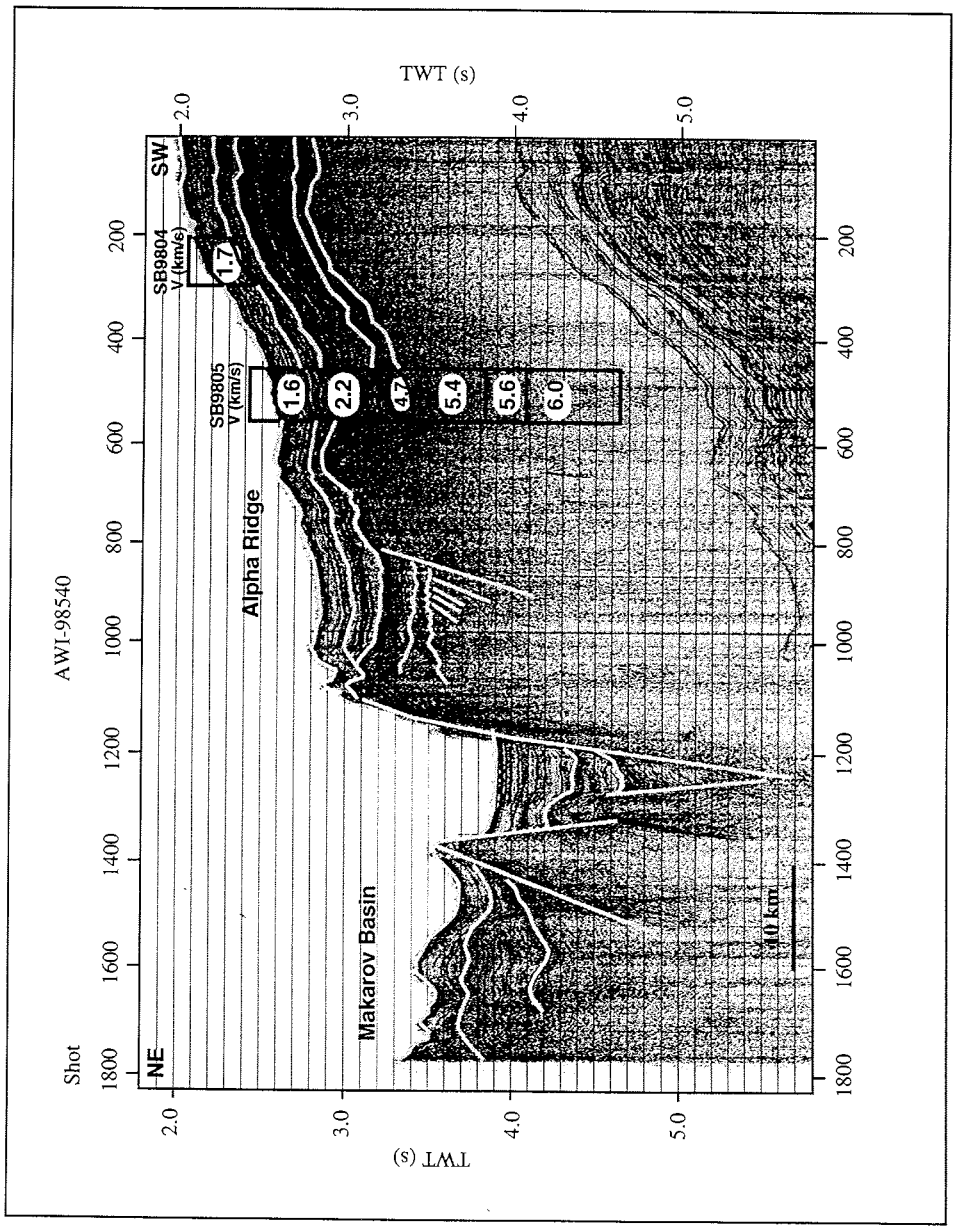

Fig. 8: Seismic profile 98540 across an escarpment at the northern flank of Alpha Ridge. The escarpment was sampled several times. For details see chapter 3 and the appendix. Sonobuoys SB 9804 and SB 9805 are overlain to the seismic reflection data. The grey lines indicate the main reflectors identified in the section based on the sonobuoys velocities.

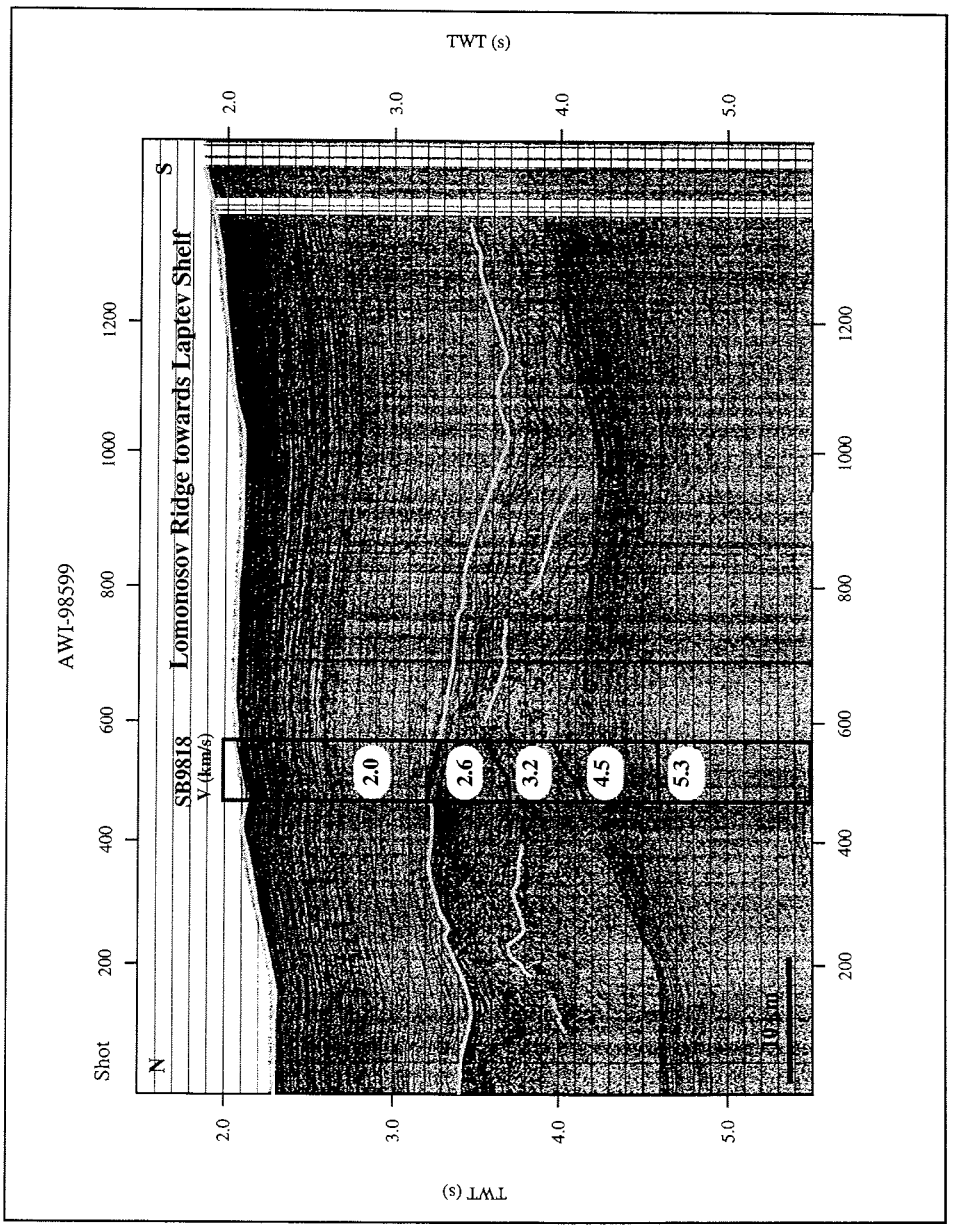

Fig. 9: Seismic profile 98599 in strike of the Lomonosov Ridge towards the Siberia Shelf. For its location see Fig. 6. Overlain are the results of the interpretation of sonobuoys SB 9818. The grey lines most likely indicate major boundaries in the sedimentary column based on velocities.

- a flat lying unit of sediments with velocities ranging between 1.8 and 2.0 km/s is most likely of Cenozoic age. The thickness of this unit is 700 and 1100 m along both lines, while thickening towards the sediment source, the Siberian Shelf (Fig. 9).
- Below this unit the velocities increase to 2.6 km/s possibly indicating the transition to older sediments. Its thickness is approximately 500 m.
- at a depth of almost 3000 m the seismic velocities gradually increase from 2.6, 3.2, 4.3 to 5.3 km/s in 6500 m depth. The MCS data shows that the sediments below this unconformity are affected by tectonics or at least shows evidences for redeposition. Here, most likely a complete section of the old continental sediment rocks of the Lomonosov Ridge are present.

In total 920 km of MCS data were acquired on the Lomonosov Ridge and to a minor part in the Makarov and Amundsen basins.

2.6 Gravimetry

(E. Weigelt, G. Jentzsch, K. Schüler)

The research vessel POLARSTERN is equipped with a sea gravimeter, system KSS 31 (BODENSEEWERKE). According to the logbook it is in operation since July 5th, 1988. It is installed in the centre of the ship, on F-deck. The system works continuously during the voyages. Gravity variations are recorded together with the ship's position, speed, and heading with a sampling rate of 12 sec. Every 10 minutes a line is printed on a printer containing date, time, relative gravity, pitch and roll accelerations, heading, speed, and latitude. In parallel, relative gravity and free air anomaly (automatically created) are plotted on the analogue plotter in the gravity room. During the voyage we noted on that plot twice a day date, time, gravity, free air anomaly and water depth provided on the digital display of the system.

Gravity connection Bremerhaven with gravimeter LCR G744

To connect the data recorded during the voyage and for correction of the instrumental drift several ties to absolute stations are needed. For this purpose a land gravimeter of type La Coste & Romberg, no. G744, is on the ship available.

Unfortunately, the measurements in Bremerhaven were not possible due to a failure in the power supply of the gravimeter. We discovered later a broken plug at one of the batteries. Since there are several readings at AWI it should be possible to use an earlier connection taking into account possible changes in water level of the harbour and the ship's draft. The small step included in this way should be neglectable.

Recording at sea

The 2-channel analogue writer is adjusted to the range of 100 mGal. The first channel (red) plots the gravity variations, and the second channel (blue) plots the free air anomaly which is computed automatically applying the Eötvös correction.

2.7 Data evaluation - Gravity -

Data quality
Travelling in open water or at good ice conditions the gravity record was relatively undisturbed. It reflects mainly the varying water depth. The filtering with SEASTATE 2 (low damping) is enough. The variations of gravity are in the range of ± 100 mGal. Under the condition of heavy ice and frequent ice breaking we see a high noise level and strong disturbances with amplitudes of up to ± 100 mGal. Further, there are episodic disturbances of up to about -15 mGal with a duration of 10 to 20 minutes. Figure 10 shows a section of the data plotted versus latitude. We can clearly identify the escarpment of the Barents Shelf, the low of the Nansen Basin, and the high of the Gakkel Ridge.

Data treatment
Final data correction and evaluation during the cruise were not possible. We first had to get started with a program system available for routine data treatment. This contains the following steps:

- merging of hourly data files to monthly data files and correction of SEASTATE filter and obvious errors (GRAVMERG);
- combination of navigation data with depth information; linear interpolation of gaps in depth data (NAVDINT);
- combination of navigation files with gravity files, computation of Bouguer anomaly (GRAVCORR);

Figure 10 gives a sample of the data for the period of July 6th to 8th, 1998. Since the depth information was still not complete only the raw gravity data (minus 985.000 mGal) are plotted, not the Bouguer anomaly.

2.8 Gravimeter tests

In the manual some tests are recommended. Those applicable during the voyage were carried out. During probing periods the ship's movements were sufficiently smooth, so that the calibration could be done. The following page numbers refer to the manual.

Control of the digital switches

The respective checks revealed:
Pitch: + 07, Roll: + 03, K: 0.8969 (calibration value)
These values are in accordance with the manual and the notes in the logbook.

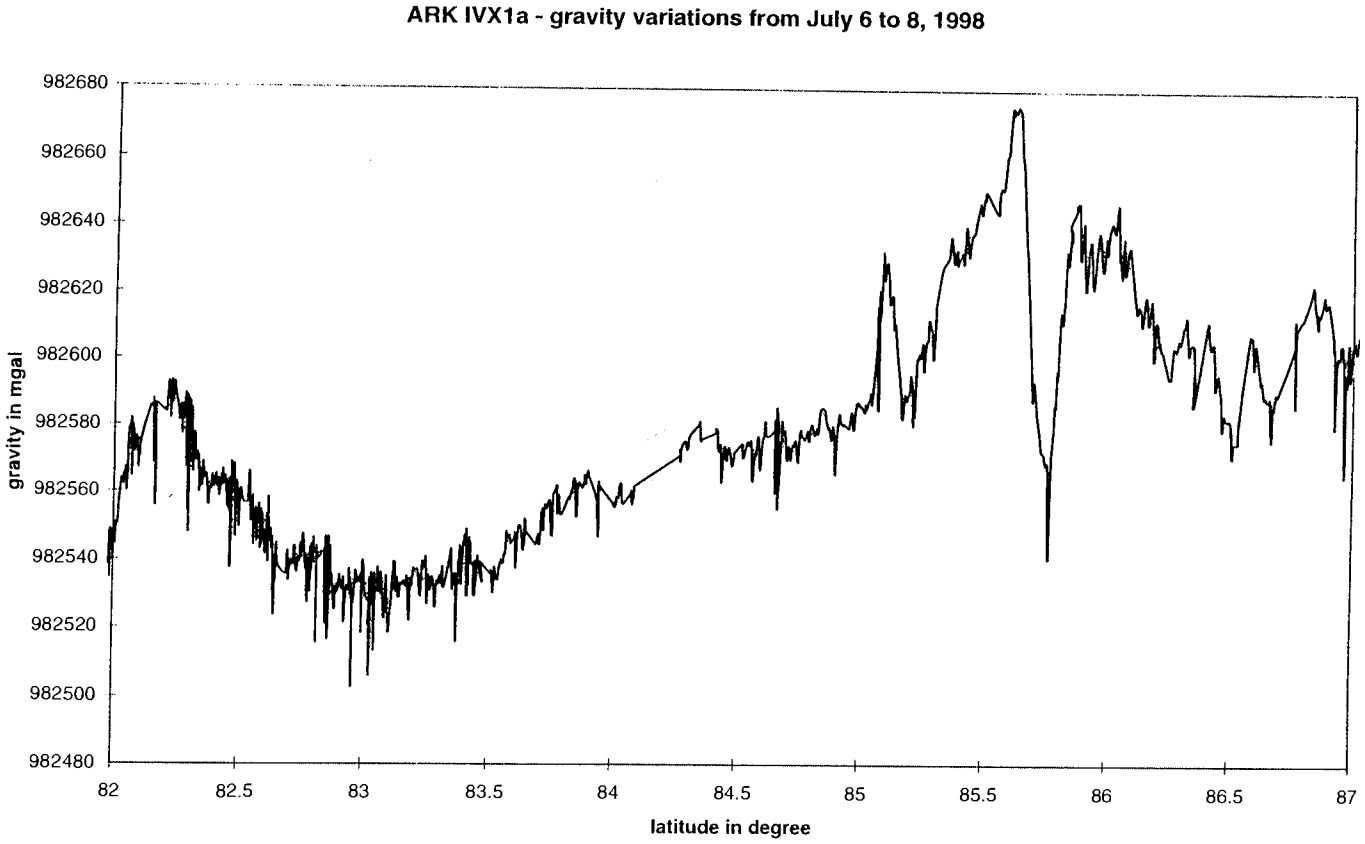

Fig. 10: Raw gravity data for the period July 6th to 8th, versus north latitude; note long period oscillation correlated with varying water depth and disturbances of negative spikes.

Test - Mode 10: Calibration
The calibration was carried out twice, on July 14th and 15th. Since the calibration step resulting from the additional weight (ball) is nearly 1000 mGal it is worth while to choose the scale of 1000 mGal on the analogue writer (p. 83: button REC, gravity '2' change to '3'). The amplitudes observed where 965.72 mGal and 966.10 mGal. Compared to the value in the manual of 964.28 mGal the deviations of less than 0.2 % are considered as very good. Therefore no further calibrations were carried out during the first leg of this cruise.

Test - Mode 11: Test V/F Converter GSS 30
Here, the gravity signal is internally decoupled and a variable test signal is created to test the voltage / frequency - conversion over the whole measuring range of +- 5.000 mGal, including the filter path. The test is performed automatically.

As a result we see oscillations on the analogue writer (scale 100 mGal) which should not exceed +- 1.5 mGal. In the manual (p. 82) a sketch of three different shifted sets of oscillations are shown, but without any time information and further explanation. In the test, only one set of oscillation appeared, and the variation observed was -2.14 mGal to +0.54 mGal. Despite of the unclear manual we take this result as a proof that the system is working properly.

CPU - loading
Using the displays (7 & 8) we find: minimum loading CPUA = 65 %; maximum loading CPUM = 74 %. The manual states that these values should be well below 100 %. Thus, also this test has a positive result.

Effect of strong tilts, tilt tests
Already shortly after leaving the harbour we observed characteristic episodic disturbances: variations of gravity over 10 to 20 minutes with amplitudes of up to -15 mGal. Later it was possible to correlate these deviations with the Interring System of the ship. This equipment is used to tilt the ship (e. g. for ice breaking purposes). The amplitude of the signal and the process of moving water excludes a direct gravity effect. A test performed during a drifting period revealed only a signal of about 1 mGal, but at a very short period, leading to slightly different results for the two different filters (little effect with SEASTATE 4, corner period 471 sec, delay 123 sec; bigger effect with SEASTATE 2, corner period 175 sec, delay 76 sec).

Long period, strong tilts during a fast voyage through the ice on July 19th proved that the signal is definitely caused by tilts. In addition, not only negative deviations, but also positive and negative variations were observed in connection with tilts causing different vertical accelerations (due to roll accelerations in connection with overriding small ice floes).

Obviously, these accelerations cannot be compensated by the gyro controlled table of the gravimeter. We cannot definitely say that there is a misadjustment or even a malfunction. But we must assume that during passages in open waters much

stronger roll and pitch movements should cause equivalent vertical accelerations. Thus, it is most likely that the observed disturbances are not standard, and that these disturbances should be avoidable.

2.9 Recommendations

General operation of the system

- CPU - loading: According to the manual this test of the system should be performed daily (no interruption of the record).

- Calibration: Calibration should be carried out several times during the cruise, maybe once a week under the condition of calm seas or during a drifting period. The deviation of the calibration pulse should be recorded over 15 to 20 minutes.

Improvement of the data

- Check of the gyro stabilised platform

We think, that the compensation provided by the platform is not sufficient. Therefore this should be checked.

- Corrections: In addition to the Eötvös - correction it would be interesting to correct the accelerations due to pitch and roll as well. Since all the data are stored and available this would require a numerical investigation.

3 Marine Geological Investigations

(R. Stein, S. Drachev, K. Fahl, J. Hefter, H. Kassens, N. Koukina, J. Matthiessen, C. Müller, E. Musatov, J. Mutterlose, N. Nörgaard-Petersen, K. Polozek, V. Shevchenko and R. Usbeck)

The overall goals of the marine-geological research program are

(1) high-resolution studies of changes in paleoclimate, paleoceanic circulation, paleoproductivity, and sea-ice distribution in the central Arctic Ocean and the adjacent continental margin during Late Quaternary times, and

(2) the long-term history of the Mesozoic and Cenozoic Arctic Ocean and its environmental evolution from a warm polar ocean to an ice-covered polar ocean.

In areas such as the Alpha-Mendeleev-Ridge, pre-quaternary sediments are cropping out (e. g., Jackson et al., 1985; Clark et al, 1986), which could even be cored with coring gears aboard RV POLARSTERN and which would allow to study the Tertiary/Cretaceous history of the (preglacial) Arctic Ocean. Especially the available data for the reconstruction of the long-term paleoclimatic history of the Arctic Ocean are very rare and only based on very short sediment cores taken from drifting ice islands.

Thus, the main working area on the Alpha-Ridge has been chosen between 84 and 86°N and 95 and 140°W. In this area, four short cores from ice islands containing lower Tertiary/Upper Cretaceous sediments were obtained from the ice island T3 and during the CESAR-Expedition (Clark et al., 1980; Jackson et al., 1985) (Fig. 11):

Core FL533:	85° 05.9'N, 98° 17.8'W	Lower Mastrichtian
Core FL437:	85° 59.5'N, 129° 58.5'W	Late Mastrichtian
Core FL422:	84° 53.3'N, 124° 32.5'W	Middle Eocene
Core CESAR-6:	85° 49.6'N, 109° 04.9'W	Late Mastrichtian

Due to too strong ice conditions, unfortunately, this area of the Alpha Ridge could not be reached by RV POLARSTERN, and the main study area on the Alpha Ridge has had to be shifted to the western part of the ridge (Fig. 11).

During ARK-XIV/1a, surface and sub-surface sediment samples were taken by the giant box corer, the multicorer, the kastenlot corer, and the gravity corer. In general, coring positions were carefully selected using PARASOUND to avoid areas of sediment redeposition and erosion. In addition, snow fields, dirty-sea-ice areas, melt ponds as well as the upper 75 m of the water column were sampled. During transit times, aerosols were routinely collected using a pump installed on the uppermost deck of the vessel.

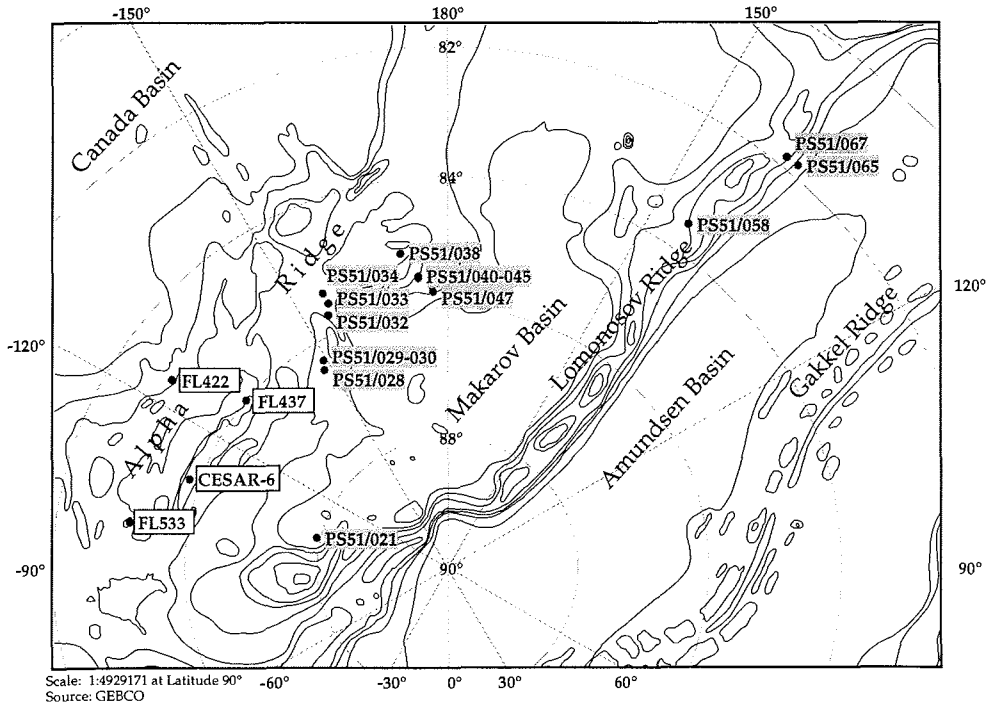

Fig. 11: Location of geological sampling stations performed during the ARK-XIV/1a Expedition. In addition, the location of the four cores taken from ice island T3 and during the CEASR-Expedition are shown. At these four locations lower Tertiary/Upper Cretaceous sediments were recovered.

The scientific investigations to be performed in the different laboratories will concentrate on:

- high-resolution stratigraphic analyses of the sediment sequences (isotopic stratigraphy, AMS 14-C-datings, amino-acids, magnetic susceptibility);
- studies of terrigenous sediment supply (grain size; clay, light, and heavy minerals; organic compounds; geochemical tracers);
- studies of the fluxes of terrigenous and marine organic carbon (total organic carbon, C/N ratios, hydrogen and oxygen indices, stable carbon and nitrogen isotopes, maceral composition, biomarker);

- reconstruction of paleoproductivity by tracer analyses (biomarkers, biogenic opal, stable isotopes, etc.);
- studies of reactions of marine biota to long- and short-term environmental changes;
- studies of physical properties (magnetic susceptibility, wet bulk density, porosity, shear strength);
- study of composition and grain size of aerosol particles;
- study of specific sedimentary environments with detailed PARASOUND surveys.

3.1 High resolution acoustic profiling by the PARASOUND echosounder system (S. Drachev, R. Usbeck)

The PARASOUND is an echosounding-type device designed to acquire a high resolution acoustic record of sub-bottom sediments. This record can be interpreted in terms of structural and facial characteristics of the sediments. According to the research program of the ARK XIV/1a cruise, the PARASOUND profiling aimed at:

- acquiring information from sub-bottom reflections for the selection of relevant sites for sampling of the sediments by gravity and kastenlot corers;

- providing a two- or even three-dimensional stratigraphic framework for lateral correlation of the sediment cores based on the sub-bottom reflection pattern;

- detecting changes in sediment facies along the transect from Spitsbergen to the Alpha Ridge and back to the continental slope of the Laptev Sea by means of interpretation of the high resolution acoustic record.

We started to run the PARASOUND on July 2nd at 74°01.5´ N, 29°37.8´ E south of Spitsbergen and kept it in 24-hour operation along the ship track until the end of the cruise on July 24th at 79°56.5´ N, 142°07.1´ E north of the New Siberian Islands (Fig. 12). This continuous profiling was interrupted only once in the Barents Shelf area between 75°50´ N, 35°00´ E and 81°28´ N, 35°00´ E where we entered the Russian economic zone, were not permitted to carry out any measurements. The following is a brief description of the obtained data and a preliminary discussion of the results.

3.1.1. Data acquisition system and data description

The PARASOUND system (Krupp Atlas Electronics, Bremen, Germany) generates two primary frequencies between 18 and 23.5 kHz transmitting in a narrow beam of 4°. As a result of the interaction of the primary frequencies within the water column, a secondary frequency is created based on the parametric effect. The parametric frequency is the difference frequency of the two primary waves transmitted. During ARK-XIV/1a cruise the parametric frequency was set to 4 kHz. This allowed sub-bottom penetration up to 100 m with a vertical resolution of ca. 30 cm. The

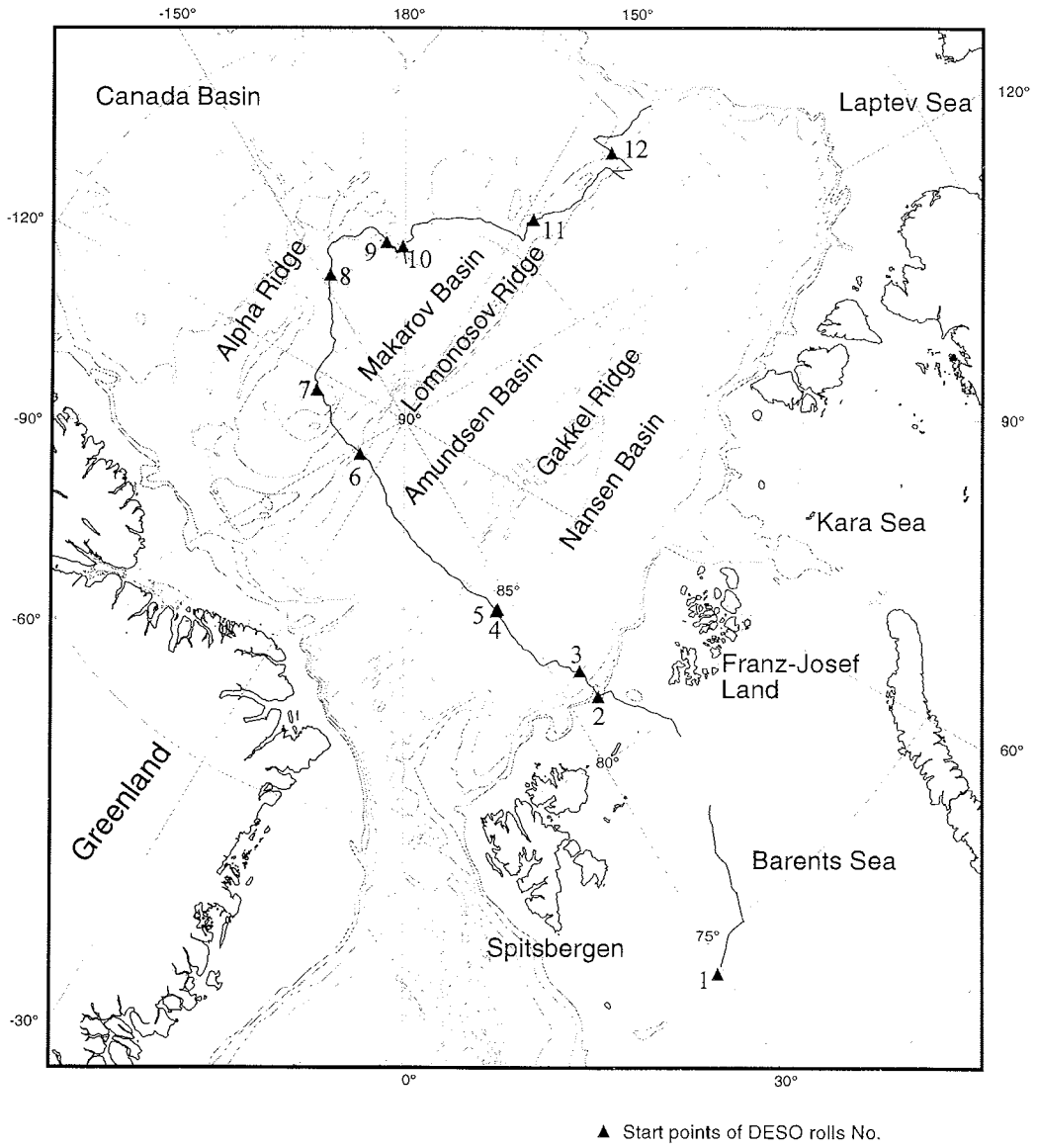

Fig. 12: Cruise track and location of the DESO paper rolls/PARASOUND profiles.

parametric pulse length was set to 2 under normal operating conditions. Under extreme conditions, such as above steep slopes and while operating in heavy sea ice, the pulse length was increased up to 8. Recorded seismograms were independently digitised by two different systems: (i) by the PARASOUND system for simultaneous printing on a chart recorder (Atlas DESO 25) and (ii) by the PARADIGMA system (Spiess, 1992) for tape storage (DAT-tapes) and post-processing. The settings of the PARADIGMA system were as follows: sampling rate 25 μs, trace length 133 or 266 ms, block size 10640 byte, format "SEG-Y packed" (Spiess, 1992).

As noted earlier (Thiede, 1988), the ship operations in sea ice covered areas produce a noise in the 3.5 - 4.5 kHz band which significantly disturbs the echosounding data. The level of this ice-breaking related noise depends on the thickness of the sea ice. Moreover, data disturbances are also related to frequent ice ramming of the vessel. Since most of the cruise took place in extremely heavy ice conditions, the PARASOUND data are strongly influenced by this kind of noise.

The complexity of the sea-bottom morphology is another strict factor which greatly limits the proper work of the PARASOUND. The operation above underwater ridges usually resulted in long-term losses of the signal and, consequently, the data.

Thus, both morphology of the sea-bottom and ice conditions caused very diverse quality of the PARASOUND data. Table 5 contains some general characteristics of the data revealed from the DESO analogue records. The location of the rolls/profiles is given in Figure 12. To estimate the data quality, we undertook a visual control of the quality of the analogue record. We applied a four-level scale of quality as follows:

- Very good quality, i. e. whole roll contains a continuous readable record slightly disturbed by ice-breaking related noise.

- Good quality, i. e. most of the roll contains a readable record disturbed by short intervals of data loss and ice-breaking related noise.

- Poor quality, i. e. most of the roll contains unreadable records, and the rare readable intervals are divided by long intervals of data missing.

- Very poor quality, i. e. almost the whole roll contains no readable records.

As follows from Table 5, the quality of the data strictly depends on the morphology of the crossed structural elements. When morphology is simple and flat, the quality of data is very good and good. These are the Barents continental shelf, Nansen, Amundsen and Makarov deep oceanic basins, and some crestal parts of the Lomonosov Ridge. In contrast, the positive structures, whose morphology is complex and variable due to presence of numerous steep slopes, reveal poor and very poor data quality. These are the Gakkel Ridge, Alpha Ridge and most of the Lomonosov Ridge.

Tab. 5: PARASOUND data characteristics

DESO paper rolls 1	Start of record: date/time, GMT latitude, longitude	End of record: date/time, GMT latitude, longitude	DAT-Tapes 1	Morphological province	Range of penetration, m	Quality, visual estimation
1	02.07.98/23:06 74°01.5′ N 29°37.8′ E	04.07.98/03:00 75°50.0′ N 35°13.5′ E	2-10	Barents Shelf	0-22	very good
2	05.07.98/17:20 81°28.5′ N 34°53.4′ E	06.07.98/08:21 82°11.8′ N 35°10.8′ E	10-12	Barents continental slope and rise	5-20	poor
3	06.07.98/09:03 82°16.4′ N 34°45.2′ E	07.07.98/14:45 84°04.2′ N 26°12.3′ E	12-16	Barents continental rise	4-25	poor
				Nansen oceanic basin	10-50	good
4	07.07.98/14:45 84°04.2′ N 26°12.3′ E	07.07.98/19:58 84°39.6′ N 25°30.1′ E	16-18	Nansen oceanic basin	24-38	good
5	07.07.98/20:00 84°39.8′ N 25°28.1′ E	09.07.98/21:45 88°37.0′ N 51°51.8′ W	18-25	Nansen oceanic basin	25-40	good/poor
				Gakkel mid-oceanic ridge	5-30	very poor
				Amundsen oceanic basin	10-30	good/poor
6	09.07.98/21:50 88°36.9′ N 52°29.2′ W	11.07.98/15:15 87°42.0′ N 109°08.6′ W	25-29	Western Lomonosov Ridge	5-25	very poor
				Western Makarov Basin	15-50	poor and very poor
7	11.07.98/16:00 87°41.9′ N 109°12.6′ W	14.07.98/19:55 85°53.8′ N 153°08.9′ W	29-36	Northern slope of central Alpha Ridge	10-25	very poor
8	14.07.98/19:55 85°53.8′ N 153°08.9′ W	17.07.98/04:22 85°29.5′ N 174°03.6′ W	36-41	Eastern Alpha Ridge	2-50	very poor
9	17.07.98/04:22 85°29.5′ N 174°03.6′ W	19.07.98/02:50 85°37.3′ N 178°58.3′ W	41-43	Eastern Alpha Ridge	–	very poor, almost no record
10	19.07.98/04:15 85°37.2′ N 179°11.7′ W	21.07.98/02:35 84°01.8′ N 147°48.0′ E	43-49	Eastern Alpha Ridge	5-15	very poor
				Eastern Makarov Basin	30-50	good
				Eastern Lomonosov Ridge	10-40	very poor
11	21.07.98/02:45 84°00.7′ N 147°41.9′ E	23.07.98/07:37 81°30.2′ N 142°22.0′ E	49-55	Eastern Lomonosov Ridge	10-110	good/poor
12	23.07.98/07:45 81°30.2′ N 142°28.6′ E	24.07.98/09:35 79°56.6′ N 142°07.6′ E	55-57	Eastern Lomonosov Ridge	40-65	good

3.1.2 Regional description

This section contains some preliminary characteristics of the different structural elements in terms of their morphology and sedimentary pattern as consistent with the PARASOUND analogue record.

Barents continental margin

The Barents continental margin extends along the cruise track from the 74°01.5′ N, 29°37.8′ E to about 82°55′ N, 28°51′ E and contains the shelf, continental slope and continental rise areas (Fig. 12, Table 5).

A very good quality of the acoustic record was revealed on the Barents Shelf with the sound penetration down to 20 - 25 m below the sea bottom. There are two distinct acoustic units (App. 1). The upper acoustically transparent unit AU-1 mostly occurs within sea-bottom depressions. It rests on a sharp erosional surface which forms the top of another unit (AU-2). The penetration below this interface is in the range of a few meters and, thus, AU-2 can be interpreted as an acoustic basement. However, in some cases steep short reflectors were observed in top of AU-2 (App. 1 and App. 2). According to the well-known geology of this shelf, we suggest, that these acoustic units represent Quaternary glacial-marine sediments (AU-1) and deformed Mesozoic rocks (AU-2). The latter are often exposed on elevated parts of the sea-floor (App. 2) whose eroded or ice-ploughed surface becomes topographically complex due to numerous small positive and negative features with amplitude variations from 1 to 20 meters.

The shelf break is located at about 81°40.5′ N, 35°07.3′ E where the water depth reaches 350 - 360 m (App. 3). The upper continental slope is rather steep causing a poor penetration of the signal. However, the slope becomes gentle downward and the penetration increases to 30 m. The penetrated sediments are characterised by moderate to low reflectivity and are believed to consist of debris flow facies. Such sediments predominate in the continental rise area. App. 4 shows a sequence of fan levees composed of four individual sedimentary units with total thickness about 30 m. The upper 2 to 5 m of each unit have a high acoustic backscatter while the lower 10 to 18 m are transparent and do not reveal any layering.

Eurasian Basin

The Eurasia Basin contains an axial mid-oceanic spreading ridge (Gakkel Ridge), which divides it into two smaller sub-basins: the Eurasia-faced Nansen Basin and the Lomonosov-faced Amundsen Basin. All these morphostructural provinces were crossed as RV POLARSTERN moved north-westward from 82°55′ N, 28°50′ E to 88°37′ N, 47°21′ E (Fig. 12).

The Nansen Basin has a very flat sea-floor. The continuous PARASOUND record over the entire basin is slightly disturbed by ice-caused noise. The signal penetration is up to 50 m below the sea-floor.

A debris flow facies extends from the Barents continental margin upon the nearest parts of the basin up to about 83°23´ N, 28°16´ E. It is well-distinguished due to high reflective acoustic characteristics and the clear absence of stratified internal structure. Toward the internal part of the basin, these sediments are gradually replaced by a facially different type of a pronounced layered sedimentary succession (App 5). The seismograms show, that it contains up to 7 individual rhythms which are highly reflective at their upper parts and transparent at the lower ones. We tentatively suggest this succession to be composed of distal turbidites.

On the acoustic record given in App. 5 one can see a slight but rather clear uplifting affecting the lower strata. The thickness of the rhythms is two time smaller than those at both sides of the uplift. This is evidence of growing of the uplift simultaneously with sediment accumulation. We consider this phenomena as an initial stage of mud diapirism which is well-developed northerly. App. 6 shows three diapirs which are in different stages of growing. The middle one, which appears to be the oldest, arises up to 30 m above the sea-floor. These diapirs have acoustically transparent cores similarly to mud-cored diapirs known from other regions (Niessen and Musatov, 1997). These features suggest that the succession of the distal turbidites in the Nansen Basin may be underlain by a mud-rich sequence of an unknown age.

The Gakkel Ridge was crossed between 84°59´ N, 24°52´ E and 86°27´ N, 10°21´ E. The PARASOUND section is characterised by a very poor record that is obviously a result of a complicated morphology of the ridge. In a few cases the seismograms contain short fragments of readable records where one can recognise some meters to 30 m thick sedimentary successions mostly occurring within local depressions (App. 7). However, such a fragmented record does not allow tracing neither the morphological features of the Gakkel Ridge nor the facial peculiarities of the sub-bottom sediments.

The Amundsen Basin is represented by a very flat deep-water plain whose major part lies at about 4.380 m. As compared to the Nansen Basin, here we have reduced signal penetration (10 - 30 m) and more ice-caused noise. Nevertheless, the acoustic record revealed a pattern which is very similar to what we observed in the Nansen Basin. The debris flow facies is predominant along the Gakkel-faced part of the section (App. 8) while the opposite part of the section contains a mostly well-stratified succession suggesting to be composed of distal turbidites.

Lomonosov Ridge

We crossed the Lomonosov Ridge twice: in its western Canadian part and in the eastern Siberian one (Fig. 12).

The western Lomonosov Ridge between 88°37´ N, 47°21´ W and 88°00´ N, 101°07´ W is characterised by a very poor PARASOUND record greatly disturbed by noise and loss of the signal due to the complex morphology of the ridge. Two examples of the

seismograms (App. 9 and App. 10) show a difference in sedimentary pattern in the Eurasia-faced slope area of the ridge (App. 9) and in its crestal part (App. 10) where the relief becomes smoother.

The Siberia-faced segment of the ridge was studied between 84°36.5´ N, 160°27.6´ E and 79°56.6´ N, 142°07.6´ E. Generally this part of the ridge reveals some asymmetry of its morphology with a very steep escarpment-bounded western flank and a more gentle eastern slope. The ship track mostly ran along the crest of the ridge where the water depth varies little and the topography is not as complicated as along both flanks of the ridge. Moreover, the whole ridge was crossed once on a W to E directed profile from the start point at 81°30´ N, 138°02´ E to the end point at 81°29.3´ N, 146°27.4´ E. Thus, the recorded PARASOUND data have different quality (Table 5) which generally depends on the relief character since the ice conditions were easier than in the Alpha Ridge area.

The majority of the recorded seismograms revealed the occurrence of well-stratified sediments with total penetrated thicknesses varying from 10 to 100 m. App. 11 gives an example from the crest of the ridge covered by a 40 m thick sedimentary sequence. Due to differences in the acoustic imaging and the presence of strong reflectors, it can be divided into three individual units. The two upper units are comparable to those reported by Niessen and Musatov (1997) southerly, where the internal structure of the penetrated sedimentary cover becomes more pronounced. These three units are typical for most of the crossed part of the ridge. However, in some cases another remarkable transparent unit "B" occurs between units "A" and "C". Over most of the crossed area this unit is lacking being truncated by Unit "A" (App. 12). This gives evidence of a distinct unconformity at the bottom of Unit "A" which can be the result of a regional tectonic and/or paleoceanographic event.

Generally one can point out that sediment thickness increases from north to the south approaching the Siberian continental margin. This appears to be related to increasing sediment supply by the large Siberian rivers. App. 13 illustrates the occurrence of a more than 100 m thick sedimentary sequence at geological station PS 051/058 which is located in the area of the western escarpment of the ridge. Here, an approx. 100 m step in sediment can be found. It might have been created by a slope instability.

Makarov Basin

The Makarov Basin separates the Alpha and Lomonosov ridges. It was also crossed twice in its western and eastern parts whose acoustic characteristics are quiet different.

The western Makarov Basin is divided into two depressions by a very narrow positive feature called Marvin Spur (Fig. 12). The PARASOUND record obtained here is of poor and very poor quality mostly because of the great noise produced by breaking of the heavy ice. Also in the area of the Marvin Spur we failed to find a real signal because of steep slopes. Thus, we illustrate this part of the Makarov Basin

with three fragments of the acoustic record obtained from those parts of the basin which are occupied by deep water plains.

The depression between the Lomonosov Ridge and Marvin Spur revealed about 20 m of penetrated sediments. This succession has an acoustic pattern very similar to those of the Amundsen Basin (App. 14). The central part of this depression contains a twenty-meters-high hill which has the same acoustic expression as the hills found in the Nansen Basin. It is a symmetrical cone-shaped feature with an acoustically transparent core. We suggest it to be the result of mud diapirism, but a possible connection to the gas releasing process has also to be taken into account.

Another depression between the Marvin Spur and Alpha Ridge is filled with well-stratified sub-bottom sediments with a thickness up to 50 m (App. 15 and App. 16). This sequence rests on a transparent acoustic unit. The interface between these units is represented by a very clear unconformity of unknown age. We found this unconformity in two areas within this part of the Makarov Basin (App. 15 and App. 16). This may be evidence of a, to some extent, regional character of this unconformity.

The eastern Makarov Basin was crossed in an area between 84°52.4´ N, 171°48.0´ E and 84°36.5´ N, 160°27.6´ E (Fig. 12). Morphologically this part of the basin is simpler. It contains a flat sea-floor which lies generally below 3.400 m of water depth. The PARASOUND data are of good quality with the penetration up to 50 m. App. 17 represents a typical example of the obtained record showing an undisturbed sedimentary sequence characterised by very thin layering. This sequence may be composed of sediments produced by gravity flows from the adjacent East Siberian continental margin.

Alpha Ridge

In this cruise we were able to reach the western part of the Alpha Ridge topped by the Lyon Sea Mount (Fig. 12). The operations in this area were carried out in extremely heavy ice conditions that resulted in considerable PARASOUND data signal loss. Especially poor data are characteristic for the northern slopes of the ridge (DESO 7, 9 and 10, Fig. 12) whose topography is much more complicated than it is shown on the existing maps. The crestal part of the ridge is the only area where the quality of the record allows to follow some peculiarities of the sub-bottom sediments (App. 18 and App. 19). As consistent with these data, the penetrated sedimentary cover has more or less the same acoustic pattern in different parts of the Lyon Sea Mount and is represented by stratified sediments. The penetration is in the range of 5 to 20 m and becomes reduced on sea-bottom highs.

3.2 Geological sampling, description, and methods applied aboard RV POLARSTERN

3.2.1 Aerosol sampling and size-distribution measurements (V. Shevchenko)

Sampling of aerosols for elemental analysis was carried out aboard RV POLARSTERN approximately 20 m above sea level by pumping of air through Filtrak-388 filters (D= 47 mm; air flow about 10 m^3 per hour). To exclude contamination from the ship, sampling was interrupted when the relative wind direction was not opposite to the ship heading. No samples were collected during rain and snow. During the expedition 3 samples were collected (Table 6). Elemental composition will be studied in Moscow by Instrumental Neutron-Activation Analysis (INAA).

Measurements of aerosol size distribution of particles larger than 0.5 µm were carried out at 61 sites (Table 7) using PC-218 photoelectrical particle counter (Royco, USA). In each series, 3 parallel measurements of particle concentrations in the ranges of 0.5 - 1, 1 - 2, 2 - 3, 3 - 5, and 5 - 10 µm were done. Aerosol size distribution of particles in the range from 0.005 µm to 1 µm were measured by DAES-3 electrostatic particle counter (Table 8).

3.2.2 Sampling of snow, melt-water ponds, and dirty sea ice (V. Shevchenko)

Aeolian transport of particulate matter onto Arctic sea ice is one source of sedimentary material in the Arctic. The annual deposition rates from eolian transport on the Central Arctic ice cover, however, are estimated to be very low to account for the high sediment loads observed in the Eurasian Basin (Pfirman et al., 1990). But atmospheric deposition of any individual components onto the Central Arctic ice surface practically has not been studied yet. In order to estimate contents of some constituents we carried out sampling of snow.

Snow and water from melt ponds samples were collected for chemical composition studies. Sampling was carried out using helictoper. Date and position of sampling are listed in the Table 9. On ice-floes samples of the upper 2 cm layer of snow and water from melt ponds were collected for chemical analysis (macrocomponents and trace elements). For sampling we used precleaned class 100 bottles, a plastic shovel, and plastic bags. Samples were stored in the refrigerator at -30 °C until processing in home laboratories. Ion chromatography and atomic absorption spectrophotometry will be carried out at AWI Bremerhaven (M. Kriews). Other subsamples will be melted and filtered through preweighted Whatman GF/F and Nuclepore filters to calculate concentrations of total suspended matter, particulate organic carbon, particulate organic nitrogen, and to determine contents and species composition of biogenic particles. It is also planned to study biomarkers and C-13 isotope

Tab. 6: List of samples of aerosol collected by filtration.

No.	Date-time (UTC)	Coordinates beginning/end	
	beginning/end	Latitude	Longitude
1	02.07-05.20	71°53.2'N	22°37.3'E
	02.07-11.20	72°38.9'N	25°01.0'E
	02.07-12.00	72°43.5'N	25°15.3'E
	02.07-18.40	73°30.1'N	27°50.3'E
	02.07-19.10	73°33.8'N	28°02.5'E
	02.07-22.10	73°54.9'N	29°14.5'E
2	04.07-05.10	76°15.0'N	35°50.2'E
	04.07-10.10	77°03.0'N	36°44.0'E
	04.07-12.30	77°25.1'N	37°28.2'E
	04.07-12.50	77°27.9'N	37°39.5'E
	04.07-14.20	77°40.7'N	38°40.3'E
	04.07-17.25	78°14.5'N	40°20.5'E
	05.07-04.40	80°08.6'N	40°35.3'E
	05.07-11.35	81°00.0'N	37°38.3'E
	05.07-12.40	81°08.9'N	36°59.1'E
	05.07-14.40	81°22.3'N	37°15.1'E
	05.07-15.05	81°24.0'N	37°11.0'E
	05.07-18.45	81°30.6'N	34°49.6'E
3	13.07-05.25	87°08.2'N	139°37.1'W
	13.07-08.05	86°56.3'N	144°03.2'W
	13.07-09.25	86°50.7'N	144°20.8'W
	13.07-11.25	86°42.8'N	146°22.4'W
	13.07-12.20	86°39.0'N	146°56.3'W
	13.07-13.30	86°33.4'N	147°38.7'W

Tab. 7: Time and locations of aerosol size distribution measurements by PC-218 (Royco, USA) particle counter

NN	Date, time (UTC)	Coordinates	
		Latitude	Longitude
1	30.06-08.00	66°21.4'N	9°35.4'E
2	30.06-09.30	66°33.6'N	9°51.2'E
3	30.06-12.30	67°00.7'N	10°27.0'E
4	30.06-14.10	67°10.8'N	10°40.6'E
5	30.06-16.25	67°29.9'N	11°07.6'E
6	30.06-20.30	67°59.9'N	12°04.8'E
7	01.07-05.40	69°11.6'N	14°34.0'E
8	01.07-09.07	69°34.5'N	15°43.2'E
9	01.07-10.00	69°40.9'N	16°02.0'E
10	01.07-12.35	69°57.5'N	16°52.0'E
11	01.07-16.50	70°17.8'N	17°55.7'E
12	02.07-04.20	71°45.0'N	22°13.1'E
13	02.07-06.12	72°00.0'N	22°56.5'E
14	02.07-10.10	72°30.7'N	24°35.4'E
15	02.07-12.15	72°45.3'N	25°21.2'E
16	02.07-14.25	73°00.1'N	26°10.3'E
17	02.07-18.40	73°30.1'N	27°50.3'E
18	02.07-19.10	73°33.8'N	28°02.5'E
19	02.07-22.10	73°54.9'N	29°14.5'E
20	04.07-04.25	76°05.7'N	35°44.4'E
21	04.07-05.10	76°15.0'N	35°50.2'E
22	04.07-07.28	76°41.1'N	35°42.5'E
23	04.07-10.10	77°03.0'N	36°44.0'E
24	04.07-13.04	77°30.0'N	37°48.2'E
25	04.07-16.14	78°01.9'N	39°41.7'E
26	04.07-22.15	79°06.2'N	40°30.5'E
27	05.07-04.40	80°08.6'N	40°35.5'E
28	05.07-07.23	80°36.2'N	39°22.3'E
29	05.07-11.35	81°00.0'N	81°00.0'E
30	05.07-15.05	81°24.0'N	37°11.0'E
31	05.07-18.45	81°30.6'N	34°49.6'E
32	06.07-00.10	81°58.9'N	34°42.0'E
33	06.07-08.53	82°15.0'N	34°50.0'E
34	06.07-17.45	82°49.7'N	31°52.8'E
35	07.07-05.15	83°26.8'N	27°23.2'E
36	07.07-17.15	84°20.0'N	25°55.0'E
37	12.07-20.45	87°31.1'N	130°45.8'W
38	12.07-22.40	87°26.8'N	136°02.0'W
39	13.07-05.25	87°08.2'N	139°37.1'W

Tab. 7 (continuation)

NN	Date, time (UTC)	Coordinates	
40	13.07-06.35	87°01.3'N	141°35.7'W
41	13.07-09.25	86°50.7'N	144°20.8'W
42	16.07-10.45	85°08.0'N	171°25.9'W
43	17.07-10.15	85°30.7'N	174°16.5'W
44	18.07-18.05	85°45.7'N	177°55.3'W
45	19.07-08.30	85°22.1'N	177°35.7'E
46	19.07-15.10	85°03.5'N	176°01.1'E
47	19.07-21.43	84°50.1'N	169°59.0'E
48	20.07-05.25	84°39.6'N	161°37.5'E
49	20.07-06.55	84°34.2'N	160°00.0'E
50	20.07-16.30	84°33.5'N	149°58.7'E
51	21.07-04.50	83°51.8'N	146°22.5'E
52	21.07-14.30	83°30.0'N	144°19.0'E
53	21.07-17.45	83°15.6'N	142°23.0'E
54	21.07-19.45	83°00.7'N	142°08.9'E
55	22.07-07.45	82°00.1'N	141°51.9'E
56	22.07-09.00	81°52.1'N	141°43.6'E
57	22.07-14.25	81°48.3'N	137°56.1'E
58	23.07-21.45	81°00.0'N	142°58.5'E
59	24.07-05.55	80°13.5'N	142°57.3'E
60	24.07-08.15	80°00.4'N	142°22.3'E
61	24.07-09.10	79°56.4'N	142°07.2'E

Tab. 8: Time and locations of aerosol size distribution measurements by DAES-3 electrostatic particle counter

NN	Date - time (UTC)	Coordinates	
		Latitude	Longitude
1	30.06-14.10	67°10.9'N	10°40.6'E
2	01.07-09.40	69°38.5'N	15°55.0'E
3	01.07-10.00	69°40.9'N	16°02.0'E
4	01.07-12.00	69°54.8'N	69°54.8'E
5	02.07-05.20	71°53.2'N	22°37.3'E
6	02.07-06.00	71°58.8'N	22°53.1'E
7	02.07-06.12	72°00.0'N	22°56.7'E
8	02.07-08.16	72°16.5'N	23°46.9'E
9	02.07-15.30	73°07.7'N	26°34.2'E
10	02.07-17.50	73°18.9'N	27°12.8'E
11	02.07-18.40	73°30.1'N	27°50.3'E
12	04.07-05.10	76°15.0'N	35°50.2'N
13	13.07-06.35	87°01.3'N	141°35.7'W

Tab. 9: Time and locations of sampling of snow, melt water ponds, and sea ice

Date	Sampler	Floe	Latitude (N)	Longitude	Snow	Water	Sea ice
06.07.1998	Shevchenko	1	82°21.27 N	33°51.18 E	1		
		2	82°21.33 N	33°20.65 E		1	
		3	82°29.18 N	33°39.34 E		2	
07.07.1998	Shevchenko	4	83°33.18 N	27°14.76 E	2	3	
		5	83°37.84 N	26°54.88 E	3		
		6	83°39.52 N	27°01.24 E		4	
		7	83°54.52 N	25°51.78 E	4	5	
		8	83°58.52 N	25°31.22 E		6	
		9	84°00.10 N	25°19.10 E			
08.07.1998	Shevchenko	10	85°53.36 N	15°56.54 E	5	7	1 +2
		11	86°04.10 N	14°54.39 E		8	3+4
		12	86°39.46 N	7°41.41 E			5+6
		13	86°51.70 N	7°52.00 E		9	7
		14	86°51.63 N	6°43.56 E	6		
10.07.1998	Müller	15	88°04.40 N	89°53.23 W	7	10	8
		16	88°02.19 N	100°56.56 W	8	11	9
		17	87°59.06 N	100°44.69 W	9	12	10
12.07.1998	Polozek	18	87°33.39 N	115°33.46 W	10	13	
		19	87°34.30 N	115°05.64 W			11
		20	87°34.65 N	116°36.35 W	11		12
		21	87°29.94 N	119°25.13 W			13
		22	87°31.20 N	118°49.48 W			14
13.07.1998	Hefter	23	86°59.54'N	143°22.71'W	12	14	
		24	86°59.54'N	143°22.71'W			15
		25	86°57.41'N	144°14.81'W	13		
		26	86°37.45'N	147°08.55'W	14	15	16
		27	86°33.09'N	148°03.64'W	15		
		28	86°32.43'N	147°14.40'W	16		17
14.07.1998	Rödle	29	86°25.36'N	148°19.85'W	17	16	
		30	86°22.38'N	148°28.66'W			18
		31	86°23.15'N	149°31.45'W	18		
15.07.1998	Usbeck	32	85°21.86'N	155°23.49'W	19	17	
		33	85°24.03'N	155°41.28'W	20		19
16.07.1998	Drachev	34	85°09.07'N	171°20.46'W	21	18	
		35	85°10.35'N	171°29.50'W			20
17.07.1998	Golikov	36	85°29.70'N	174°44.44'W	22	19	21
		37	85°35.68'N	173°43.74'W	23		
		38	85°37.01'N	174°05.21'W	24		
18.07.1998	Yoon	39	85°45.14'N	177°01.22'W	25	20	
		40	85°43.24'N	178°43.21'W			22
18.07.1998	Sokolov	41	85°40.40'N	176°56.23'W	26		23
		42	85°39.19'N	177°51.71'W			24+25
19.07.1998	Musatov	43	85°21.04'N	177°43.80'E	27	21	26
		44	85°13.90'N	178°26.70'E	28		
21.07.1998	Rödle	45	83°31.00'N	144°46.59'E	29	22	
		46	83°33.57'N	144°58.95'E	30	23	27
		47	83°33.29'N	144°49.77'E	31		
22.07.1998	Norgaard-Pedersen	48	81°52.59'N	141°36.00'E	32	24	
		49	81°48.69'N	141°44.90'E	33		
		50	81°51.19'N	141°16.87'E	34		
23.07.1998	Matthiessen	51	81°26.05'N	142°32.32'E	35		
		52	81°31.50'N	141°50.59'E	36		
		54	81°33.50'N	141°44.77'E	37	25	
		55	81°36.06'N	142°17.85'E			28
23.07.1998	Müller	56	81°28.40'N	145°03.88 E	38	26	29
		57	81°28.86'N	145°25.92'E	39		

composition in these samples. The obtained data will be used for the estimation of deposition of chemical components to the Arctic Ocean surface from the atmosphere. Later scanning electron microscopy with X-ray micro analysis will be carried out to study the composition of individual particles. The studies of composition of particulate matter contained in snow are to be carried out at AWI Bremerhaven, IORAS Moscow, and University of Antwerpen.

Sediment transport via sea ice is expected to contribute significantly to deep-sea sedimentation at least in regions of ice ablation (Pfirman et al., 1990; Nürnberg et al., 1994). It is important to study the role of different sources in supplying the Central Arctic, especially the Alpha Rigde area, with ice-rafted sediments. Thus, "dirty sea ice" has been samples at numerous locations during the ARK-XIV/1a Expedition (Table 9). At AWI the "dirty ice" samples will be melted and filtered. After that grain size analyses, mineral and elemental composition, contents of organic compounds, isotope composition of C species composition of algae will be studied at AWI, IORAS and MMBI. Using the obtained data we try to estimate the input of matter from different source regions delivered in the study area by the Transpolar Drift or Beaufort Gyre systems.

3.2.3 Sampling in the water column using sediment traps (V. Shevchenko)

In order to elucidate the contribution of ice-derived mineral and organic material to particle flux rates, sedimenting material was collected by short-term deployments of sediment traps attached to the ice floes. The sediment traps were deployed by hand over the edge of ice floes, at a distance of at least 200 m away from the ship (Table 10). Helicopter was used to bring people and equipment onto the ice floes. Deployments consisted of two single traps (D= 12 cm) positioned at 50 and 75 m of water depth. The traps are fitted with a baffler at the top. The sampling bottles were filled with prefiltered sea water to which NaCl was added to increase the density (to salinity of about 40 ‰). The solution was poisoned with $HgCl_2$ prior and after the deployment. Samples collected by sediment traps will be analyzed for particulate organic carbon, particulate organic nitrogen, Chl-a and seston content. Light and scanning electron microscopic analyses will also be performed. At the same stations water samples for microalgae studies were taken from the sea surface (0 m) manually from the edge of ice floes and from the 25, 50 and 75 m depths from the rosette Niskin bottles. Aggregates (colonies) of diatoms were collected from the edge of ice floes where sediment traps were deployed. The trap data, combined with related data from the water column, will allow quantitative and qualitative evaluations of daily vertical particle flux rates.

Tab. 10: Sediment trap deployments; phytoplankton (0, 25, 50 and 75 m depths) and ice flora (0 m) sampling.

Station No.	Date	Position		Duration (hr)	Quantity of ice flora samples
		Latitude	Longitude		
51/034	15.07	85°22.3'N	155°25.2'W	6	4
51/038	16.07	85°08.0'N	171°25.6'W	3	3
51/046	18.08	85°45.1'N	177°00.5W	6.25	4

3.2.4 Sea floor sediment sampling and description
(K. Fahl, J. Hefter, H. Kassens, N. Koukina, J. Matthiessen, C. Müller, E. Musatov, J. Mutterlose, N. Nörgaard-Petersen, K. Polozek, and R. Stein)

Sampling of Near-Surface Sediments
Surface sediments were taken routinely at almost all geological stations (Fig. 11) with the giant box corer (GKG; 50 x 50 x 60 cm). The surface sediments of the GKG were sampled for sedimentological, micropaleontological, and geochemical investigations. In addition, three plastic tubes (12 cm in diameter) and one plastic box (cross section of 7.5 x 15) covering the entire sediment column gained by GKG were taken for sedimentological, geochemical, and stable isotope investigations, and for archiving at AWI.

At several stations (see station list), the AWI multicorer ("MUC"; manufactured by Fa. Wuttke, Henstedt-Ulzburg) with 12 tubes of 6 cm in diameter was used. The penetration weight of the MUC is 250 kg.

Coring and Sampling of Long Sediment Cores
The gravity corer (SL) and the kastenlot corer (KAL) were used to obtain long sediment cores. The gravity corer has a penetration weight of 1.5 t, and a core barrel segment length of 5 m with a diameter of 120 mm. The core barrels used during ARK-XIV/1a had lengths of 5 and 10 m. The length of the obtained cores vary between 0 and 635 cm (Fig. 13). The kastenlot (Kögler, 1963), a gravity corer with a rectangular cross section of 30 x 30 cm, has a penetration weight of 3.5 t and a corebox segment sized 30 x 30 x 575 cm (manufactured by Hydrowerkstätten Kiel). The length of the box core boxes used was 11.75 m plus about 30 cm for the core catcher. The great advantage of this kastenlot is the wall-thickness of only 0.2 cm. Because of the great cross-sectional area (900 cm^2) and the small thickness of the walls, the quality of the core was generally excellent. The length of the obtained core was 719 cm (PS51/038-4) (Fig. 13).

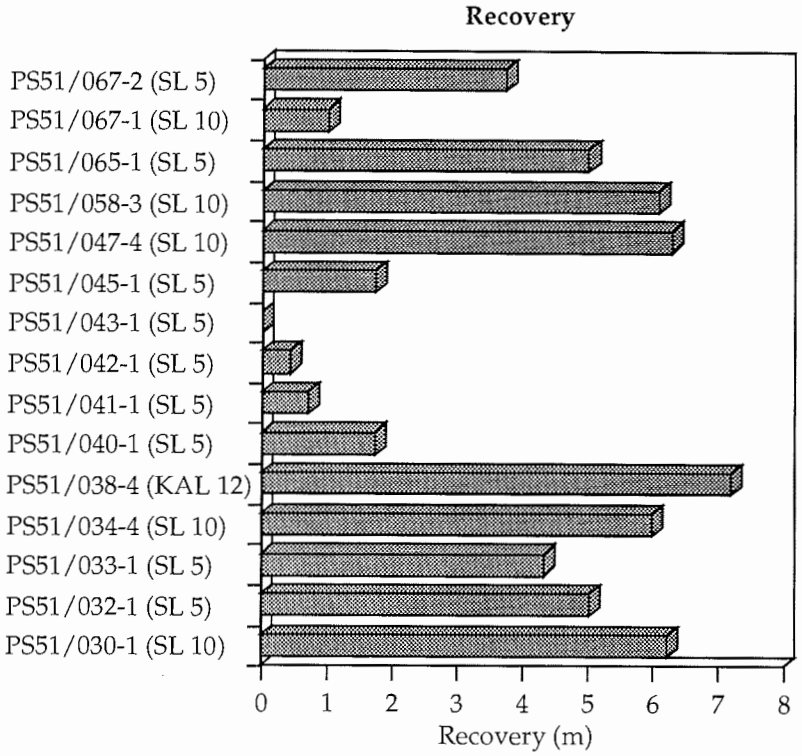

Fig. 13: Recovery of kastenlot (KAL) and gravity (SL) cores.

Six of the gravity cores were opened, described, and sampled for smear-slide analysis onboard POLARSTERN. Before opening of the SL cores, core logging was performed (see chapter 3.3.1). Sampling of SL cores will be performed onshore for stratigraphical, sedimentological, geochemical, and micropaleontological studies (AMS^{14}C dating, stable isotopes, grain size, mineral composition, major and minor elements, carbonate, organic carbon, biomarker, microfossil assemblages, etc.).

Sampling of the KAL core for the same investigations was performed as follows: three plastic boxes (100 x 16 x 7.5 cm) covering the entire core (AWI Archive; AWI geochemistry, sedimentology, mineralogy, and stable isotopes; GEOMAR sedimentology and stable isotopes). One plastic box (100 x 9 x 7.5 cm) covering the entire core was taken for core logging and afterwards deep-frozen at -30°C for organic-geochemical studies to be later performed at the home laboratory. In addition, single samples were taken from the entire core for specific mineralogical and micropaleontological studies (IORAS Moscow, VNIIO St. Petersburg, MMBI Murmansk).

Sediment Description and Characterization

• Visual core description
The sediment cores were routinely photographed and described, and are graphically displayed within the annex. Sediment colors were identified according to the "Munsell Soil Color Chart".

• Smear slide investigations
Smear-slide investigations were performed to obtain estimates of the grain size and sediment composition (i. e., biogenic and terrigenous components) and for the classification of the sediment type (e. g., silty clay, sandy silt, etc.).

• Radiographs
Sediment slabs of 0.5 cm in thickness were taken continuously from KAL and all opened SL cores. X-ray images has been produced onboard POLARSTERN in order to elucidate sedimentary and biogenic structures and to determine the number of coarse-grained detritus >2 mm for evaluation of the contents of ice-rafted debris (IRD; cf., Fig. 21) (for method see Grobe, 1987).

3.3 Physical properties in marine sediments

During ARK-XIV/1a physical properties were determined on whole cores by logging (magnetic susceptibilty, P-wave velocity, wet bulk density and porosity) and on discrete samples after core opening (wet bulk density, water content, porosity). Physical properties of marine sediments are important parameters for the interpretation of the sedimentary record. These data allow to enhance the paleoceanographic interpretation of each site (e. g. to determine sediment accumulation rates) and to provide data for lateral core correlation and stratigraphic control. Furthermore, the magnetic susceptibility which is defined as the dimensionless proportional factor of an applied magnetic field in relation to the magnetization in the sample, can be used as an indicator for marine versus terrestrial origin of the sediments (e. g., Nowaczyk, 1991). In addition, P-wave velocity and wet bulk density are basic parameters for the calculation of synthetic seismograms in order to compare the cored sedimentary record with high resolution seismic profiles obtained with the PARASOUND system.

3.3.1 Continuous whole-core logging of wet bulk density, P-wave velocity and magnetic suceptibility
(R. Stein, R. Usbeck and K. Polozek)

Wet Bulk Density (WBD) and P-wave velocity and magnetic susceptibility were measured in 1-cm intervals on gravity and kastenlot cores taken during the cruise. We have used the "Multi Sensor Core Logger (MSCL-14)", manufactured by Geotek (UK), which allows the determination of core diameter, P-wave travel time, gamma-

ray attenuation and magnetic susceptibility. The system is automated (PC based) and designed for non-destructive logging of up to 1.3 m long whole-core sections. In case of kastenlot cores, polystyrene boxes (size inside 82.5 x 72 x 1000 mm) were logged which were previously filled with sediments by pushing the boxes into the cores shortly after the kastenlot was opened. Because the loop sensor used has a different response to varying core diameter, all magnetic susceptibility values determined for kastenlot boxes are multiplied by 0.82 (Table 11) according to the manufacturer's correction instructions. The data is expressed in SI-units, although no correct volume susceptibility can be assessed due to the loop sensor geometry.

A detailed description of the MSCL system is given by Kuhn (1995), its calibration is described by Niessen (1997) and Weber et al. (1997). The characteristics are summarized in Table 11. During the time of the cruise the gamma ray attenuation was calibrated to density using aluminum, graphite and water. The raw data was processed using the Geotek Software Version 3.0. Additionally, a Kaleidagraph Macro was improved during the cruise in order to calculate the correction for count rate effects on the attenuated gamma data as described in Weber et al. (1997).

For all sediment cores logged aboard RV POLARSTERN during the ARK-XIX/1a Expedition, the records of porosity, WBD and magnetic susceptibility are listed in the Appendix. The porosity values have been calculated from the measured WBD and a grain density of 2.65 g cm^{-3} (Weber et al., 1997). As an example, the data of Kastenlot Core PS51/038-4 are shown in Figure 14. All three variables show rhythmic/cyclic variations with changing amplitudes, suggesting changes in sediment composition and/or grain size (cf., Chapter 3.5). In general, the WBD values calculated from the MSCL correlate with those determined on discrete samples. There is a similar trend, although the MSCL densities are mostly lower than those of discrete samples (Fig. 14). Based on the porosity and WBD records, the sedimentary sequence can be divided in three intervals. Interval I (445 cmbsf to bottom of core) is characterized by porositiy and WBD values ranging between 50 and 70 % and between 1.55 and 1.8 g cm^{-3}, respectively. Interval II (250 to 445 cmbsf) is characterized by low-amplitude variations in porosity and WBD (60 - 65% and 1.58 - 1.68 g cm^{-3}). In the upper 250 cmbsf (Interval III) the amplitude of both parameters distinctly increases, reaching a maximum range in the uppermost 150 cmbsf. The increase in magnetic susceptibility at about 350 cmbsf coincides with increased occurrence of IRD (cf., Fig. 21) and a change in the grey scale record (cf., Fig. 16).

Based on whole-core logging records, a lateral correlation between sediment cores is possible as shown for the Alpha-Ridge Transect PS51/030-1 to PS51/034-4 (Fig. 15 a and b). The WBD records of all four cores (Fig. 15 a) display a similar very prominent pattern. The lower part of the records is characterized by WBD values fluctuating around a constant mean values of about 1.64 to 1.68 g cm^{-3}; the amplitude is significantly lower than in the upper part. The upper part is characterized by a trend to lower mean values and a distinct increase in the amplitude of fluctuation. At least four major cycles superimposed by shorter-term cycles, are observed in the records (Fig. 15 a). In the magnetic susceptibility records (Fig. 15 b), distinct minimum values

can be correlated in all four cores. Based on the MSCL records, the sedimentation rate of the shallower core PS51/034-4 (water depth 2071 m) appears to be lower (by a factor of about two) than that of the deeper cores from water depths between about 2690 and 2950 m (cf., Chapter 3.5).

Tab. 11: Multi Sensor Core Logger (MSCL-14) specifications

P-wave Velocity and Core Diameter	
Transducer diameter	5 cm
Transmitter pulse frequency	500 kHz
Transmitted pulse repetition rate:	1 kHz
Received pulse resolution	50 ns
P-wave travel-time offset	8.47 µs (KAL, 2*3 mm box wall thickness) 7.79 µs (SL, 2*2.5 cm liner wall thickness)
Density	
Gamma ray source	Cs-137
Source activity	356 MBq
Source energy	0.662 MeV
Collimator diameter	5 mm
Gamma detector	Scintillation Counter (John Count Scientific Ltd.)
Magnetic Susceptibility	
Loop sensor type	MS-2B (Bartington Ltd.)
Loop sensor diameter	14 cm
Alternating field frequency	0.565 kHz
Magnetic field intensity	approx. 80 A/m RMS
Loop sensor correction coefficient SL K-rel	2 (113 cm^2 core cross section)
Loop sensor correction coefficient KAL K-rel	0.82 (59.4 cm^2 box cross section)

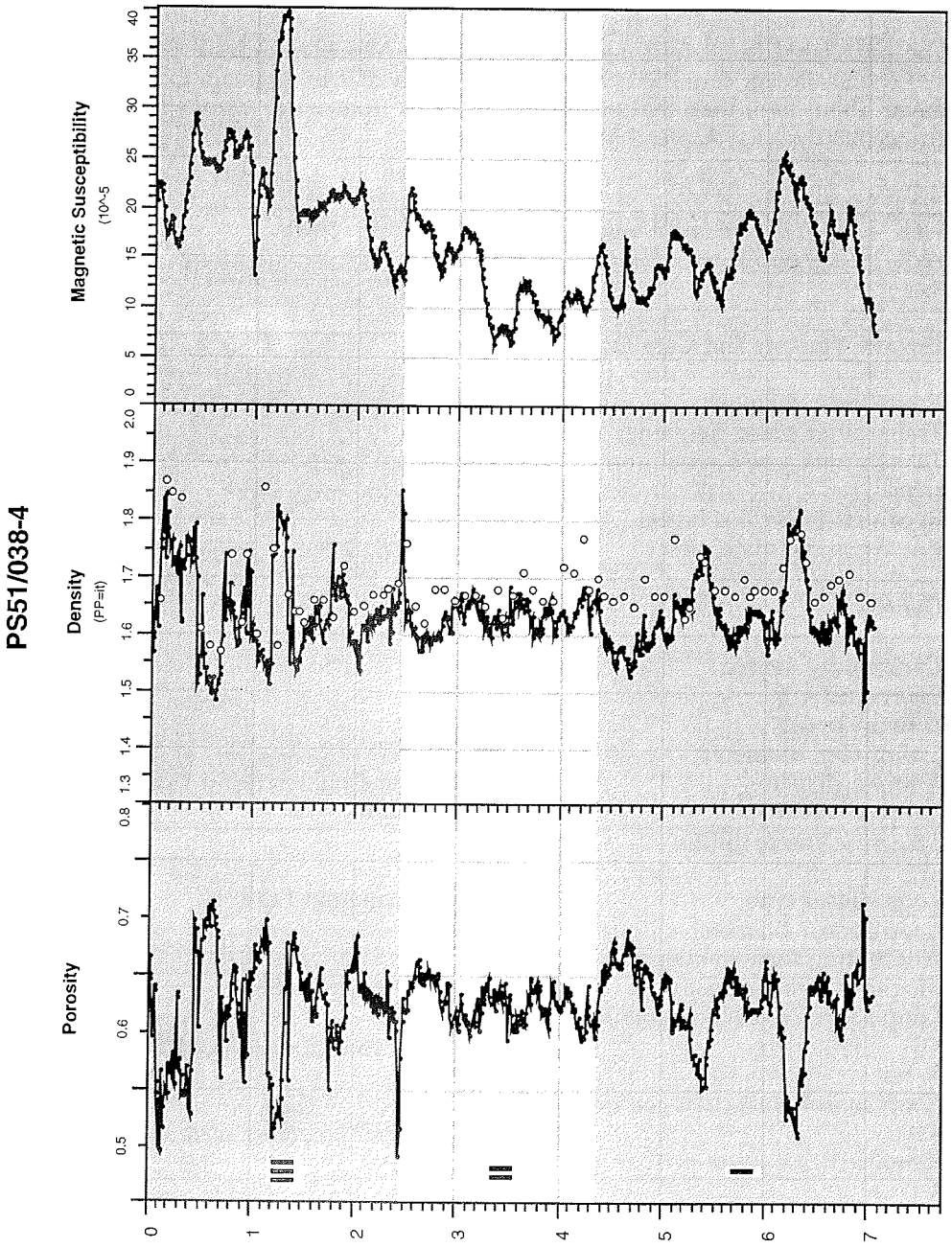

Fig. 14: Porosity, wet bulk density, and magnetic susceptibility records from Kastenlot Core PS51/038-4, obtained by Multi Sensor Logging. Open circles are wet bulk density values measured on discrete samples (cf., Fig. 16).

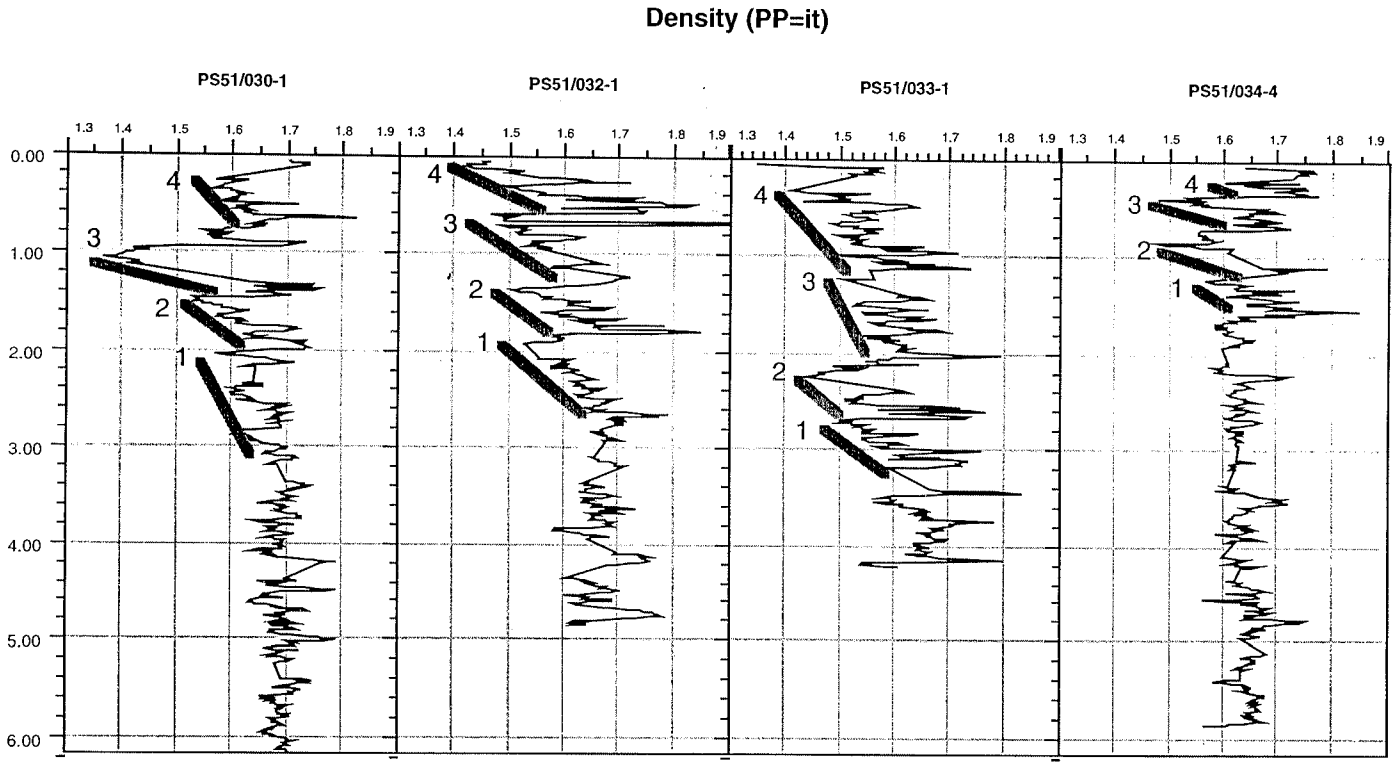

Fig. 15 a: Lateral correlation of whole-core logging results of the Alpha-Ridge-Transect PS51/030-1 to PS51/034-4.
(a) wet bulk density records
Grey-shadded interval of the upper part of the records in (a) and (b) indicates a general change in the pattern of the density records (i. e., decrease in mean value and increase in amplitude of fluctuation).

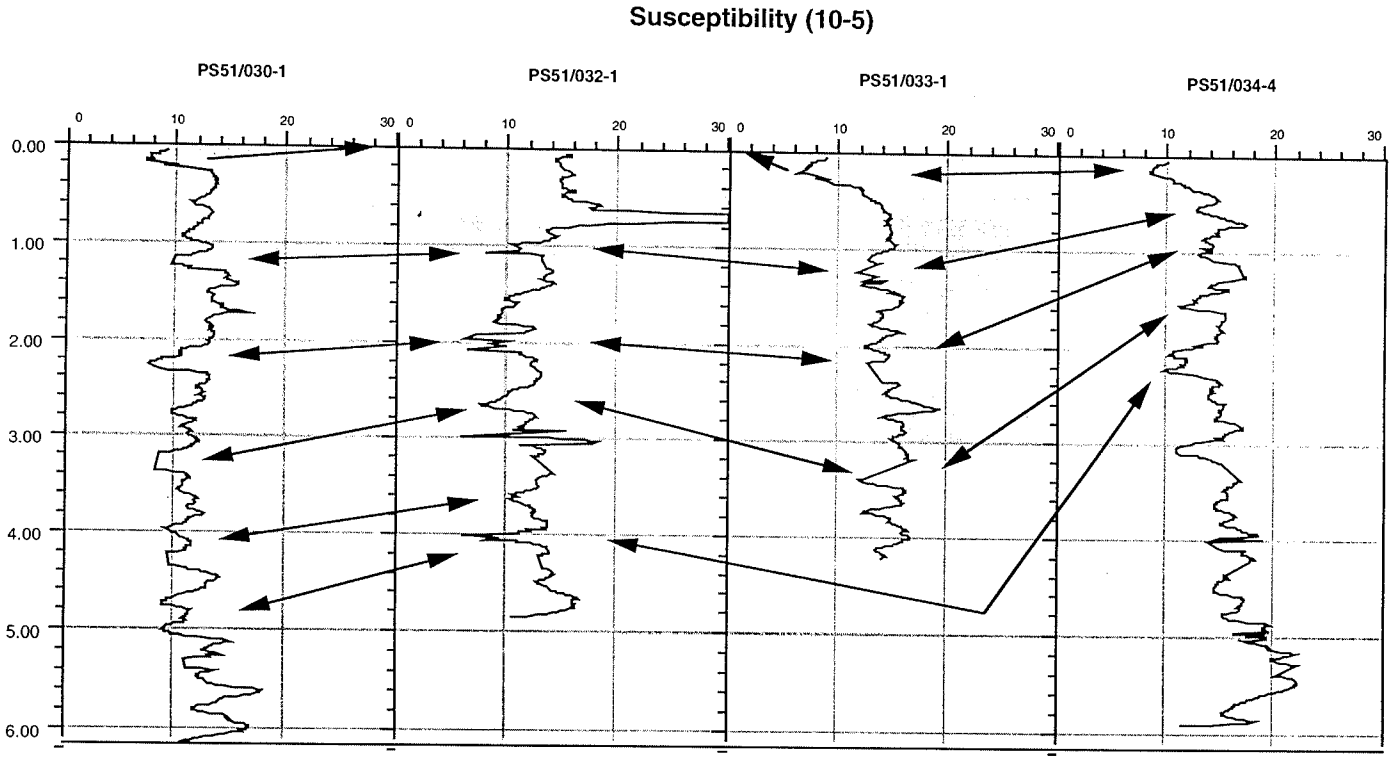

Fig. 15 b: Lateral correlation of whole-core logging results of the Alpha-Ridge-Transect PS51/030-1 to PS51/034-4.
(b) magnetic susceptibility records
Grey-shadded interval of the upper part of the records in (a) and (b) indicates a general change in the pattern of the density records (i. e., decrease in mean value and increase in amplitude of fluctuation).

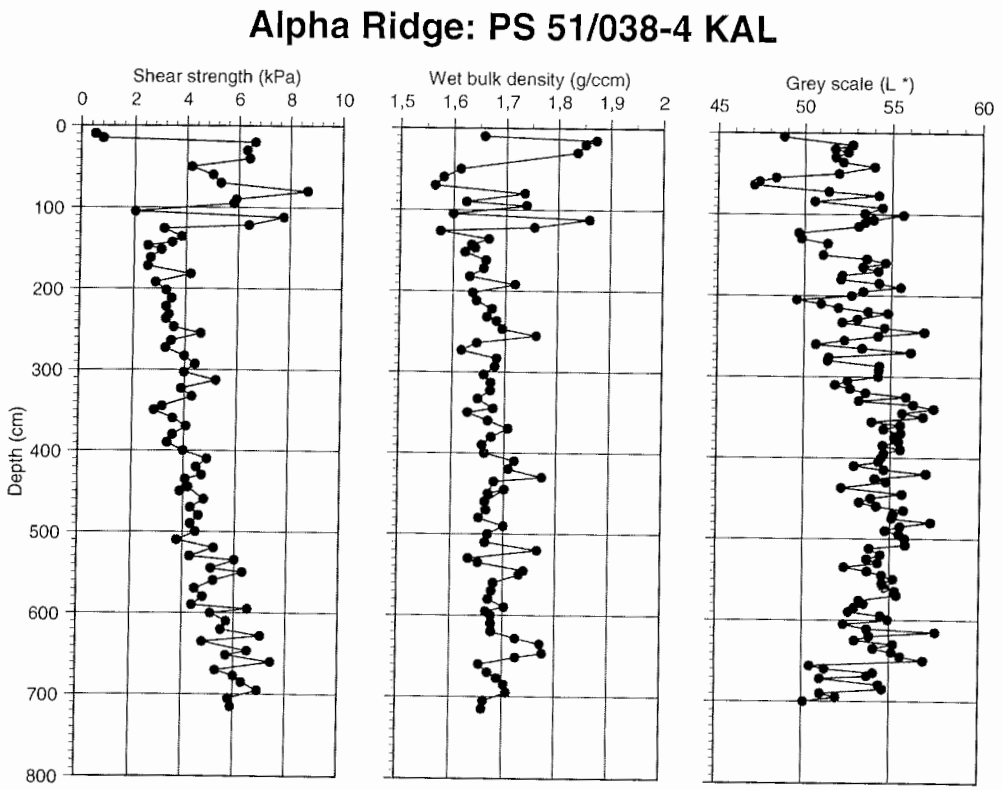

Fig. 16: Physical property record of sediment Core PS 51/038-4 KAL from the ALPHA Ridge at 1473 m water depth.

3.3.2. Physical properties of discrete samples
(H. Kassens and N. Nörgaard-Petersen)

Sediment physical properties measured aboard on discrete samples included shear strength, index properties (e. g. wet bulk density, water content, porosity), and colour reflectance.

Shear strength: A vane shear instrument (Haake viscometer, RV 3) was used to measure undrained shear strength of undisturbed box and gravity cores (kasten

corer; 30 x 30 x 600 cm). A 20 mm x 8.8 mm vane was used with this instrument, inserted 1 cm deep into the sediment and rotated at a speed of 4 rotations per minute (24°/sec). The measurement interval ranged from 2.5 to 10 cm depending on the down-core variability of sediments. At each depth interval 2 - 4 measurements were taken in order to determine the scatter associated with sediment inhomogenities, such as bioturbation. Shear strength was measured at peak failure. All values are reported in kPa.

Index properties: From the index properties water content and bulk density, sediment phase relationships as dry density, porosity and void ratio were derived. The index properties were determined from the direct measurement of the total mass of the sample (Mt), the dry mass of the sample (Md) and the total volume of the saturated sample (Vt). To compensate for ship's motion, mass was determined using a technique of differential counterbalancing on twin top loading electronic balances (Childress and Mickel, 1980). A constant volume sampling tube of 10 ccm was used. The tube was carefully pushed into the sediment, then cut out, trimmed and weighed. After determination of the total (wet) mass and volume, samples were stored for later freeze drying and determination of water content and dry mass in the home laboratory. Wet bulk density (Mw) is the density of the total sample, including pore fluid (Mw = Mt/Vt). Units are reported in g/ccm. In addition to being one of the most basic measurements for determining material properties, bulk density is also one of the two variables required for calculation of sediment accumulation rates.

Colour reflectance: Colour reflectance was determined directly after core recovery in order to avoid colour changes due to e. g. air contact alteration of the sediments. Measurements were carried out by using the MINOLTA spectrophotometer CM 2002. This system is measuring the spectral reflectance of sediments at wave length from 400 to 700 nm (L * a * b * colour space; also referred to as the CIELAB space). To average colour inhomogenities as a result of bioturbation 2 - 3 measurements were taken at each depth interval (field of view 0.8 cm^2). Lightness, hue, and saturation were registrated, whereas only the lightness variable L* (grey scale) is reported here.

Preliminary results of Kastenlot Core PS 51/038-4 from the northern slope of the Alpha Ridge at 1.473 m water depth are reported here (Fig. 16):

In general, the uppermost sediment cover (<10 m) on the Alpha Ridge is dominated by Quaternary hemipelagic sediments. The frequency and amplitude variations of the physical property curves represent alternating sediment intervals of silty clay with intervals of sandy silty clay as well as frequent mud clasts-rich units. Sediments show normally consolidated behaviour (e. g. linearly increasing shear strength with depth), with intervals showing deviations from this trend between 20 and 125 cm below sea floor. The deviations can be directly correlated with lithologic changes, such as event deposits of ice-rafted debris and mud clasts (cf., Chapter 3.5), and therefore do not represent past erosional or seabed loading events. From 125 cm to the base of the core at 720 cm below sea floor the shear strength values show a rather

constant downward increase of about 0.5 kPa/m and wet bulk density variations of decreased amplitude. This pattern reflects the rather homogeneous and fine-grained character of the sediments.

The cyclic alternation of yellowish brown (10YR5/4) and dark yellowish brown (10YR4/3) sediment units (cf. core description) seen throughout the core was documented also by colour reflectance measurements. A grey scale record produced (Fig. 16) shows the cyclic character, but reveals also a change in grey scale and cyclic amplitude at about 350 cm below sea floor. This change apparently is not documented by the shear strength and wet bulk density records, but coincides with changes in magnetic susceptibility and IRD content (cf., Figs. 14 and 21, respectively). More investigations are needed to explain the relationship between colour variation and other lithological and physical properties in more detail.

Physical property records of sediment core PS 51/038-4 from the Alpha Ridge correspond to records of sediment core PS 2185-6 from the Lomonosov Ridge at 1052 m water depth (Fütterer, 1992). The high-amplitude physical property pattern observed within the uppermost 125 cm of sediment core PS 51/038-4 correlates well with the pattern observed within the upper 300 cm of sediment core PS 2185-6 from the Lomonosov Ridge (Fig. 17). According to Spielhagen et al. (1997) the Brunhes/Matuyama boundary is at 342 cm below sea floor in the Lomonosov Ridge core. This age correlation also correlates well with the lithostratigraphy (cf., Fig. 22). Thus, sediment accumulation rates during the Late Quaternary seem to have been almost 3 times lower on the Alpha Ridge in comparison to the Lomonosov Ridge.

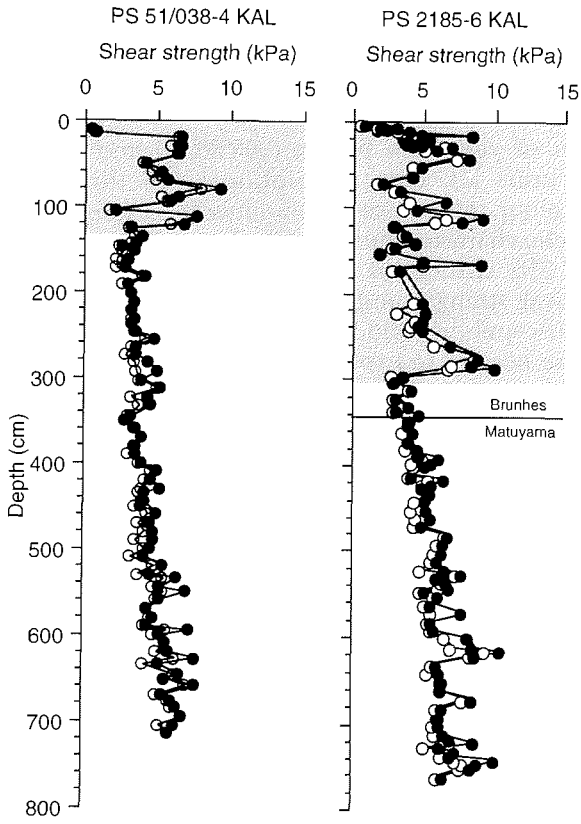

Fig. 17: Shear strength distribution of Alpha Ridge Core PS 51/038-4 and Lomonosov Ridge Core PS 2185-6. Open/solid circles indicate minimum/maximum values. Remarkable is the similarity of both records. Sediment units of different thickness in these two cores are showing comparable shear strength pattern.

3.4. Biostratigraphy
(J. Mutterlose and J. Matthiessen)

3.4.1 Material and methods

A total of 127 samples were studied with respect to their micropalaeontological contents. The samples are derived from the following sediment cores: PS51/028 MUC, PS51/029-1 GKG, PS51/030-1 SL, PS51/032-1 SL, PS51/033-1 SL, PS51/034-4 SL, PS51/038-3 GKG, PS51/038-4 KAL, PS51/040-1 SL, PS51/041-1 SL, PS51/067-1 SL and PS51/067-2 SL. For location of the sections compare Table 12.

Tab. 12: List of samples studied for calcareous nannofossils. 1 samples = total of samples studied for each section, 2 nannos " samples yielding calcareous nannfossils, 3 depth = interval from which nannofossils were recovered.

station	1) samples	2) nannos	3) depth
28 - MUC	15	3	22 - 25cm
29-1 GKG	5	3	5 - 30cm
30-1 SL	27	10	30 - 235cm
32-1 SL	3	0	
33-1 SL	6	2	130 - 230cm
34-4 Sl	18	2	39 - 77cm
38-3 GKG	5	0	
38-4 KAL	33	4	51 - 151cm
40-1 SL	2	0	
41-1 SL	1	0	
67-1 SL	11	1	40cm
67-2 SL	7	0	

Simple smear-slide preparations were examined under the light microscope using a magnification of 1.500 x. Norland Optical Adhesive was used to attach the cover glasses to the microscope slide. The abundance of microfossils in the material recovered in general is low. Microfossils constitute less than 1 % of the rock, most of the smear slide were made up by quartz, feldspar and mica. One sample (67-2, CC) was disaggregated in hot water and washed over a 63 µm sieve in order to gain foraminifera. However, this sample is barren.

In addition 20 samples were disaggregated and washed over a 21 µm sieve for palynological analyses. Samples, smear slides and residues are housed at the AWI in Bremerhaven.

3.4.2 Results

Calcareous nannofossils

None of the samples studied yield rich and/or abundant assemblages of calcareous nannofossils. Most of the samples are barren, only 25 of 127 samples contain nannofossils of low diversity. All of the taxa encountered are of Quaternary age: *Gephyrocapsa oceanica, Emiliania huxleyi.* The preservation of *Gephyrocapsa* is quite good, in most specimens the oblique bridge is still preserved. More solid coccoliths were observed as well. These, however, can not be assigned to a specific

genus due to fragmentary preservation. Abundance is low as well, coccoliths are extremely rare. In those samples where coccoliths were observed, abundances may be estimated as 1 specimen per 10 fields of view.

Based on the occurrence of *Gephyrocapsa oceanica* the nannofossil bearing strata can be assigned to the nannofossil zones NN 19 - 12 of Martini (1971). Only cores 28 - 1, 24 - 25 cm and 67 - 1, 40 cm yielded definitive specimens of *Emiliania huxleyi*. These samples have latest Pleistocene age and correlate to NN 21.

Foraminifera
Rare planktonic foraminifera have been observed, they are, however less common than calcareous nannofossils.

Palynomorphs
Only few samples from near-surface sediments washed over 21 µm sieve contained palynomorphs, whereas the smear slides proved to be barren. The low palynomorph recovery may be caused by the strong dilution of residues with coarse silt particles. Processing with hydrofluoric acid is required to further enrich the organic matter. The dark brown silty clays from near-surface sediments contained relatively abundant dinoflagellate cysts, consisting of a monospecific assemblage of *Algidasphaeridium? minutum*. This species is characteristic of relatively low saline cold waters of the high northern latitudes and is in particular common in Holocene sediments.

3.5 Lithostratigraphy
(R. Stein, N. Kukina, J. Matthiessen, C. Müller, N. Nörgaard-Petersen and R. Usbeck)

Six long sediment cores with a recovery between 4.5 to 7.2 meters (Fig. 13) were obtained along the northern flank of the western Alpha Ridge (Fig. 11: Cores PS51/030-1, PS51/032-1, PS51/033-1, PS51/034-4, PS51/038-4, PS51/047-4). At the steep slope of a graben-like structure in the westernmost part of the Alpha Ridge, a gravity corer equipped with a short core barrel segment of five meters was used to get pre-Quaternary sediments/basaltic basement. The recovery of these cores PS51/040-1 to PS51/045-1 range between zero and 1.7 meters (Figs. 11 and 13). At the Lomonosov Ridge four sediment cores PS51/058-3, PS51/065-1, PS51/067-1 and PS51/067-2 with lengths between 1 and 6 meters were recovered (Figs. 11 and 13). The lithostratigraphy described below is mainly based on the lithological core description (see Appendix) and smear slide estimates as well as MSCL data.

Alpha Ridge
The predominent lithology of the Alpha Ridge sediment cores is silty clay of brown, light to dark yellowish brown, and light olive brown colours. In the upper about 0.5 to 1.4 m of the cores, more sandy intervals and mud clasts occur. The most prominent features of all cores are colour cycles of light olive brown and brownish

yellow/yellowish brown sediments occurring down to the bottom of the cores. These distinct colour cycles seem not to be related neither to changes of grain-size or composition. Most of the sediments are slightly to moderately bioturbated. The main sedimentary components are quartz, feldspar and mica. In few layers detrital carbonates are enriched. Biogenic components are always rare contributing less than 1 % to the components. Near-surface sediments which usually are dark brown silty clays contain slightly higher amounts of microfossils including planktic and benthic foraminifera, fragments of radiolarian and diatoms. Rare sponge spicules were observed.

For the cores PS51/034-4 and PS51/038-4 (including GKG PS51/038-3) a more detailed study of the composition of the sediments were performed, using smear-slide analysis (Figs. 18 to 20; Table 13 to 15) and IRD counts (Fig. 21). Based on smear-slide estimates, terrigenous (mineral) particles are predominent, with the only exception of two samples from Core PS51/038-4 where very high amounts of biogenic carbonate occur at 79 and 248 cmbsf (Fig. 20 a; Table 15). In general, the sediments consist of 30 to 60 % quartz as the most dominent compound. Feldspars and mica, reaching up to 25 % each, are the next important compounds. Occasionally, terrigenous carbonate (i. e., calcite and dolomite) may reach values of 10 - 20 %. Heavy minerals occur in very variable amounts (1 - 30 %; Tables 13. - 15). In the heavy mineral fraction, amphiboles and pyroxenes are the dominent components (Figs. 18 b - 20 b; Tables 13 - 15) as already described by other authors for sediments cores from the Alpha Ridge (Darby et al., 1989 and further references therein). Both amphiboles and pyroxenes display high-amplitude variations between about 10 - 80 % and 10 - 60 %, respectively, and are generally anticorrelated (Figs. 18 b and 20 b). At Core PS51/034-4, maximum amounts of amphiboles were counted in the intervals between 5 and 50 cmbsf and below 340 cmbsf (Fig. 18 b). At Core PS51/038-4, the amphibole maxima occur between about 20 and 90 cmbsf, 160 and 200 cmbsf and below 550 cmbsf (Fig. 20 b). This suggests changes in terrigenous sediment supply from different source areas. Fe-Mn nodules occur in significant amounts in the sediments from Core PS51/038-4 at depth intervals of about 100 - 150 cmbsf, 250 cmbsf, and 530 - 630 cmbsf (Fig. 20 b).

According to the counts of IRD in X-radiographs, distinct variations in the supply of coarse-grained material by icebergs is suggested. There is a general trend towards higher IRD values in the upper part of the sedimentary sequences of cores PS51/030-1, PS51/034-4, and PS51/038-4 (Fig. 21). Based on a first rough stratigraphic framework (see below), increases in IRD input probably occur at about 1.6 Ma and 1.2 Ma.

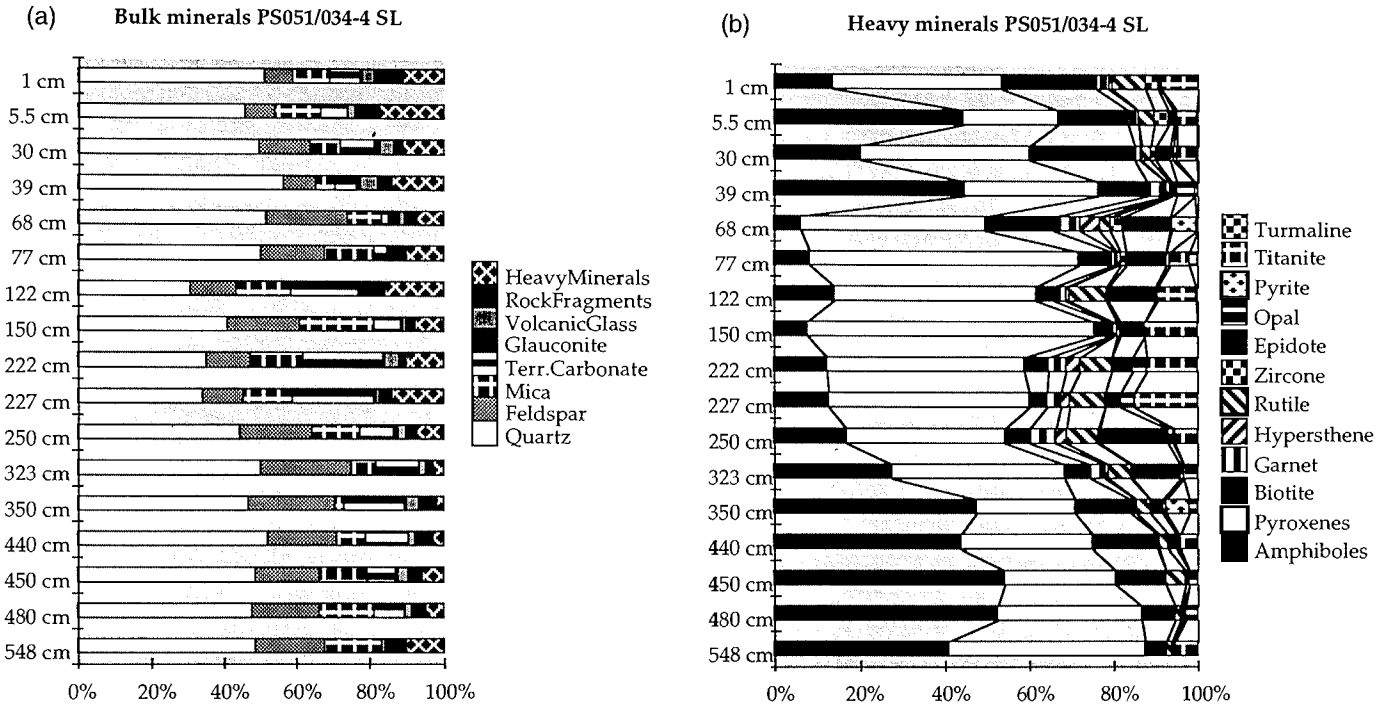

Fig. 18: Bulk (a) and heavy (b) mineralogy of sediments from gravity core (GKG) PS51/034-4, based on smear-slide counts.

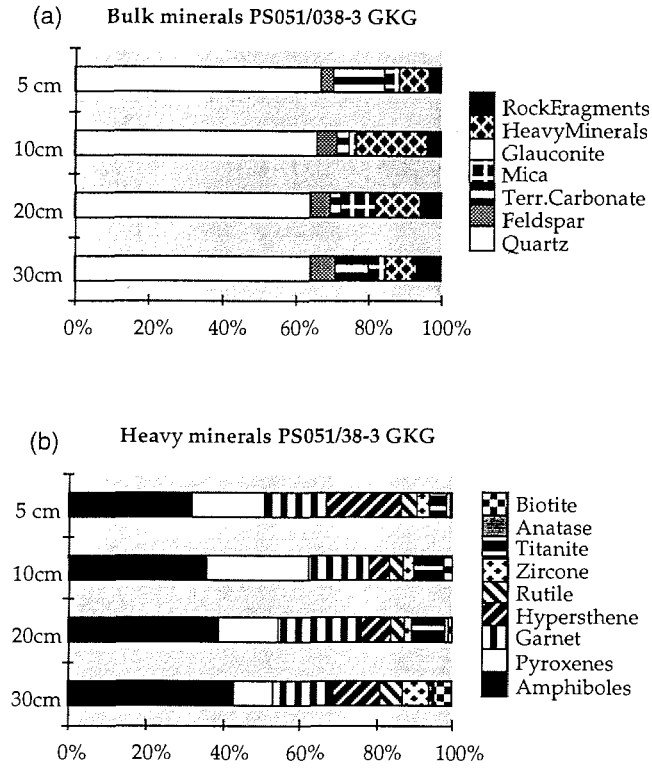

Fig. 19: Bulk (a) and heavy (b) mineralogy of sediments from giant box core (GKG) PS51/038-3, based on smear-slide counts.

In order to discuss the new records obtained during the Cruise ARK-XIV/1a in context with other sedimentary records already available from the Alpha Ridge area and to get a rough stratigraphic framework, the lithology of cores PS51/034-4, PS51/030-1 and PS51/038-4 are related to the "Standard Arctic Lithological Units" and the paleomagnetostratigraphy published by Clark et al. (1980), Jackson et al. (1985), Mudie and Blasco (1985), Jones (1987), and Darby et al. (1989) (Fig. 22). Based on this correlation, the upper standard units F to M can be identified in the sedimentary sequences of the three cores. At Core PS51/034-4, the Brunhes/Matuyama boundary and the base of the Jaramillo Event are probably at about 0.75 and 1 mbsf, respectively. The resulting sedimentation rates are about 1 1.2 mm/ky in the upper part (i. e., units H to M) and about 2 mm/ky in the underlying interval (units G and F). This agrees well with similar estimates of sedimentation rates by Darby et al. (1989) from this area. Using the sedimentation rate of 2 mm/ky, the extrapolated age of the base of Core PS51/034-4 is about 3.5 Ma. At cores PS51/030-1 and PS51/038-4, the sedimentation rates appears to by higher by a factor of 2 - 3 in comparison to Core PS51/034-4 (Fig. 22).

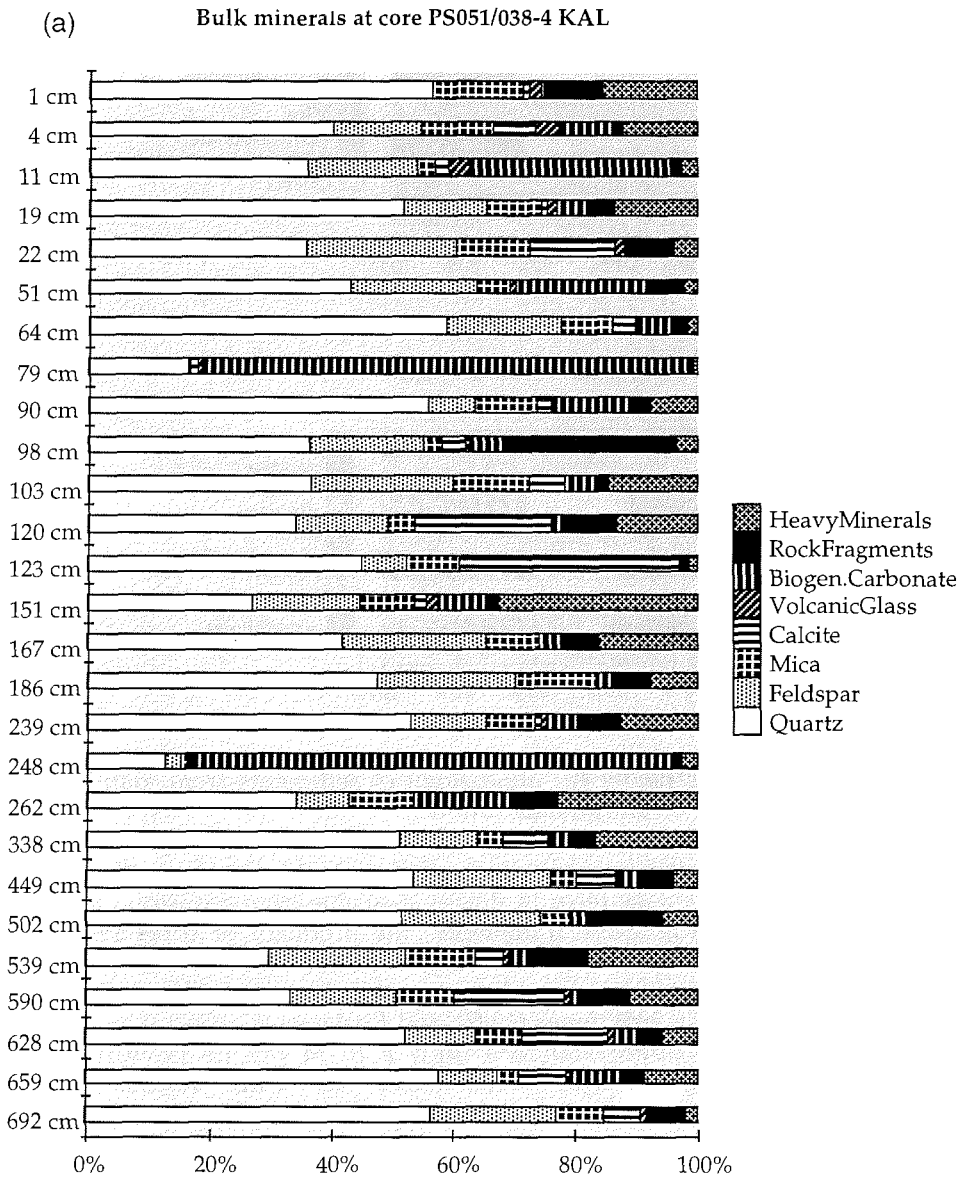

Fig. 20 a: Bulk (a) and heavy (b) mineralogy of sediments from kastenlot core PS51/038-4, based on smear-slide counts.

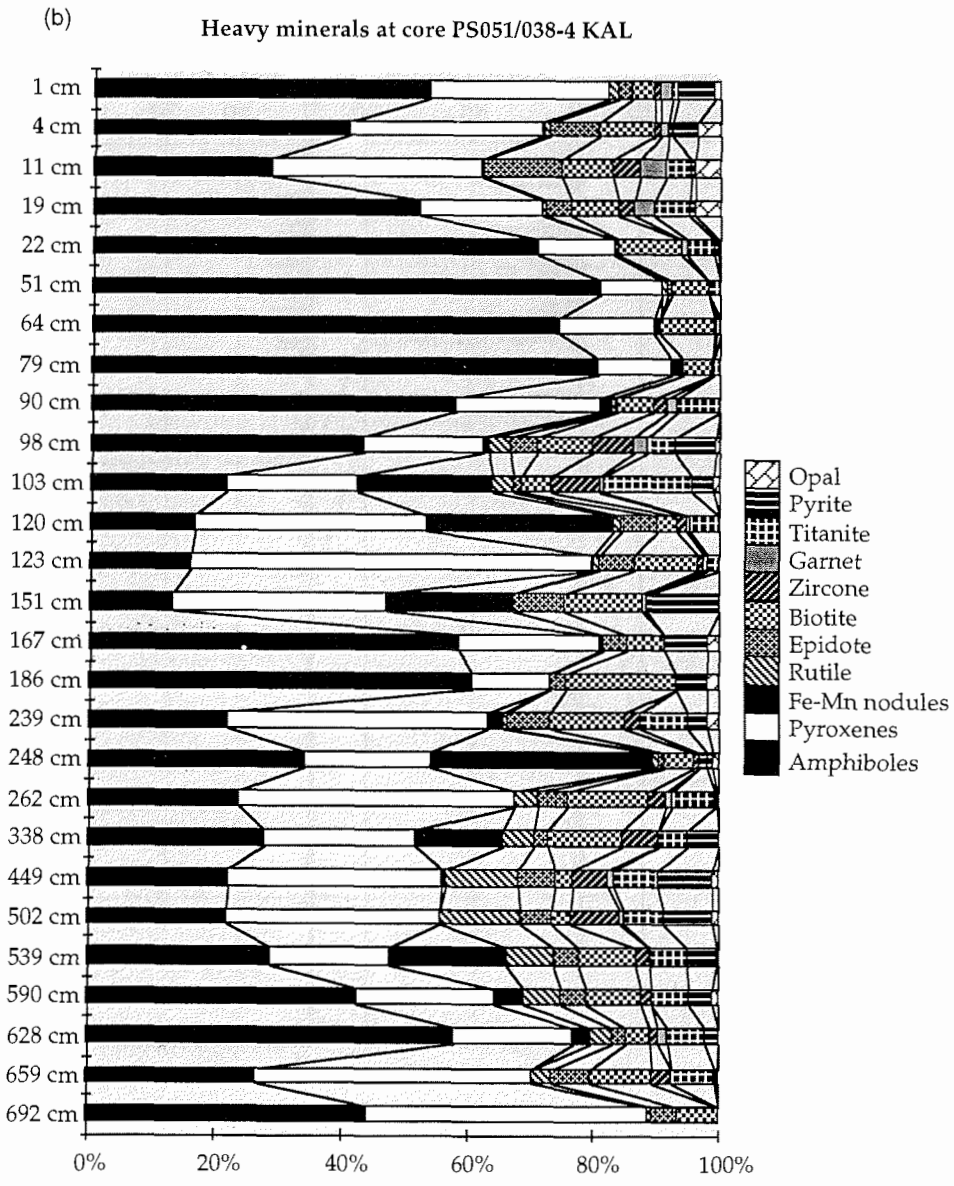

Fig. 20 b: Bulk (a) and heavy (b) mineralogy of sediments from kastenlot core PS51/038-4, based on smear-slide counts.

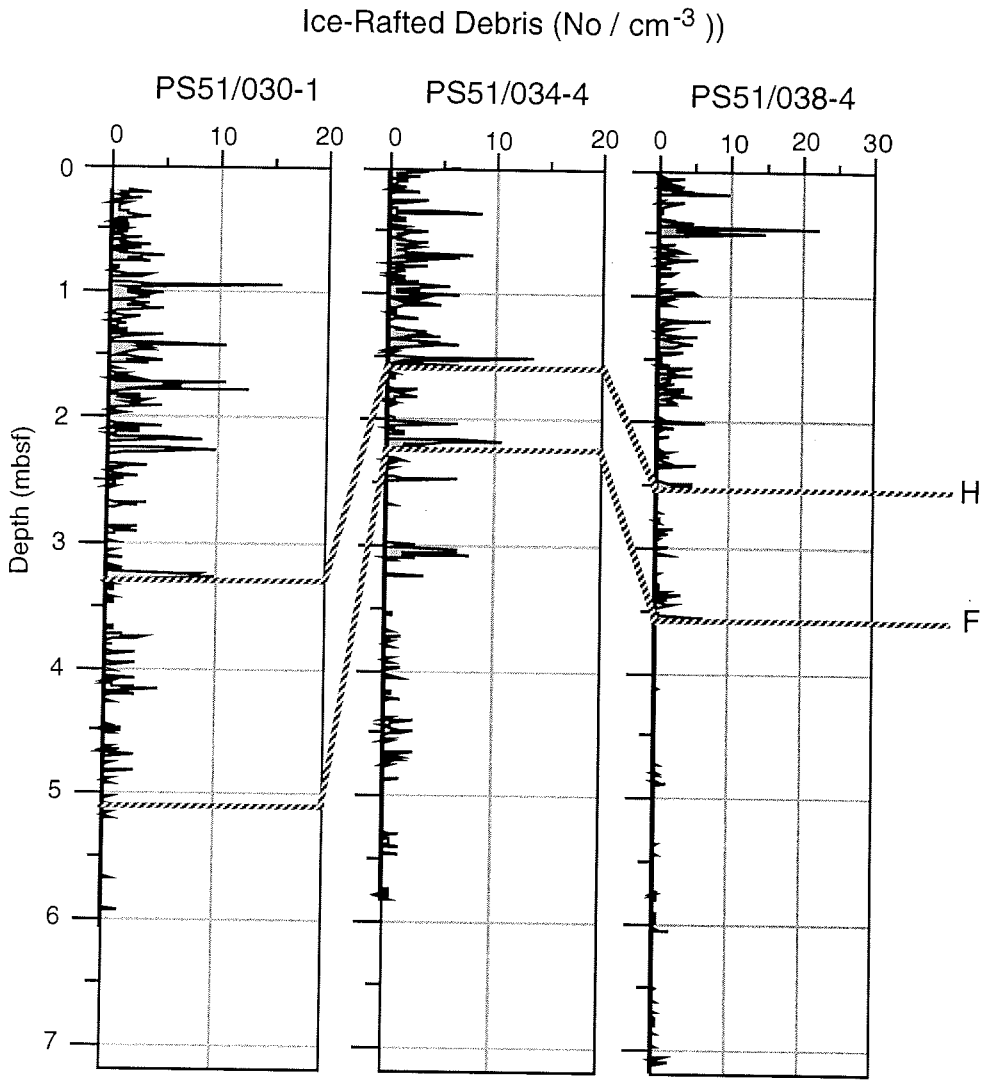

Fig. 21: Content of ice-rafted debris > 2 mm, counted in X-radiographs and expressed as numbers per 10 cm^{-3}. Correlation lines are based on magnetic susceptibility and lithology records and indicate the basis of Standard Arctic Lithological Units H and F with an estimated age of 1.25 Ma and 1.6 Ma, respectively (cf. Fig. 22)

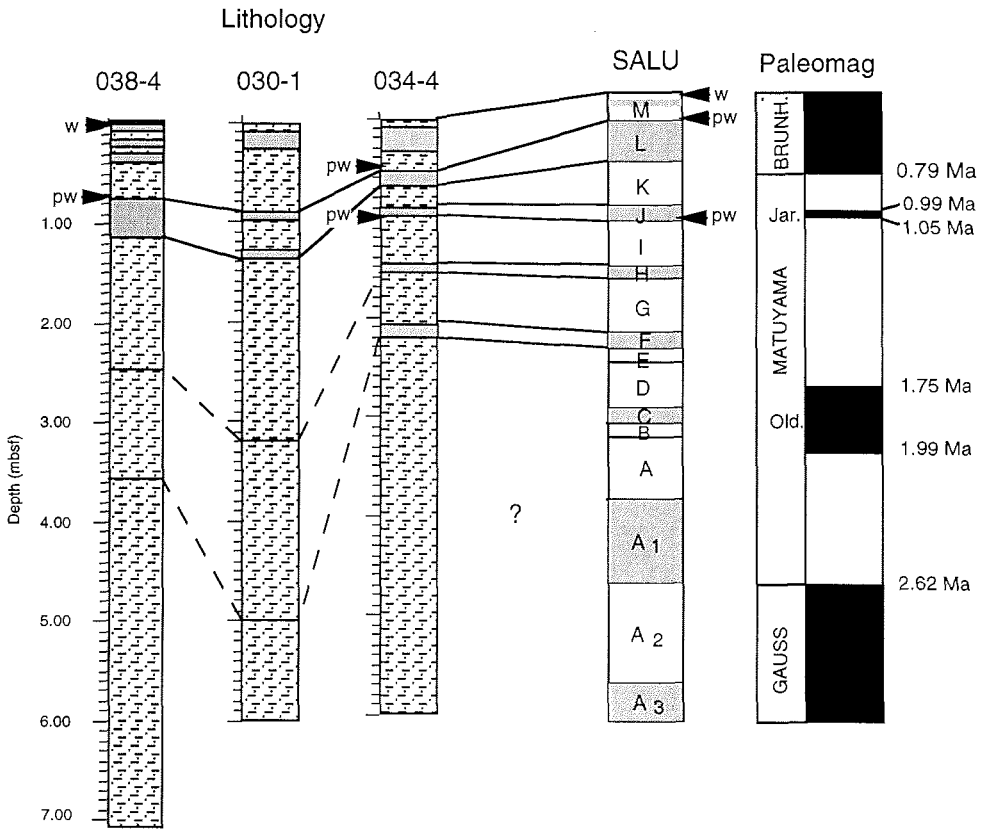

Fig. 22: Lithostratigraphy of cores PS51/030-1, PS51/034-4 and PS51/038-4, based on the lithological core description. Gray intervals in the lithology column indicate more sandy and mud clast intervals. The lithology columns are correlated with the Standard Arctic Lithological Units (SALU) and the paleomagnetostratigraphy (Clark et al., 1980; Mudie and Blasco, 1985; Jones, 1987; Darby et al., 1989); paleomagnetic time scale according to Cande and Kent (1992). Units A3, A2, C, F, H, J, L, and parts of M are more sandy intervals. "w" and "pw" indicate white and pink-white layers which can be used for core correlation. The stippled correlation lines are based on the magnetic susceptibility records.

Tab. 13: Bulk (a) and heavy (b) mineralogy of sediments from Core PS51/034-4, based on smear-slide estimates.

(a)

PS051/034-4 SL	548 cm	480 cm	450 cm	440 cm	350 cm	323 cm	250 cm	227 cm	222 cm	150 cm	122 cm	77 cm	68 cm	39 cm	30 cm	5.5 cm	1 cm
Quartz	48.9	47.9	48.6	52.1	46.8	50.4	44.6	34.2	35.2	41.1	30.6	50.1	51.6	56.3	49.8	45.8	51
Feldspar	18.8	18.5	17.9	18.9	23.8	24.8	19.8	11.2	12.2	19.8	12.6	17.6	22.3	8.9	13.8	8.3	7.9
Mica	15.5	14.9	12.8	7.8	2.4	6.8	12.8	13.4	14.6	20.3	15.2	13.8	9.4	5.3	8.6	12.5	10.3
Glauconite	0	0	0.2	0.1	0.1	0.3	0.6	0.4	0.2	0.5	3.7	2.1	2.8	0.8	1.5	0	0.3
Volcanic Glass	1.2	1.8	2.9	1.8	3.7	1.8	2.7	1.2	4.3	0.9	0.3	0.9	1.8	5.2	3.8	1.7	3.4
Terr. Carbon.	7,6	8.5	7.9	11.7	16.8	11.3	9.6	22.5	21.8	7.3	18.6	3.3	1.9	5.9	9.3	7.5	8.4
Rock Fragm.	5.8	3.7	4.3	4.8	4.5	1.9	2.6	3.4	1.7	2.4	3.4	2.1	2.9	3.9	2.3	6.9	7.8
Heavy Minerals	9.8	4.7	5.4	2.8	1.9	2.7	7.3	13.7	10	7.7	15.6	10.1	7.3	13.7	10.9	17.3	10.9

(b)

PS051/034-4 SL	548 cm	480 cm	450 cm	440 cm	350 cm	323 cm	250 cm	227 cm	222 cm	150 cm	122 cm	77 cm	68 cm	39 cm	30 cm	5.5 cm	1 cm
Amphiboles	41	52.8	54.4	43.7	47.6	27.8	16.7	12.7	12.4	7.6	14.1	8.2	5.9	44.9	20.1	44.4	13.5
Garnet	0	0	0	0.4	1.2	3.2	6.4	3.3	4.2	0.3	2.7	0.9	6.1	4.7	1.4	2.4	2.9
Hypersthene	0	0	0	0.2	0	0.9	2.5	2.1	3.1	0.4	0.9	0.2	4.6	0.2	0.2	0.2	0.9
Rutile	1.3	1.3	4.2	2.2	3.3	5.4	7.4	8.2	7.8	0.9	8.8	0.9	2.3	0.7	2.1	3.8	7.8
Zircone	0	0.2	0	0.1	0	0.5	0.3	0	0	0.8	0.3	1.3	3.1	0.4	1.3	3.2	2.8
Titanite	5.3	3.1	2.1	4.1	2.1	3.2	5.4	15.2	12.1	12.7	9.2	4.3	0.4	0.6	4.2	4.5	8.9
Pyroxenes	46.6	33.7	26.2	31.2	23.4	40.7	37.5	47.5	46.6	67.8	47.7	63.3	44	31.5	40.2	22.3	39.8
Biotite	4.8	8.1	12.1	15.3	13.2	6.1	5.8	4.2	5.7	3.9	4.1	8.3	16.2	11.4	24.7	16.6	22.6
Epidote	0.8	0.7	0.9	2.1	3.1	11.2	16.5	3.5	4.8	5.6	11.5	9.6	11.3	1.2	3.3	1.1	0.8
Turmaline	0	0	0	0	0	0.1	0.2	0	0	0	0.3	2.2	0	0.1	0.6	0.6	0
Opaque	0.2	0.1	0.1	0.1	0.9	0.9	1.1	3.3	3.3	0	0.1	0	0.2	4.1	0.7	0.4	0
Pyrite	0	0	0	0.6	5.2	0	0.2	0	0	0	0.3	0.8	5.9	0.2	1.2	0.5	0

Tab. 14: Bulk (a) and heavy (b) mineralogy of sediments from Core PS51/038-3, based on smear-slide estimates.

(a)

PS051/38-3 GKG	30 cm	20 cm	10 cm	5 cm
Quartz	64.1	64.2	65.8	67.1
Feldspar	6.8	5.3	5.4	3.1
Mica	4.6	9.7	1.8	4
Glauconite	0	0.1	0.1	0.2
Terr. Carbonate	9.2	2.7	3.6	14.3
Rock Fragments	6.7	5.7	3.8	3.2
Heavy Minerals	8.6	12.3	19.5	8.1

(b)

PS051/38-3 GKG	30 cm	20 cm	10 cm	5 cm
Amphiboles	42.8	38.8	35.4	31.6
Garnet	15.9	21.7	15.6	16.2
Hypersthene	12.4	7.4	5.4	19.6
Rutile	5.7	3.7	3.6	3.9
Zircone	7.2	2.2	2.8	3.2
Titanite	0.8	8.6	7.7	4.7
Anatase	0.2	0.8	1,1	1.2
Pyroxenes	10	15.6	26.8	19.1
Biotite	5	1.2	2.7	0.5

Tab. 15 a: Bulk (a) and heavy (b) mineralogy of sediments from Core PS51/038-4, based on smear-slide estimates.

(a)

PS051/038-4 KAL	692 cm	659 cm	628 cm	590 cm	539 cm	502 cm	449 cm	338 cm	262 cm	248 cm	239 cm	186 cm	167 cm	151 cm
Quartz	56.7	57.8	52.2	33.1	29.5	51.8	53.4	51.2	34.1	12.6	52.9	47.5	41.6	26.9
Feldspar	20.3	9.4	11.7	17.6	22.8	22.8	22.6	12.9	8.9	2.5	12.7	22.8	23.8	17.6
Mica	7.8	3.8	7.9	9.8	11.7	4.7	4.6	4.1	10.6	0.9	7.8	13.3	8.7	8.8
Calcite	5.9	7.8	13.9	17.9	4.6	5,3	6.2	7.6	0	0.3	0.9	0	0	2.2
Volcanic Glass	0.9	0.8	0.6	0.8	0.8	0.4	0.2	0.3	0.1	0.6	1.3	0.3	0	1.9
Biogen Carbonate	0.6	7.9	4.5	1.9	2.9	2.5	3.3	3.8	16.7	79.8	4.8	2.9	3.9	8.8
Rock Fragments	5.9	3.9	3.3	7.9	9.8	11.9	5.9	3.6	6.9	0.7	6.9	5.3	5.9	1.2
Heavy Minerals	1.9	8.6	5.9	11	17.9	5.9	3.8	16.5	22.7	2.6	12.7	7.9	16.1	32.6

123 cm	120 cm	103 cm	98 cm	90 cm	79 cm	64 cm	51 cm	22 cm	19 cm	11 cm	4 cm	1 cm
44.9	33.9	36.6	36.1	55.8	16.2	58.9	42.9	35.5	51.7	35.9	39.9	56.7
7.4	15.2	23.3	18.8	7.5	0.3	19	21.1	25.1	13.8	17.9	14.7	17,7
8.6	4.6	12.6	3.1	10.6	0.2	8.2	5.4	11.8	9	3.1	11.9	14.8
36.1	22.5	5.7	3.9	2.2	0.9	3.7	0.1	13.9	0.9	2.1	6.9	1.1
0	0	0.2	0.9	0	0.7	0	0.8	1.7	1.7	3.5	3.9	2.1
0.9	1.8	4.9	5.7	12.9	80.1	6.8	21.7	0.2	5.3	33.1	9.7	0.7
0.9	8.9	2.2	27.9	3.3	0.8	1.6	5.9	7.9	3.9	1.8	0.9	8.9
1.2	13.1	14.5	3.6	7.7	0.8	1.8	2.1	3.9	13.7	2.6	12.1	15.7

Tab. 15 b: Bulk (a) and heavy (b) mineralogy of sediments from Core PS51/038-4, based on smear-slide estimates.

(b)

PS051/038-4 KAL	692 cm	659 cm	628 cm	590 cm	539 cm	502 cm	449 cm	338 cm	262 cm	248 cm	239 cm	186 cm	167 cm	151 cm
Amphiboles	43.9	26.4	57.9	42.5	28.7	21.7	22.2	27.8	23.7	33.9	21.8	60.6	58.3	13
Garnet	0	0.1	1.8	0	0	0.4	0.8	0	0.9	0	0.1	0	0	0.3
Fe-Mn nodules	0	0	3.2	4.8	18.9	0.1	0.3	13.9	0	35.6	2.5	0.1	0.3	20
Rutile	0.8	3.1	3.3	5.8	7.3	12.8	11.8	4.9	3.7	0.9	0.7	0	0	0.4
Zircone	0	2.9	1	1.8	2.1	8	5.7	5.8	2.9	0.9	2.4	0	0	0.1
Titanite	0	6.9	5.8	5.7	6	6.5	6.8	4.6	6.9	0.9	7.7	0	0	0
Pyroxenes	44.7	43.8	18.7	21.9	18.7	33.8	33.8	23.9	43.8	20	41.3	12.5	22.7	33.9
Biotite	6.7	9.7	3.8	8.8	9.1	3.1	2.8	11.9	12.8	4.8	11.8	17.8	5.9	12.5
Epidote	3.9	6.5	2.1	3.9	4.1	4.9	5.9	2.2	4.7	0.8	6.7	2.2	3.8	7.9
Opaque	0	0.4	0.3	1	0.5	0.9	1.1	0.1	0.4	1	2.1	2	2.1	0
Pyrite	0	0.2	2.1	3.8	4.6	7.8	8.8	4.9	0.2	1.2	2.9	4.8	6.9	11.9

123 cm	120 cm	103 cm	98 cm	90 cm	79 cm	64 cm	51 cm	22 cm	19 cm	11 cm	4 cm	1 cm
15.7	16.5	21.5	43.2	57.9	80.6	74.3	80.8	71.1	51.8	28.5	40.6	53.3
0.9	0.7	0.8	1.7	1.6	0.6	0.7	0	0.9	2.9	4.1	1.1	1.9
0.3	29.9	21.7	1.2	1.9	2.2	0.9	0	0	0	0.2	0.1	0
0.9	1.3	3.5	3.1	0.9	0	0	0.9	0	0.7	0.1	1.2	1.7
0.9	1.4	7.8	6.9	2.1	0	0.4	0	0	2.5	4.2	0.9	0.9
1.7	4.7	13.9	4.5	6.9	0.9	0	2.2	4.3	5.9	4.2	0.9	0.7
64	36.6	20.5	18.9	22.9	11.3	14.8	9.8	11.9	19.6	33.3	30.9	28.7
9.9	3.3	4.6	8.8	5.7	4.4	8.9	5.6	9.9	7.5	8.3	8.9	3.7
5.6	5.6	1.3	4.3	0.1	0	0	0.7	0.7	4.1	12.5	7.7	2.1
0	0	1.1	0.6	0	0	0	0	0.5	4.1	4.1	3.8	1.2
0.1	0	3.3	6.8	0	0	0	0	0.7	0.9	0.5	3.9	5.8

Graben in the westernmost part of the Alpha Ridge

At the steep slope of a graben-like structure in the westernmost part of the Alpha Ridge the Seismic Profile 98540 suggests that older sediment strata and/or basaltic basement are cropping out (Fig. 23). Thus, a coring program was carried out to try getting pre-Quaternary sediments/basaltic basement. In four of the cores (PS51/040-1, PS041-1, PS51/042-1 and PS51/043-1; cf., Fig. 11), pieces of basalts were recovered. From these cores, only Core PS51/040-1 was opened and described yet. In this core, a large piece of basalt (7 cm in diameter) was found at 160 - 166 cmbsf; the core catcher contains further pieces of basalt. The overlying sediments are dark brown, light olive brown to yellowish brown silty clays with some amounts of sand and mud clasts in the uppermost part (Fig. 23), i. e., very similar to those recovered in cores PS51/30-1 to PS51/038-4 (see above). Thus, the age of the sediments is probably Quaternary and a major hiatus should occur between basalts and overlying sediments. Further more detailed investigations of the basalts as well as the sediments of the up to now unopened sediment cores will hopefully allow to date the basalts and to study the Quaternary (/pre-Quaternary?) paleoenvironmental history of the Alpha-Ridge area.

Lomonosov Ridge

During the cruise track along the Lomonosov Ridge RV POLARSTERN crossed a steep, north-south striking slope at about 81° 50´N, 140° 30´E where older sediments may crop out. From this slope, gravity cores PS51/067-1 and PS51/67-2 (Fig. 11) with a length of 1 and 3.7 m, respectively, were obtained. The sedimentary sequence of the long Core PS51/067-2 can be divided into three lithological units (Fig. 24). Unit III (332 cmbsf to bottom of core) consists of dark gray, firm sandy silty clay. Unit II (209 - 332 cmbsf) is an olive to light olive brown (sandy) silty clay. The upper part of this unit is slightly bioturbated. Unit I (0 to 209 cmbsf) consists of dark brown, yellowish brown and light olive brown, partly bioturbated silty clay. A pink layer occurs at 60 cmbsf. These lithological units are similar to those of sediment cores recovered from the Lomonosov Ridge during POLARSTERN Cruise ARK-XI/1 (Stein et al., 1997). The boundary between lithological units II and I coincides with a distinct jump in the porosity and wet bulk density suggesting a hiatus at that depth (Fig. 24). The lowermost Unit III may be of Oxygen Isotope Stage 6 age, based on the correlation with the ARK-XI/1 cores (Stein et al., 1997). Whether this age correlation is correct or whether the sedimentary sequence even represents older time intervals has to be verified by further more detailed investigations.

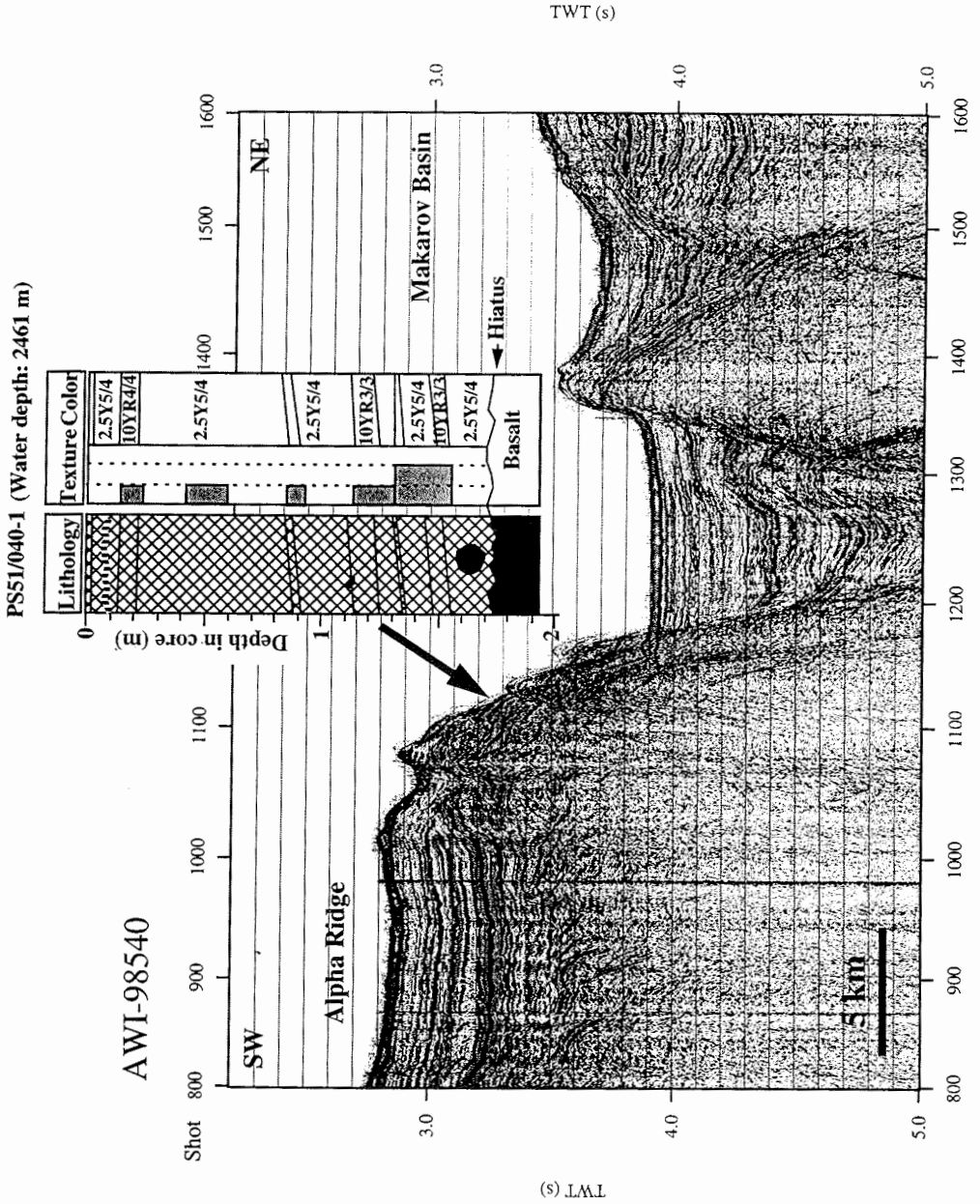

Fig. 23: Seismic profile 98540 and location and lithology of Core PS51/040-1. At 1.73 mbsf, the gravity corer stucked in the basalt.

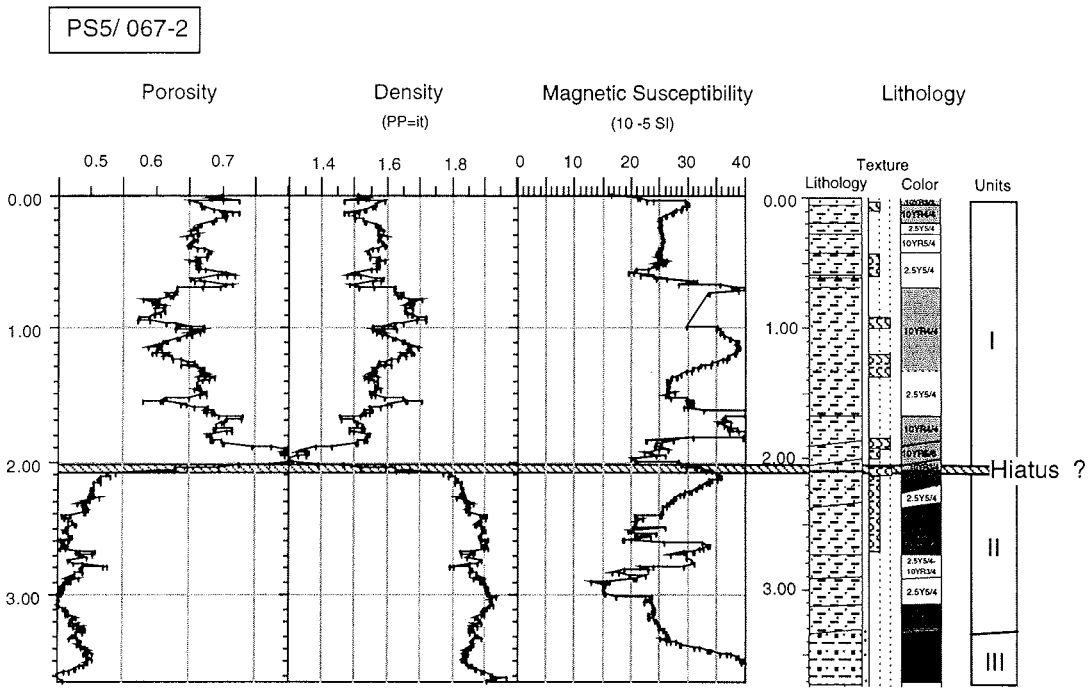

Fig. 24: Lithology and porotiy, wet wulk density, and magnetic susceptibility records from Lomonosov Ridge Core PS51/067-2. Roman numbers indicate lithological units.

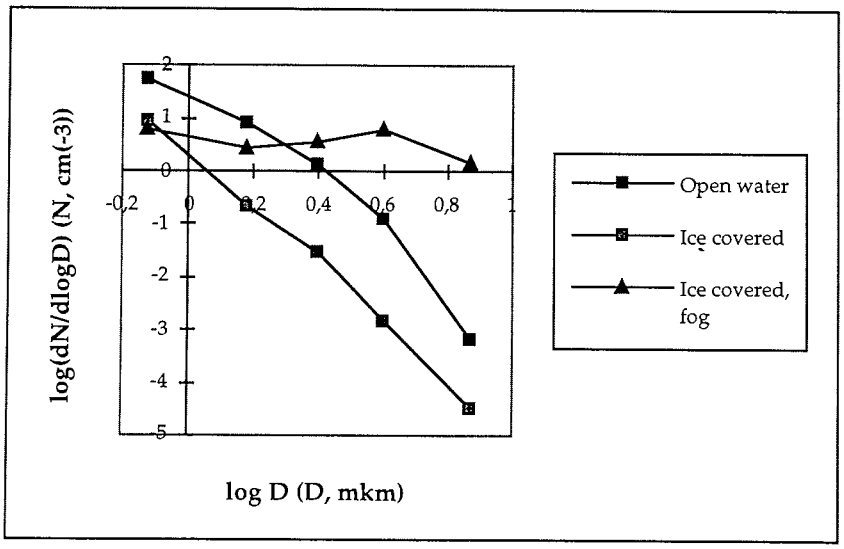

Fig. 25: Typical aerosol particle size distribution in the study area. Series: 1 - over the open water; 2 - over the ice covered sea; 3 - over the ice covered sea during fog condition.

3.6 Aerosols
(V. Shevchenko)

Numerous studies have shown that aerosols in the Arctic are of importance for atmospheric chemistry and climate (Barrie, 1986). But up to now aerosols in the marine boundary layer in the high Arctic have been studied little. Here, preliminary results of the studies of aerosol size distribution over the NW Barents Sea and the Central Arctic are presented. During the ARK-XIV-1a Expedition 183 measurements of aerosol size spectra at 61 sites and 14 measurements by DAES-3 were carried out (Tables 7 and 8). In general, there is a much greater number of small particles (with sizes from 0.5 μm to 2 μm) in comparison to large particles, as it is described elsewhere (O'Dowd et al., 1997). The observed particle size spectra are on whole conservative to changes of temperature, relative humidity, wind velocity and direction. In ice-covered areas we find much lower concentrations of particles from all size classes (Fig. 25). This could testify the input of sea salt particles from the sea surface microlayer by wind and the importance of these particles for the chemical composition of marine aerosols, as it has been shown in other regions (O'Dowd et al., 1997). We shall see the input of wind blown sea salt after the elemental analysis of aerosol samples in home laboratory. During a fog formation concentration of large particles (from 3 to 5 mm) sharply increased as it has been found in the Laptev Sea (Smirnov et al., 1997). A more detailed study of the parameters of aerosol size distribution and controlling factors will be carried out later in comparison with other areas.

4 Bathymetric measurements
(N. Tsoukalas, C. Roedle, G. Schwab)

4.1 Introduction

The morphology of the Alpha Mendeleev Ridge in the Amerasian Basin, is little known, since no bathymetric charts of sufficient detail exist. The expedition ARK XIV/1a provided an opportunity to obtain new bathymetric data and to densify the existing depth information. These bathymetric data may be used for morphologic interpretation. They are also valuable for planning and conducting detailed geological and geophysical studies in this region. The HYDROSWEEP multibeam sonar system was used for the collection of these data.

4.2 Survey instrumentation

The HYDROSWEEP DS 2 system is permanentely installed on board RV POLARSTERN. The transducers are flush mounted in the ship´s hull. It uses a transmitting frequency of 15.5 kHz. This frequency was chosen as a compromise between depth range and resolution. The operating principle is to transmit a signal from the transducers and measure the two way travel time of this signal to 59 locations in a narrow swath perpendicular to the ship's axis on the seafloor. Simultaneously, a time series of the envelope of the returned signal is stored, which is used to construct synthetic side scan sonar imagery data (S. Dijkstra, et. al. 1998). HYDROSWEEP uses a self-calibration process to determine the local mean sound velocity. This is necessary for the conversion of travel times to a model of the path traversed by the signals through the water column. Upon start-up the DS-2 searches for the seafloor, when this is found the system switches over to the so-called survey mode. Raw data was stored on DAT tapes at ten minute intervals by the HYDROSWEEP DS-2 system itself.

4.3 System operation

HYDROSWEEP was used with a 90° coverage angle, generating a swath width of approximately twice the water depth. Due to heavy ice conditions it was not possible to derive the local mean sound speed using the system´s self calibration mechanism. Instead we used information obtained by CTD measurements during geological and oceanographic stations.

4.4 Navigation

POLARSTERN uses the Global Positioning System (GPS) in on line differential mode (DGPS) to obtain position coordinates DGPS corrections are determined by installing a station at known coordinates and determining the adjustments

necessary to the range observations to arrive at the correct position solution. We received normally the differential corrections via the SkyFix system that uses the InMarSat (International Maritime Satellite) satellites. North of 87° N no differential corrections were available, because the elevation angle of the satellite above the horizon was insufficient.

4.5 System software

In November 1997, the existing HYDROSWEEP DS was updated to the DS-2 version. Included with the new DS-2 system two independent software packages, namely Hydromap online and Hydromap offline are provided. Hydromap online is designed for data acquisition, mapping and storage of hydrographic observation data. With HYDROSWEEP offline it is possible to edit the recorded data, e. g. positions. The main advantage of these software packages, which complement one another, is the consistent concept from real-time data acquisition (Hydromap online) through to post-processing (Hydromap offline).

4.6 Data collection

HYDROSWEEP data acquisition started at position 74°10' N, 30°10' E on July 3rd, 1998 at 00:25 .Universal Time Coordinated (UTC). From July 3rd, 1998 15:15 UTC until July 5th, 1998 17:15 UTC, when we were in the area where both Norway and Russia have territory claims, all data acquisition on POLARSTERN was interrupted. During the remaining period the system was running continuously.A survey of the eastern flank of the Lomonosov Ridge was performed which was mentioned in the GEBCO (General bathymetric charts of the oceans) map allusively. After completing this survey we went on with observations between 81°30' N, 140° E and 81°25' N 147° E, and headed then to the south in direction of Tiksi (Jacutia). The HYDROSWEEP measurements were stopped on July 24th, 1998, when entering the Russian EEZ.

4.7 Data processing

The post-processing of the recorded data, in which the plausibility of navigation of the observed depths is analyzed, was carried out completely on POLARSTERN. Raw data was separated in eight hour segments and transformed in the SURF (**S**ystem **U**nabhaengiges **R**ohdaten **F**ormat) format. The navigation data was then processed using Hydromap offline. It was decided to extract missing navigation data, caused by HYDROSWEEP failures, at one second intervals from POLDAT (POLarstern DATenbank). Depth editing was done using the HDCS (**H**ydrographic **D**ata **C**leaning **S**ystem). For that, SURF data had to be transformed to the HDCS format. The HDCS is part of the Hydrographic Information Processing System (HIPS) that also includes CARIS (Computer Aided Resource Information System) (Dijkstra et. al., 1998).

After finishing depth editing with HDCS the data were converted into an internal AWI data format. So-called NAK files were created (corrected navigation files). Following a brief summary of the data processing chain is given.

- conversion of raw data to SURF data (separated in eight hour sections)
- navigation editing (Hydromap offline)
- conversion of SURF to HDCS
- depth editing (HDCS)
- conversion of HDCS to *.hyd files (using hdcsToAWI) and *.nak files (using HYDROSWEEPToNak)

The NAK files were used by the geophysical work group for the location of their seismic profiles. Additionally, track plots were provided.

4.8 Survey results

In the Lomonosov Ridge area we have seen differences of over 500 m between observed depths and depth values indicated by GEBCO sheet 5.17. Additionally at 81°50' N, 140°28' E a slope of nearly 25 % was observed which is not present in the available maps. The relative depth elevation over the sector of this feature is approximately 1.100 m - 2.100 m with an extension of nearly 1.1 NM in west-east direction. (Fig. 26) At 81°49' N, 138°54' E a second minor slope was found (Fig. 26). We surveyed the specific areas in detail and geological stations with gravity cores where then taken at both locations.

4.9 Problems encountered

Due to heavy ice conditions, there were numerous system failures on route to Alpha Ridge. Often the system was not able to obtain reasonable depth values. As a solution, the system was restarted every time it did not obtain bottom returns or when unreasonable depths were given. Every new start interrupted the data flow and data storage. This caused gaps in the data records (Fig. 27).

We suspect that ice caught under the ship may have damaged the transducers. The recorded signal strength may be interpreted as evidence of damage to these devices (personal communication Helmut Muhle). An inspection of the transducers will therefore be necessary at POLARSTERN's next visit to a dry dock.

Software problems also occured, often in conjunction with heavy ice. Several times it was not possible to transform eight hour of raw data into the SURF format. This problem was solved by reducing the time span over which the data was converted,

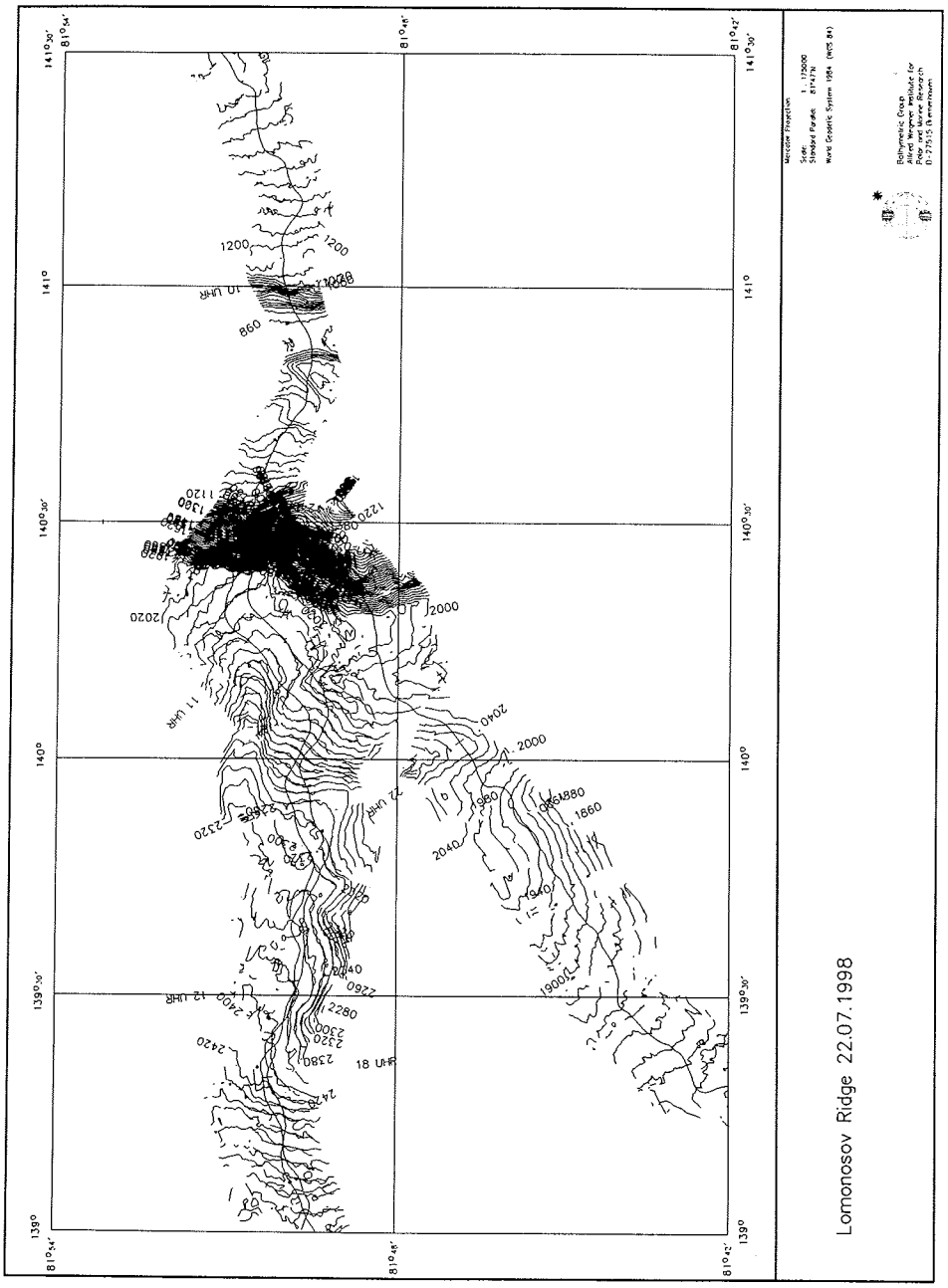

Fig. 26: Western flank of the Lomonosov Ridge close to the Laptev Sea at 81°50' N. The two topographic steps at 140°30' E and 141° E were sampled with gravity cores.

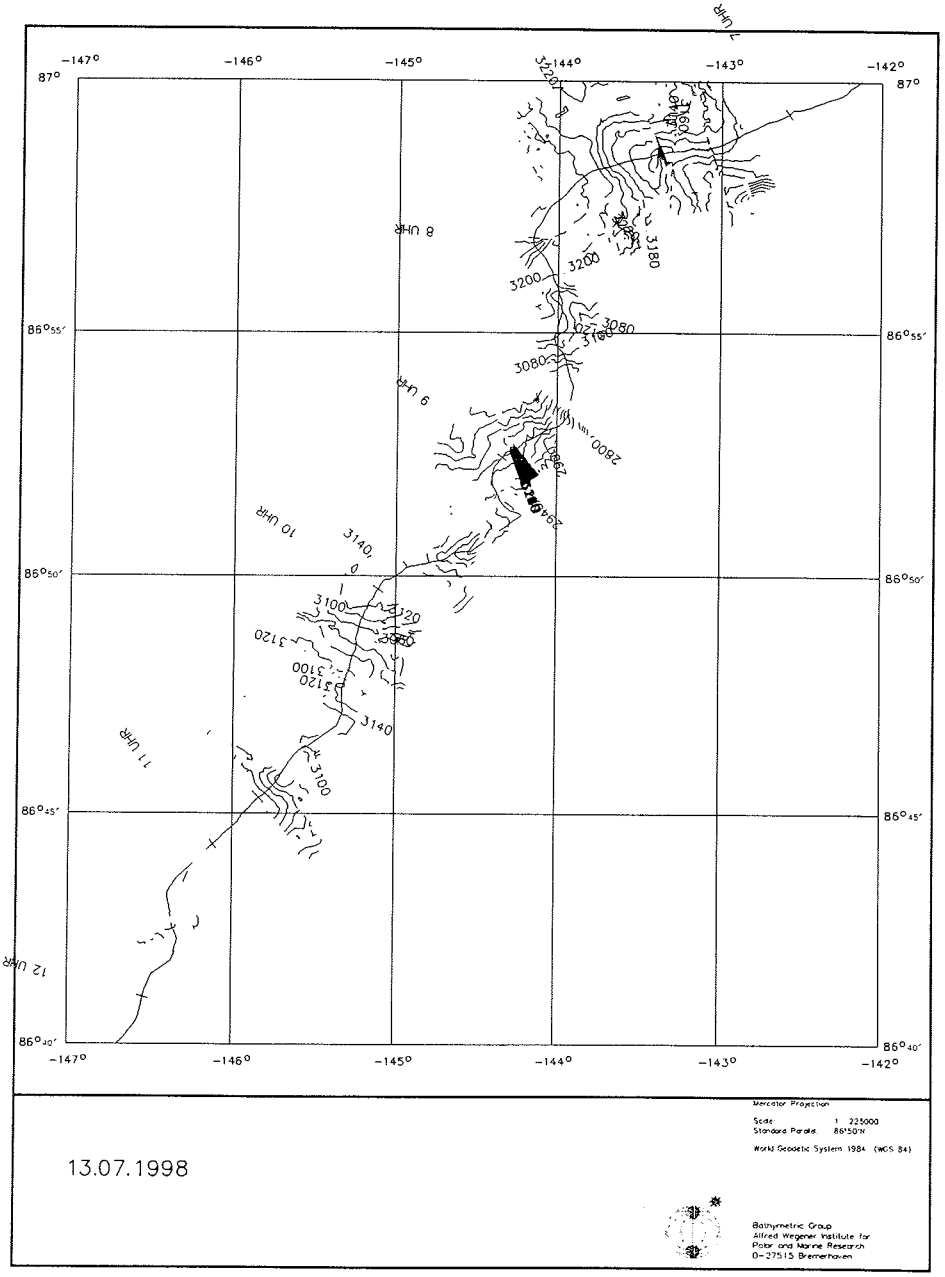

Fig. 27: Ship's bathymetry along the northern flank of the Alpha Ridge. The difficult ice conditions produced several failures of the Hydrosweep system, visible as gaps on the map.

thus, enabling us to isolate the problem. Sometimes complete system failures occured in heavy ice conditions. It was then necessary to restart the system. A system test was performed and all error messages are stored and will be analysed by the manufacturer after the expedition.

4.10 Summary

During this expedition we collected a lot of exiting data. Especially in the region of the eastern Lomonosov Ridge we were able to obtain high resolution data, which forms a large improvement on the existing data base. Although, we encountered some hard- and software problems in heavy pack ice, that need to be adressed, the overal result during this cruise was positive. Although there is space for software improvement, the new HYDROSWEEP and Sidescan system offers an improvement with respect to data handling and control of HYDROSWEEP.

We would like to express our gratitude to Helmut Muhle (POLARSTERN's electronic engineer for HYDROSWEEP), Semme Dijkstra and all the others who assisted us for their enthusiastic support during the cruise.

5 Biology: Zooplankton and macrozoobenthos. Contributions to the ecology of the deep Arctic Ocean with special reference to the Alpha-Ridge, Lomonosov-Ridge and Makarov-Basin areas

(E. Rachor, A. Golikov, B. Strohscher, T. Zöller)

The ecosystems of the ice-covered deep Arctic basins including the ridges, and especially the benthic compartments, suffer from shortage of organic matter produced in situ. Thus, many areas seem to a high degree dependent of the horizontal advection of particulate organic matter from the more productive marginal Arctic seas. The significance of such transportation processes for pelagic and benthic communities is a main target of the ongoing biological activities of AWI in the Arctic Ocean.

The ARK-XIV/1a-expedition of the German RV POLARSTERN in summer 1998 offered a unique opportunity to penetrate into such areas that have not been sufficiently explored so far and to compare the results with findings of expeditions into the Eurasian Arctic (e. g. in 1991, 1993, 1995, 1996 and 1997). As the Eurasian basins are under the strong influences of currents of Atlantic water masses and the Transpolar Drift, while the Amerasian basins are more re-circulating systems, the significance of such differences may be revealed by comparative studies in both areas.

Beyond such principal differences, the anticipated gradients from the Lomonosov-Ridge (separating both areas) across the Makarov-Basin up to the Canadian Basin and the specific life conditions and patterns of organisms at the Alpha-Ridge are of special interest. Moreover, biogeographical distribution patterns and the role of water masses of Pacific origin for biological productivity are poorly known in the target area and had to be considered during the investigations. In brief, the general scientific objectives were:

- Description of distribution patterns or zooplankton and zoobenthos according to the morphology of the sea floor and the hydrology;
- Evaluation of metabolic activities of the benthos;
- Investigation of the possible role of advection (of food) to the Alpha-Ridge area in comparison with the Lomonosov-Ridge.

5.1 Working plan

Pelagic communities, especially the meso-zooplankton, were to be sampled from the whole water column along the planned transect across the Alpha-Ridge from the Makarov Basin up to deeper waters of the Canadian Basin. The main analyses were directed to the calanoid copepods, which are transported especially with the Atlantic

water masses circulating in the Arctic Ocean and which form a major grazer group in the pelagial. Thus, and by the formation of larger fecal pellets as well as their destruction and repeated use (by coprophagy) they are among the important transformers of particulate organic matter in the water column. High densities of such grazers together with a well developed microbial loop may substantially reduce the organic matter settling down on the sea floor.

Beyond contributing to these aspects, the analyses of zooplankton distribution patterns were intended to show how far the high Arctic ridges (Alpha and Lomonosov) may act as faunistic barriers even in these well transportable organisms.

Zoobenthos, especially the larger macrofauna, is an integrating indicator of the environmental conditions during longer periods, among which the availability of food particles is of greatest significance. This organic matter may originate from in-situ production and direct vertical flux or/and from horizontal advection from more productive areas like the open Arctic shelf seas (e. g. the Laptev Sea). The deep sea floor of the Eurasian basins (including the Gakkel-Ridge) has proven to be a very poor benthic environment (see e. g. Kröncke, 1998), while there seem to be a few exceptions from this general pattern, among which the Lomonosov Ridge appears to be the most prominent. The planned investigations on the Alpha-Ridge would allow a better understanding of such differences and answer the question, whether water depths is the main controlling factor of such patterns or whether advection together with differences in the regional productivity may be more important.

The biogeographical, diversity and density distribution patterns of the Arctic macrozoobenthos are a sensitive result of the post-glacial development of their life conditions. They are expected to change substantially during any new developments in the ice cover, the circulation patterns and the primary production in the course of climatic alterations. The description of nowadays distribution patterns and activities of biota are the pre-conditions for an early recognition of ecosystem changes and for the prediction of possible future developments.

5.2 Methods

Zooplankton was collected with a new version of the HYDROBIOS multiple closing net, the so-called deep-sea multi-net. It allowed the stratified sampling of nine different water layers from the near-bottom waters up to the surface during one haul. The opening of the catching net is 0.5 m^2; and the filtered volume is estimated by a combination of two small flow meters. The mesh size of all nets was 150 µm. Accordingly, meso-zooplankton and slow-moving larger plankton were mainly collected by the net hauls. The material was preserved and will be evaluated in detail at AWI Bremerhaven.

Zoobenthos was obtained with the large box corer (Grosskastengreifer, GKG, 0.25 m^2 surface area), in most cases as small box sub-samples (227 cm^2) from common hauls

with the sediment geologists. Some single benthos GKGs were additionally taken and evaluated in total. The surface material (from the first 2 cm) was sieved on 0,25 mm screens, while the deeper layers (down to more than 15 cm) were sieved on 0.5 mm screens. The material was preserved in 4 % formaldehyde, buffered with a saturated borax solution in sea water. A part of these samples were pre-evaluated on board under 10-fold magnification. The remainders and all the other material will be evaluated in the home laboratories (Bremerhaven and St. Petersburg). For the investigation of smaller zoobenthos, 2 to 3 cores of the multiple sediment corer (MUC, inner single core diameter 5.7 cm) were taken. Most of these cores were first used for measurements of total sediment oxygen uptake rates; thereafter, they were separated into the uppermost 2 cm layer and the following 8 cm. These samples were preserved in total and are to be analysed in Bremerhaven for smaller macro- and the main groups of meiofauna (see also deep-sea group, chapter 6).

For the measurements of sediment biota oxygen uptake rates, multicorer tubes were incubated for 1 to 5 days with an overlaying original water volume of ca. 10 cm thickness at temperatures of 0° Celsius in darkness. The water was gently circulated by a peristaltic pump, connected with the multicorer tubes by a closed hose system. Oxygen concentrations were measured at the start and at the end of each incubation with very sensitive oxygen probes (ME, according to Clark's principle) or/and by the chemical Winkler method (thanks to Sergey Pivovarov).
After incubation, the upper 10 cm of the sediment cores were preserved for faunal density counts as described above.

5.3 Preliminary results

Biological sampling was performed only at a part of the planned stations, as severe ice conditions and shortage of time did not allow to penetrate into the waters beyond the Alpha-Ridge (Canadian Basin). The single samples obtained at most stations do only allow rough estimations of quantitative structural and of activity parameters of the pelagic and benthic communities investigated. Nevertheless, they indicate general trends, especially in connection with previous results from neighbouring areas. Table 16 summarises all our sampling activities (see also station map and station Table of the general part of the cruise report):

Tab. 16: Biological sampling statistics. The locations of the station are shown in Fig. 30.

Station No.	Date	UTC	Latitude	Longitude	Water depth	CTD	MN	MUC	GKG
001	03.07.	09.08	74°48.3'N	33°59.5'E	236m	+	-	+	-
021	10.07.	14.46	87°56.5'N	102°42.4'W	3336m	+	-	+	-
028	13.07.	18.27	86°25.3'N	148°11.0'W	3105m	-	-	+	-
029	14.07.	09.48	86°23.1'N	148°05.8'W	2870m	-	-	-	+
034	15.07.	06.47	85°22.3'N	155°24.1'W	2092m	+	+	+	+
038	16.07.	08.37	85°08.0'N	171°24.5'W	1518m	+	+	+	+
047	18.07.	05.47	85°45.0'N	177°03.5'W	2452m	+	+	+	++
058	21.07.	09.40	83°33.5'N	144°50.5'E	1298m	-	-	+	++

001: Barents Sea; 021: Makarov Basin;
028 - 047: Alpha-Ridge area; 058: Lomonosov-Ridge

Location (Latitude, Longitude), Water depth, Time: at the beginning of the station
CTD: Vertical profile for salinity, temperature, depths, together with "Rosette" water bottle sampling
MN: Deep sea multi-net for meso-zooplankton (9 nets for 9 layers; mesh = 150 µm)
MUC: Multi-corer for undisturbed sediment and near-bottom water samples (12 tubes)
GKG: Large box sampler (Grosskastengreifer; 0.25 m^2 sample surface area)

Table 17 Overview on the zooplankton sampling at three stations in the Alpha-Ridge area. There seemed to be a relatively well developed zooplankton fauna, dominated by *Calanus hyperboreus* and *C. glacialis* in the upper water layers and in the layers of Atlantically influenced waters.

Tab. 17: Zooplankton sampling statistics

Stat. No.	Depth (m)	Filtrated water vol. (m^3)	Vol. Zoopl. (cm^3)	Vol. plankton/ Vol. filt. water (cm^3/m^3)	Conspicuous plankton organisms	Hyd & Cten (%)	Copepodes (%)
034	2030-1500	247	4	0.016	Hyd & Cten	20	30
	1500-1000	256	15	0.059	Hyd & Cten	70	10
	1000-750	120	10	0.083	Hyd & Cten	20	10
	750-500	124	7.5	0.060	Hyd & Cten	50	20
	500-200	152	20	0.132	Pareuchaeta spp.	0	60
	200-100	52	10	0.192	C. hyp. & C. glac.	0	70
	100-50	25	7.5	0.300	C. hyp. & C. glac.	0	50
	50-0	26	25	0.962	C. hyp. & C. glac.	0	90
038	1450-1000	253	7.5	0.030	Hyd. & Cten.	30	30
	1000-750	128	2.5	0.020	Hyd & Cten	20	20
	750-500	123	4	0.033	Hyd & Cten	20	30
	500-200	142	25.5	0.180	Hyd & C. hyp.	10	70
	200-100	47	20	0.426	C. hyp. & C. glac.	0	80
	100-50	23	5	0.217	C. hyp. & C. glac.	0	70
	50-0	23	25	1.087	C. hyp. & C. glac.	0	90
045	2350-2000	186	12.5	0.067	Hyd & Cten	90	10
	2000-1500	265	8	0.030	Hyd & Cten	30	10
	1500-1000	275	12.5	0.045	Hyd & Cten	70	1(
	1000-750	136	27	0.199	Shrimps (Natantia)	50	5
	750-500	136	20	0.147	Amphipods	50	20
	500-200	158	37.5	0.237	C. hyp. & C. glac.	0	50
	200-100	52	12.5	0.240	C. hyp. & C. glac.	0	70
	100-50	23	10	0.435	C. Hyp. & C. glac.	0	80
	50 -0	23	20	0.870	C. hyp. & C. glac.	0	90

Hyd = Hydromedusae; Cten = Ctenophora; C. hyp. = Calanus hyperboreus; C. glac. = Calanus glacialis

The preliminary results of the analyses of the macro-zoobenthos samples are summarised in Table 18. It is obvious that the fauna in the Alpha-Ridge area is extremely poor (both in species diversity and in density, individual numbers per area). Polychaetes form the only dominant group; they seemed to be sediment reworking (deposit feeding) animals. Suspension feeders like small sponges were also found, but only as very tiny individuals, while living bivalves were totally lacking. Echinoderms were not found, too.

The station sampled on the Lomonosov-Ridge (058) proved to be much richer than the majority of the Alpha-Ridge stations.

Tab. 18: Macrozoobenthos sampling (preliminary results)

Taxa / Stations	001	021	028/029	034	038	047	058
Spongia	(*)	(-)	1	1	0	1	3
Coelenterata	(*)	(-)	0	0	0	+	2
Polychaeta	++	(-)	0	2	2	3	2
Mollusca							
Bivalvia	(*)	(-)	0	0	0	0	0
Gastropoda	(*)	(-)	0	0	0	0	0
Misc.	(-)	(-)	0	0	0	0	0
Crustacea							
Amphipoda	(*)	(-)	0	0	0	+	+
Isopoda	(-)	(-)	+	0	0	+	0
Cumacea	(*)	(-)	0	0	0	-	1
Misc.	(*)	(-)	0	0	0	-	1
Echinodermata							
Holothur.	(*)	+?	0	0	0	-	0
Ophiurids	(*)	(-)	0	0	0	-	0
Misc.	(*)	(-)	0	0	0	-	0
Others	(*)	(-)	0	0	0	-	0
Species numbers	*>20*	*1*	*2*	*2*	*2*	*10*	*>10*
Abundance (m^{-2})	*2000*	*<10*	*<10*	*<10*	*<10*	*<100*	*100*

numbers: individuals found in box sample of 227 cm^2
+: present in any other sample (MUC-core or qual. sample from GKG)
(-): absent from MUC sample
(*): absent from MUC sample,
but occurring in the area (central Barents Sea)

These results are compared with the oxygen uptake rates obtained from core tube incubations in Fig. 28. The trends indicated by the arrangement of the stations according to depths should not be stressed too much, while the regional differences found seem to be the more interesting.

Station number	Depth, m	Location	Species numbers	Numbers of individuals per square meter	Oxygen uptake rates, mmol O_2 m^{-2} $hour^{-1}$
1	235	Barents Sea	50	2000	150
58	1273	Lomonosov-Ridge	7	60	116
38	1476	Alpha-Ridge, Lyon seamount	2	10	39
34	2025	Alpha-Ridge	2.5	10	73
47	2450	NW Alpha-Ridge	3	20	25
21	3171	Makarov Basin	2	10	25

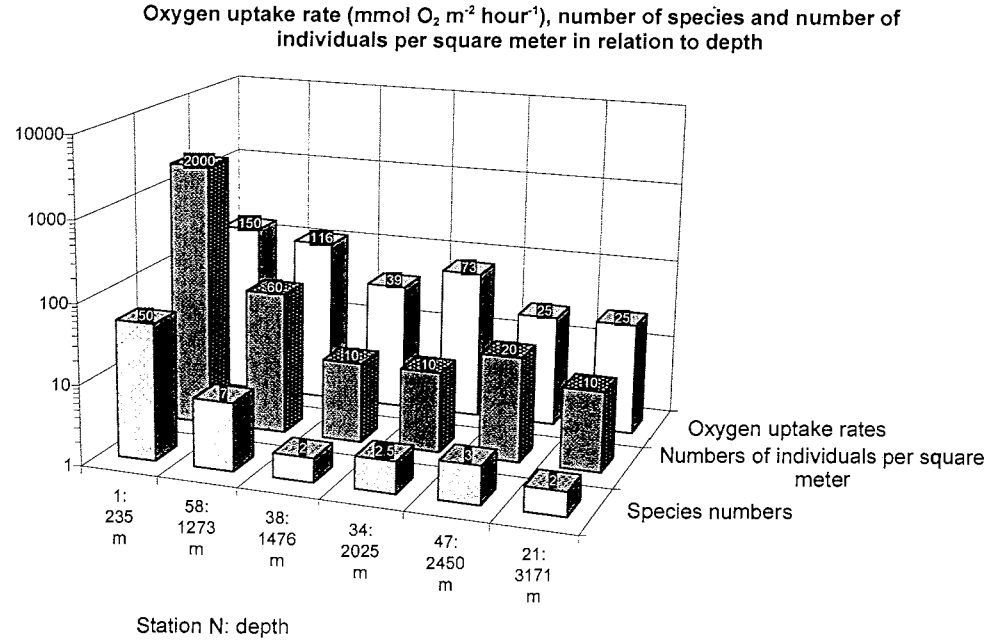

Fig. 28: Benthic oxygen uptake rates (mmol O_2 m^{-2} $hour^{-1}$) numbers of macro-zoobenthos species and of individuals per square meter in relation to depths (preliminary data).

5.4 Conclusions

Compared with the results from earlier expeditions (see e. g. Kröncke 1998), the deep water stations in the Makarov-Basin and in the adjacent Alpha-Ridge area proved again to be very poor in macro-zoobenthos, while the richer fauna met on the Lomonosov-Ridge fits into the pictures presented already by Kröncke in 1994, Anisimova et al. (1997) and Deubel & Rachor (1998). It even seems as if the Alpha-Ridge is among the poorest benthic environments ever investigated in the Arctic

Ocean (the "Arctic benthic desert"), which was also seen in the bottom images made during the MUC sampling and supported by the measurements of benthic micro-organism activities and pigment analyses made by the AWI deep sea group (see chapter 6.0). The zooplankton compartment above the ridge, however, may be less impoverished.

While the enrichment along the Lomonosov-Ridge was explained mainly by advection of particulate organic matter produced in the northeastern Laptev Sea area, to which an increased primary production in the leads and polynyas regularly seen over the ridge may add matter, the Alpha-Ridge area seems to be remote from any supporting production source as well as very poor in in-situ-production due to the very heavy ice cover prevailing there. In addition, the relatively rich zooplankton community is supposed to consume and almost totally work up any organic particles available in the water column.

The relatively high oxygen uptake rates measured in the poor ("desert") environments may be explained as stress induced artefacts, as a recovery (if any) of a deep sea fauna after hauling on board the ship may need much more days than the maximum time (5 days) used for incubations. In addition, dead animals may have increased bacterial activities and their oxygen uptake rates in our experiments.

The evaluations and analyses to be done in the home laboratories will show, whether the hypotheses presented here are to be rejected or modified. Moreover, it would be very promising to study such different ecosystems as tackled during this cruise (Alpha and Lomonosov Ridges) in more detail during any other future expeditions, as such different influences as water depths, role of zooplankton (from total grazing up to enhancing sedimentation by fecal pellet production), advection/isolation from productive areas and the significance of in-situ production could be evaluated.

6 Smallest benthic biota of the central Arctic Ocean (I. Schewe, S. Hülse)

During POLARSTERN Cruise ARK-XIV/1a we were able to get, for the first time, quantitative sediment samples form the Alpha Ridge region (central Arctic Ocean) for qualitative and quantitative investigations on sediment-inhabiting organisms of smallest body size (<1000 µm).

Meiofauna	1000 µm - 32 µm		(including foraminiferans)
Nanofauna	32 µm - 2 µm		(mainly protozoans)
Bacteria		<2 µm	

Furthermore we carried out biochemical analysis to assess informations about food availability at the seafloor, bacterial activity and total biomass of organisms living in the sediments.

6.1 Sediment sampling and processing

Sediment samples were obtained by a multicorer (MUC), taking up to 12 sediment cores per haul with an inner diameter of 6 cm. The MUC was equipped with a video camera system to get a first impression of the benthic realm and to allow a (semi-)targeted sampling at the seafloor. Samples were taken at 6 stations, in the deep Makarov Basin (>3000 m), on the Alpha Ridge between 155°W and 180°W and at a station on the top of the Lomonosov Ridge (1270 m) at 83°N (Tab. 19).

Immediately after recovery of the MUC, we sampled the sediment-overlying water to analyse oxygen concentrations in bottom waters (Winkler-Titration). The uppermost five centimetres of the sediment cores were subsampled using plastic syringes with cut off anterior ends. Three replicate subsamples from different MUC tubes were taken for each parameter investigated. Samples were either processed directly on board or fixated with Formalin and Glutaraldehyde or stored at –20°C for later analyses at the home laboratory.

Measurement of bacterial exoenzymatic activity and determinations of sediment bound chloroplastic pigments (indicating the input of organic matter phytoplankton production), as well as microscopic observations of living nanofauna organisms were carried out on board the ship.

Quantitative estimations of meiofauna, nanofauna and bacteria will be performed on fixated samples later in the lab. Phospholipid concentrations in the sediment will be analysed to quantify total biomass of sediment inhabiting micro-organisms. Determinations of the sediment water content (porosity) and grain size analyses will complete these investigations.

Tab. 19: List of multicorer stations

Latitude	Longitude	Depth [m]	Date	Station
87,561 N	102,595 W	3170	10.07.98	PS 51/21
86,333 N	147,386 W	3130	13.07.98	PS 51/28
85,223 N	155,240 W	2070	15.07.98	PS 51/34
85,015 N	171,270 W	1470	16.07.98	PS 51/38
85,450 N	176,560 W	2450	18.07.98	PS 51/47
83,335 N	144,477 E	1270	21.07.98	PS 51/58

6.2 Preliminary results

As expected, all parameters so far measured range on very low levels, characterising especially the area around the Alpha Ridge as an extremely oligotrophic desert region. Nevertheless, clear water depth depending tendencies of sediment bound chloroplastic plant-pigments and coupled bacterial activities could be established in the data (Fig. 29).

Preliminary results from station 21 in the Makarov Basin and station 58 on the Lomonosov Ridge showed slightly higher values than the stations directly located on the Alpha Ridge. Nevertheless, they nicely fit to data determined during the Arctic Ocean expedition in the summer 1996 with the Swedish ice-breaker ODEN and may confirm a possible lateral input of organic matter from the Siberian shelf regions into the Arctic deep-sea.

However, only in combination with following carefully evaluation of further biochemical parameters and quantitative faunistic analyses an improved interpretation of the results will be possible.

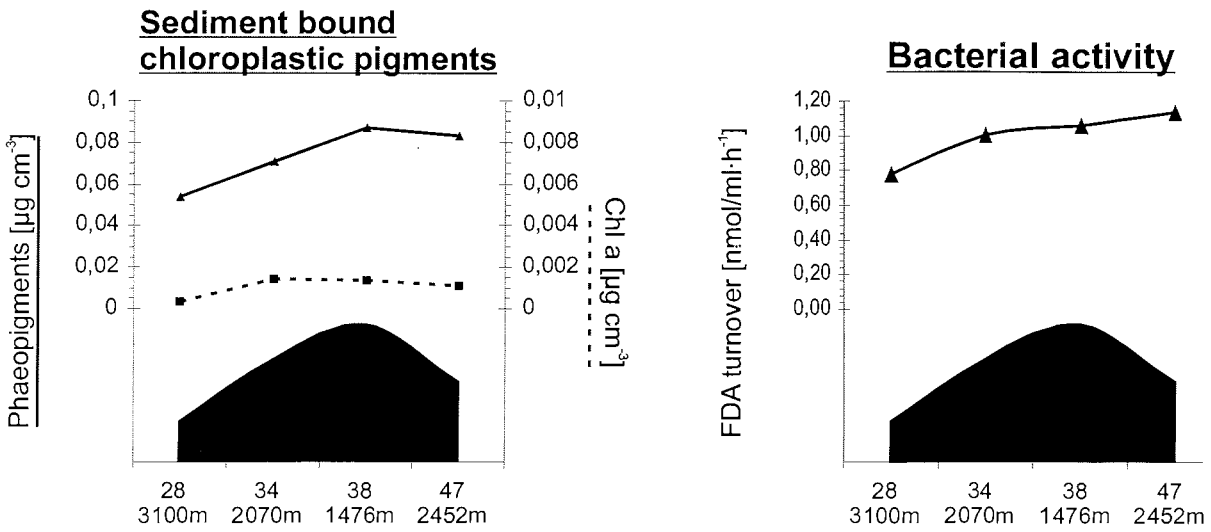

Fig. 29: Plant pigments and bacterial exoenzymatic activity on Alpha Ridge stations.

7 Oceanography
(V. Solokov, S. Pivovarev, W. Schneider)

7.1 Introduction

The work of the oceanographic group on board of the RV POLARTSERN continues the previous investigations of the Arctic Ocean. During the last few years an increase of temperature in Atlantic water in the Arctic Ocean was observed. The results of the previous investigations indicated that the influence of Atlantic water on the Arctic Ocean had increased significantly (Quardfasel et al., 1993; Morrison et al., 1996; Alekseev et al., 1997). The front between waters with an Atlantic versus Pacific character has shifted from over the Lomonosov Ridge to roughly over the Alpha and Mendeleev Ridges.

Nutrient and oxygen concentrations in the water provide a valuable tool to trace different kind of water masses in the Arctic Ocean. For example, silicon was widely used as a tracer of river waters in the Kara and Laptev Seas in summer (Rusanov et al., 1979). Pacific water with high silicon concentration which flows through Bering Strait can be traced via the Chukchi Sea to Fram Strait and the Greenland Sea.

Moreover inorganic silicon, dissolved in a marine water, is a very important biogeochemical parameter. Marine planktonic organisms diatoms, radiolarians and silicoflagellates build amorphous silica shells using dissolved silica for construction their skeleton. The surface layer of the Arctic Ocean, where photosynthesis occurs, is enriched by silicon as well as other nutrients as a result of mixing with under layered water, in which a rests of phytoplankton are dissolved.

Phosphate and nitrate are the mineral basement of the primary production of phytoplankton in the surface structural zone of the Arctic Ocean.

7.2 Working programme

The aim of the oceanographic studies during the cruise was to obtain the data of the distribution of physical and chemical parameters of sea water in the Arctic Ocean along the cruise way. These data are necessary for a better understanding of the water mass structure and condition of the Atlantic water.

The specific oceanographic goals are following:

- to perform vertical profiles of temperature, salinity and nutrients in the Nansen, Amundsen and Makarov Basins, and over the Mendelyev and Lomonosov ridges;
- to study the anomaly of the temperature in the Atlantic water;
- to determine the influence of the Pacific water over the Alpha Ridge by chemical tracers.

7.3 Equipment and methods

General information about temperature and salinity distribution was obtained by CTD, XBT and XCTD casts along the route. The vertical profiles of temperature salinity were measured by CTD-system a Seabird 911 plus, equipped with dual temperature and conductivity sensors, yellow substance fluorescence sensor combined with 24-bottle rosette. The CTD was also equipped with three resistance thermometers were used to control the stability of its temperature sensors.

The XBT-systems, Sippican T-7, equipped with temperature sensor have been used during the cruise. The XBT is capable of temperature accuracy's of +/- 0.1C, with a resolution of better then 0.01C. Vertical profiles of temperature can be measured to a maximum depth of 760 m. The XCTD-systems, Sippican MK-12, were equipped with temperature and conductivity sensors, with capable accuracy's of +/- 0.1 C and a resolution of better then 0.01 C. Vertical profiles can be measure to a maximum depth of 1.000 m. The XBT and XCTD measurements are sampled at a rate that provides a vertical resolution of one meter at a nominal depth accuracy of +1-5 meters or 2 % of depth, whichever is greater.

Dissolved inorganic silicon was analyzed from all sampling depth at all stations. The samples were drawn in 250 ml plastic bottles and analyzed within one hour after collection by standard procedures. Analyses were carried out with a photoelectrocolorimeter KFK-2M. More then 100 samples have been frozen for to analyze phosphate and nitrate. The dissolved oxygen concentration was determined by means of the Winkler method (Manual, 1993).

7.4 Preliminary results

During the cruise from July 5 to 24, 1998 were carried out:

- 7 CTD stations;
- 44 XBT;
- 6 XCTD;
- 139 measurements of silicon in the water samples;
- 93 measurements of oxygen.

Positions of the stations are shown on the Fig. 30.

Temperature, salinity and silicon profiles of some CTD stations are shown on the Fig. 31 a - d Over the Makarov Basin and the Alpha Ridge well pronounced signal of the Pacific water was observed at the depth 40 - 60 m.

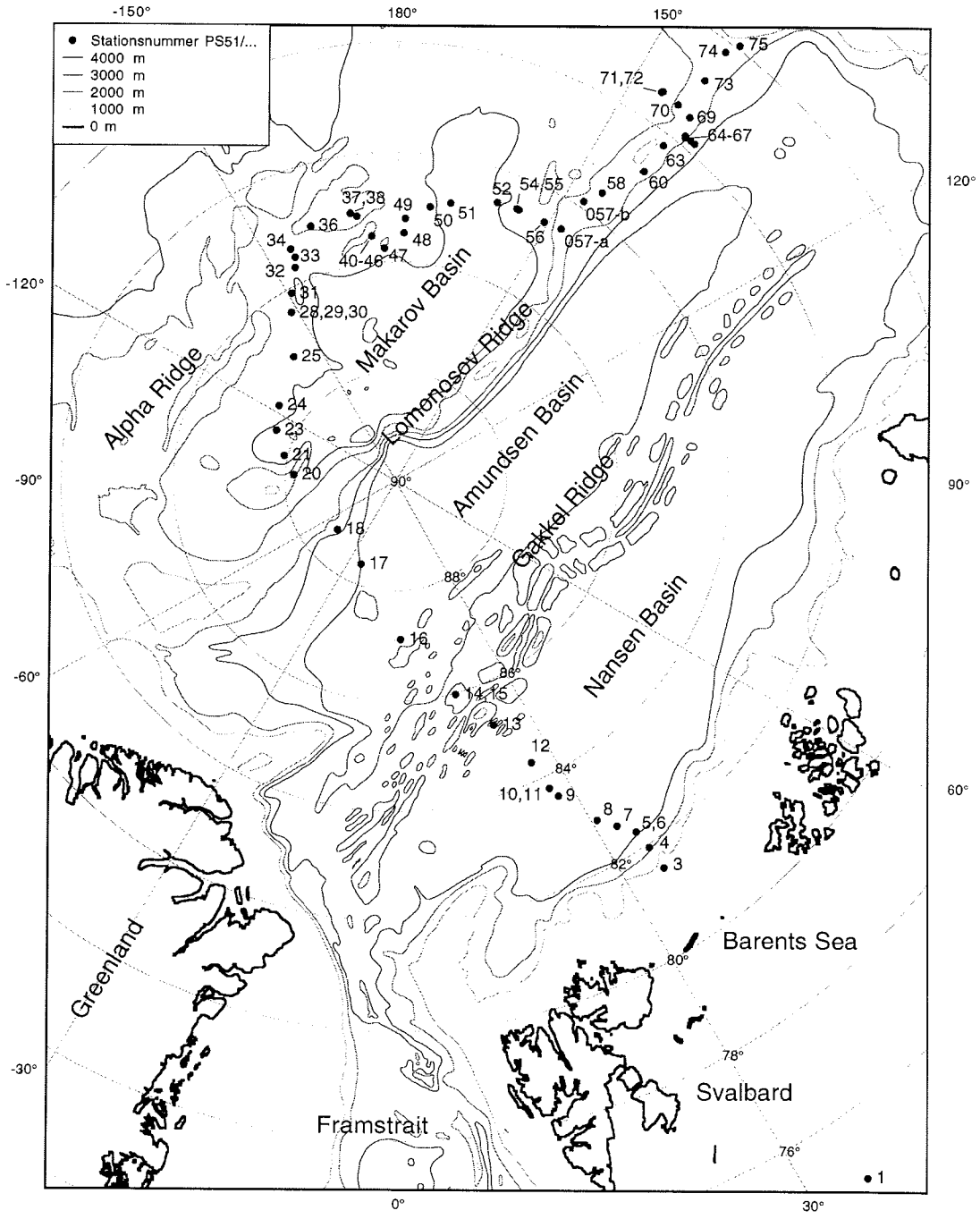

Fig. 30 a: Biologic, geologic and oceanograhic stations

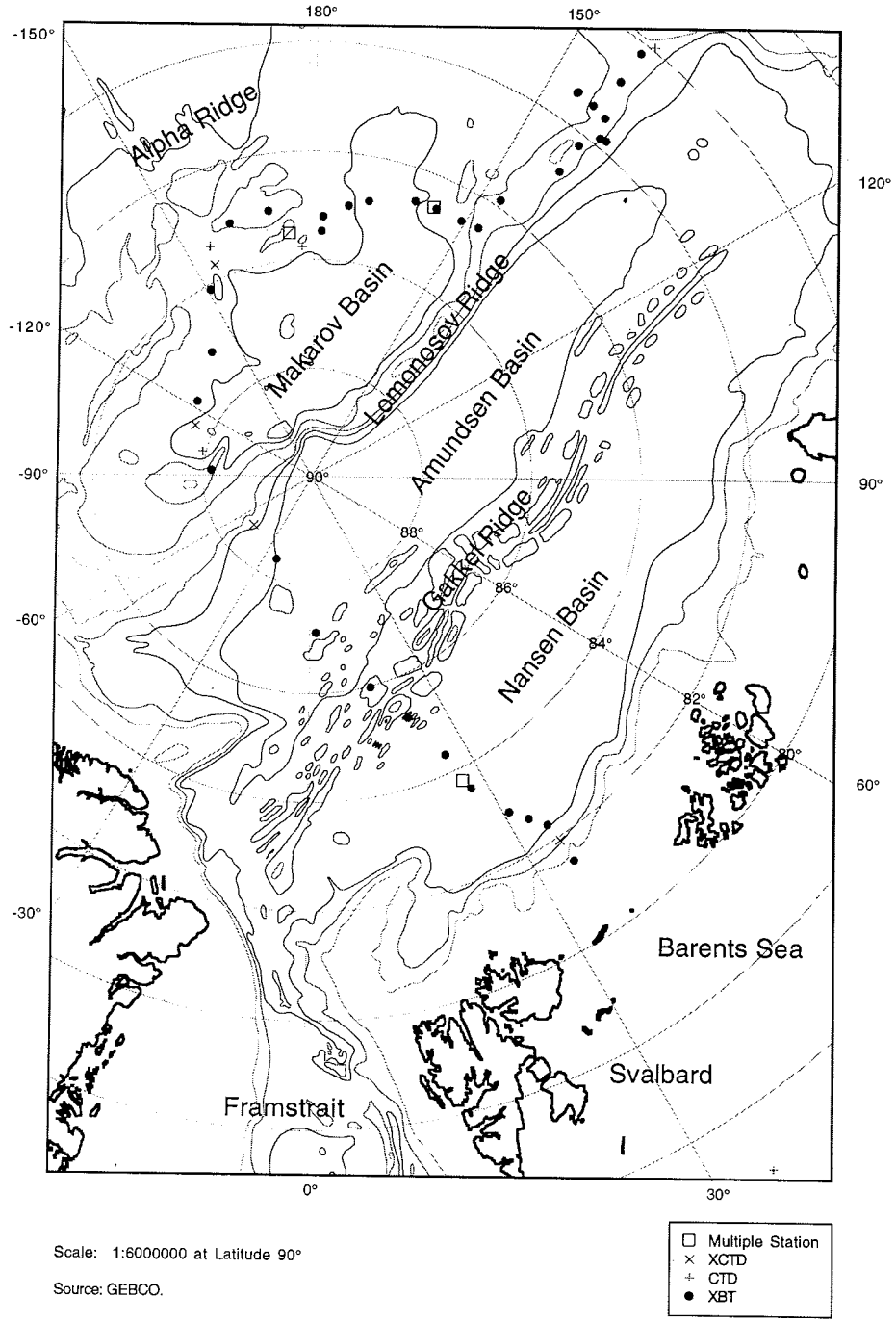

Fig. 30b: Oceanographic stations during the expedition

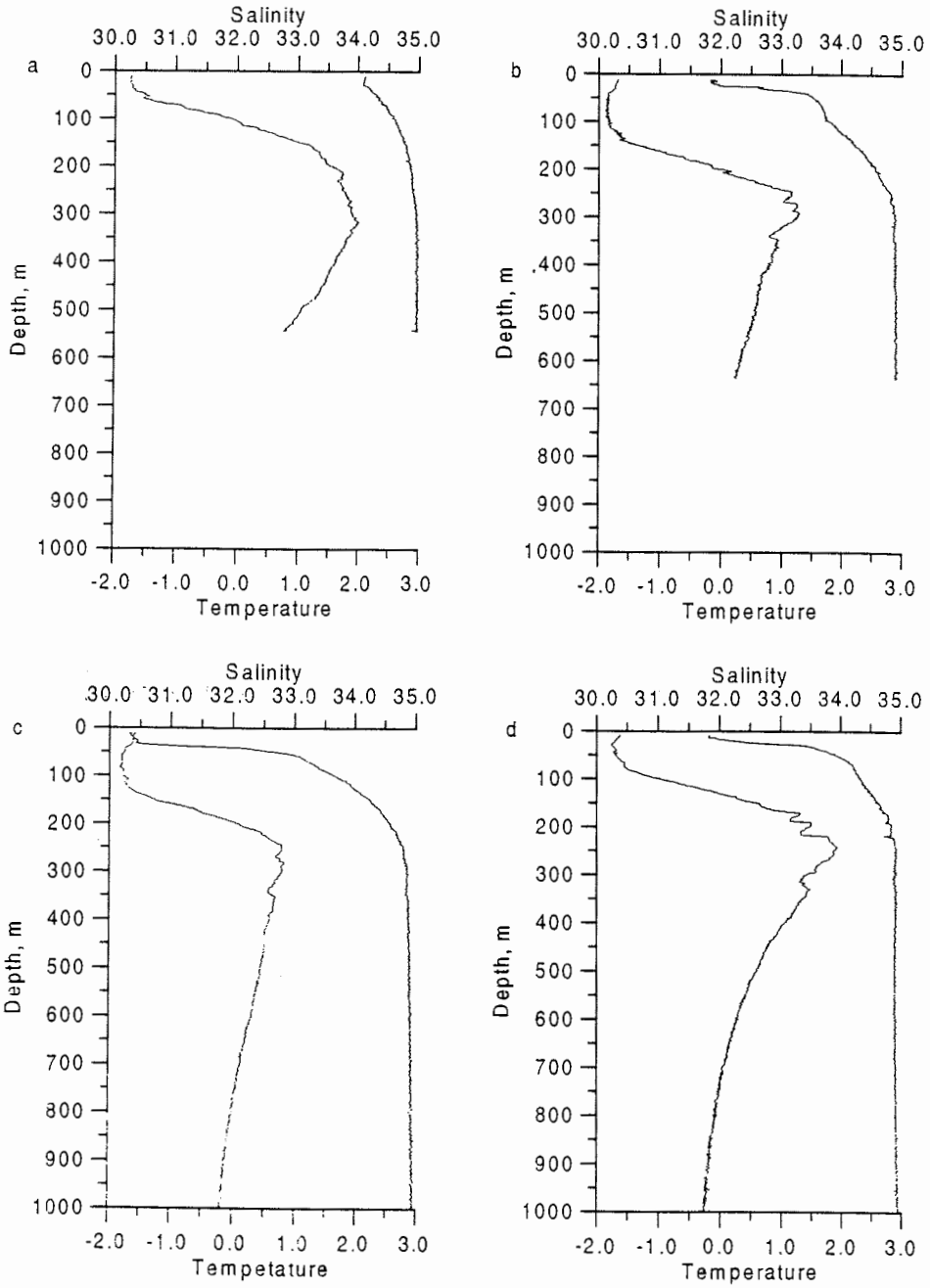

Fig. 31 a - d: Temperature distribution at the XCTD stations: a - 4; b - 18; c - 32; d - 58. Location see fig. 30 a.

The results of the XBT data shown on the Fig. 32. The cruise track was divided onto the three transacts: the first - from the Barents sea to the Alpha Ridge slope, the second - from the Alpha Ridge to the Lomonosov Ridge and the third - along the Lomonosov Ridge up to the continental slope in the Laptev Sea. The temperature distribution at the upper 700 m layer of the most all parts of the transacts is in according with the previous results. Atlantic water with a temperature more then +1.6 C was observed at the third transact (Fig. 32 c) over the Lomonosov Ridge. That temperature is higher then maximum temperature have ever been observed in that area.

Many of the vertical temperature profiles exhibit step-like structures and even inversions, with vertical scales from 10 up to tens of meters (Fig. 31). The inversions are believed to result from interleaving of different water masses at the frontal zones. Finally double-diffusion processes may to a certain extent alter the vertical temperature and salinity distribution of the layered structure (Augstein, 1997).

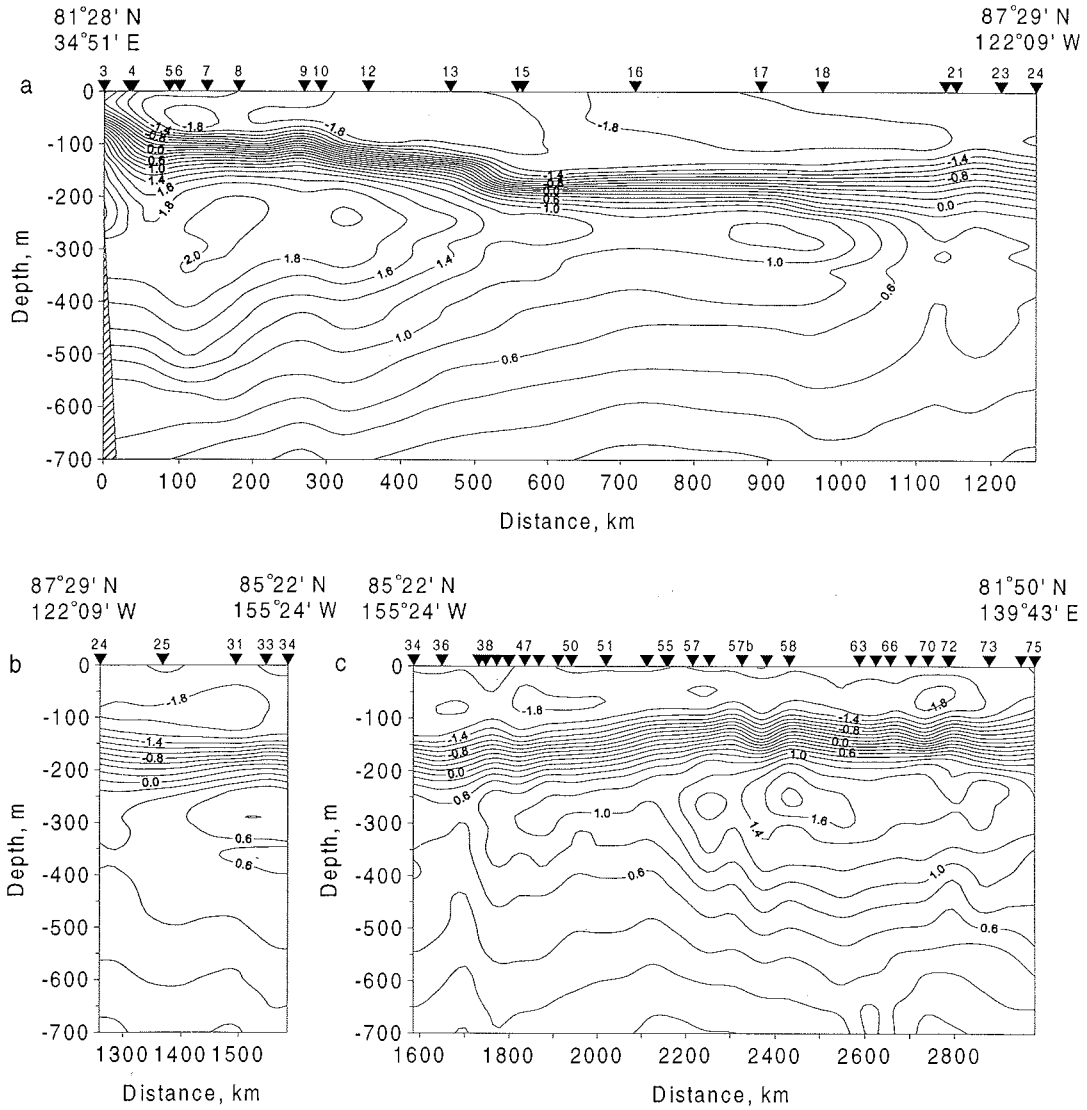

Fig. 32: Temperature (°C) distribution across the Arctic Ocean a - 05-12.07; b - 12-15.07; c - 15-24.07 1998. CTD , XCTD and XBT-7 data.

8 Electromagnetic ice thickness measurements (E. Weigelt)

The ARK XIV/1a leg offered the rare opportunity to observe the distribution of sea-ice thickness along the transpolar current system. The thickness of ice floes characterises ice of different age and helps to identify different ice regimes. Whereas the surface roughness and extension of the pack ice could be observed from the air or the space, the thickness of even ice created by freezing can only directly be measured on ice by drilling or electromagnetic techniques.

The significant contrast of the conductivity between the sea ice as nearly isolator and the good conductivity of sea water enables ice thickness measurements be made with electromagnetic methods. Here, the thickness of the sea ice was determined indirectly by the measure of underground apparent electrical conductivity.

For the measurements a commercially available portable instrument (Geonics EM31) was used. The instrument consists of two coils with a distance of 3.66 m for transmitting and receiving electrical signals with an operating frequency of 9.8 kHz. The instrument was used in the horizontal dipole mode and placed directly on the surface. From the measured values of the apparent conductivity a preliminary thickness can be calculated by the relation:

Thickness = 8.32- ln (Ac -5.85)/0.826) (C. Haas; 1998)
Ac = apparent conduchivity

8.1 First results

Along the whole transect thickness samples of 3 to 6 ice floes a day were acquired with the help of a helicopter. Only a few gaps occurred on the transect because the weather conditions were not favourable for flights. The samples were acquired from 82.35°N, 33.85°E along the ships track through the Eurasian Basin towards the Alpha Ridge to 87.58°N, 116.61°W and from this position towards the Laptev Sea, where the position of the last investigated floe is 81.48°N, 145.43°E at the eastern edge of the Lomonosov Ridge. Figure 33 shows the positions of the investigated floes.

Thickness data from 54 ice floes were collected along profiles with a total length of 5935 m and a measuring point distance of 5 m. The floes were chosen to be representative for the ice cover of the surrounding region. If possible the profiles were positioned in more than 50 m distance from rafted ridges to avoid influence of such disturbed areas on thickness values. The depth of melt-puddles and the thickness of the snow cover were determined at typical points of the floes with a ruler.
A typical example for a 100 m long profile (85° 21.04'N, 177°43.8'E) is shown in figure 34. Most floes on the cruise were covered with 20 to 50 % of melt puddles that formed the major part of the surface variations. In some regions the floes were

significantly rafted, so that ice thickness over 6 m may not representative for the investigated area.

In the Eurasian Basin the most of the sampled ice floes have a thickness between 1.6 m and 2.5 m. The mean thickness of the floes in the Makarov Basin is about 2.5 m. Along the slope of the Alpha Ridge two kinds of ice floes occurred: floes with an even surface and an average thickness of 2 m; and floes with a rough, by crevasses and little ridges disturbed surface and a thickness over 3 - 4 m. At the eastern end of the Lomonosov Ridge the floes show again a flat surface and the most measured thickness values amount 1.6 m.

Figure 35 shows the distribution of sea-ice thickness for all 1076 recorded data points. The ice thickness along the observed transect varies between 0.6 m and 5 m beside thicker spots close to rafted ridges, but the most observed thickness is between 1.5 and 2.3 m. A region with significant thicker sea ice about 4 m thickness and more was observed around the western part of the Alpha Ridge.

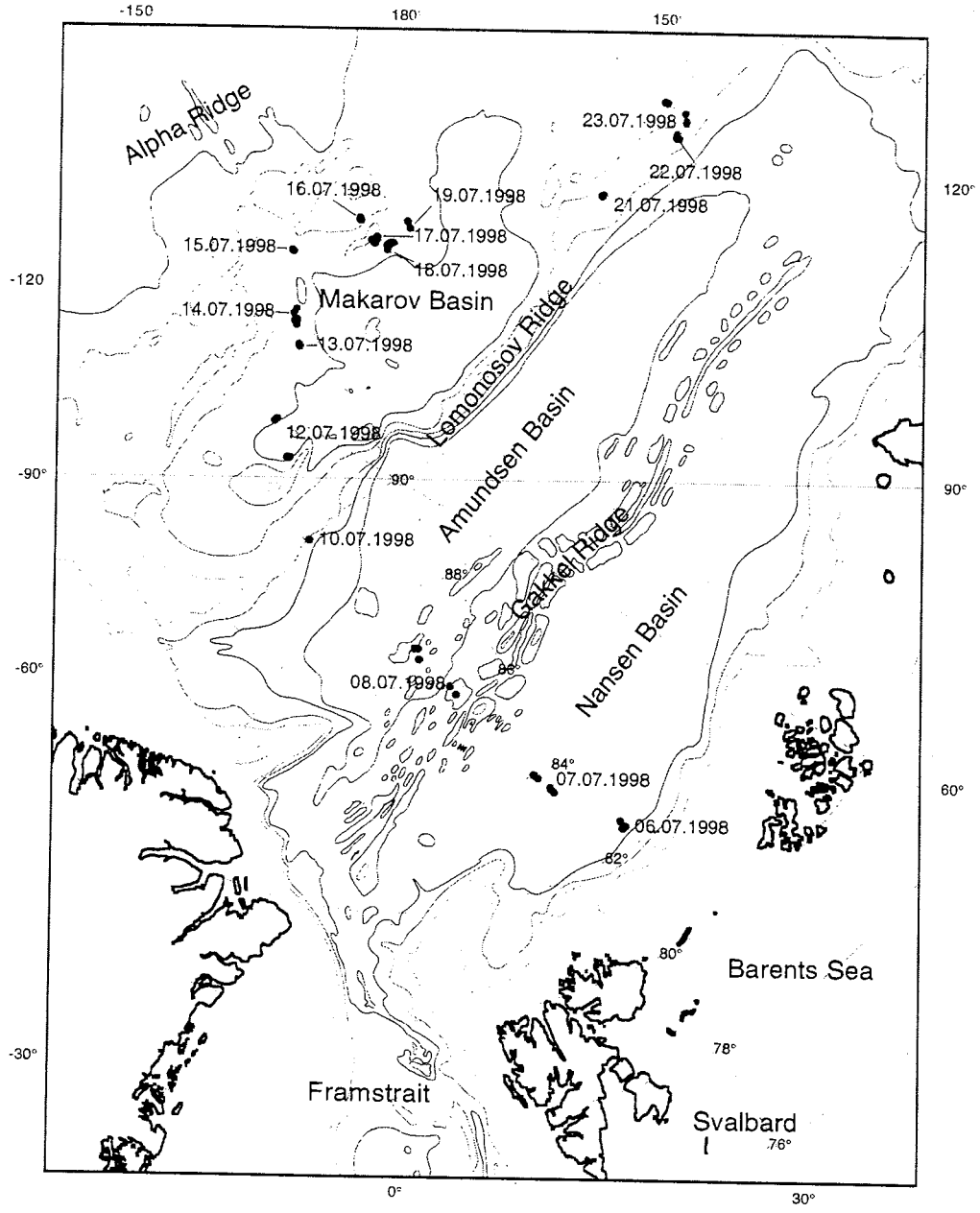

Fig. 33: Location map of all ice floes sampled for thickness measurements during the cruise.

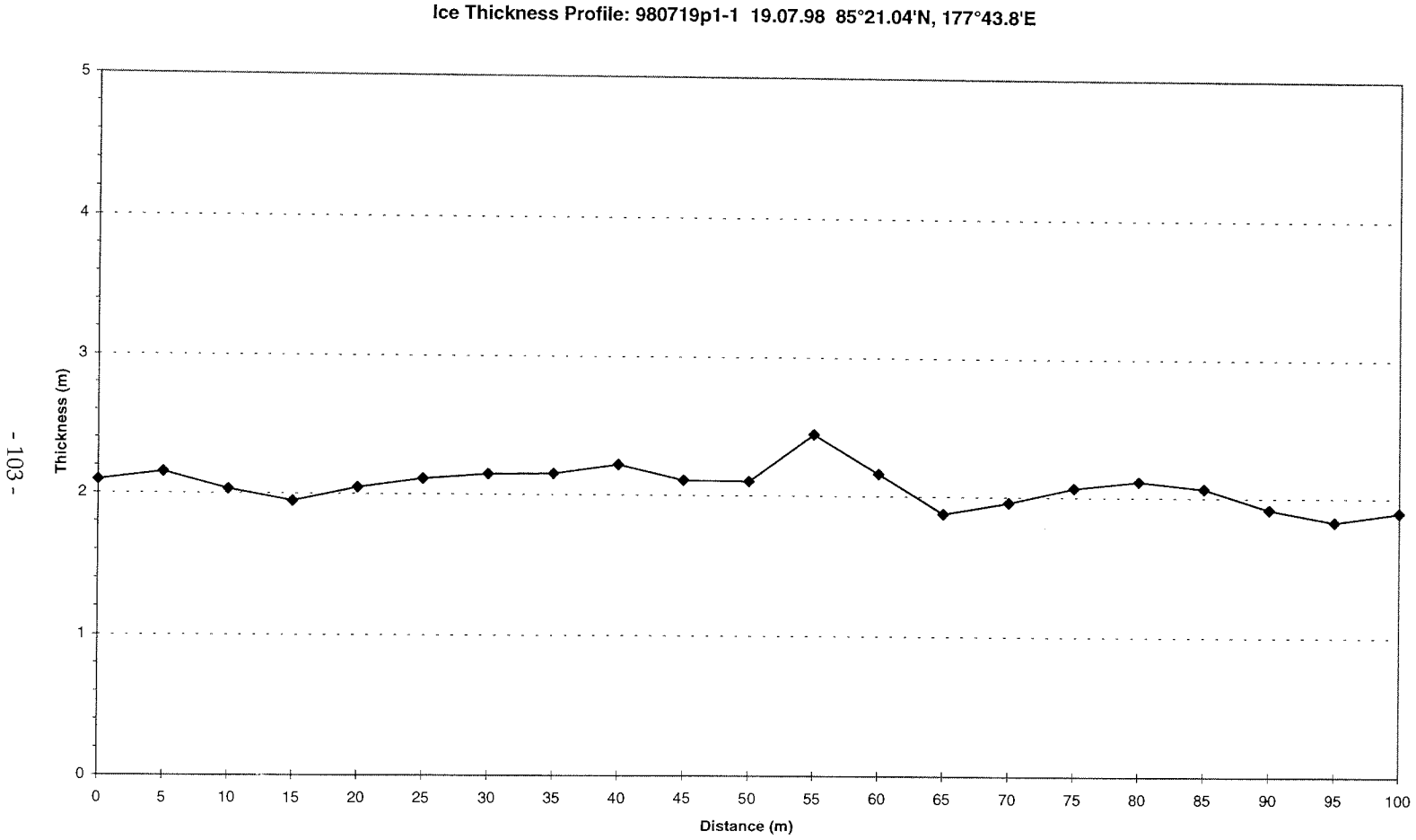

Fig. 34: Example of an ice-thickness profile

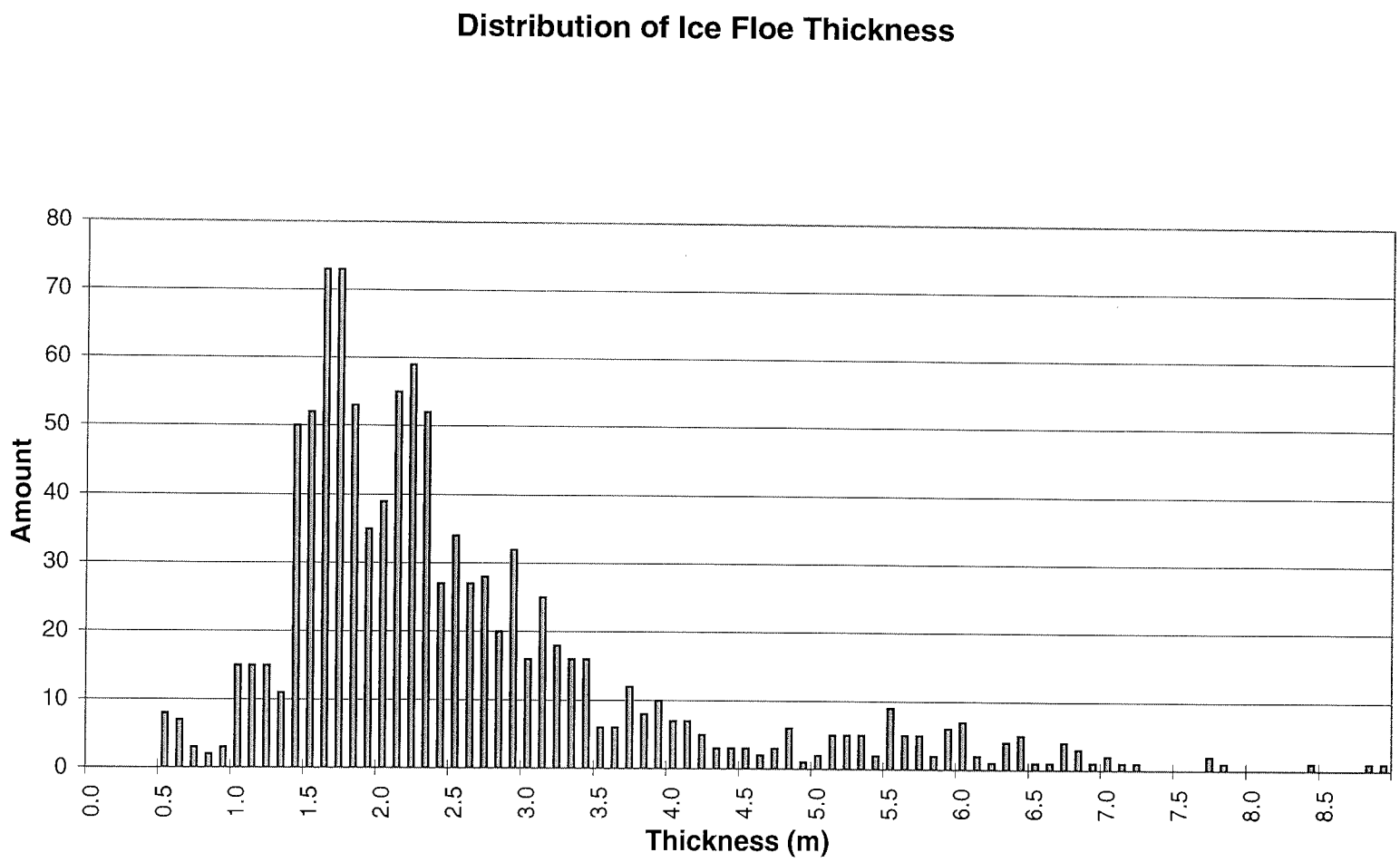

Fig. 35: Thickness distribution of all samples of the floe thickness along the ship's track.

References

Alekseev G.V., Bulatov G.V., Ivanov V.V. Temperature anomaly of the Atlantic Warte at Arctic Ocean, DAN RAN, 1997.

Anisimova, N., Deubel, H., Potin, S. & E. Rachor (1997): Zoobenthos (in Cruise Report ARK-XI/1, ed. by E. Rachor). Ber. Polarforsch. 226: 103 - 110.

Augstein, E., Report on Polar Research., The expedition Arctic 96 of RV „POLARSTERN"(ARKXII). No. 234, 1997

Barrie, L. A., 1986: Arctic air pollution: an overview of current knowledge. Atmos. Environ., 20, 643-663.

Cande, S.C. and Kent, D.V., 1992. A new geomagnetic polarity time scale for the Late Cretaceous and Cenozoic, Journ. Geophys. Res., 97: 13917-13951.

Childress, J. J. and Michel, T. J., 1980. A motion compensated shipboard precision balance system. Deep Sea Res., 27, 965-970.

Clark, D. L., Byers, C. W. & Pratt, L. M., 1986. Cretaceous black mud from the Central Arctic Ocean. Palaeoceanography, 1(3): 265-271.

Clark, D. L., Whitman, R. R., Morgan, K. A. and Mackey, S. C., 1980. Stratigraphy and glacial-marine sediments of the Amerasian Basin, central Arctic Ocean. GSA Special Paper, 181, 57 pp.

Darby, D. A., Naidu, A. S., Mowatt, T. C. and Jones, G., 1989. Sediment Composition and Sedimentary Processes in the Arctic Ocean. In: Herman, Y. (Ed.), The Arctic Seas, Van Nostrand Reinhold Company, New York, 657 - 720.

Deubel, H. & E. Rachor (1998): AWI, Biannual Report: 40-42.

Dijkstra, S., Stober, M., Tsoukalas, N., 1998. Hydrosweep DS bathymetry and Side Scan Sonar Surveys in: Jokat, W. and Oerter, H. (edg): The expedition AntarktisXIV of RV Polarstern in 1997, Report of leg ANT-XIV/3, 267, 31-47.

Fütterer, D. K., 1992. ARCTIC'91: The Expedition ARK-VIII/3 of RV "POLARSTERN" in 1991. Ber. zur. Polarforsch., 107, 267 pp.

Grobe, H., 1987. A Simple Method for the Determination of Ice-Rafted Debris in Sediment Cores. Polarforschung 57 (3), 123 - 126.

Jackson, H. R., Mudie, P. J. and Blasco, S. M., 1985. Initial geological report on CESAR - The Canadian Expedition to study the Alpha Ridge, Arctic Ocean. Geol. Surv. Canada, Paper 84 - 22, 177 pp.

Jokat, W., Buravtsev, V., Miller, H., 1995. Marine seismic profiling in sea ice covered regions, Polarforschung 64(1), 9-17

Jones, G. A., 1987. The central Arctic Ocean sediment record: Current progress in moving from a litho- to a chronostratigraphy. Pol. Res., 5: 309 - 311.

Kögler, F., 1963. Das Kastenlot. In: Meyniania, 13, 1-7.

Kröncke, I. (1994): Macrobenthos composition, abundance and biomass in the Arctic Ocean along a transect between Svalbard and the Makarov Basin. Polar Biol. 14: 519-529

Kröncke, I. (1998): Macrofauna communities in the Amundsen Basin, at the Morris Jesup Rise and at the Yermak Plateau (Eurasian Arctic Ocean). Polar Biol. 19: 383-392.

Kuhn, G., 1995. Sedimentphysikalische Untersuchungen. In: GERSONDE, R. (Ed.), Die Expedition ANTARKTIS-XI/2 mit FS "POLARSTERN" 1993/94.- Berichte zur Polarforschung 163, 66 - 74.

Martini, E., 1971. Standard Tertiary and Quaternary calcareous nanno-plankton zonation. In: Farinacci, A. (Ed.), Proceedings of the Second Planktonic Conference, Roma 1970, Edizioni Technoscienza, Rome, 739 - 785.

Morrison, J., Steele, M. and Anderson, R. Hydrography of the Upper Arctic Ocean Measured from the Nuclear Submarine USS Pargo., Draft at Deap-Sea Research., 1996.

Mudie, P. J. and Blasco, S. M., 1985. Lithostratigraphy of the CESAR cores. In: Jackson, H. R., Mudie, P. J. and Blasco, S. M. (Eds.), Initial geological report on CESAR - The Canadian Expedition to study the Alpha Ridge, Arctic Ocean, Geol. Surv. Canada, Paper 84 - 22, 59 - 100.

Niessen, F., 1997. Physical Properties in Marine Sediments. In: Kuhn, G. (Ed.): Die Expedition ANTARKTIS-XI/4 mit FS "POLARSTERN" 1994. Berichte zur Polarforschung (in press).

Niessen, F., and Musatov, E., 1997. Marine sediment echosounding using PARASOUND. In: E. Rachor (Ed.),

Niessen, F., and Musatov, E., 1997. Marine sediment echosounding using PARASOUND. In: E. Rachor (Editor), Reports on Polar Research. V. 226. Alfred Wegener Institute for Polar and Marine Research, Bremerhaven, Germany, pp. 118 - 128.

Nowaczyk, N. R., 1991. Hochauflösende Magnetostratigraphie spätquatärer Sedimente arktischer Meeresgebiete. Berichte zur Polarforschung 78, 187 p.

Nürnberg, D., Wollenburg, I., Dethleff, D., Eicken, H., Kassens, H., Letzig, T., Reimnitz, E., Thiede, J., 1994. Sediments in Arctic sea ice: Implications for entrainment, transport and release. Marine Geology. V. 119. P. 185-214.

O'Dowd, C. D., Smith, M. H., Consterdine, I. E. & Lowe, J. A., 1997: Marine aerosol, sea-salt, and the marine sulphur cycle: A short review. Atmos. Environ., 1, 73 - 80.

Pfirman S., Lange, M. A., Wollenburg I., Schlosser P., 1990. Sea ice characteristics and the role of sediment inclusion in deep-sea deposition: Arctic and Antarctic comparisons. In: U. Blei and J. Thide (Editors), Geological History of the Polar Oceans: Arctic versus Antarctic. Kluwer, Dordrecht. P.187 - 211.

Quadfasel, D., Sy A., Rudels, B. A ships of opportunity section to the North Pole: upper ocean temperature observation. Deap-Sea Research, vol. 40,No 4, p.777-789, 1993.

Rachor, E., 1997, "Scientific Cruise Report of the Arctic Expedition ARK-XI/1 of RV 'Polarstern' in 1995", Reports on Polar Research, 226, 118 - 128.

Smirnov, V.V., Shevchenko, V.P., Stein, R. et al., 1997. Aerosol size distribution over the Laptev Sea in July - September 1995: First results. - Berichte zur Polarforschung, 212, 139 - 143.

Spielhagen RF, Eisenhauer A, Frank M, Frederichs T, Kassens H, Mangini A, Nowaczyk NR, Nørgaard-Pedersen N, Schäper S, Stein R, Thiede J, Tiedemann R, Wahsner M, Bonani G, and Kubik PW (1997) Arctic Ocean evidence for Late Quaternary initiation of northern Eurasian ice sheets, Geology 25, 769-864.

Spiess, V., 1992. Digitale Sedimentechographie - Neue Wege zu einer hochauflösenden Akustostratigraphie. - Ber. Fachb. Geowiss. Univ. Bremen, 35, 199 pp.

Spiess, V., 1992. Digitale Sedimentechographie - Neue Wege zu einer hochauflösenden Akustostratigraphie. - Ber. Fachb. Geowiss. Univ. Bremen, Nr. 35, 199 pp.

Stein, R., Behrends, M. and Spielhagen, R., 1997. Lithostratigraphy and sediment characteristics. In: Rachor, E. (Ed.), Scientific Cruise Report of the Arctic Expedition ARK-XI/1 of RV "POLARSTERN" in 1995, Berichte zur Polarforschung, 226, 143 - 153.

Thiede, J., 1988. Scientific cruise report of Arctic Expedition ARK IV/3. Reports on Polar Research, 43, 237 p.

Thiede, J., 1988. Scientific cruise report of Arctic Expedition ARK IV/3. Reports on the Polar Research, v. 43. 237 p.

Weber, M.E., Niessen, F., Kuhn, G., and Wiedicke, M., 1997. Calibration and application of marine sedimentary physical properties using a multi-sensor core logger. Marine Geology, 136, 151 - 172.

Stationsliste ARK-XIV (27.6.98 - 27.7.98)

Stat. No.	Date Datum 1998	Time (UTC) Start End	Position N		Position W/E		Depth Lottiefe	Heading Kurs	Speed (kn)	Station Work Equipment applied Arbeiten/Geräte
PS 51/001-1	03.07	9:08	74°	48.3'N	33°	59.5'E	236 (HS)	304°	STOP	CTD z. Wasser
		9:17								CTD a.T. (218m), Hieven
	03.07	9:23	74°	48.4'N	33°	59.3'E	241 (HS)	304°	STOP	CTD a.d. Wasser, a. Deck
PS 51/001-2	03.07	9:44	74°	48.4'N	33°	59.3'E	244 (HS)	304°	STOP	MUC z. Wasser
		9:55								MUC a. Grund (236)
		10:02	74°	485'N	33°	58.4'E	248 (HS)			MUC a. D. Wasser, a. Deck
PS 51/002	05.07	17:52	81°	28.6'N	34°	51.1'E	249 (HS)	270°	2.5	Streamer z. Wasser
		18:03	81°	28.7'N	34°	49.1'E	245 (HS)	270°	2.5	Airgun z. Wasser, 18:07 First Shot
PS 51/003	05.07	18:24	81°	28.8'N	34°	43.8'E	244 (HS)	30°	3.0	XBT
PS 51/004	05.07	23:30	81°	55.9'N	34°	44.6'E	1834 (HS)	360°	5.0	XCTD
PS 51/002	06.07	00:00	81°	58.1'N	34°	43.3'E	1936 (HS)	011°	STOP	Profilende - Streamer & Airguns werden eingeholt
PS 51/005	06.07	09:07	82°	16.7'N	34°	42.7'E	2568 (HS)	315°	3.5	XBT
PS 51/006	06.07	10:11	82°	17.9'N	34°	17.6'E	2695 (HS)	260°	3.5	XBT
PS 51/007	06.07	13:02	82°	34.1'N	32°	45.0'E	3319 (HS)	320°	5.0	XBT
PS 51/008	06.07	19:59	82°	51.2'N	30°	48.2'E	3782 (HS)	282°	4.0	XBT
PS 51/009	06.07	06:55	83°	34.3'N	27°	23.3'E	4076 (HS)	300°	5.0	XBT
PS 51/010	07.07	09:09	83°	45.5'N	26°	43.1'E	4082 (HS)	016°	STOP	CTD z. Wasser,
		10:08								CTD a. Tiefe (4001m), Hieven
		11:07	83°	45.4'N	26°	44.6'E	4081 (HS)	013°	STOP	CTDa. D. Wasser, a. Deck
PS 51/011	07.07	11:15	83°	45.4'N	26°	44.7'E	4082 (HS)	358°	STOP	XBT
PS 51/012	07.07	17:10	84°	19.6'N	25°	56.6'E	3900 (HS)	340°	5.0	XBT
PS 51/013	08.07	01:41	84°	13.4'N	22°	10.1'E	3580 (HS)	300°	5.0	XBT
PS 51/014	08.07	05:56	85°	55.5'N	16°	08.6'E	2762 (HS)	340°	9.0	XBT
PS 51/015	08.07	07:20	85°	59.8'N	15°	58.5'E	2876 (HS)	360°	5.0	XBT
PS 51/016	08.07	17:59	87°	07.4'N	2°	12.9'E	4395 (HS)	360°	5.0	XBT
PS 51/017	09.07	14:47	88°	21.7'N	22°	04.7'W	4282 (HS)	306°	2.0	XBT
PS 51/018	09.07	21:09	88°	37.8'N	49°	29.2'W	2444 (HS)	190°	2.0	XCTD
PS 51/019	10.07	07:20	88°	11.3'N	86°	28.7'W	3661 (HS)	230°	4.0	Airgun v. Deck
	10.07	07:20	88°	11.4'N	86°	48.8'W	3506 (HS)	230°	4.0	Streamer z. Wasser
	10.07	07:35	88°	11.2'N	86°	57.6'W	2912 (HS)	270°	4.0	Firstshot, Airgun Array z. Wasser
	10.07	09:01	88°	09.5'N	91°	36.8'W	2432 (HS)	258°	6.0	Sonoboje ausgesetzt
PS 51/020	10.07	09:30	88°	09.8'N	93°	05.5'W	2358(LZ)	301°	4.0	XBT
PS 51/019	10.07	10:20	88°	09.7'N	95°	53.5'W	2541 (LZ)	268°	4.0	Sonoboje ausgesetzt
		14:22	87°	56.6'N	102°	41.3'W	3216 (LZ)	099°	0.1	Airgun a. Deck
PS 51/021	10.07	14:46	87°	56.5'N	102°	42.4'W	3236 (HS)	204°	STOP	CTD zu Wasser
		15:41								CTD a. Tiefe, Hieven
PS 51/021	10.07	16:34	87°	56.5'N	102°	42.4'W	3245 (HS)	204°	STOP	CTD a. d. Wasser u. a. Deck
PS 51/021-1	10.07	16:40	87°	56.3'N	102°	50.8'W	3247 (HS)	204°	STOP	MUC z. Wasser
PS 51/021-2	10.07	18:51	87°	56.0'N	103°	06.0'W	3245 (HS)	204°	STOP	MUC a. d. Wasser u. a. Deck
PS 51/022	10.07	20:05	87°	55.6'N	104°	01.7'W	3018 (HS)	294°	3.0	Streamer u. Airgun z.Wasser
		20:08	87°	55.6'N	104°	01.7'W	3018 (HS)	294°	3.0	First Shot
		20:24	87°	55.6'N	104°	19.0'W	3260 (PS)	294°	STOP	Airgun Array a. Deck, Hieven Streamer
PS 51/023	12.07	13:29	87°	39.3'N	113°	10.6'W	2898 (PS)	292°	0.5	XCTD
PS 51/023	12.07	13:41	87°	39.3'N	113°	10.6'W	2898 (PS)	292°	STOP	2. XCTD
PS 51/024	12.07	18:29	87°	29.5'N	122°	52.4'W	2838 (PS)	280°	6.5	XBT

Stat. No	Date Datum 1998	Time (UTC) Start End	Position N	Position W/E	Depth Lottiefe	Heading Kurs	Speed (kn)	Station Work Equipment applied Arbeiten/Geräte
PS 51/025	13.07	06:02	87° 04.7'N	140° 34.4'W	3084 (PS)	200°	6.0	XBT
PS 51/026	13.07	07:11	86° 58.9'N	142° 56.1'W	3169 (PS)	244°	5.5	Airgun Array ausgeschwungen
PS 51/026	13.07	07:27	86° 58.6'N	143° 17.4'W	3156 (PS)	282°	3.5	Streamer z. Wasser
PS 51/026	13.07	07:29	86° 58.6'N	143° 23.6'W	3160 (PS)	258°	3.5	Airgun Array z. Wasser, 11:33 First Shot
PS 51/027	13.07	09:10	86° 51.5'N	144° 20.6'W	3027 (HS)	133°	4.8	Sonoboje ausgesetzt
PS 51/026	13.07	11:56	86° 41.3'N	146° 03.0'W	3275 (HS)	320°	1.0	Airgun Array und Streamer ein
PS 51/028	13.07	18:27	86° 25.3'N	148° 11.0'W	3105 (LZ)	200°	STOP	MUC z.Wasser
		19:22						MUC a. Tiefe (3053m)
		20:29	86° 25.0'N	148° 06.0'W	3117 (HS)	202°	STOP	MUC a. d. Wasser, a. Deck
PS 51/029	14.07	09:40	86° 23.1'N	148° 05.8'W	2880 (HS)	261°	STOP	GKG z. Wasser
		10:26	86° 23.08'N	148° 07.07'W				GKG a. Grund (2823m)
		11:07	86° 23.0'N		2837 (HS)	261°	STOP	GKG a. d. Wasser, a. Deck
PS 51/030	14.07	12:30	86° 23.0'N	148° 11.1'W	2841 (PS)	257°	STOP	SL z. Wasser
		13:05					STOP	SL i. Grund
		13:45	86° 23.0'N	148° 12.4'W	2837 (PS)	257°	STOP	SL a. Deck
PS 51/031	14.07	17:42	86° 06.0'N	150° 55.0'W	3160 (PS)	190°	5.0	XBT
PS 51/32	14.07	22:06	86° 42.7'N	154° 51.5'W	2950	270°	STOP	XCTD
PS 51/032-1	14.07	22:13	85° 42.7'N	154° 41.5'W	2950 (HS)	268°	STOP	SL z. Wasser
		23:30	85° 42.81'N	154° 42.4'W				SL a. Grund (2890m)
		00:09	85° 42.8'N	154° 42.9'W	2935 (PS)	268°	STOP	SL a. d. Wasser, a. Deck
PS 51/033	15.07	03:16	85° 32.5'N	155° 40.4'W	2699 (HS)	206°	STOP	SL z. Wasser
		03:52						SL a. Grund
		04:48	85° 32.6'N	155° 40.3'W	2687 (HS)	207°	STOP	SL a. Deck
PS 51/034-1	15.07	06:47	85° 22.3'N	155° 24.1'W	2699 (HS)	315°	STOP	CTD z. Wasser
		07:27						CTD a. Tiefe
		08:16	85° 22.3'N	155° 24.8'W	2687 (HS)	297°	STOP	CTD a. d. Wasser, a. Deck
PS 51/034-2	15.07	08:27	85° 22.3'N	155° 25.0'W	2111 (HS)	297°	STOP	MN z. Wasser
		09:10					STOP	MN a. Tiefe (2030m), Hieven
		10:20	85° 22.4'N	155° 26.2'W	2098 (HS)	297°	STOP	MN a. d. Wasser, a. Deck
PS 51/034-3	15.07	10:34	85° 22.4'N	155° 26.5'W	2095 (HS)	297°	STOP	MUC z. Wasser
		11:12	85° 22.47'N	155° 26.85'W			STOP	MUC a. Tiefe (2029m), Hieven
		11:59	85° 22.5'N	155° 27.4'W	2076 (HS)	294°	STOP	MUC a. d. Wasser, a. Deck
PS 51/034-4	15.07	12:06	85° 22.6'N	155° 27.3'W	2073 (HS)	294°	STOP	SL z. Wasser
		12:27	85° 22.6'N	155° 27.8'W			STOP	SL a. Grund
		12:52	85° 22.6'N	155° 28.0W	2072 (HS)	294°	STOP	SL a. Deck
PS 51/034-5	15.07	13:09	85° 22.6'N	155° 28.4'W	2075 (HS)	294°	STOP	KG z. Wasser
		13:34	85° 22.6'N	155° 28.4'W			STOP	KG a. Grund
		14:06	85° 22.7'N	155° 28.8'W	2093 (HS)	297°	STOP	KG a. Deck

Stat. No.	Date Datum 1998	Time (UTC) Start End	Position N	Position W/E	Depth Lottiefe	Heading Kurs	Speed (kn)	Station Work Equipment applied Arbeiten/Geräte
PS 51/034-1	15.07	14:58	85° 22.8'N	155° 28.4'W	2103 (HS)	218°	3.0	Streamer z. Wasser
		15:05	85° 22.5'N	155° 31.5'W	2120 (HS)	211°	6.5	Airgun Array z. Wasser, 11:33 First Shot
PS 51/034-2	15.07	15:35	85° 20.2'N	155° 41.3'W		218°	6.0	Sonoboje ausgesetzt
PS 51/034-3	15.07	16:29	85° 15.4'N	155° 16.0'W	2283 (LZ)	236°	6.0	Sonoboje ausgesetzt
PS 51/034-4	15.07	17:30	85° 12.5'N	155° 10.3'W		236°	6.0	Sonoboje ausgesetzt
PS 51/036	15.07	21:38	85° 06.8'N	161° 24.0'W	2047 (HS)	230°	6.0	XBT
PS 51/034-5	16.07	00:11	85° 12.0'N	163° 58.0'W	1833 (HS)	275°	5.8	Sonoboje ausgesetzt
PS 51/037	16.07	06:10	85° 02.9'N	170° 03.6'W	1615 (HS)	270°	5.6	XBT
PS 51/034-5	16.07	07:00	85° 07.8'N	171° 23.2'W	1514 (HS)	340°	3.0	Airgun Array a. Deck
		08:10						Streamer ein
PS 51/038-1	16.07	08:37	85° 08.0'N	171° 24.5'W	1518 (HS)	320°	STOP	CTD z. Wasser
		09:06					STOP	CTD a. Tiefe (1476m)
		09:44	85° 08.0'N	171° 24.5'W	1518 (HS)	013°	STOP	CTD a. d. Wasser, a. Deck
PS 51/038-2	16.07	09:55	85° 08.0'N	171° 25.2'W	1516 (HS)	013°	STOP	MN z. Wasser
		10:27					STOP	MN a. Tiefe (1450), Hieven
		11:23	85° 08.0'N	171° 26.0'W	1514 (HS)	013°	STOP	MN a. d. Wasser, a. Deck
PS 51/038-3	16.07	11:37	85° 08.0'N	171° 25.9'W	1515 (HS)	014°	STOP	GKG z. Wasser
		11:59	85° 08.2'N	171° 26.06'W			STOP	GKG a. Grund (1448m)
		12:33	85° 08.0'N	171° 26.1'W	1512 (HS)	018°	STOP	GKG a. d. Wasser, a. Deck
PS 51/038-4	16.07	12:59	85° 08.1'N	171° 26.6'W	1513 (HS)	018°	STOP	Kastenlot z. Wasser
		13:16	85° 08.1'N	171° 24.4'W			STOP	Kastenlot a. Tiefe
		13:40	85° 08.1'N	171° 26.6'W	1512 (HS)	018°	STOP	Kastenlot a. d. Wasser, a. Deck
PS 51/038-5	16.07	14:00	85° 08.2'N	171° 26.8'W	1512 (HS)	355°	STOP	MUC z. Wasser
		14:36	85° 08.1'N	171° 27.0'W			STOP	MUC a. Tiefe
		15:02	85° 08.2'N	171° 27.1'W	1509 (HS)	354°	STOP	MUC a. d. Wasser, a. Deck
PS 51/039	16.07	15:43	85° 08.2'N	171° 26.8'W	1512 (HS)	334°	3.4	Streamer z. Wasser
		15:51	85° 08.4'N	171° 30.7'W	2128 (HS)	299°	5.5	Airgun Array z. Wasser, 15:52 First Shot
PS 51/039-1	16.07	16:48	85° 13.3'N	171° 56.6'W	1583 (HS)	353°	6.0	Sonoboje ausgesetzt
PS 51/039-2	16.07	17:41	85° 16.7'N	172° 44.0'W	1643 (PS)	308°	6.0	Sonoboje ausgesetzt
PS 51/040-2	16.07	18:13	85° 18.6'N	173° 03.3'W	1739 (PS)	350°	7.0	XBT
PS 51/041-2	16.07	20:44	85° 30.7'N	174° 20.5'W	928 (LZ)	330°	5.0	XBT
PS 51/039	16.07	23:15	85° 39.6'N	176° 53.1'W	1600 (LZ)	306°	4.0	Hieven Airgun Array und Streamer
		23:39	85° 40.4'N	177° 04.6'W	-	321°	STOP	Streamer und Array ein
PS 51/040-1	17.07	05:18	85° 30.6'N	174° 11.0'W	2442 (PS)	320°	STOP	SL z. Wasser
			85° 30.62'N	174° 10.38'W			STOP	SL a. Grund
		06:23	85° 30.7'N	175° 00.0'W	2435 (LZ)	355°	STOP	SL a. Deck
PS 51/041-1	17.07	10:41	85° 30.8'N	174° 11.2'W	2402 (HS)	044°	STOP	SL z. Wasser

Stat. No.	Date Datum 1998	Time (UTC) Start End	Position N	Position W/E	Depth Lottiefe	Heading Kurs	Speed (kn)	Station Work Equipment applied Arbeiten/Geräte
		11:08	85° 30.81'N	174° 11.37'W			STOP	SL a. Grund (2351m)
		11:40	85° 30.8'N	174° 11.6'W	2424 (HS)	057°	STOP	SL a. Deck
PS 51/042	17.07	12:16	85° 30.9'N	174° 11.6'W	2349 (HS)	058°	STOP	SL z. Wasser
		12:40	85° 30.9'N	174° 11.6'W			STOP	SL a. Grund
		13:10	85° 31.0'N	174° 10.8'W	2345 (HS)	077°	STOP	SL a. Deck
PS 51/043	17.07	13:33	85° 31.1'N	174° 11.0'W	2373 (HS)	067°	STOP	SL z. Wasser
		14:00	85° 31.1'N	174° 10.7'W			STOP	SL a. Grund
		14:41	85° 31.2'N	174° 10.3'W	2399 (HS)	065°	STOP	SL a. Deck
PS 51/044	17.07	15:00	85° 31.2'N	174° 09.9'W	2425 (HS)	078°	STOP	CTD z. Wasser
		15:23	85° 31.3'N	174° 09.5'W			STOP	CTD a. Tiefe
		15:53	85° 31.4'N	174° 09.4'W	2599 (HS)	080°	STOP	CTD a. d. Wasser, a. Deck
PS 51/045	17.07	16:08	85° 31.4'N	174° 08.9'W	2632 (HS)	080°	STOP	SL z. Wasser
		16:35	85° 31.5'N	174° 08.45'W		080°	STOP	SL a. Grund
		17:12	85° 31.6'N	174° 08.1'W	2620 (PS)		STOP	SL a. Deck
PS 51/046	17.07	19:46	85° 31.0'N	174° 27.8'W	2919 (HS)		6.0	XBT
PS 51/047-1	18.07	05:47	85° 45.0'N	177° 03.5'W	2452 (HS)	325°	STOP	CTD z. Wasser
		06:27					STOP	CTD a. Tiefe
		07:23	85° 45.2'N	176° 59.9'W	2468 (HS)	325°	STOP	CTD a. d. Wasser, a. Deck
PS 51/047-2	18.07	07:31	85° 45.2'N	177° 03.5'W	2468 (HS)	317°	STOP	MN z. Wasser
		08:15					STOP	MN a. Tiefe (2350 m), Hieven
		09:39	85° 45.4'N	176° 57.8'W	2502 (HS)	328°	STOP	MN a. d. Wasser, a. Deck
PS 51/047-3	18.07	09:59	85° 45.4'N	176° 57.3'W	2501 (HS)	386°	STOP	MUC z. Wasser
		10:44	85° 45.54'N	176° 57.8'W			STOP	MUC a. Tiefe (2435 m)
		11:30	85° 45.6'N	176° 56.0'W	2510 (HS)	385°	STOP	MUC a. d. Wasser, a. Deck
PS 51/047-4	18.07	11:36	85° 45.7'N	176° 56.3'W	2512 (HS)	312°	STOP	SL z. Wasser
		12:05	85° 45.54'N	176° 55.8'W			STOP	SL a. Grund
		12:37	85° 45.8'N	176° 55.1'W	2511 (HS)		STOP	SL a. Deck
PS 51/047-5	18.07	12:52	85° 45.8'N	176° 55.3'W	2510 (HS)	341°	STOP	GKG z. Wasser
		13:23	85° 45.9'N	176° 54.6'W			STOP	GKG a. Grund (1448m)
		14:00	85° 46.0'N	176° 54.4'W	2510 (HS)	341°	STOP	GKG a. d. Wasser, a. Deck
PS 51/047-6	18.07	14:21	85° 46.0'N	176° 53.9'W	2512 (HS)	341°	STOP	GKG z. Wasser
		14:57	85° 46.2'N	176° 53.6'W			STOP	GKG a. Grund (1448m)
		15:38	85° 46.0'N	176° 54.4'W	2521 (HS)	341°	STOP	GKG a. d. Wasser, a. Deck
PS 51/048	18.07	06:55	85° 28.8'N	178° 26.2'E	2778(HS)	272°	6.0	XBT
PS 51/049	19.07	10:40	85° 18.8'N	178° 07.6'E	2709 (HS)	140°	6.0	XBT
PS 51/050	19.07	18:26	85° 57.9'N	178° 00.1'E	3112 (HS)	245°	6.0	XBT

Stat. No.	Date Datum 1998	Time (UTC) Start End	Position N	Position W/E	Depth Lottiefe	Heading Kurs	Speed (kn)	Station Work Equipment applied Arbeiten/Geräte
PS 51/051	19.07	21:51	84° 49.8'N	169° 51.4'E	3398 (HS)	252°	2.0	Streamer z. Wasser, Airgun Array z. Wasser, First Shot
		22:09	84° 49.7'N	169° 48.9'E	3411 (HS)	250°	STOP	Streamer ein
PS 51/051	19.07	23:19	84° 50.0'N	169° 03.8'E	3427 (HS)	270°	6.0	XBT
PS 51/052	20.07	06:33	84° 36.0'N	160° 20.2'E	3474 (HS)	190°	6.0	XBT
PS 51/053-1	20.07	08:18	84° 35.5'N	158° 41.4'E	2897 (HS)	280°	2.5	Streamer z. Wasser
		08:23						Airgun Array z. Wasser
		08:26	84° 35.6'N	158° 36.4'E	3021 (HS)	285°	5.5	First Shot
PS 51/054	20.07	10:37	84° 35.0'N	156° 24.4'E		217°	6.0	XCTD
PS 51/053-2	20.07	10:44	84° 34.6'N	156° 16.4'E	2839 (HS)	257°	6.0	Sonoboje z. Wasser
PS 51/055	20.07	11:06	84° 35.0'N	155° 56.5'E	1955 (HS)	231°	6.0	XBT
PS 51/056	20.07	15:53	84° 33.9'N	150° 40.9'E	1317 (HS)	282°	4.5	XBT
PS 51/053-3	20.07	16:45	84° 34.0'N	149° 52.0'E	1685 (HS)	290°	6.0	Sonoboje z.Wasser
PS 51/057a	20.07	21:17	84° 31'N	147° 11.7'E	2526 (HS)	070°	6.5	XBT
PS 51/053-3	21.07	01:35	84° 31'N	147° 11.7'E	1239 (HS)	211°	6.0	Sonoboje z.Wasser
PS 51/057b	21.07	04:35	83° 52.7'N	146° 33.6'E	1138 (HS)	240°	6.0	XBT
PS 51/053-4	21.07	07:32	83° 34.3'N	145° 25.8'E	1370 (HS)	240°	6.0	Sonoboje z.Wasser, Radio Silence
PS 51/053-5	21.07	08:43	83° 34.0'N	144° 54.7'E	1344 (HS)	230°	4.0	Hieven Airgun Array
		08:54				230°	STOP	Streamer ein
PS 51/058-1	21.07	09:20	83° 33.5'N	144° 50.5'E	1338 (HS)	254°	STOP	GKG z. Wasser
		09:45	83° 33.55'N	144° 50.21'E				GKG a. Grund (1293m)
		10:02	83° 33.5'N	144° 50.0'E	1333 (HS)	251°	STOP	GKG a. d. Wasser, a. Deck
PS 51/058-2	21.07	10:29	83° 33.5'N	144° 49.7'E	1329 (HS)	249°	STOP	GKG z. Wasser
		10:46	83° 33.5'N	144° 49.46'E				GKG a. Grund (1288m)
		11:04	83° 33.5'N	144° 49.0'E	1327 (HS)	248°	STOP	GKG a. d. Wasser, a. Deck
PS 51/058-3	21.07	11:22	83° 33.5'N	144° 48.8'E	1322 (HS)	248°	STOP	SL z. Wasser
		11:39	83° 33.5'N	144° 48.39'E				SL auf Tiefe (1292 m)
		11:55	83° 33.5'N	144° 48.5'E	1320 (HS)	248°	STOP	SL a. Grund
PS 51/058-4	21.07	12:08	83° 33.5'N	144° 48.2'E	1326 (HS)	245°	STOP	MUC z. Wasser
		12:35	83° 33.5'N	144° 47.7 'E			STOP	MUC a. Tiefe (1235 m)
		13:08	83° 33.6'N	144° 47.5'E	1320 (HS)	245°	STOP	MUC a. d. Wasser, a. Deck
PS 51/058-5	21.07	13:22	83° 33.6'N	144° 47.5'E	1310 (HS)	245°	STOP	XCTD z. Wasser
PS 51/059-1	21.07	21:42	82° 51.7'N	141° 39.7'E	2155 (HS)	155°	3.0	Streamer z. Wasser
		21:48					6.0	Airgun Array z. Wasser
		21:50	82° 51.0'N	141° 39.8'E	2145 (HS)	188°	6.0	First Shot
PS 51/060	21.07	22:23	82° 48.1'N	141° 45.6	2040 (HS)	155°	7.0	XBT
PS 51/059-2	21.07	22:33	82° 47.0'N	141° 49.5'E	1792 (HS)	170°	7.2	Sonoboje z. Wasser

Stat. No.	Date Datum 1998	Time (UTC) Start End	Position N	Position W/E	Depth Lottiefe	Heading Kurs	Speed (kn)	Station Work Equipment applied Arbeiten/Geräte
PS 51/059-3	21.07	23:20	82° 44.1'N	142° 03.5'E	1346 (HS)	090°	STOP	Airgun Array a. d. Wasser
		23:30						Streamer ein
PS 51/061-0	22.07	00:41	82° 38.7'N	142° 05.4'E	1336 (HS)	140°	3.0	Streamer z. Wasser
		00:49						Airgun Array z. Wasser
		00:53	82° 37.2'N	142° 08.0'E	1253 (HS)	195°	6.0	First Shot
PS 51/061-1	22.07	01:41	82° 32.7'N	142° 04.8'E	1079 (HS)	177°	5.7	Sonoboje z. Wasser
PS 51/061-0	22.07	02:08	82° 32.1'N	142° 04.8'E	1072 (HS)	257°	4.0	Airgun Array ein
		02:23						Streamer ein
PS 51/062	22.07	04:45	82° 13.4'N	141° 59.0'E	1486 (HS)	190°	3.0	Airgun Array z. Wasser
		04:55	82° 12.6'N	141° 54.0'E	1488 (HS)	200°	3.0	Streamer z. Wasser, First Shot 05:12
PS 51/063	22.07	04:55	82° 12.6'N	141° 54.0'E	1488 (HS)	200°	3.0	XBT
PS 51/062-1	22.07	05:50	82° 08.8'N	142° 07.9'E	1448 (HS)	240°	6.0	Sonoboje, Radio Silence
PS 51/064	22.07	09:06	81° 51.4'N	141° 40.0'E	1456 (HS)	190°	6.0	XBT
PS 51/062	22.07	14:00	81° 48.1'N	137° '58.2E	3452 (HS)	290°	3.5	Ende Streamer
		14:05						Array ein
		14:15	81° 48.2'N	137° 55.0'E	3463 (HS)	295°	1.0	Streamer und Airgun Array a. Deck
PS 51/065	22.07	16:34	81° 49.5'N	138° 54.7'E	2754 (HS)	279°	STOP	SL z. Wasser
		17:02	81° 49.5'N	138° 55.0'E				SL a. Grund
		17:32	81° 49.5'N	138° 55.5'E	2705 (HS)	105°		SL a. Deck
PS 51/066	22.07	18:20	81° 49.5'N	139° 34.1'E	2397 (HS)	115°	6.0	XBT
PS 51/067-1	22.07	19:20	81° 50.1'N	140° 28.7'E	1616 (HS)	090°	STOP	SL z. Wasser
		19:40	81° 50.1'N	138° 28.5'E				SL a. Grund
		19:59	81° 50.0'N	140° 29.2'E	1575 (HS)	110°		SL a. Deck
PS 51/067-2	22.07	20:26	81° 50.5'N	140° 29.5'E	1550 (HS)	130°		SL z. Wasser
		20:42	81° 49.94'N	140° 29.78'E				SL a. Grund (1525 m)
		21:05	81° 49.9'N	140° 30.1'E	1495 (HS)	146°		SL a. Deck
PS 51/068	23.07	00:59	81° 29.8'N	138° 04.8'E	3316 (HS)	089°	3.1	Streamer z. Wasser
		01:06						Airgun Array z. Wasser
		01:09						First Shot
PS 51/068-1	23.07	04:12	81° 28.8'N	140° 16.5'E	1211 (HS)	094°	6.0	Sonoboje, Radio Silence
PS 51/069	23.07	06:13	81° 31.1'N	141° 30.3'E	1190 (HS)	110°	6.0	XBT
PS 51/068-2	23.07	08:48	81° 28.8'N	143° 08.9'E	1333 (HS)	108°	6.0	Sonoboje z. Wasser
PS 51/070	23.07	09:26	81° 27.8'N	143° 35.6'E	1544 (HS)	060°	6.0	XBT
PS 51/076	23.07	10:00	81° 30.0'N	143° 34.0'E				ARGOS BOJE 14955 auf Scholle
PS 51/068-3	23.07	11:37	81° 29.2'N	145° 04.5'E	2070(HS)	066°	6.5	Sonoboje z. Wasser
PS 51/071	23.07	14:39	81° 26.1'N	146° 06.0'E	2360(HS)	226°	5.6	XBT
PS 51/068	23.07	14:45	81° 25.4'N	146° 01.3'E	2341(HS)	233°	3.2	Airguns ein

Stat. No.	Date Datum 1998	Time (UTC) Start End	Position N		Position W/E		Depth Lottiefe	Heading Kurs	Speed (kn)	Station Work Equipment applied Arbeiten/Geräte
PS 51/072	23.07	14:49	81°	25.3'N	146°	00.9'E	2339(HS)	180°	2.9	XBT
PS 51/068	23.07	14:58	81°	24.8'N	146°	06.0'E	2334(HS)	245°	5.6	Airgun Array z. Wasser, First Shot
PS 51/068-4	23.07	16:30	81°	18.9'N	145°	34.1'E	2295(HS)	245°	6.0	Sonoboje z. Wasser
PS 51/068-5	23.07	20:23	81°	06.0'N	143°	46.3'E	1802(HS)	246°	6.0	Sonoboje z. Wasser
PS 51/073	23.07	23:33	80°	49.0'N	142°	48.5'E	1757(HS)	225°	6.0	XBT
PS 51/068	24.07	02:09	80°	33.1'N	142°	57.7'E	1802(HS)	241°	4.2	Airguns ein - Arraywechsel
PS 51/068	24.07	02:44	80°	31.2'N	142°	51.8'E	1739(HS)	184°	3.2	Airgun Array z. Wasser
		02:47								First Shot
PS 51/068	24.07	04:50	80°	19.5'N	142°	44.6'E	1612(HS)	122°	6.0	Sonoboje
PS51/077	24.07	06:00	80°	07.32'N	142°	03.91'E				ARGOS BOJE 14954 auf Scholle
PS 51/074	24.07	06:19	80°	11.0'N	142°	52.6'E	1579(HS)	199°	6.0	XBT
PS 51/068	24.07	08:50	79°	57.1'N	142°	12.5'E	1434(HS)	237°	4.0	Airgun Array a. d. Wasser
		08:55							4.0	Streamer ein
PS 51/075		09:14	79°	56.5'N	142°	07.1'E	1436 (HS)	295°	STOP	CTD z. Wasser
		09:29							STOP	CTD a. d. Wasser, a. Deck, (defekt)
PS 51/075	24.07	09:40	79°	56.6	142°	07.6'E	1406 (LZ)	307°	STOP	CTD z. Wasser
		10:05							STOP	CTD a. Tiefe (1361 m)
		10:35	79°	56.7	142°	08.2'E	1410 (LZ)	307°	STOP	CTD a. d. Wasser, a. Deck

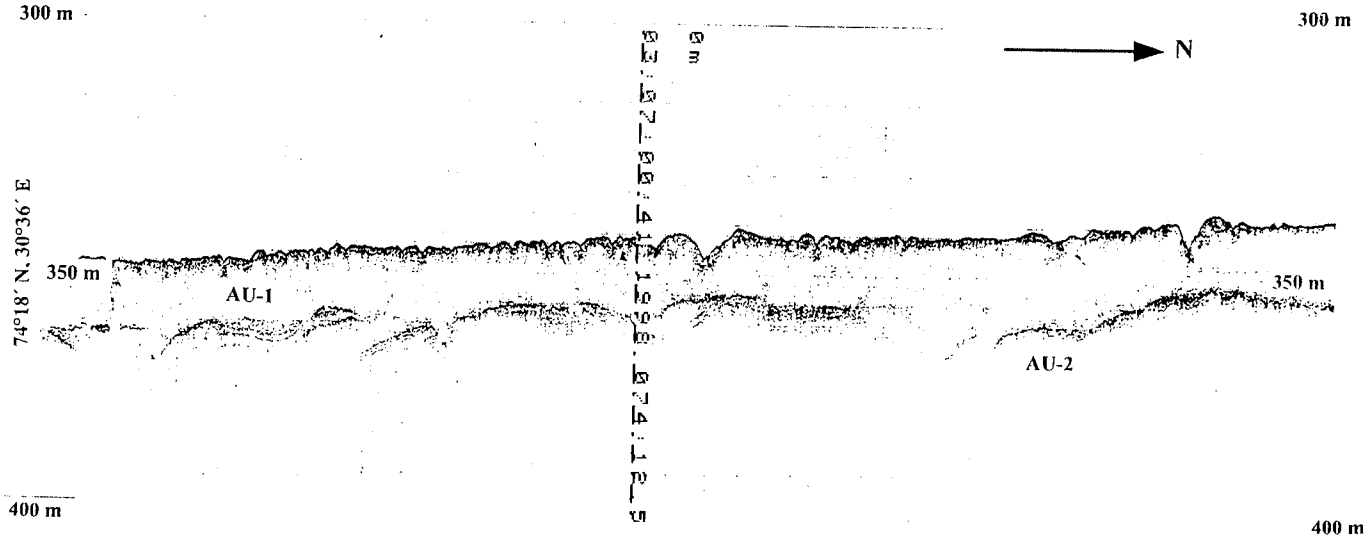

App. 1: Fragment of the PARASOUND record showing two acoustic units on the Barents Shelf. Note the reflectors at the top of AU-2 which are believed to coincide with slightly deformed Mesozoic rocks (DESO roll No. 1).

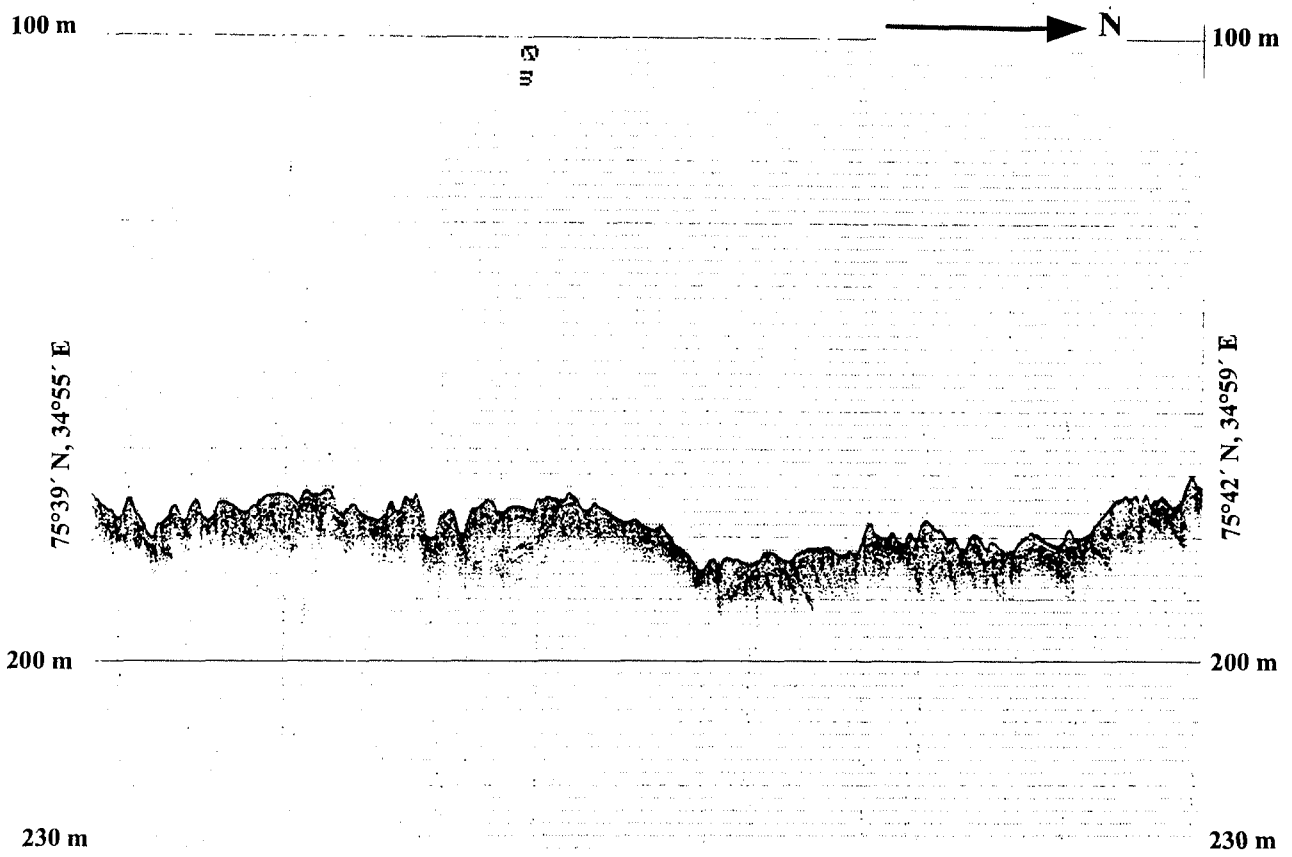

App. 2: Fragment of the PARASOUND record (DESO roll No. 1) showing a character of the sea-bottom of the Barents shelf in area of the exposed Mesozoic bed-rocks. The steep reflectors at the top of AU-2 are suggested to represent deformed Mesozoic complexes.

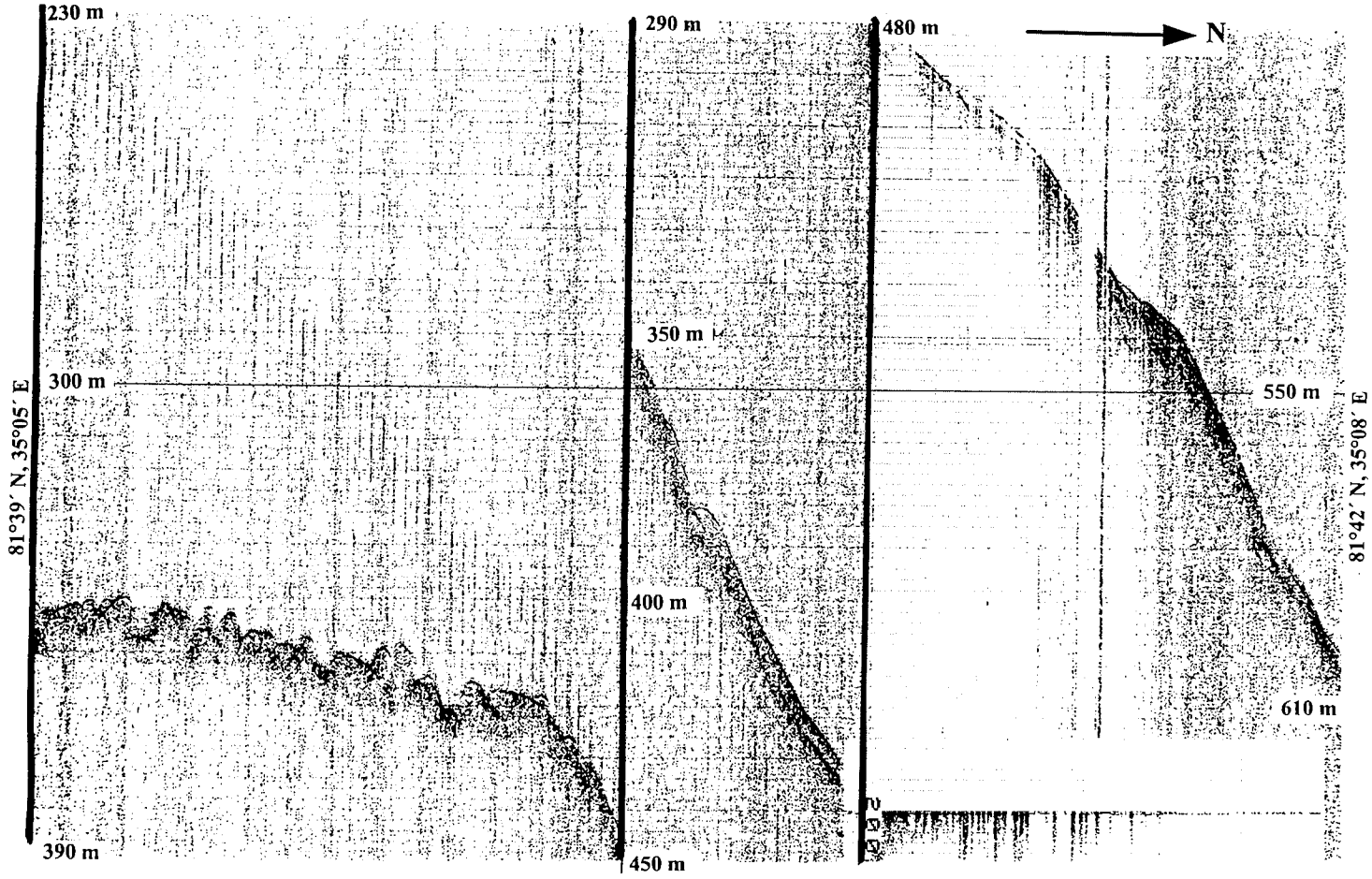

App. 3: Fragment of the PARASOUND record from transition area between shelf and slope of the Barents continental margin (DESO roll No. 2). Slump structures can be seen on the slope.

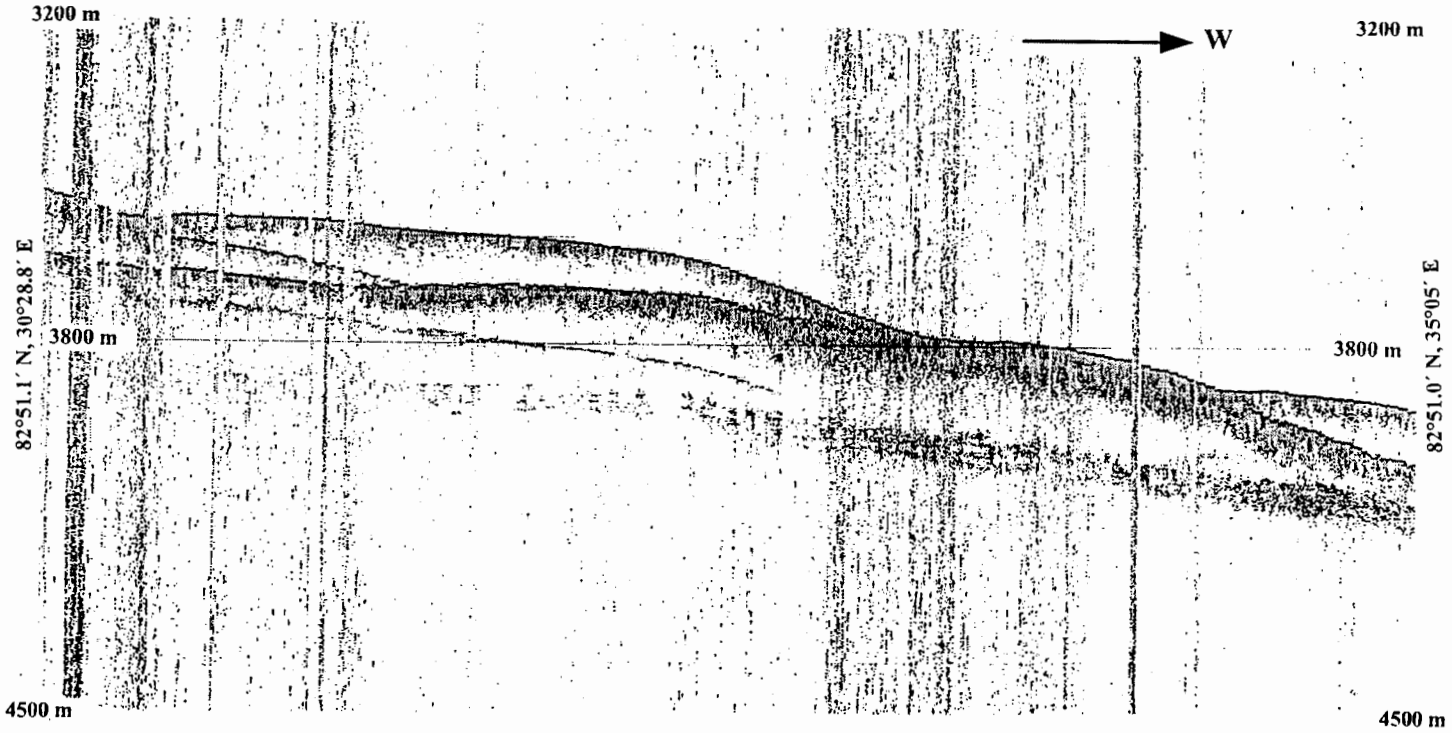

App. 4: Fragment of the PARASOUND record from area of the continental rise of the Barents passive margin (DESO roll No. 3). Four individual lens-shaped fan levees are well-distinguished.

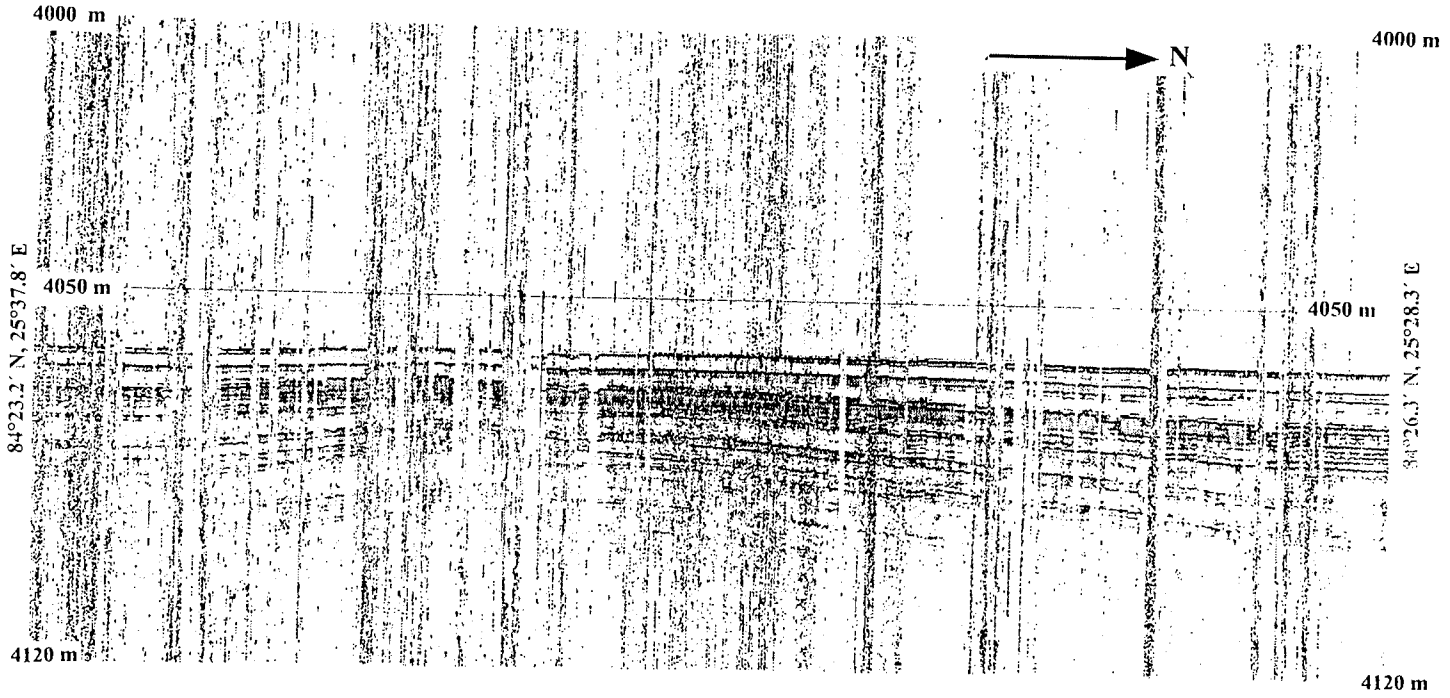

App. 5: Fragment of the PARASOUND record from Nansen oceanic basin (DESO roll No. 4). Sub-bottom sediments are well-layered and are considered to consist of the distal turbidites. Note an uplifting of the lower strata.

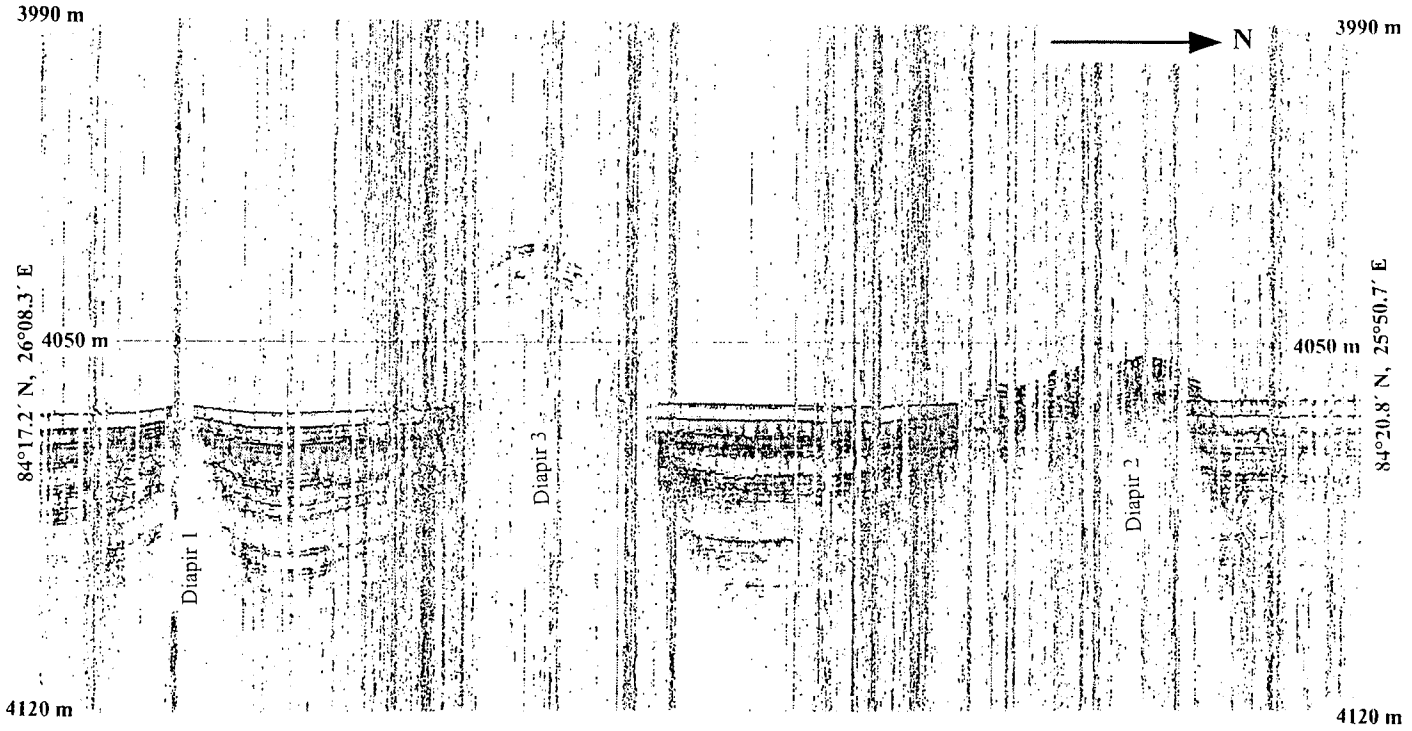

App. 6: Fragment of the PARASOUND record from Nansen oceanic basin (DESO roll No. 4) showing three specific features which are considered to represent the mud-cored diapirs.

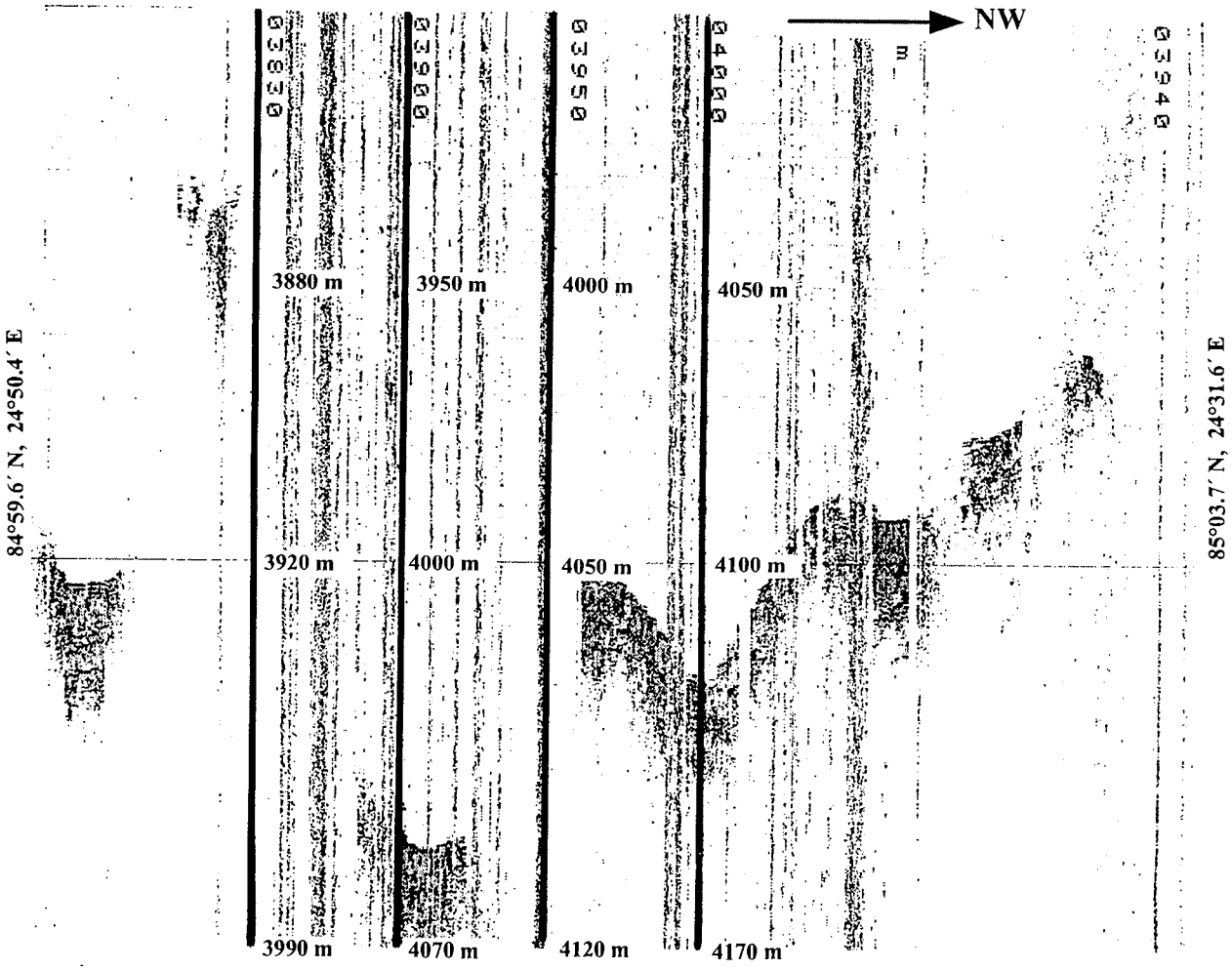

App. 7: An example of poor PARASOUND record from area of the Gakkel Ridge (DESO roll No. 5).
One can see very complicated morphology and thin nonstratified sediments characterized by high reflectivity.

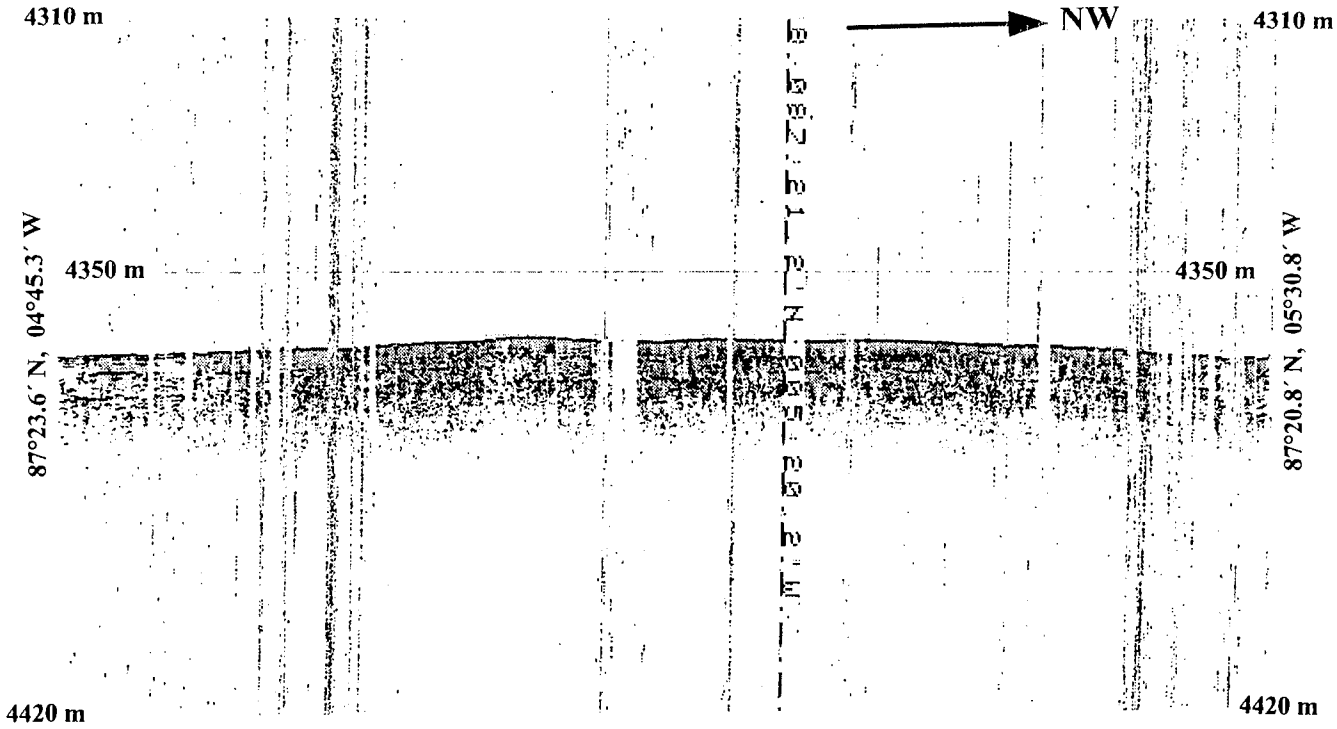

App. 8: Fragment of the PARASOUND record showing acoustic pattern of sub-bottom sediments in the Amundsen oceanic basin (DESO roll No. 5).

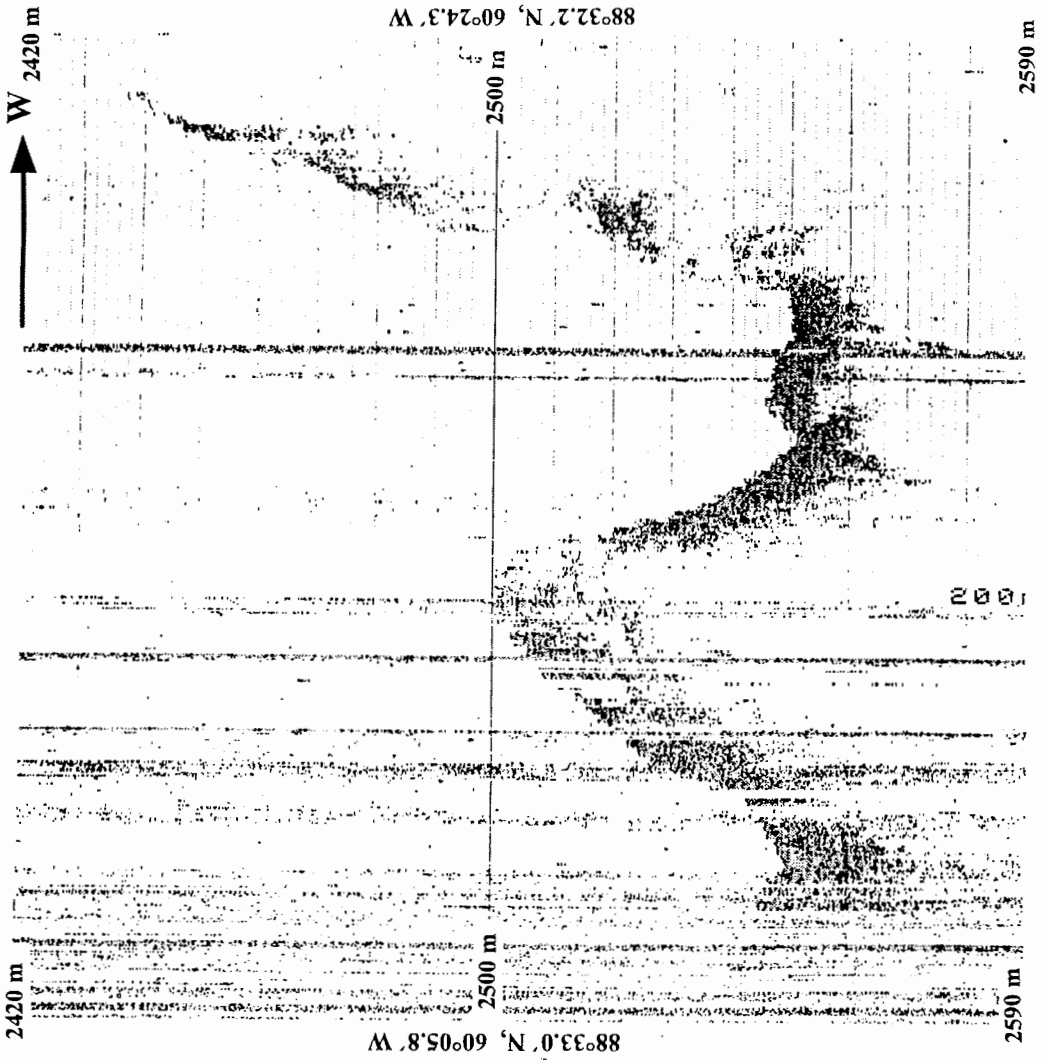

App. 9: An example of poor PARASOUND record from area of the western Eurasia-faced Lomonosov Ridge (DESO roll No. 6). The acoustic expression of the sub-bottom sediments is very similar to those recorded in area of the Gakkel Ridge.

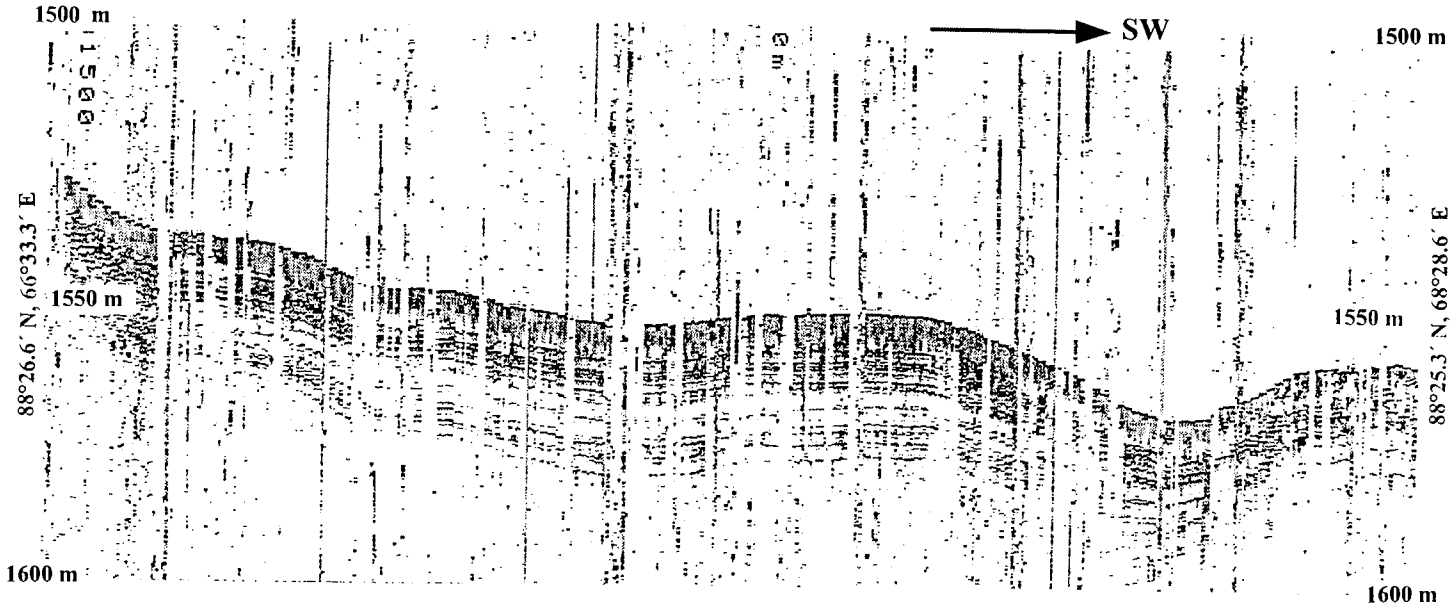

App. 10: Fragment of the PARASOUND record showing an acoustic pattern from crestal part of the western Lomonosov Ridge (DESO roll No. 6). One can notice a flat relief and an occurrence of the well-stratified sediments.

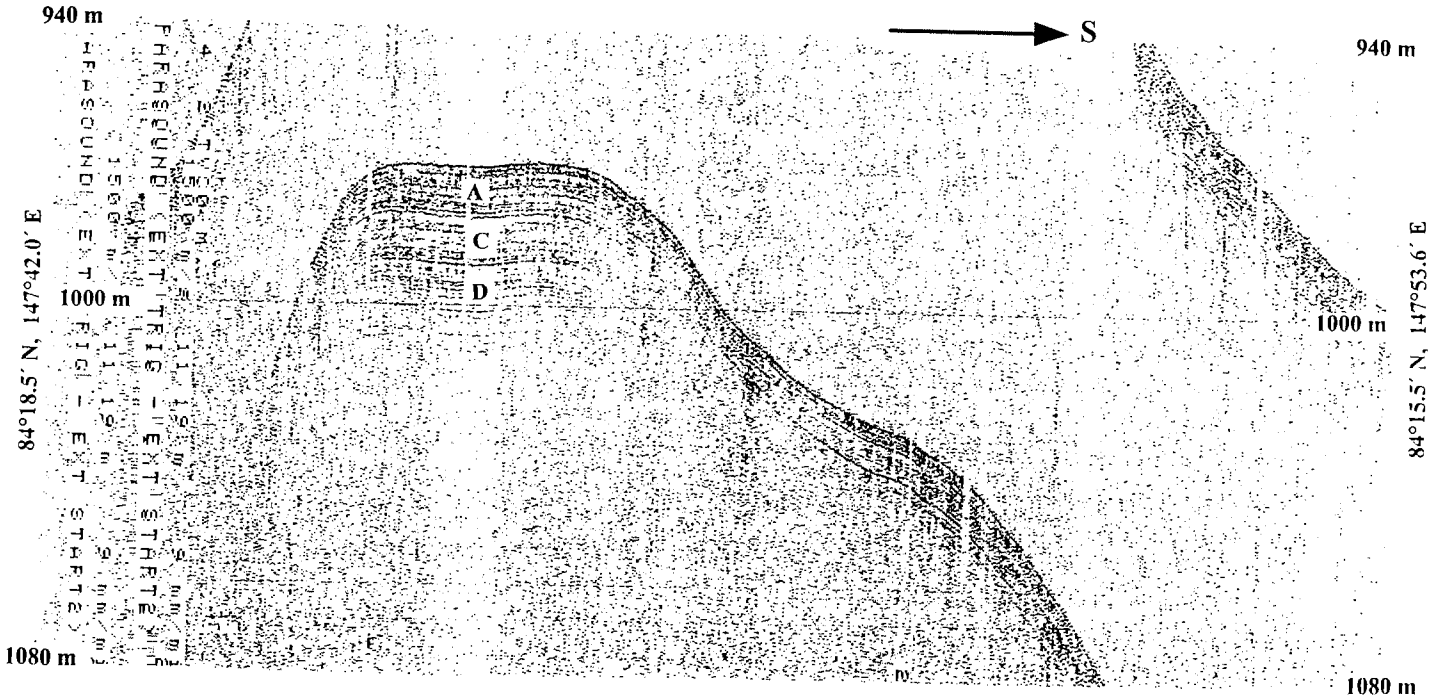

App. 11: Fragment of the PARASOUND record from a crestal part of the eastern Lomonosov Ridge (DESO roll No. 10). The 50 m thick sedimentary succession is suggested to consist of three individual units.

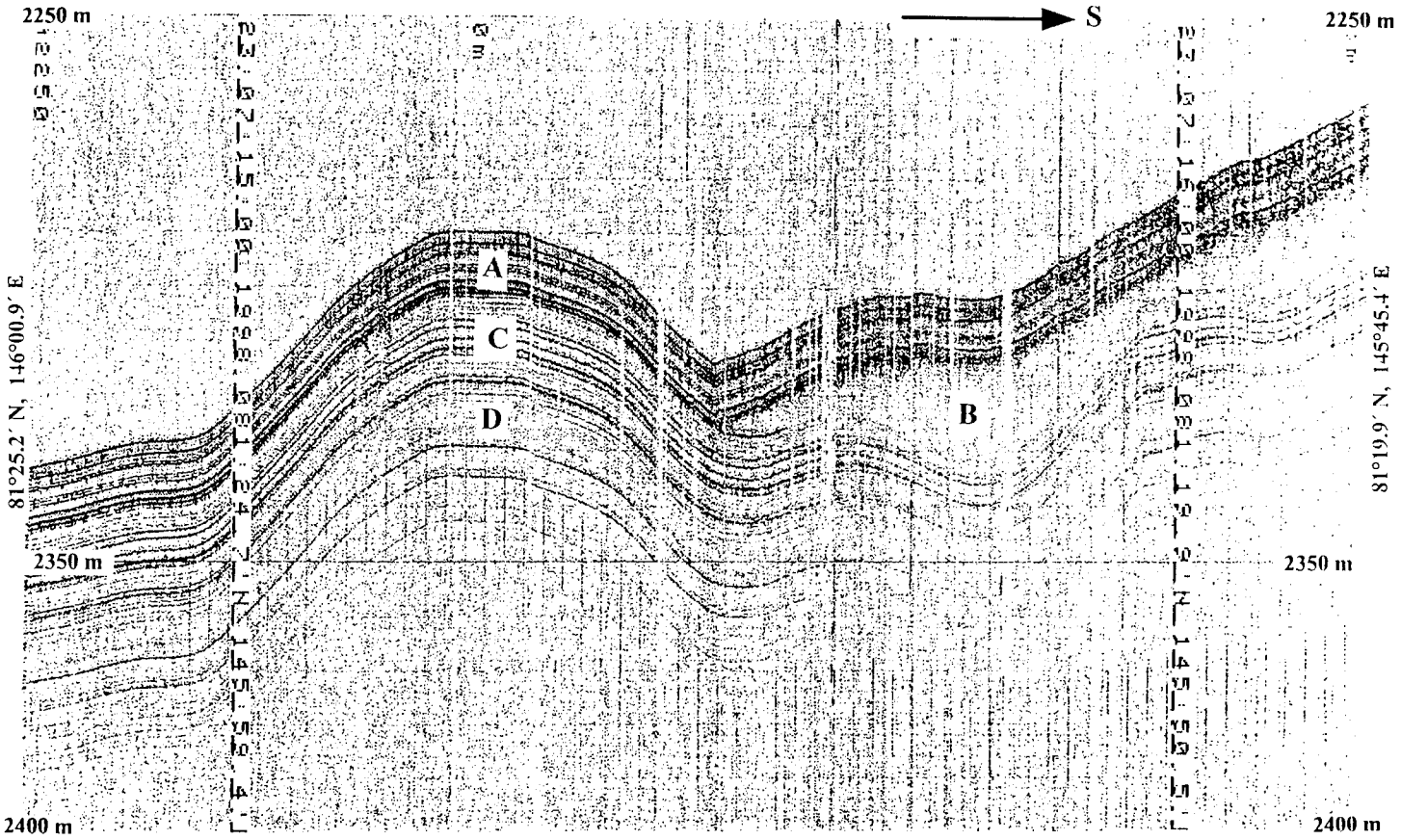

App. 12: Fragment of the PARASOUND record from eastern Lomonosov Ridge (DESO roll No. 12) showing a presence of four individual pronounceable-stratified sedimentary units. Note the sharp unconformity at the base of unit „A„.

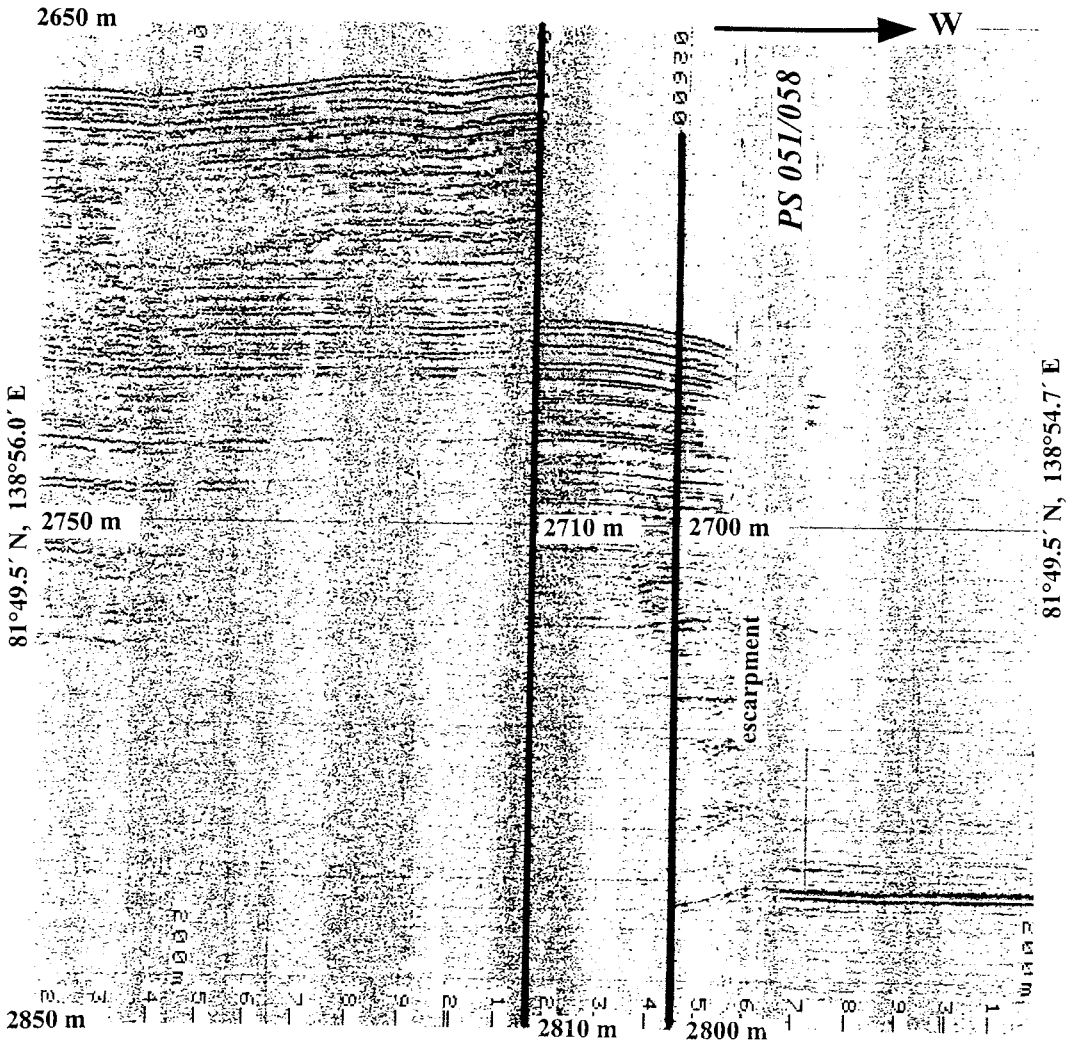

App. 13: Fragment of the PARASOUND record from an area of western escarpment of the eastern Lomonosov Ridge (DESO roll No. 11) illustrating the occurrence of more than 110 m thick sedimentary succession at the geological station PS 051/058.

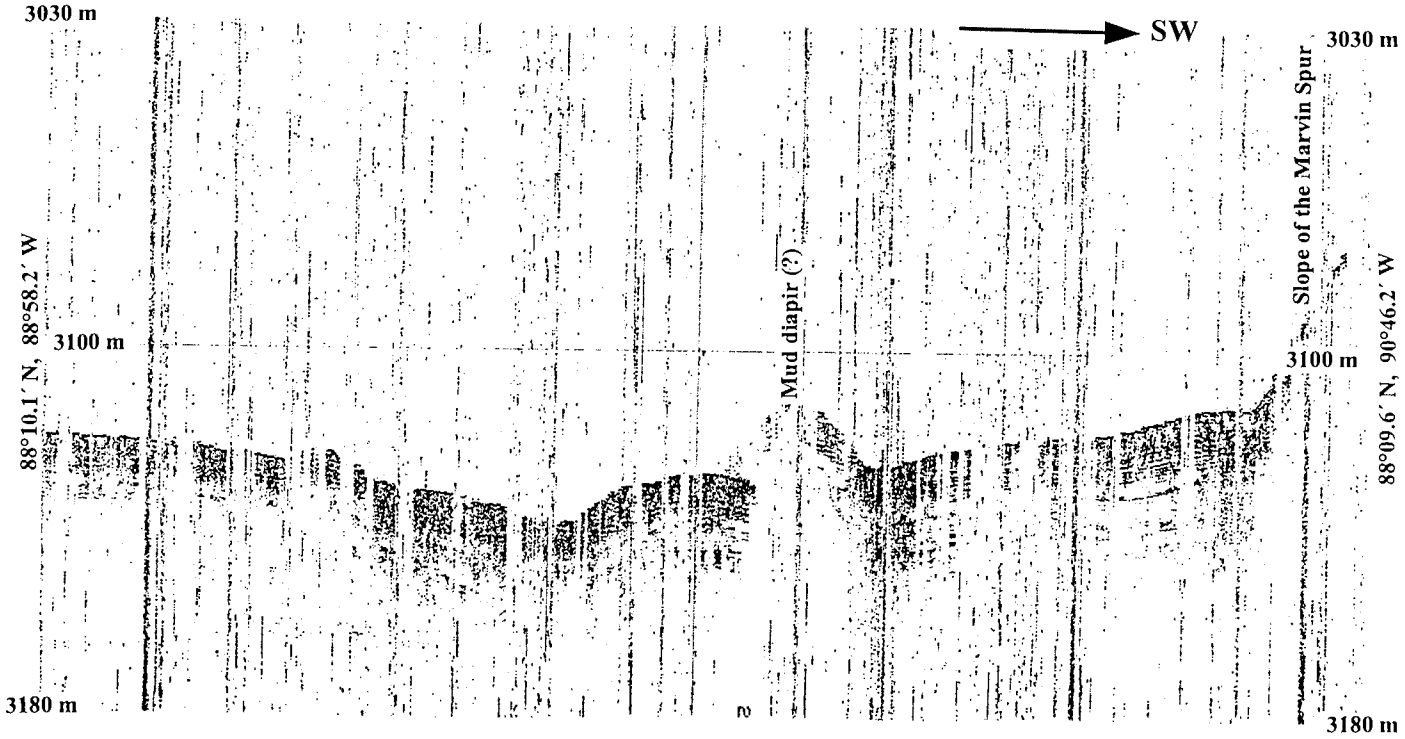

App. 14: Fragment of the PARASOUND record from an area of the Makarov Basin between the Lomonosov Ridge and Marvin Spur (DESO roll No. 6). There is an positive feature in central part of the section inferred to be a mud-cored diapir. One can note a similarity between acoustic pattern of the sediments of the Makarov and Amundsen basins.

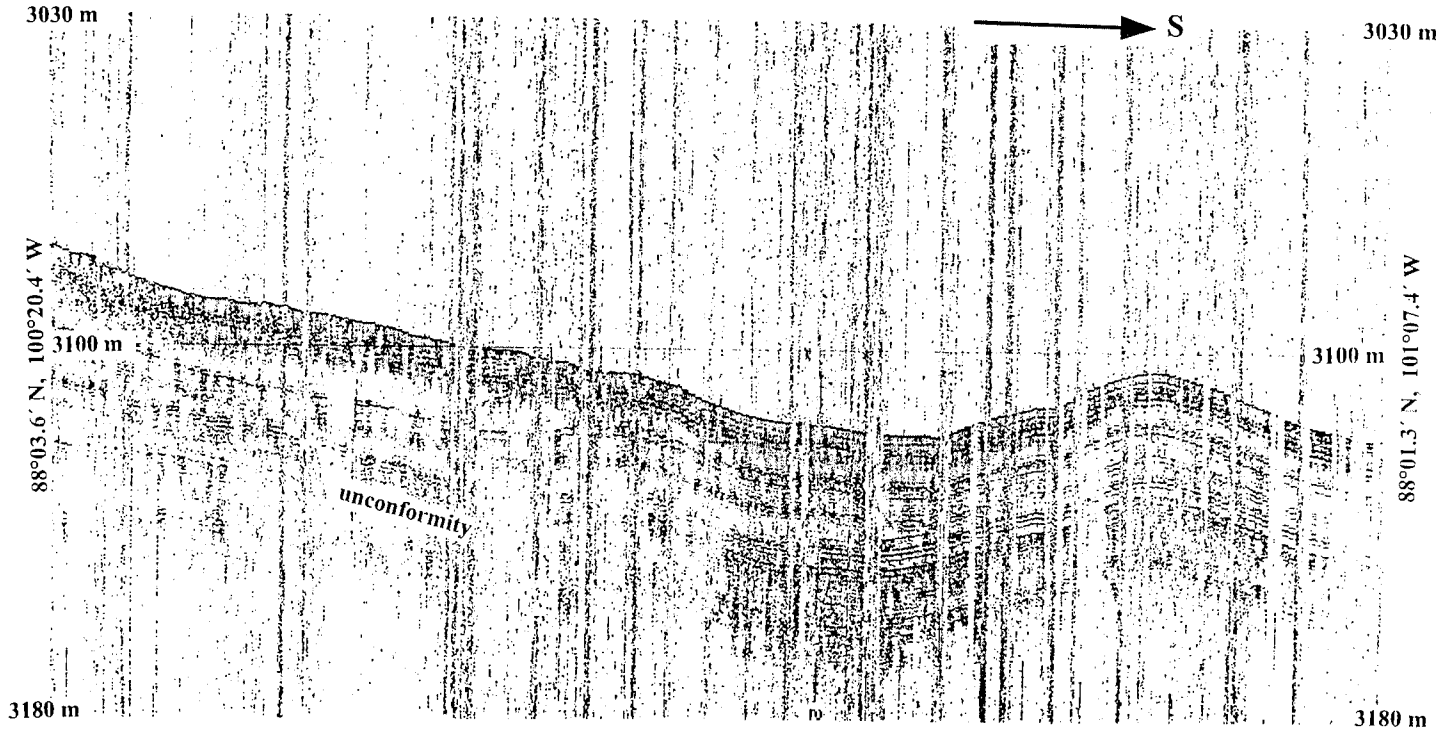

App. 15: Fragment of the PARASOUND record from an area of the Makarov Basin between the Marvin Spur and Alpha Ridge (DESO roll No. 6) showing 50 m thick well-stratified sedimentary unit. Note an unconformity below this unit in the left part of the fragment.

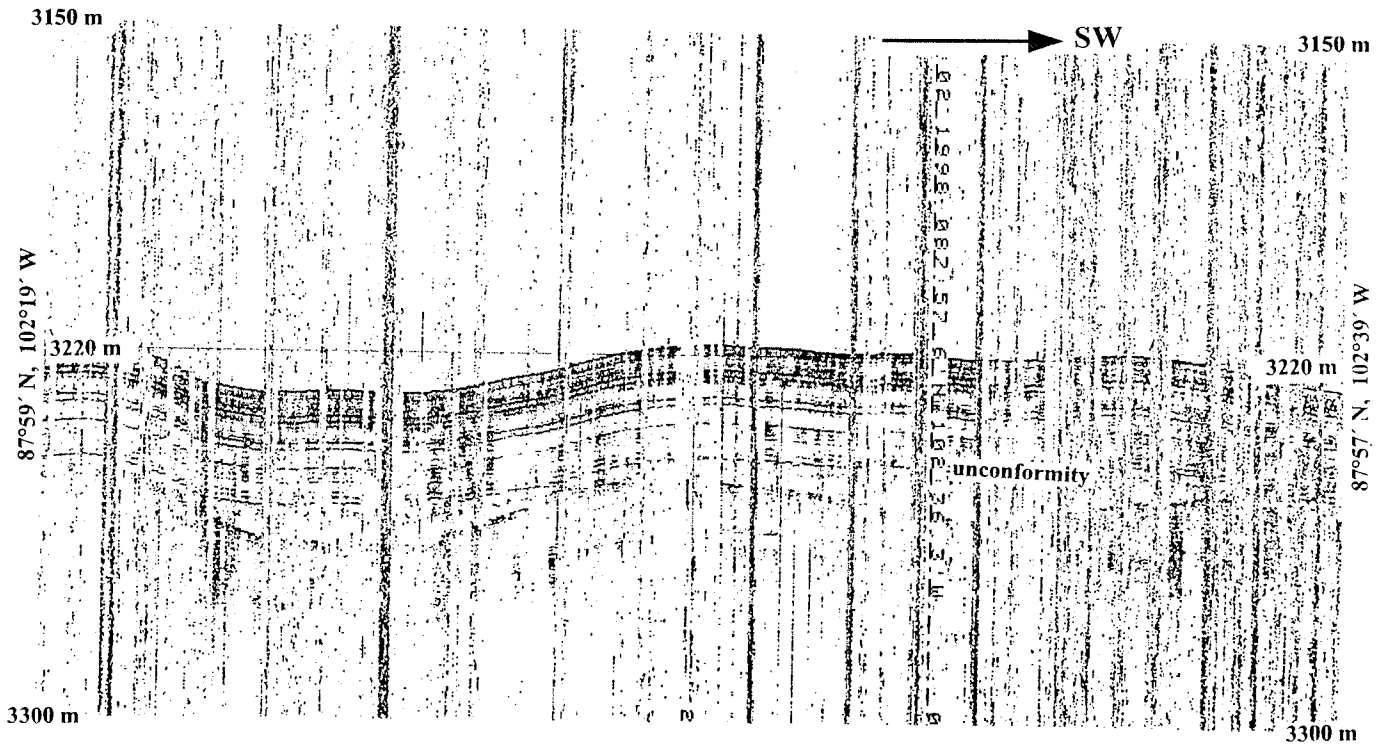

App. 16: Fragment of the PARASOUND record from an area of the Makarov Basin between the Marvin Spur and Alpha Ridge (DESO roll No. 6) illustrating well pronounced unconformity below the stratified sedimentary unit.

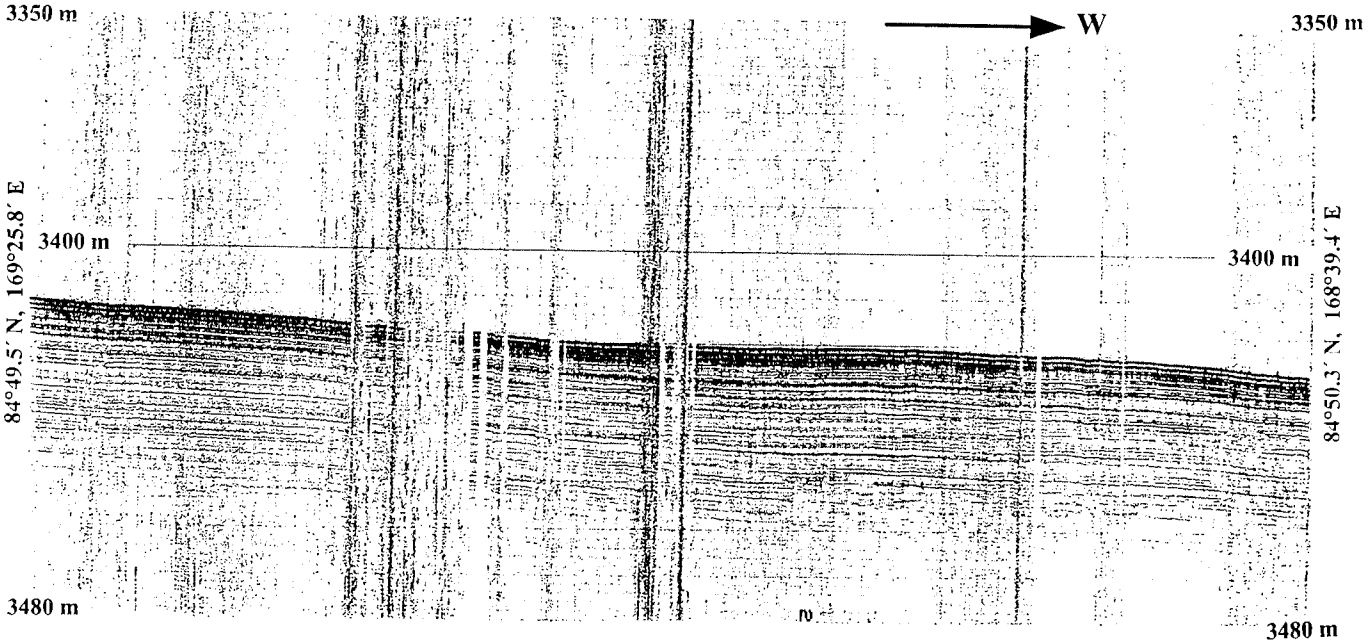

App. 17: Fragment of the PARASOUND record from the eastern Makarov Basin (DESO roll No. 10) showing 50 m thick thin-layered sedimentary unit.

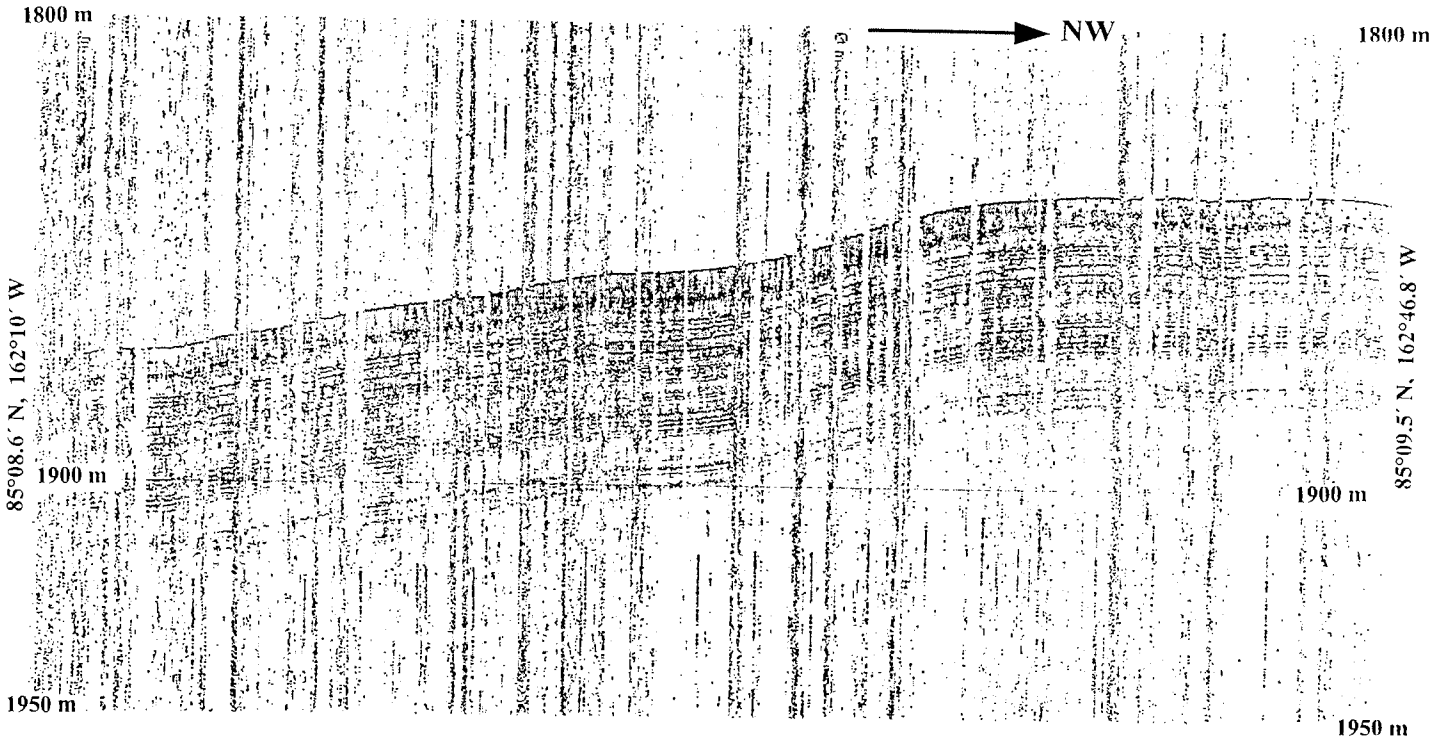

App. 18: Fragment of the PARASOUND record showing an acoustic sub-bottom pattern of eastern slope of the Lyon Sea Mount (Eastern Alpha Ridge; DESO roll No. 8).

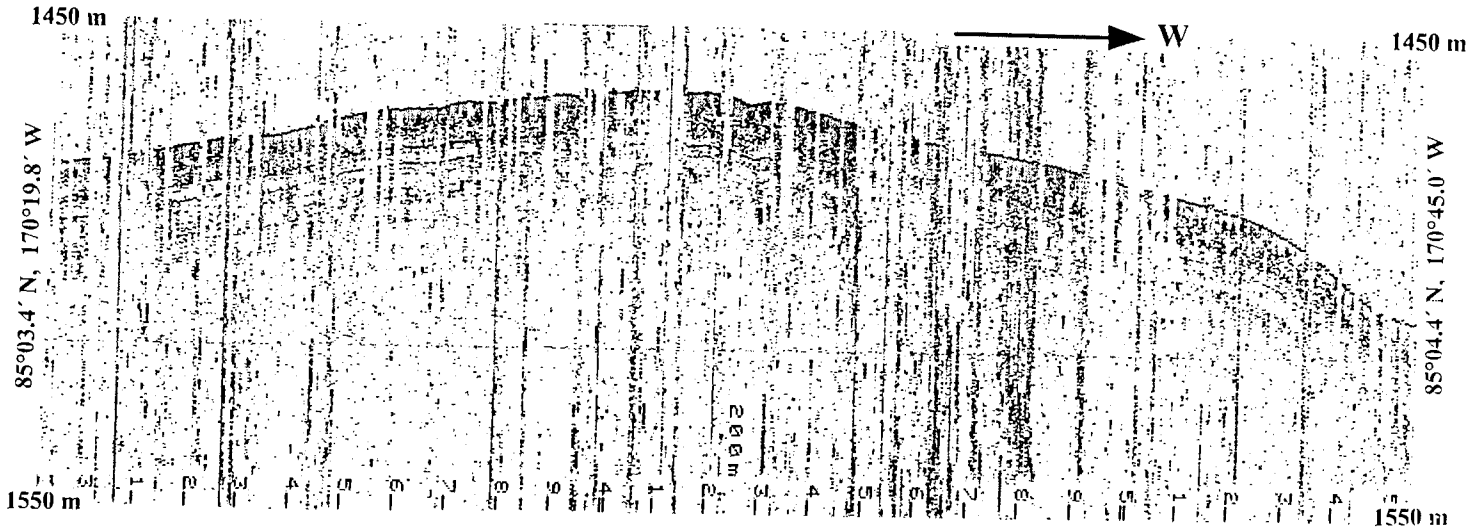

App. 19: Fragment of the PARASOUND record showing an acoustic sub-bottom pattern of the top of Lyon Sea Mount (Eastern Alpha Ridge; DESO roll No. 8).

Legende:

Lithology

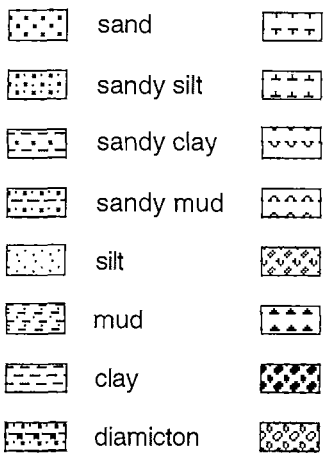

Structure

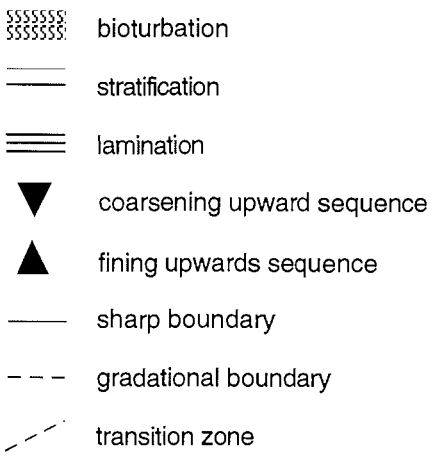

B microfossil barren
N occurrence of nannofossils

PS051/029-1 (GKG) Alpha Ridge **ARK XIV/1a (ARCTIC 98)**

Recovery: 0.40 m 86° 23.1'N 148° 05.8'W Water depth: 2876 m

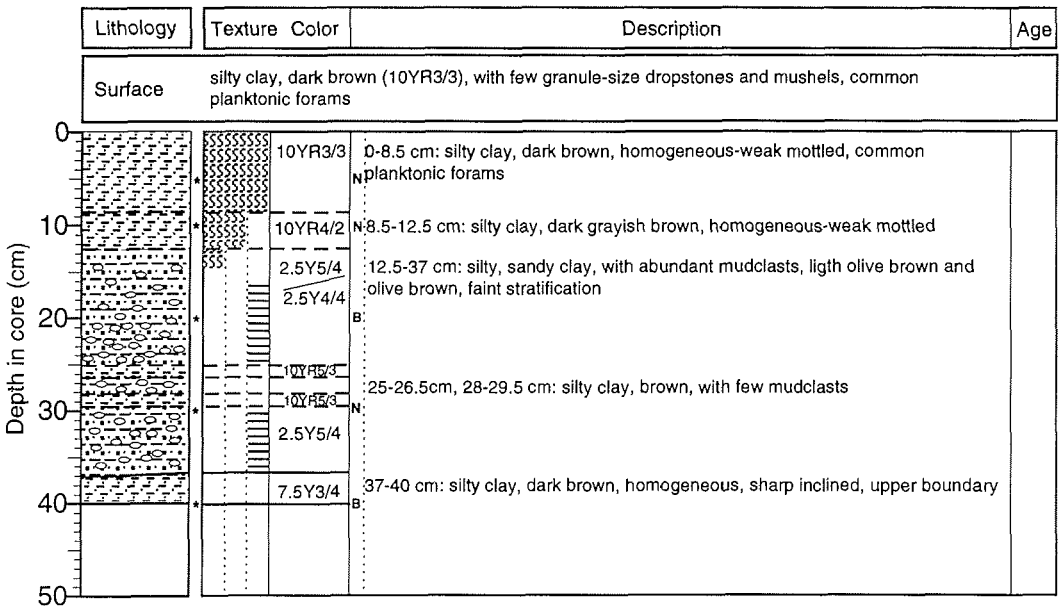

PS51/030-1 (SL) Northern Slope of Alpha Ridge **ARK-XIV/1a**

Recovery: 6.25 m N 86° 22.96´ N, 148° 11.87´ W Water depth: 2869 m

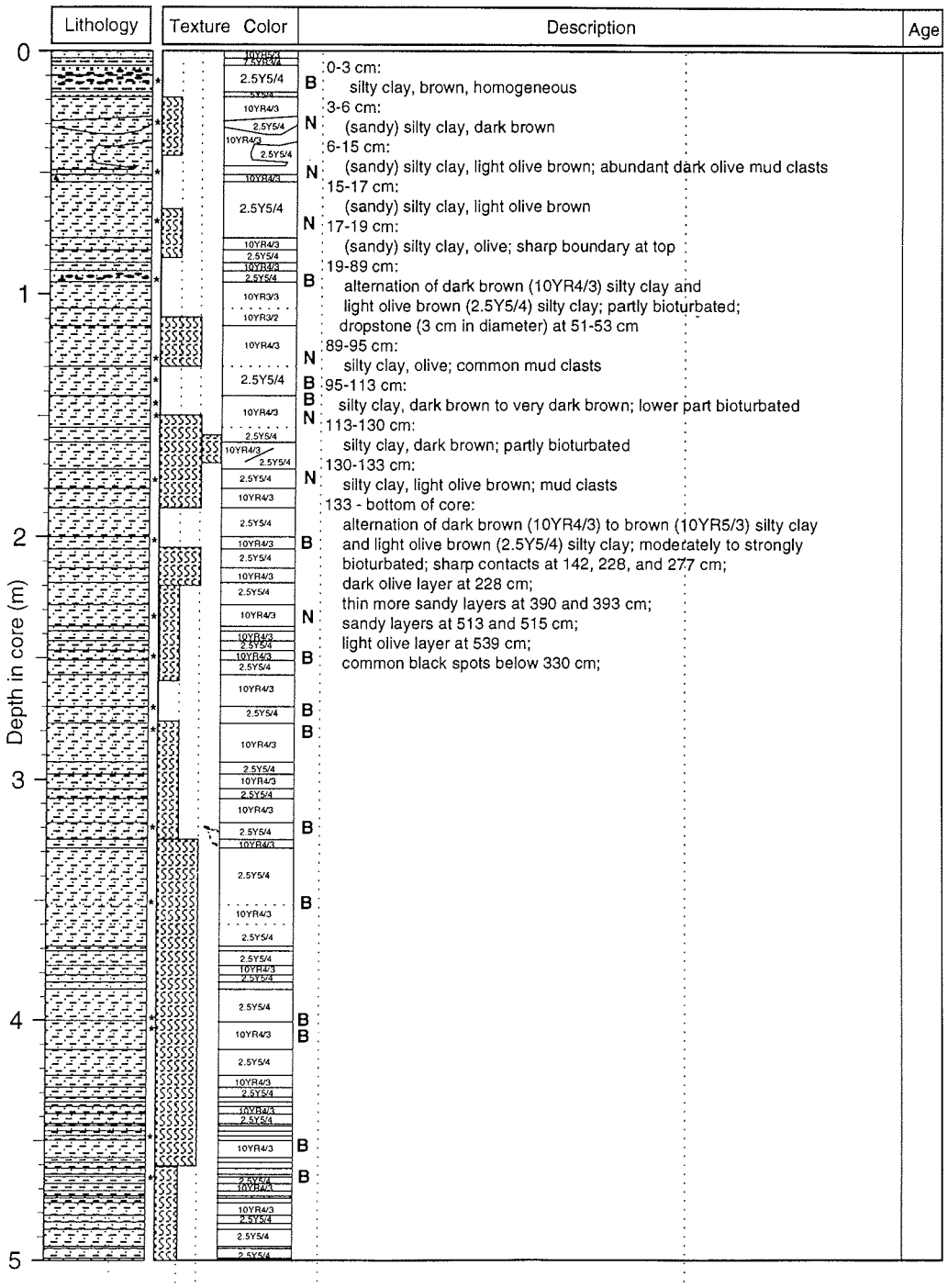

ARK-XIV/1a

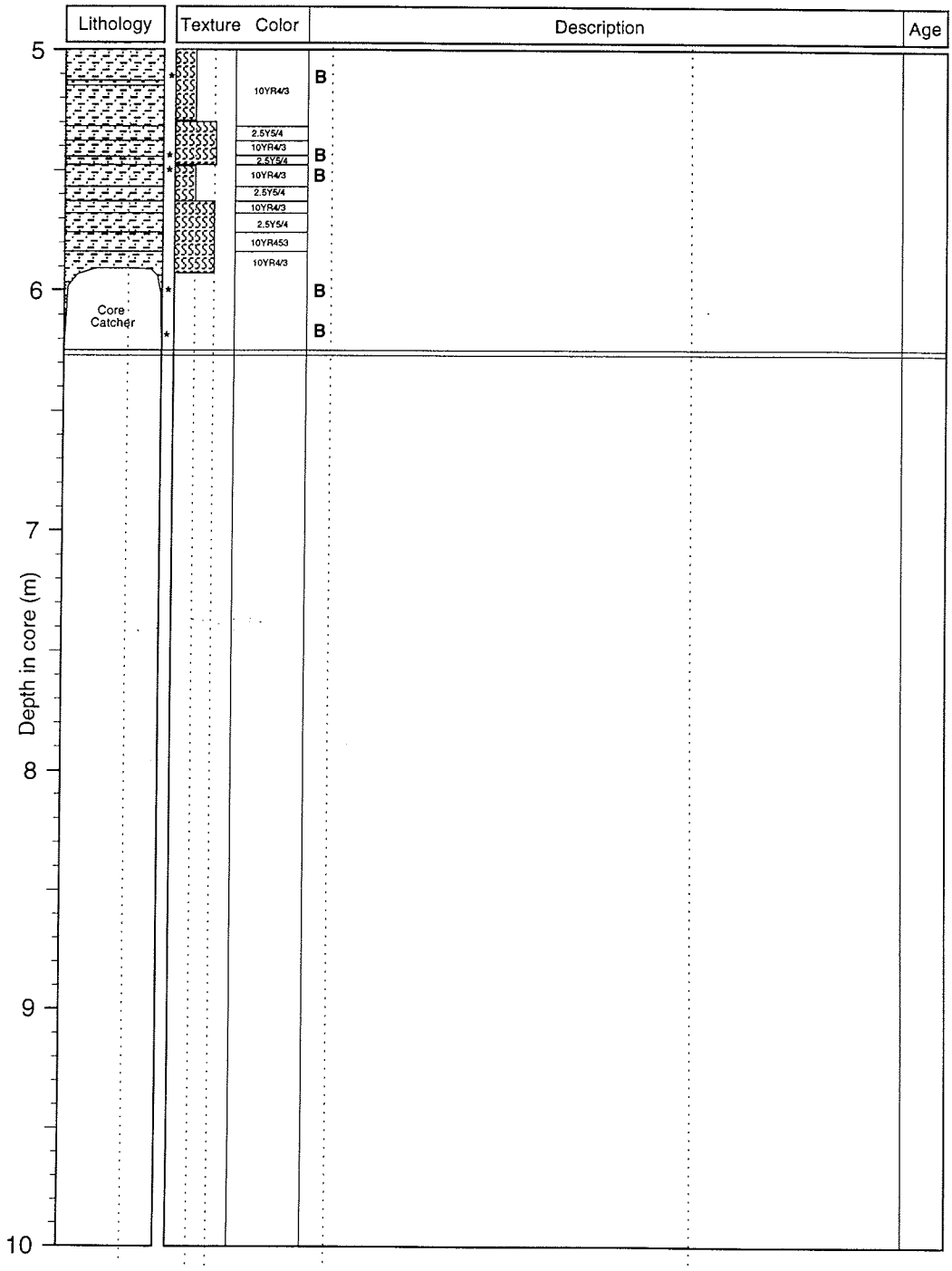
Lithology
Texture
Color
Description
Age
Depth in core (m)
5
6
7
8
9
10
Core Catcher
10YR4/3
2.5Y5/4
10YR4/3
2.5Y5/4
10YR4/3
2.5Y5/4
10YR4/3
2.5Y5/4
10YR453
10YR4/3
B
B
B
B
B

PS51/034-4 (SL) Alpha Ridge **ARK-XIV/1a**

Recovery: 6.0 m 85° 22.58´ N, 155° 27.72´ W Water depth: 2071 m

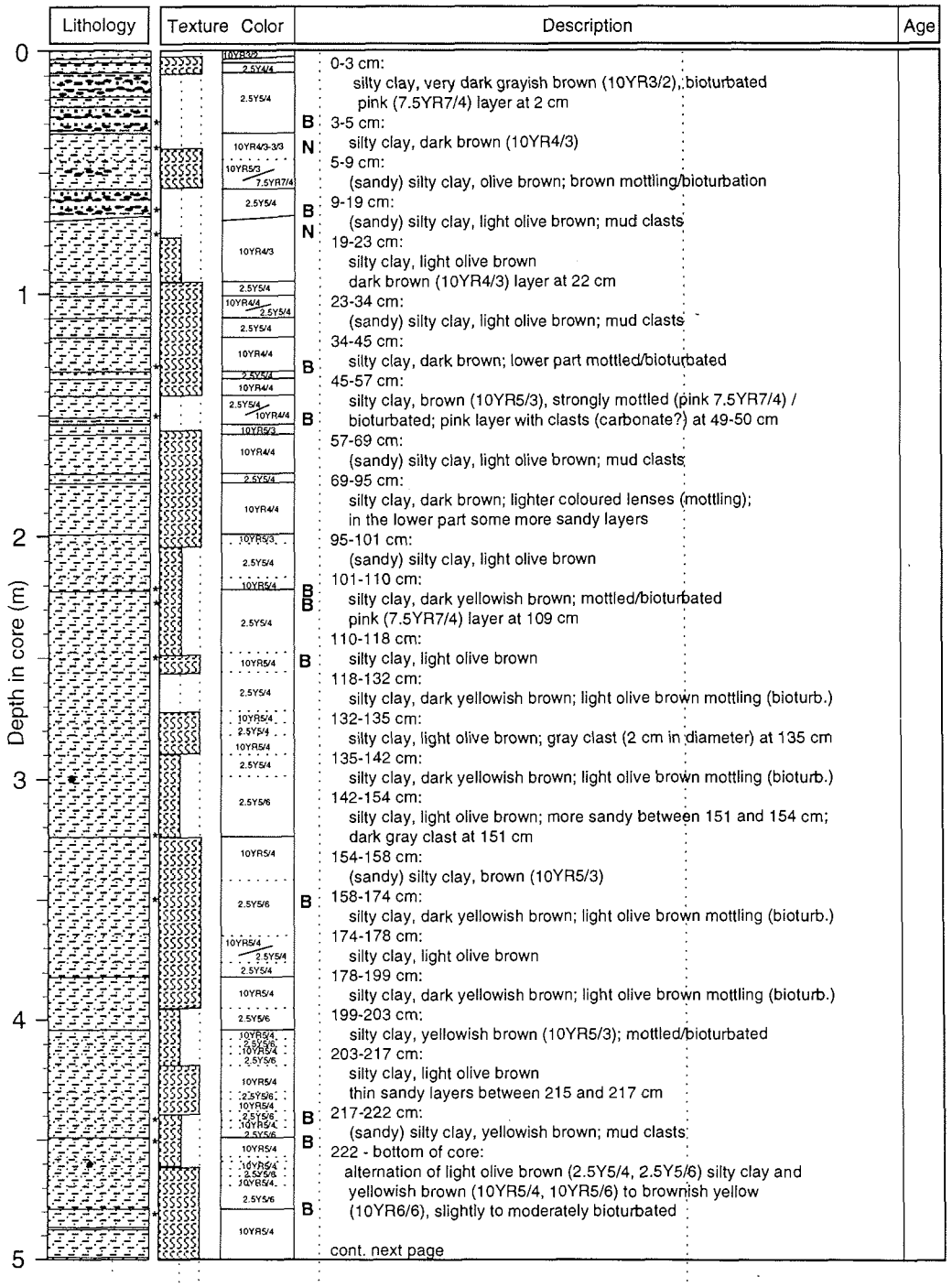

ARK-XIV/1a

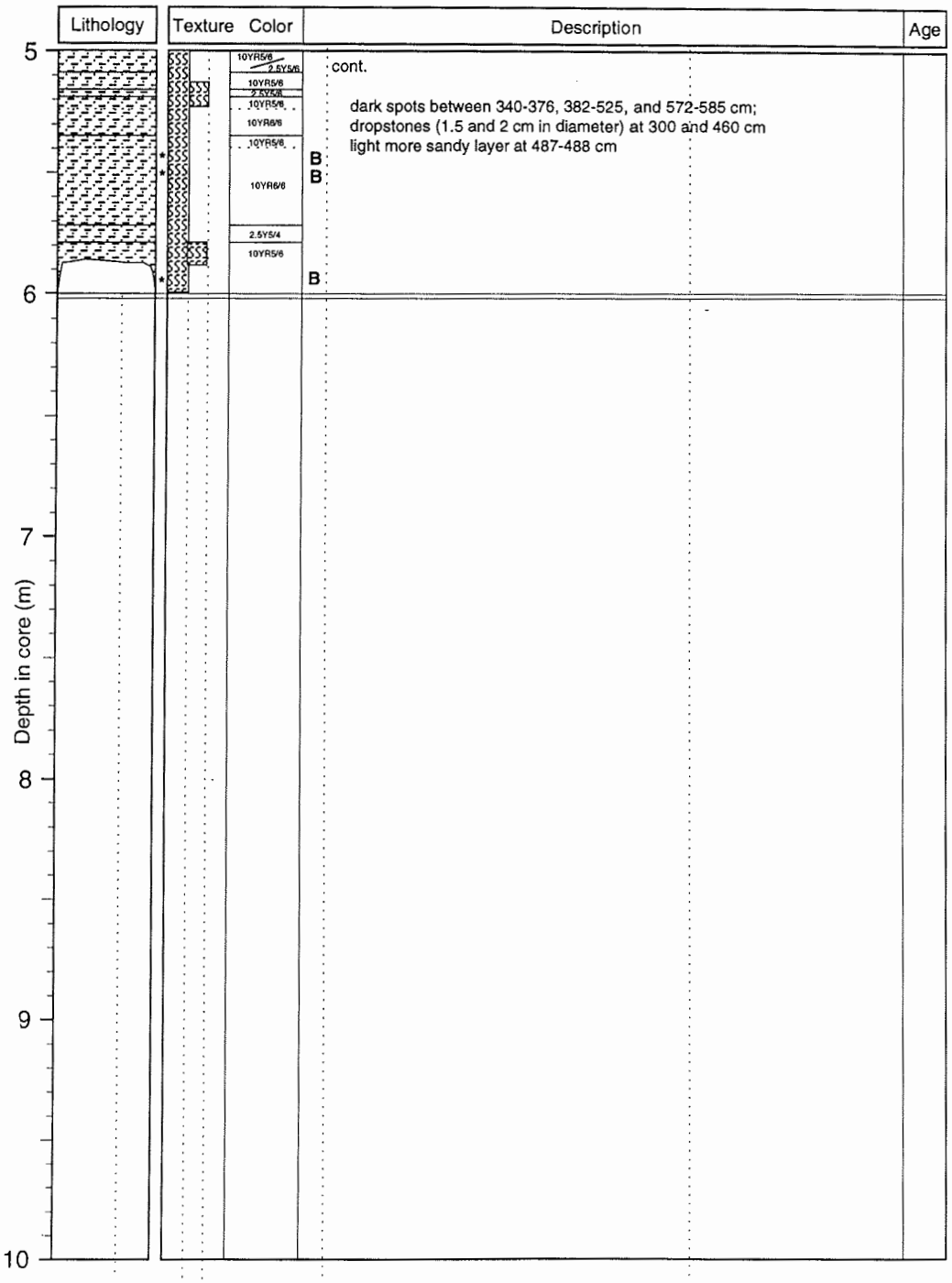
Lithology
Texture
Color
Description
Age
5
6
7
8
9
10
Depth in core (m)
10YR5/6
2.5Y5/6
10YR5/6
2.5Y5/6
10YR5/6
10YR6/6
10YR5/6
10YR6/6
2.5Y5/4
10YR5/6
cont.
dark spots between 340-376, 382-525, and 572-585 cm;
dropstones (1.5 and 2 cm in diameter) at 300 and 460 cm
light more sandy layer at 487-488 cm
B
B
B

PS051/034-5 (GKG) Alpha Ridge **ARK XIV/1a** (ARCTIC 98)

Recovery: 0.36 m 85° 22.7'N 155° 28.4'W Water depth: 2082 m

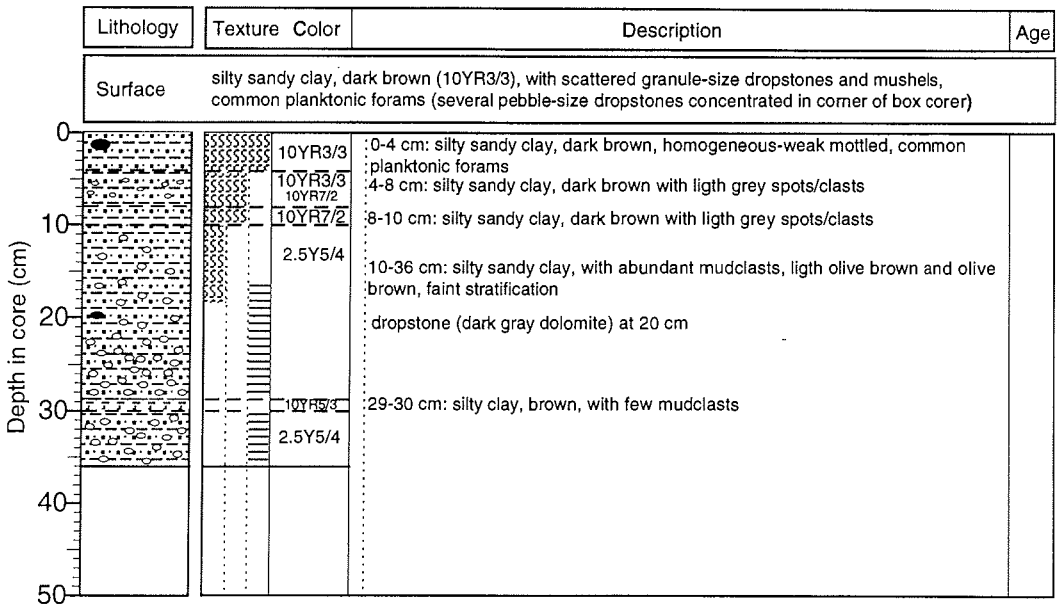

PS051/038-3 (GKG) Alpha Ridge **ARK XIV/1a** (ARCTIC 98)

Recovery: 0.39 m 85° 08.0'N 171° 26.0'W Water depth: 1515 m

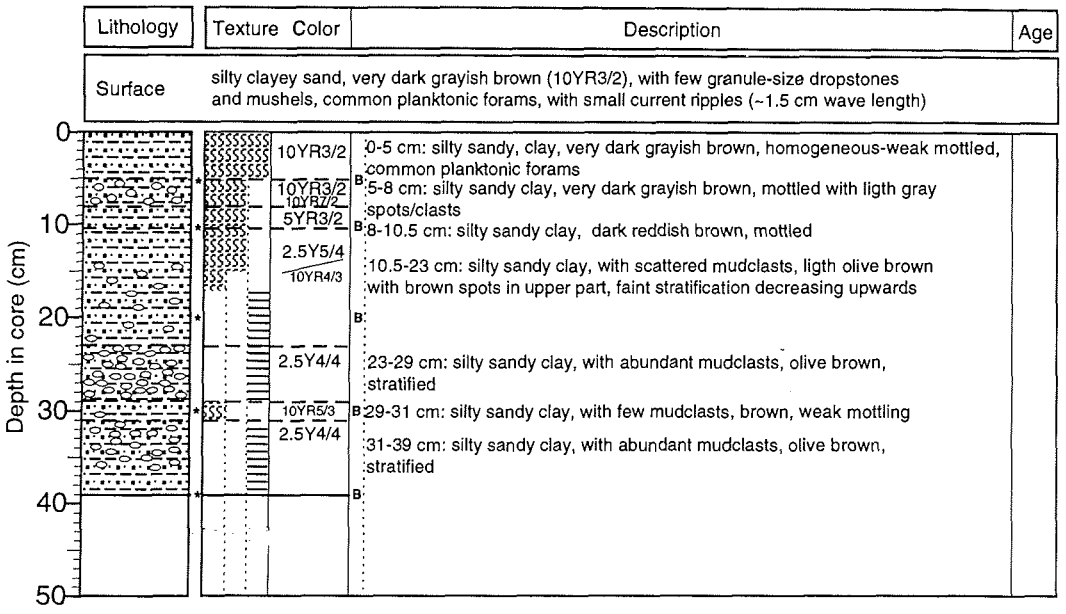

PS51/038-4 (KAL) Northern Slope of Alpha Ridge **ARK-XIV/1a**

Recovery: 7.19 m 85° 08.08´ N, 171° 26.41´ W Water depth: 1473 m

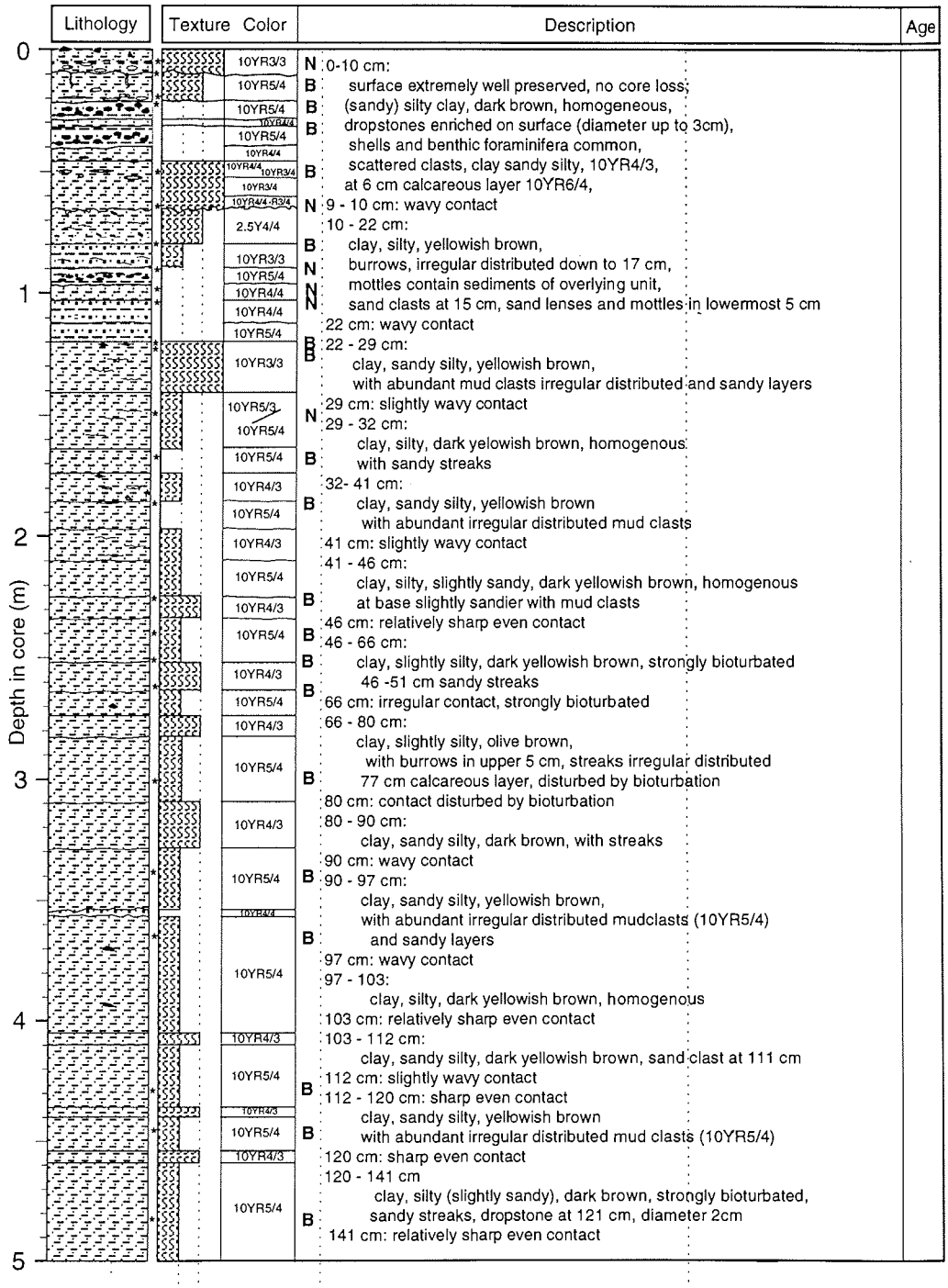

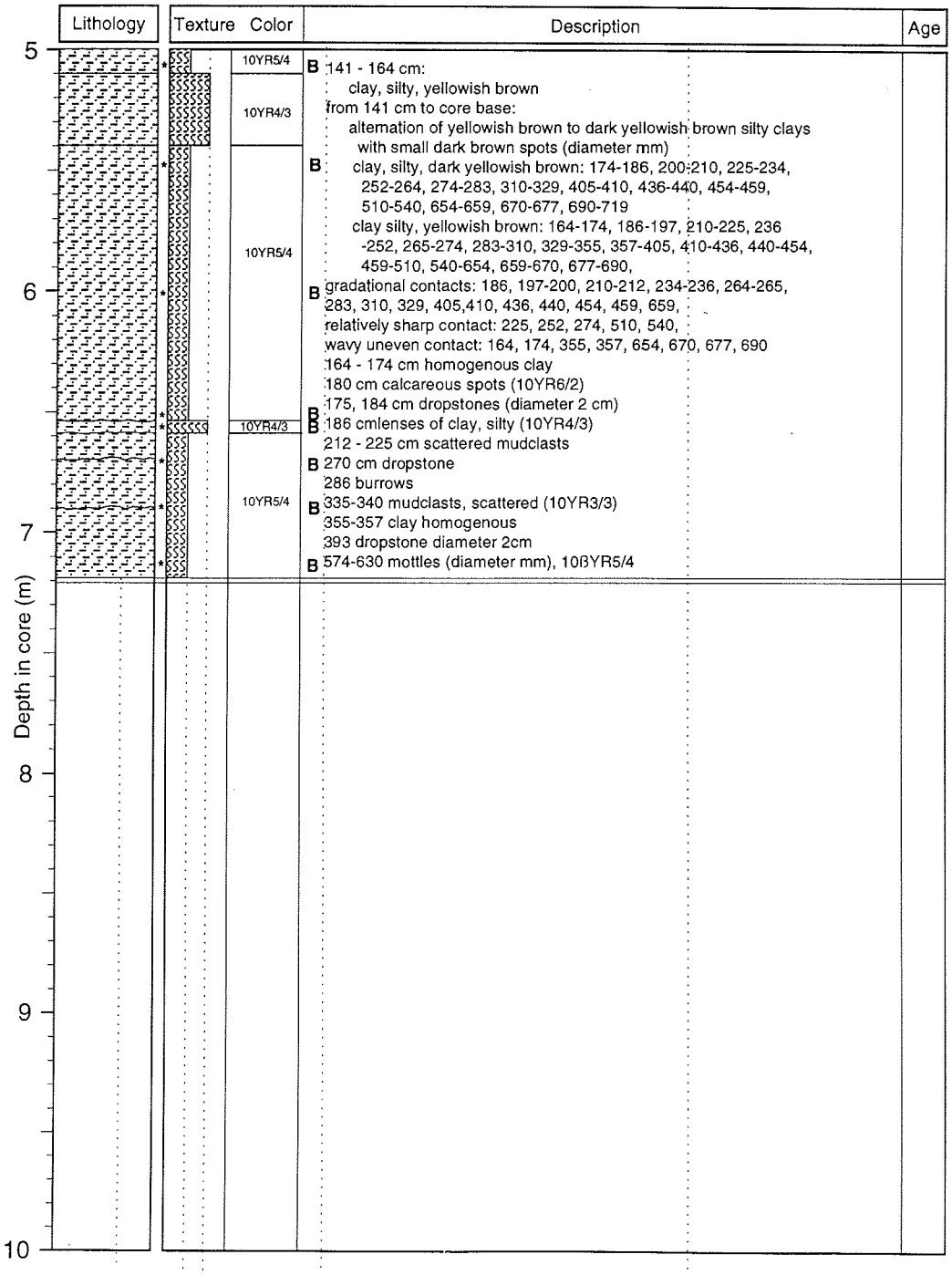
Lithology
Texture
Color
Description
Age
Depth in core (m)
5
6
7
8
9
10
10YR5/4
10YR4/3
10YR5/4
10YR4/3
10YR5/4
B 141 - 164 cm:
clay, silty, yellowish brown
from 141 cm to core base:
alternation of yellowish brown to dark yellowish brown silty clays
with small dark brown spots (diameter mm)
B clay, silty, dark yellowish brown: 174-186, 200-210, 225-234,
252-264, 274-283, 310-329, 405-410, 436-440, 454-459,
510-540, 654-659, 670-677, 690-719
clay silty, yellowish brown: 164-174, 186-197, 210-225, 236
-252, 265-274, 283-310, 329-355, 357-405, 410-436, 440-454,
459-510, 540-654, 659-670, 677-690,
B gradational contacts: 186, 197-200, 210-212, 234-236, 264-265,
283, 310, 329, 405,410, 436, 440, 454, 459, 659,
relatively sharp contact: 225, 252, 274, 510, 540,
wavy uneven contact: 164, 174, 355, 357, 654, 670, 677, 690
164 - 174 cm homogenous clay
180 cm calcareous spots (10YR6/2)
175, 184 cm dropstones (diameter 2 cm)
B
B 186 cmlenses of clay, silty (10YR4/3)
212 - 225 cm scattered mudclasts
B 270 cm dropstone
286 burrows
B 335-340 mudclasts, scattered (10YR3/3)
355-357 clay homogenous
393 dropstone diameter 2cm
B 574-630 mottles (diameter mm), 10ßYR5/4

PS51/040-1 (SL) Graben NW Slope of Alpha Ridge **ARK-XIV/1a**

Recovery: 1.73 m 85° 30.64´ N, 174° 10.20´ W Water depth: 2461 m

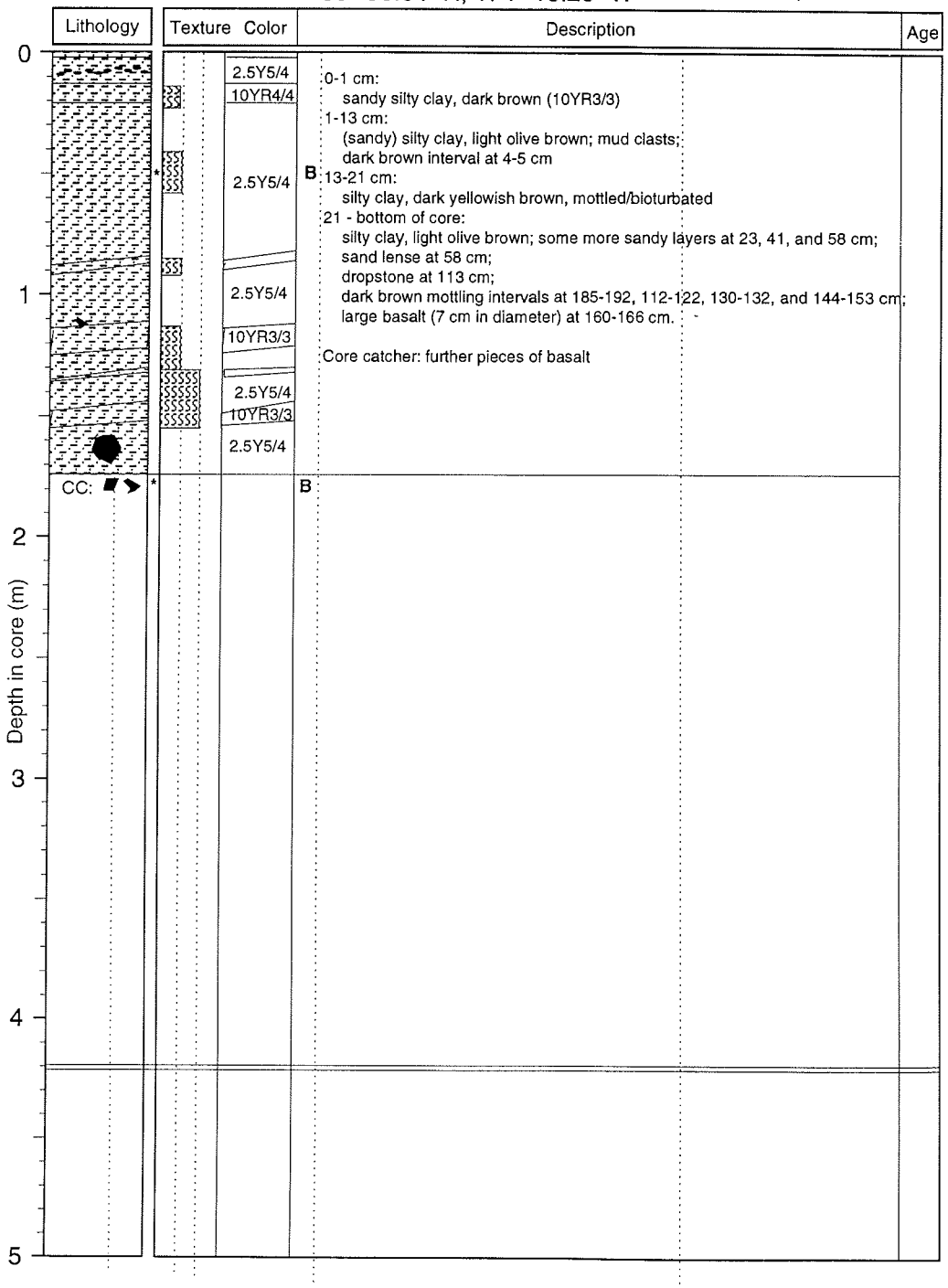

PS051/047-5 (GKG) Alpha Ridge **ARK XIV/1a** (ARCTIC 98)

Recovery: 0.39 m 85° 45.9'N 176.° 54.6'W Water depth: 2453 m

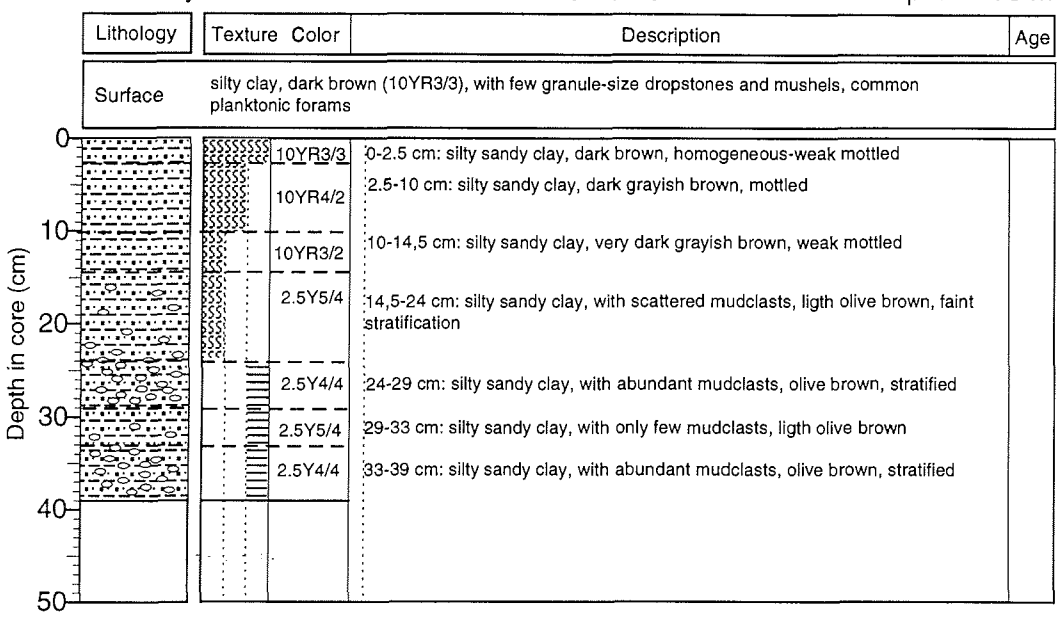

PS051/058-1 (GKG) Lomonosov Ridge **ARK XIV/1a (ARCTIC 98)**

Recovery: 0.42 m 83° 33.6'N 144° 50.3'E Water depth: 1298 m

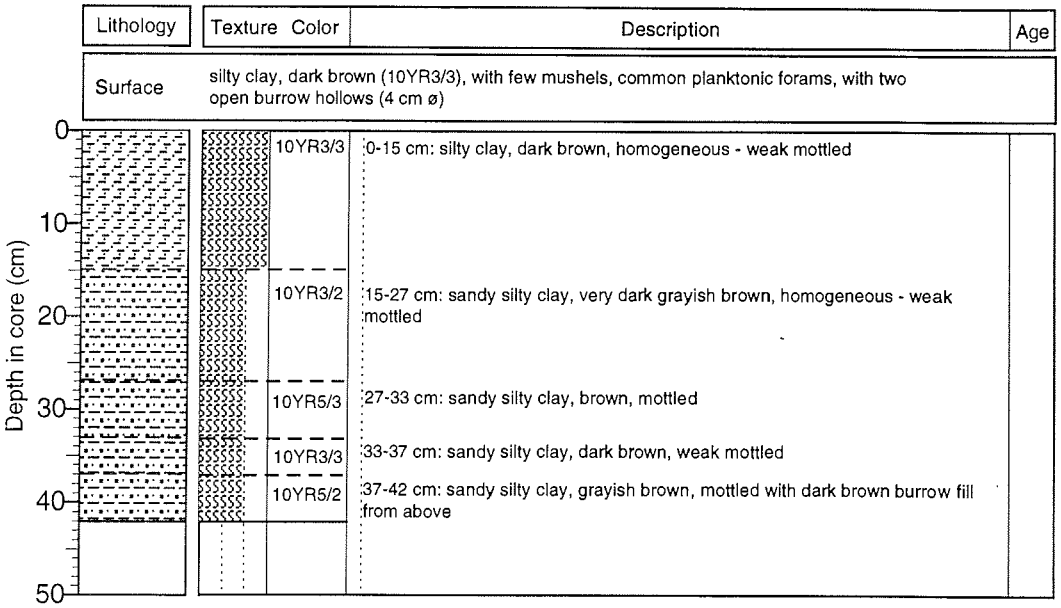

PS51/067-1 (SL) Lomonosov Ridge **ARK-XIV/1a**

Recovery: 1.0 m 81° 50.67´ N, 140° 28.53´ E Water depth: 1594 m

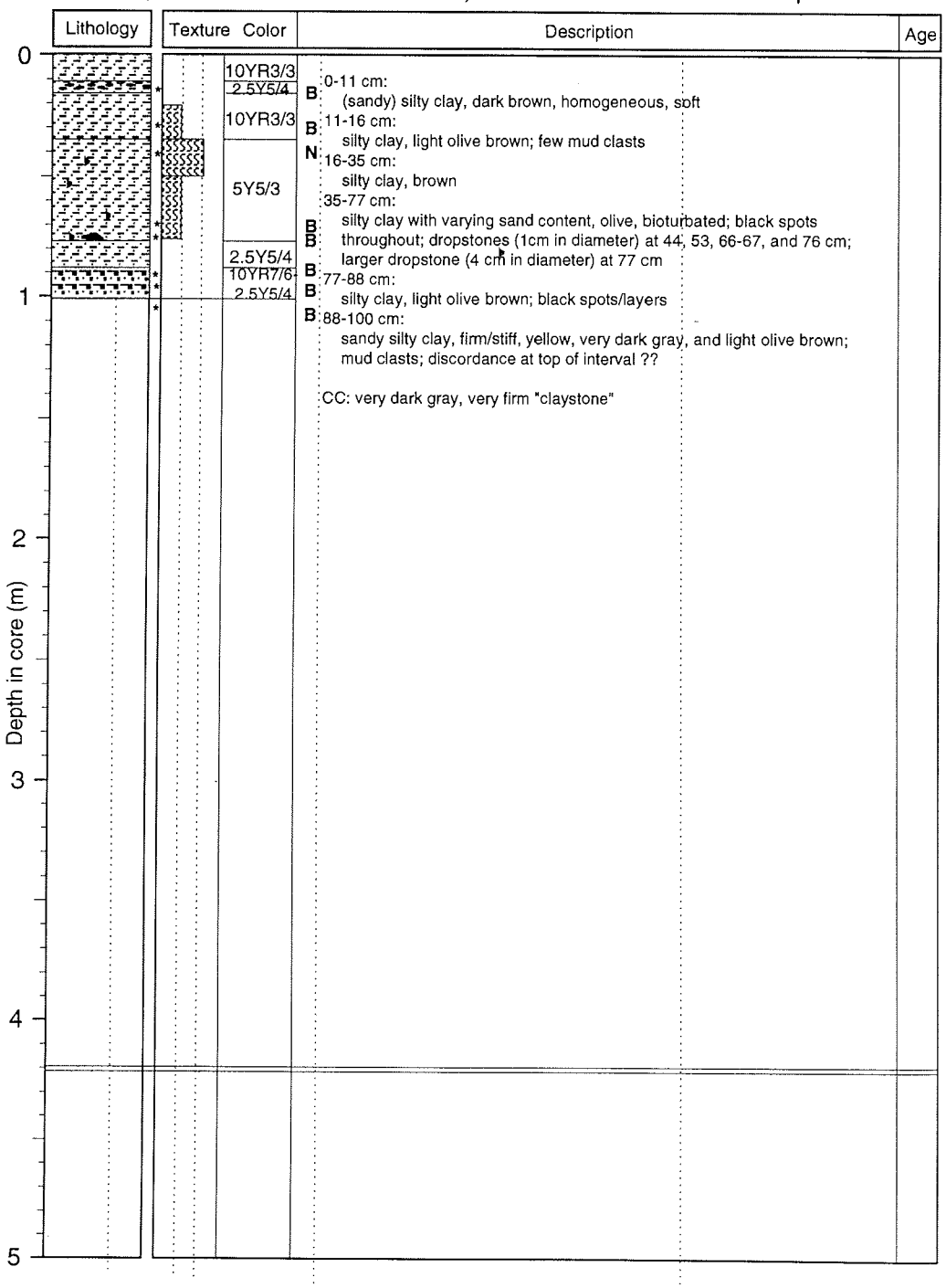

PS51/067-2 (SL) Lomonosov Ridge **ARK-XIV/1a**

Recovery: 3.73 m 81° 49.95´ N, 140° 29.74´ E Water depth: 1514 m

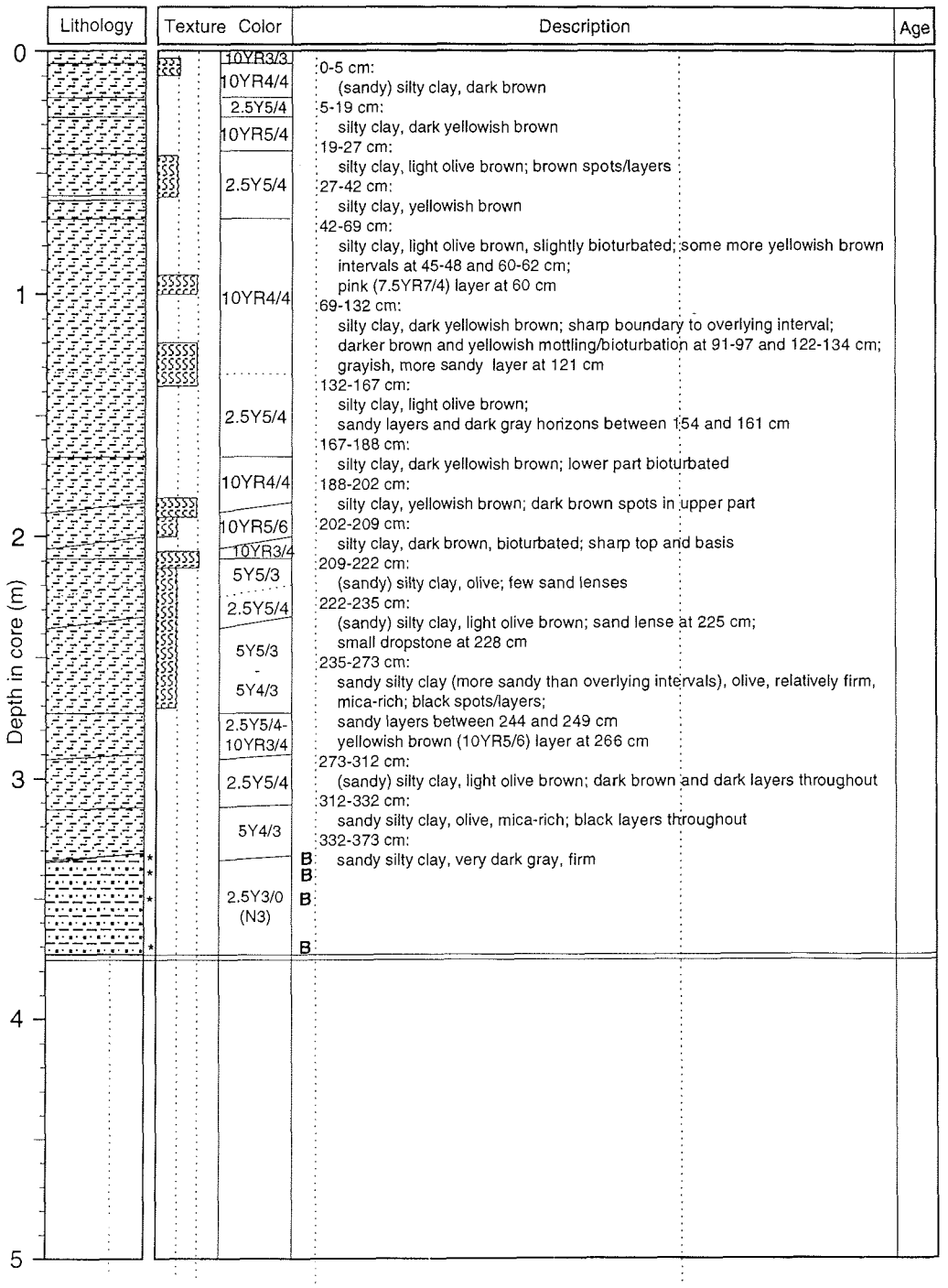

Appendix Core logging graphs

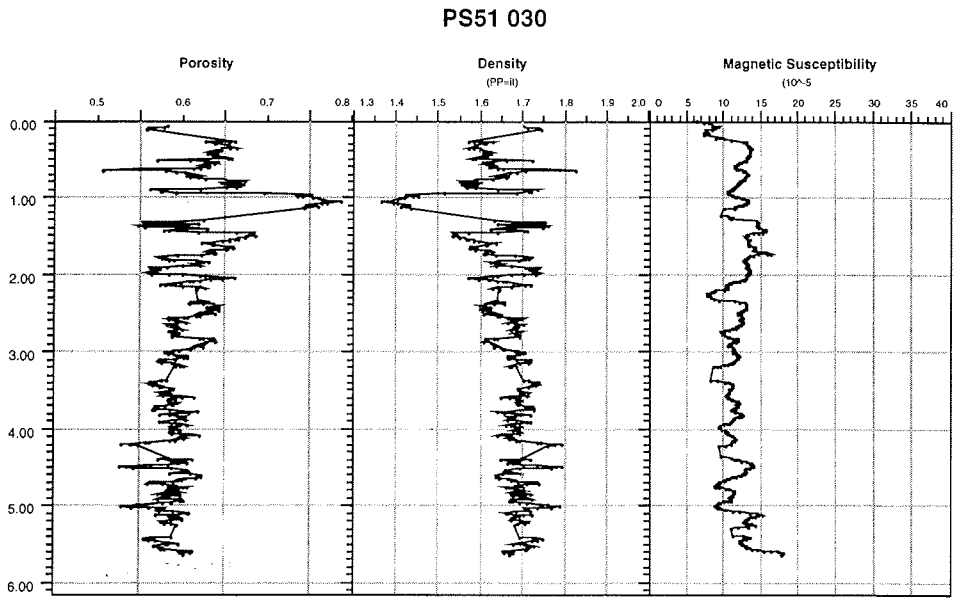

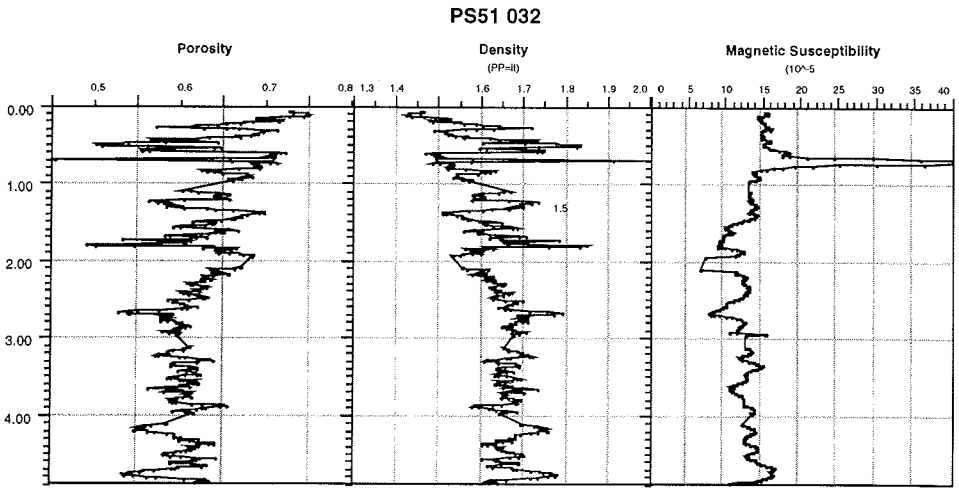

PS51 033

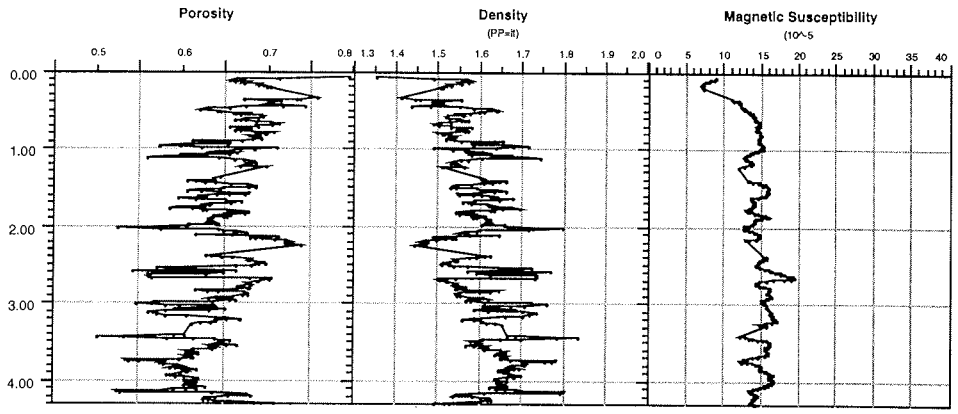

PS51 034

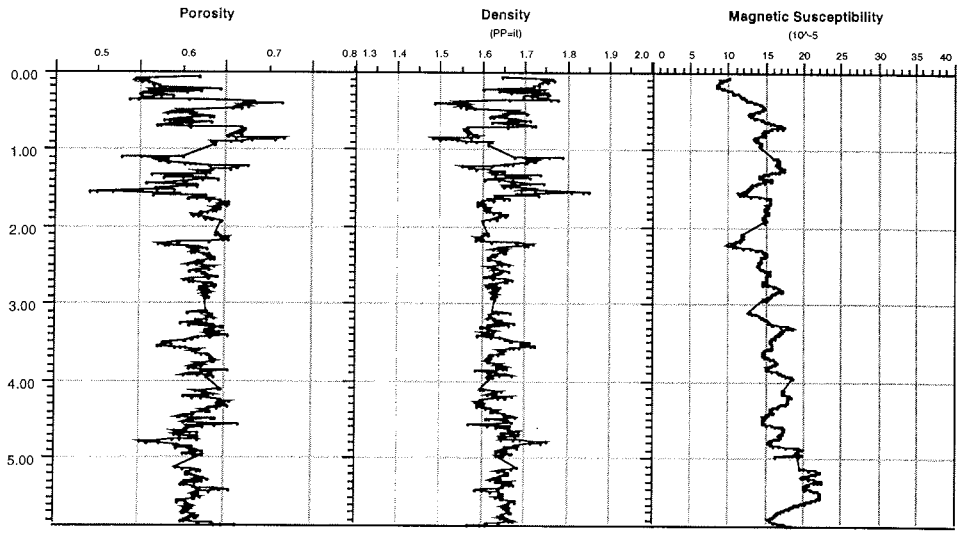

PS51 038

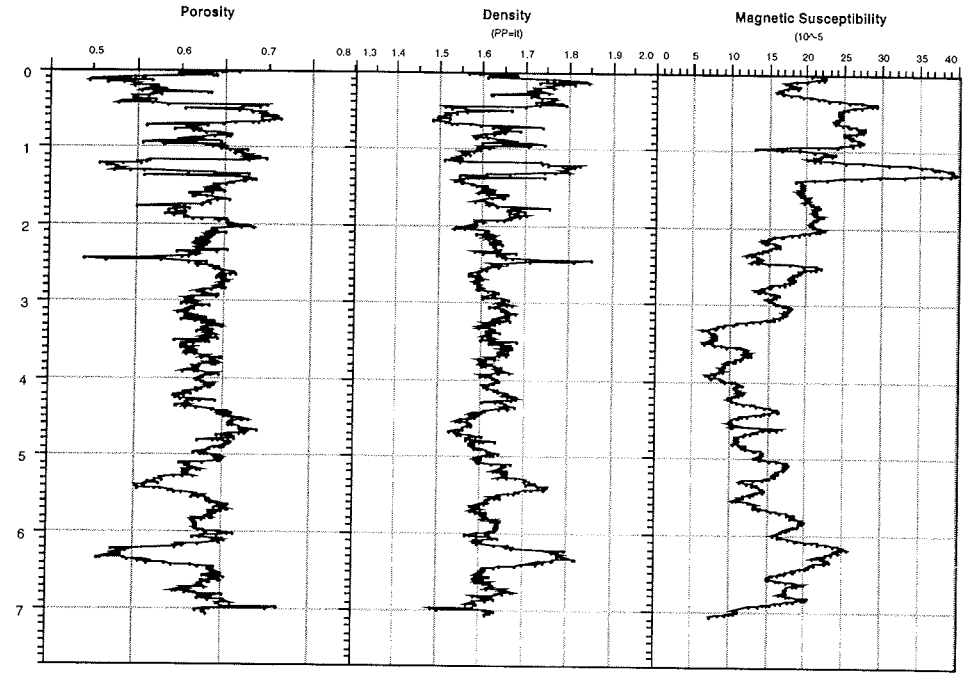

PS51 040

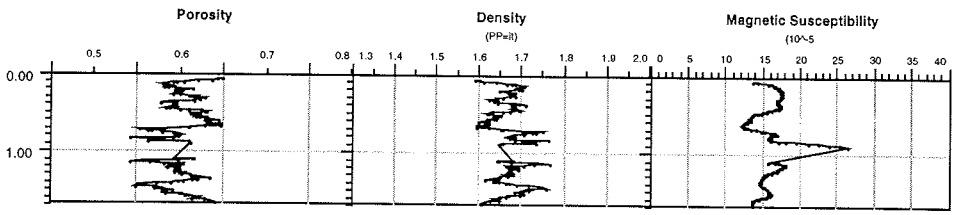

PS51 041

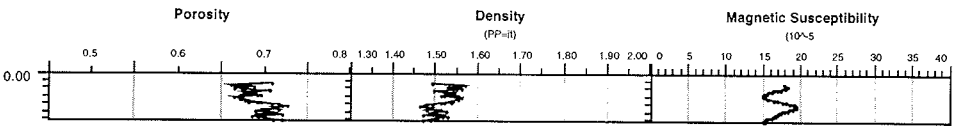

PS51 045

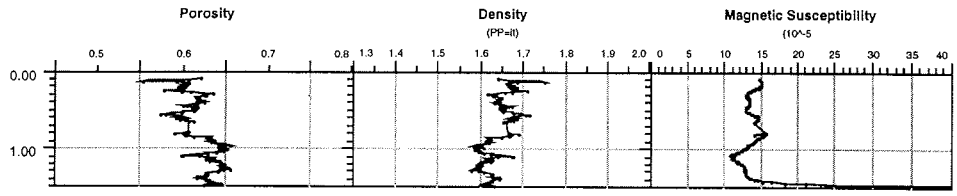

PS51 047

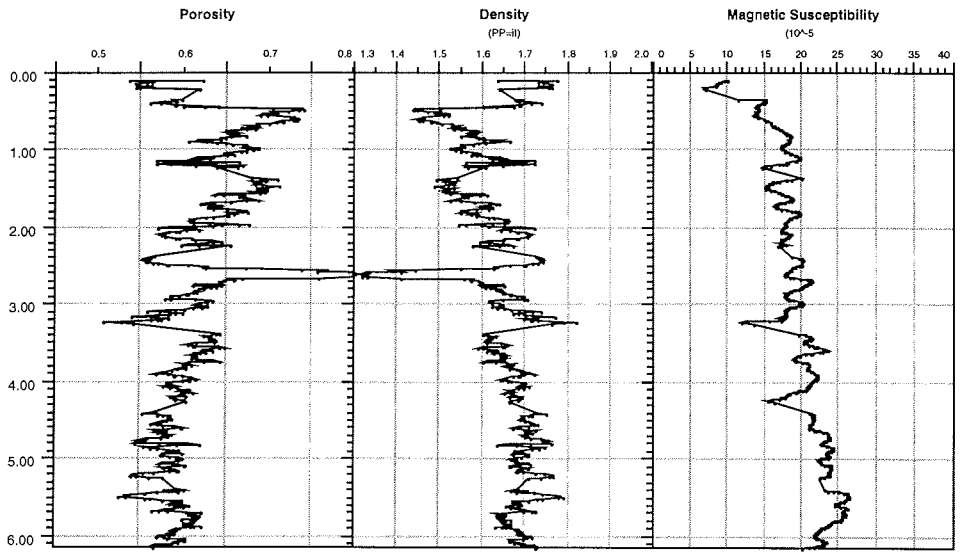

PS51 058

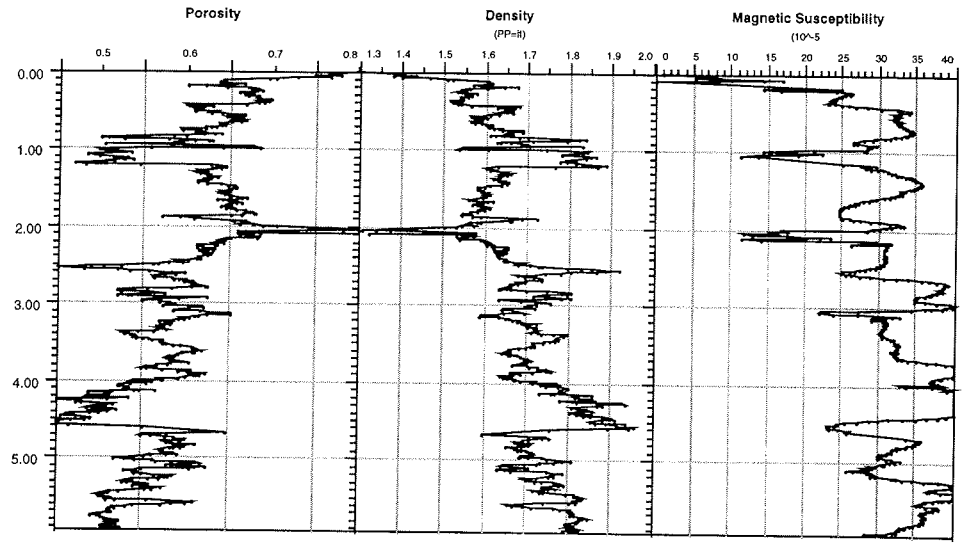

PS51 065

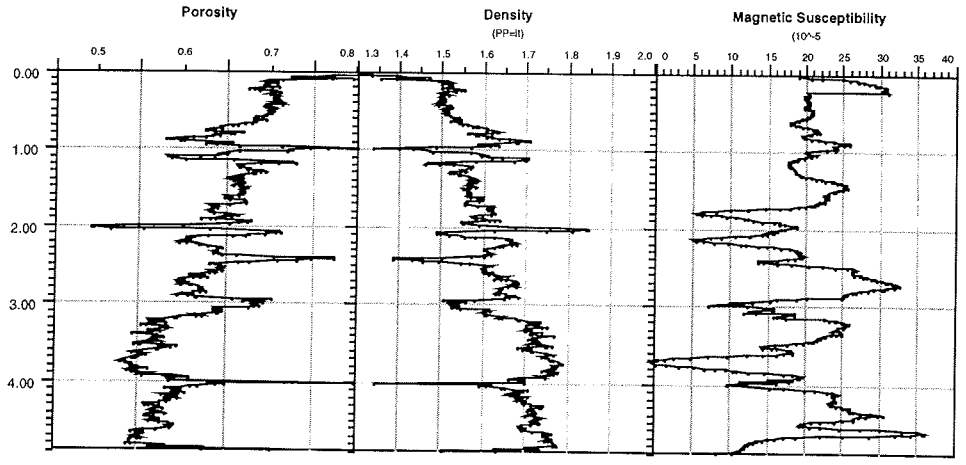

PS51 067-1

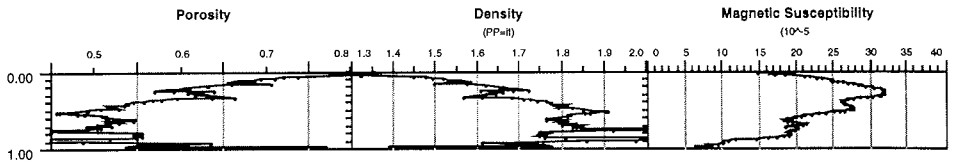

PS51 067-2

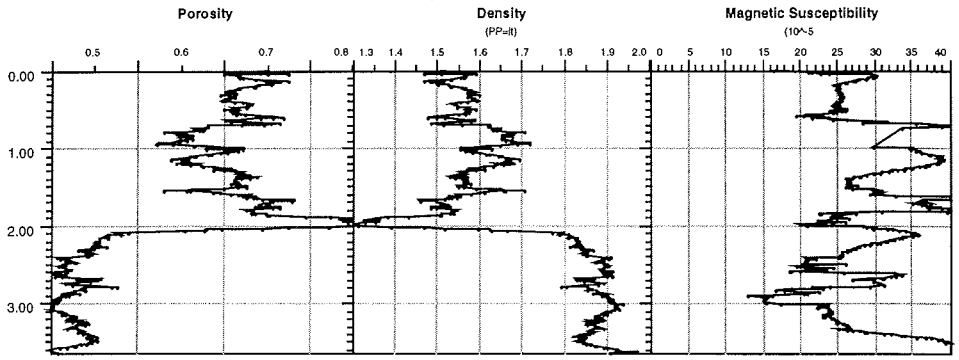

Participating Institutions

	Adress	Participants
Germany		
AWI	Alfred-Wegener-Institut für Polar-und Meeresforschung 27515 Bremerhaven	29
DWD	Deutscher Wetterdienst Seewetteramt Postfach 30 11 90 20304 Hamburg	2
HSW	Helikopter Service Wasserthal GmbH Kätnerweg 43 22393 Hamburg	3
GEOMAR	Forschungszentrum für marine Geowissenschaften der Christian-Albrechts-Universität Wischhofstraße 1 - 3 24148 Kiel	2
IGB	Institut f. Geologie Ruhruniversität Bochum Postfach 10 21 48 44780 Bochum	1
FSUJ	Friedrich-Schiller-Universität Jena Institut f. Geowissenschaften Lehrstuhl f. Angewandte Geophysik Burgweg 11 07749 Jena	1
Canada		
GSC	Geological Survey of Canada Box 1006 Dartmouth, N.S. B2Y 4A2	1

Participating Institutions

Adress		Participants
Russia		
AARI	Arctic and Antarctic Research Institute 38 Bering str. St. Petersburg 199397	2
MMBI	Murmansk Marine Biological Institute Russian Academy of Sciences 17, Vladimirskaya Street Murmansk, 183019	2
Shirshov	P.P. Shirshov Institute of Oceanology Nakhimovskii Prospekt 36 Moscow 117851	2
VNIIO	VNIIOkeangeologia 1, Angliysky ave. St. Petersburg 190121	4
ZISP	Zoological Institute of Russian Academy of Sciences Universitetskaya nab., 1 St. Petersburg, 199034	1

Cruise Participants

ARK-XIV/1a

Name		Institute
Böhm,	Joachim	HSW
Büchner,	Jürgen	HSW
Butzenko,	Viktor	VNIIO
Dratchev,	Sergej	Shirshov
Dürr,	Arndt	AWI
Dunker,	Erich	AWI
Fahl,	Kirsten	AWI
Gierlichs,	Annette	AWI
Golikov,	Alexey	ZISP
Hefter,	Jens	AWI
Hülse,	Sandra	AWI
Jackson,	Ruth	GSC
Jentzsch,	Gerhard	FSUJ
Jokat,	Wilfried (Fahrtleiter 1a)	AWI
Kassens,	Heidemarie (Fahrtleiter 1b)	GEOMAR
Kaufeld,	Lothar	DWD
König,	Matthias	AWI
Krause,	Reinhard	AWI
Lange,	Gert	Journalist
Lensch,	Norbert	AWI
Martens,	Hartmut	AWI
Matthiessen,	Jens	AWI
Müller,	Claudia	AWI
Musatov,	Evgeny	VNIIO
Mutterlose,	Jörg	IGB
Nørgaard-Pedersen,	Niels	GEOMAR
Pivovarov,	Sergey	AARI
Posselov,	Viktor	VNIIO
Polozek,	Kerstin	AWI
Rachor,	Eike	AWI
Rödle,	Claudia	AWI
Schewe,	Ingo	AWI
Schmidt,	Ebba	AWI
Schneider	Wolfgang	AWI
Schüler,	Karsten	AWI
Schwab,	Georg	AWI
Shevchenko,	Vladimir	Shirshov
Sokolov,	Vladimir	AARI
Sonnabend,	Hartmut	DWD

Name		Institute
Stein,	Rüdiger	AWI
Stepanov,	Sergei	VNIIO
Strohscher,	Birgit	AWI
Thalmann,	Kerstin	AWI
Tsoukalas	Nikolaus	AWI
Usbek,	Regina	AWI
Weigelt,	Estella	AWI
Yoon,	Mi-Kyung	AWI
Zepick,	Burkhard	HSW
Zöller,	Tobias	AWI
NN (MMBI)		
NN (MMBI)		

Ship's Crew

Greve, Ernst-Peter	Kapitän
Grundmann, Uwe	1. Offizier
Rodewald, Martin	1. Offizier
Knoop, Detlef	Ltd. Ingenieur
Spielke, Steffen	2. Offizier
Fallei, Holger	2. Offizier
N N	Arzt
Koch, Georg	Funker
Erreth, Mon. Gyula	2. Ingenieur
Ziemann, Olaf	2. Ingenieur
Fleischer, Martin	2. Ingenieur
Bretfeld, Holger	Elektroniker
Muhle, Helmut	Elektroniker
Greitemann-Hackl, A.	Elektroniker
Roschinsky, Jörg	Elektroniker
Muhle, Heiko	Elektroniker
Clasen, Burkhard	Bootsmann
Reise, Lutz	Zimmermann
Gil Iglesias, Luis	Matrose
Pousada Martinez, S.	Matrose
Kreis, Reinhard	Matrose
Bindernagel, Knuth	Matrose
Schultz, Ottomar	Matrose
Burzan, G.-Ekkehard	Matrose
Hagemann, Manfred	Matrose
Schmidt, Uwe	Matrose
Müller, Klaus	Lagerhalter
Ipsen, Michael	Masch. Wart
Voy, Bernd	Masch. Wart
Grafe, Jens	Masch. Wart
Hartmann, Ernst-Uwe	Masch. Wart
Preußner, Jörg	Masch. Wart
Haubold, Wolfgang	Koch
Völske, Thomas	Kochsmaat
Martens, Michael	Kochsmaat
Jürgens, Monika	1. Stewardess
N N	Stewardess/K.
Czyborra, Bärbel	2. Stewardess
Deuß, Stefanie	2. Stewardess
Neves, Alexandre	2. Stewardess
Huang, Wu-Mei	2. Steward
Mui, Kee Fung	2. Steward
Yu, Kwok Yuen	Wäscher

Folgende Hefte der Reihe „Berichte zur Polarforschung" sind bisher erschienen:

* **Sonderheft Nr. 1/1981** – „Die Antarktis und ihr Lebensraum"
Eine Einführung für Besucher – Herausgegeben im Auftrag von SCAR

Heft Nr. 1/1982 – „Die Filchner-Schelfeis-Expedition 1980/81"
zusammengestellt von Heinz Kohnen

* **Heft-Nr. 2/1982** – „Deutsche Antarktis-Expedition1980/81 mit FS ‚Meteor'"
First International BIOMASS Experiment (FIBEX) – Liste der Zooplankton- und Mikronektonnetzfänge
zusammengestellt von Norbert Klages.

Heft Nr. 3/1982 – „Digitale und analoge Krill-Echolot-Rohdatenerfassung an Bord des Forschungsschiffes ‚Meteor'" (im Rahmen von FIBEX 1980/81, Fahrtabschnitt ANT III), von Bodo Morgenstern

Heft Nr. 4/1982 – „Filchner-Schelfeis-Expedition 1980/81"
Liste der Planktonfänge und Lichtstärkemessungen
zusammengestellt von Gerd Hubold und H. Eberhard Drescher

* **Heft Nr. 5/1982** – "Joint Biological Expedition on RRS 'John Biscoe', February 1982"
by G. Hempel and R. B. Heywood

* **Heft Nr. 6/1982** – „Antarktis-Expedition 1981/82 (Unternehmen ‚Eiswarte')"
zusammengestellt von Gode Gravenhorst

Heft Nr. 7/1982 – „Marin-Biologisches Begleitprogramm zur Standorterkundung 1979/80 mit MS ‚Polarsirkel' (Pre-Site Survey)" – Stationslisten der Mikronekton- und Zooplanktonfänge sowie der Bodenfischerei
zusammengestellt von R. Schneppenheim

Heft Nr. 8/1983 – "The Post-Fibex Data Interpretation Workshop"
by D. L. Cram and J.-C. Freytag with the collaboration of J. W. Schmidt, M. Mall, R. Kresse, T. Schwinghammer

* **Heft Nr. 9/1983** – "Distribution of some groups of zooplankton in the inner Weddell Sea in summer 1979/80"
by I. Hempel, G. Hubold, B. Kaczmaruk, R. Keller, R. Weigmann-Haass

Heft Nr. 10/1983 – „Fluor im antarktischen Ökosystem" – DFG-Symposium November 1982
zusammengestellt von Dieter Adelung

Heft Nr. 11/1983 – "Joint Biological Expedition on RRS 'John Biscoe', February 1982 (II)"
Data of micronecton and zooplankton hauls, by Uwe Piatkowski

Heft Nr. 12/1983 – „Das biologische Programm der ANTARKTIS-I-Expedition 1983 mit FS ‚Polarstern'"
Stationslisten der Plankton-, Benthos- und Grundschleppnetzfänge und Liste der Probennahme an Robben und Vögeln, von H. E. Drescher, G. Hubold, U. Piatkowski, J. Plötz und J. Voß

* **Heft Nr. 13/1983** – „Die Antarktis-Expedition von MS ‚Polarbjörn' 1982/83" (Sommerkampagne zur Atka-Bucht und zu den Kraul-Bergen), zusammengestellt von Heinz Kohnen

* **Sonderheft Nr. 2/1983** – „Die erste Antarktis-Expedition von FS ‚Polarstern' (Kapstadt, 20. Januar 1983 – Rio de Janeiro, 25. März 1983)", Bericht des Fahrtleiters Prof. Dr. Gotthilf Hempel

Sonderheft Nr. 3/1983 – „Sicherheit und Überleben bei Polarexpeditionen"
zusammengestellt von Heinz Kohnen

* **Heft Nr. 14/1983** – „Die erste Antarktis-Expedition (ANTARKTIS I) von FS ‚Polarstern' 1982/83"
herausgegeben von Gotthilf Hempel

Sonderheft Nr. 4/1983 – "On the Biology of Krill *Euphausia superba*" – Proceedings of the Seminar and Report of the Krill Ecology Group, Bremerhaven 12.–16. May 1983, edited by S. B. Schnack

Heft Nr. 15/1983 – "German Antarctic Expedition 1980/81 with FRV 'Walther Herwig' and RV 'Meteor'" – First International BIOMASS Experiment (FIBEX) – Data of micronekton and zooplankton hauls
by Uwe Piatkowski and Norbert Klages

Sonderheft Nr. 5/1984 – "The observatories of the Georg von Neumayer Station", by Ernst Augstein

Heft Nr. 16/1984 – "FIBEX cruise zooplankton data"
by U. Piatkowski, I. Hempel and S. Rakusa-Suszczewski

Heft Nr. 17/1984 – „Fahrtbericht (cruise report) der ‚Polarstern'-Reise ARKTIS I, 1983"
von E. Augstein, G. Hempel und J. Thiede

Heft Nr. 18/1984 – „Die Expedition ANTARKTIS II mit FS ‚Polarstern' 1983/84",
Bericht von den Fahrtabschnitten 1, 2 und 3, herausgegeben von D. Fütterer

Heft Nr. 19/1984 – „Die Expedition ANTARKTIS II mit FS ‚Polarstern' 1983/84",
Bericht vom Fahrtabschnitt 4, Punta Arenas–Kapstadt (Ant-II/4), herausgegeben von H. Kohnen

Heft Nr. 20/1984 – „Die Expedition ARKTIS II des FS ‚Polarstern' 1984, mit Beiträgen des FS ‚Valdivia' und des Forschungsflugzeuges ‚Falcon 20' zum Marginal Ice Zone Experiment 1984 (MIZEX)"
von E. Augstein, G. Hempel, J. Schwarz, J. Thiede und W. Weigel

Heft Nr. 21/1985 – "Euphausiid larvae in plankton samples from the vicinity of the Antarctic Peninsula, February 1982" by Sigrid Marschall and Elke Mizdalski

Heft Nr. 22/1985 – "Maps of the geographical distribution of macrozooplankton in the Atlantic sector of the Southern Ocean" by Uwe Piatkowski

Heft Nr. 23/1985 – „Untersuchungen zur Funktionsmorphologie und Nahrungsaufnahme der Larven des Antarktischen Krills *Euphausia superba* Dana" von Hans-Peter Marschall

Heft Nr. 24/1985 – „Untersuchungen zum Periglazial auf der König-Georg-Insel Südshetlandinseln/ Antarktika. Deutsche physiogeographische Forschungen in der Antarktis. – Bericht über die Kampagne 1983/84" von Dietrich Barsch, Wolf-Dieter Blümel, Wolfgang Flügel, Roland Mäusbacher, Gerhard Stablein, Wolfgang Zick

* **Heft-Nr. 25/1985** – „Die Expedition ANTARKTIS III mit FS ‚Polarstern' 1984/1985" herausgegeben von Gotthilf Hempel.

***Heft-Nr. 26/1985** – "The Southern Ocean"; A survey of oceanographic and marine meteorological research work by Hellmer et al.

Heft Nr. 27/1986 – „Spatpleistozäne Sedimentationsprozesse am antarktischen Kontinentalhang vor Kapp Norvegia, östliche Weddell-See" von Hannes Grobe

Heft Nr. 28/1986 – „Die Expedition ARKTIS III mit ‚Polarstern' 1985" mit Beiträgen der Fahrtteilnehmer, herausgegeben von Rainer Gersonde

* **Heft Nr. 29/1986** – „5 Jahre Schwerpunktprogramm ‚Antarktisforschung' der Deutschen Forschungsgemeinschaft." Rückblick und Ausblick. Zusammengestellt von Gotthilf Hempel, Sprecher des Schwerpunktprogramms

Heft Nr. 30/1986 – "The Meteorological Data of the Georg-von-Neumayer-Station for 1981 and 1982" by Marianne Gube and Friedrich Obleitner

Heft Nr. 31/1986 – „Zur Biologie der Jugendstadien der Notothenioidei (Pisces) an der Antarktischen Halbinsel" von A. Kellermann

Heft Nr. 32/1986 – „Die Expedition ANTARKTIS IV mit FS ‚Polarstern' 1985/86" mit Beiträgen der Fahrtteilnehmer, herausgegeben von Dieter Fütterer

Heft Nr. 33/1987 – „Die Expedition ANTARKTIS-IV mit FS ‚Polarstern' 1985/86 – Bericht zu den Fahrtabschnitten ANT-IV/3–4" von Dieter Karl Fütterer

Heft Nr. 34/1987 – „Zoogeographische Untersuchungen und Gemeinschaftsanalysen an antarktischem Makroplankton" von U. Piatkowski

Heft Nr. 35/1987 – „Zur Verbreitung des Meso- und Makrozooplanktons in Oberflächenwasser der Weddell See (Antarktis)" von E. Boysen-Ennen

Heft Nr. 36/1987 – „Zur Nahrungs- und Bewegungsphysiologie von *Salpa thompsoni* und *Salpa fusiformis*" von M. Reinke

Heft Nr. 37/1987 – "The Eastern Weddell Sea Drifting Buoy Data Set of the Winter Weddell Sea Project (WWSP)" 1986 by Heinrich Hoeber und Marianne Gube-Lehnhardt

Heft Nr. 38/1987 – "The Meteorological Data of the Georg von Neumayer Station for 1983 and 1984" by M. Gube-Lenhardt

Heft Nr. 39/1987 – „Die Winter-Expedition mit FS ‚Polarstern' in die Antarktis (ANT V/1–3)" herausgegeben von Sigrid Schnack-Schiel

Heft Nr. 40/1987 – "Weather and Synoptic Situation during Winter Weddell Sea Project 1986 (ANT V/2) July 16–September 10, 1986" by Werner Rabe

Heft Nr. 41/1988 – „Zur Verbreitung und Ökologie der Seegurken im Weddellmeer (Antarktis)" von Julian Gutt

Heft Nr. 42/1988 – "The zooplankton community in the deep bathyal and abyssal zones of the eastern North Atlantic" by Werner Beckmann

Heft Nr. 43/1988 – "Scientific cruise report of Arctic Expedition ARK IV/3" Wissenschaftlicher Fahrtbericht der Arktis-Expedition ARK IV/3, compiled by Jörn Thiede

Heft Nr. 44/1988 – "Data Report for FV 'Polarstern' Cruise ARK IV/1, 1987 to the Arctic and Polar Fronts" by Hans-Jürgen Hirche

Heft Nr. 45/1988 – „Zoogeographie und Gemeinschaftsanalyse des Makrozoobenthos des Weddellmeeres (Antarktis)" von Joachim Voß

Heft Nr. 46/1988 – "Meteorological and Oceanographic Data of the Winter-Weddell-Sea Project 1986 (ANT V/3)" by Eberhard Fahrbach

Heft Nr. 47/1988 – „Verteilung und Herkunft glazial-mariner Gerölle am Antarktischen Kontinentalrand des östlichen Weddellmeeres" von Wolfgang Oskierski

Heft Nr. 48/1988 – „Variationen des Erdmagnetfeldes an der GvN-Station" von Arnold Brodscholl

* **Heft Nr. 49/1988** – „Zur Bedeutung der Lipide im antarktischen Zooplankton" von Wilhelm Hagen

Heft Nr. 50/1988 – „Die gezeitenbedingte Dynamik des Ekström-Schelfeises, Antarktis" von Wolfgang Kobarg

Heft Nr. 51/1988 – „Ökomorphologie notothenioider Fische aus dem Weddellmeer, Antarktis" von Werner Ekau

Heft Nr. 52/1988 – „Zusammensetzung der Bodenfauna in der westlichen Fram-Straße" von Dieter Piepenburg

* **Heft Nr. 53/1988** – „Untersuchungen zur Ökologie des Phytoplanktons im südöstlichen Weddellmeer (Antarktis) im Jan./Febr. 1985" von Eva-Maria Nöthig

Heft Nr. 54/1988 – „Die Fischfauna des östlichen und südlichen Weddellmeeres: geographische Verbreitung, Nahrung und trophische Stellung der Fischarten" von Wiebke Schwarzbach

Heft Nr. 55/1988 – "Weight and length data of zooplankton in the Weddell Sea in austral spring 1986 (Ant V/3)" by Elke Mizdalski

Heft Nr. 56/1989 – "Scientific cruise report of Arctic expeditions ARK IV/1, 2 & 3" by G. Krause, J. Meincke und J. Thiede

Heft Nr. 57/1989 – „Die Expedition ANTARKTIS V mit FS ‚Polarstern' 1986/87"
Bericht von den Fahrtabschnitten ANT V/4–5 von H. Miller und H. Oerter

* **Heft Nr. 58/1989** – „Die Expedition ANTARKTIS VI mit FS ‚Polarstern' 1987/88"
von D. K. Fütterer

Heft Nr. 59/1989 – „Die Expedition ARKTIS V/1a, 1b und 2 mit FS ‚Polarstern' 1988"
von M. Spindler

Heft Nr. 60/1989 – „Ein zweidimensionales Modell zur thermohalinen Zirkulation unter dem Schelfeis"
von H. H. Hellmer

Heft Nr. 61/1989 – „Die Vulkanite im westlichen und mittleren Neuschwabenland,
Vestfjella und Ahlmannryggen, Antarktika" von M. Peters

* **Heft-Nr. 62/1989** – "The Expedition ANTARKTIS VII/1 and 2 (EPOS I) of RV 'Polarstern'
in 1988/89", by I. Hempel

Heft Nr. 63/1989 – „Die Eisalgenflora des Weddellmeeres (Antarktis): Artenzusammensetzung und Biomasse
sowie Ökophysiologie ausgewählter Arten" von Annette Bartsch

Heft Nr. 64/1989 – "Meteorological Data of the G.-v.-Neumayer-Station (Antarctica)" by L. Helmes

Heft Nr. 65/1989 – „Expedition Antarktis VII/3 in 1988/89" by I. Hempel, P. H. Schalk, V. Smetacek

Heft Nr. 66/1989 – „Geomorphologisch-glaziologische Detailkartierung
des arid-hochpolaren Borgmassivet, Neuschwabenland, Antarktika" von Karsten Brunk

Heft-Nr. 67/1990 – „Identification key and catalogue of larval Antarctic fishes",
edited by Adolf Kellermann

Heft-Nr. 68/1990 – „The Expediton Antarktis VII/4 (Epos leg 3) and VII/5 of RV 'Polarstern' in 1989",
edited by W. Arntz, W. Ernst, I. Hempel

Heft-Nr. 69/1990 – „Abhängigkeiten elastischer und rheologischer Eigenschaften des Meereises vom
Eisgefüge", von Harald Hellmann

Heft-Nr. 70/1990 – „Die beschalten benthischen Mollusken (Gastropoda und Bivalvia) des
Weddellmeeres, Antarktis", von Stefan Hain

Heft-Nr. 71/1990 – „Sedimentologie und Paläomagnetik an Sedimenten der Maudkuppe (Nordöstliches
Weddellmeer)", von Dieter Cordes.

Heft-Nr. 72/1990 – „Distribution and abundance of planktonic copepods (Crustacea) in the Weddell Sea
in summer 1980/81", by F. Kurbjeweit and S. Ali-Khan

Heft-Nr. 73/1990 – „Zur Frühdiagenese von organischem Kohlenstoff und Opal in Sedimenten des südlichen
und östlichen Weddellmeeres", von M. Schlüter

Heft-Nr. 74/1990 – „Expeditionen ANTARKTIS-VIII/3 und VIII/4 mit FS ‚Polarstern' 1989"
von Rainer Gersonde und Gotthilf Hempel

Heft-Nr. 75/1991 – „Quartäre Sedimentationsprozesse am Kontinentalhang des Süd-Orkey-Plateaus im
nordwestlichen Weddellmeer (Antarktis)", von Sigrun Grünig

Heft-Nr. 76/1990 – „Ergebnisse der faunistischen Arbeiten im Benthal von King George Island
(Südshetlandinseln, Antarktis)", von Martin Rauschert

Heft-Nr. 77/1990 – „Verteilung von Mikroplankton-Organismen nordwestlich der Antarktischen Halbinsel
unter dem Einfluß sich ändernder Umweltbedingungen im Herbst", von Heinz Klöser

Heft-Nr. 78/1991 – „Hochauflösende Magnetostratigraphie spätquartärer Sedimente arktischer
Meeresgebiete", von Norbert R. Nowaczyk

Heft-Nr. 79/1991 – „Ökophysiologische Untersuchungen zur Salinitäts- und Temperaturtoleranz
antarktischer Grünalgen unter besonderer Berücksichtigung des ß-Dimethylsulfoniumpropionat
(DMSP) - Stoffwechsels", von Ulf Karsten

Heft-Nr. 80/1991 – „Die Expedition ARKTIS VII/1 mit FS ‚Polarstern' 1990",
herausgegeben von Jörn Thiede und Gotthilf Hempel

Heft-Nr. 81/1991 – „Paläoglaziologie und Paläozeanographie im Spätquartär am Kontinentalrand des
südlichen Weddellmeeres, Antarktis", von Martin Melles

Heft-Nr. 82/1991 – „Quantifizierung von Meereseigenschaften: Automatische Bildanalyse von
Dünnschnitten und Parametrisierung von Chlorophyll- und Salzgehaltsverteilungen", von Hajo Eicken

Heft-Nr. 83/1991 – „Das Fließen von Schelfeisen - numerische Simulationen
mit der Methode der finiten Differenzen", von Jürgen Determann

Heft-Nr. 84/1991 – „Die Expedition ANTARKTIS-VIII/1-2, 1989 mit der Winter Weddell Gyre Study
der Forschungsschiffe „Polarstern" und „Akademik Fedorov", von Ernst Augstein,
Nikolai Bagriantsev und Hans Werner Schenke

Heft-Nr. 85/1991 – „Zur Entstehung von Unterwassereis und das Wachstum und die Energiebilanz
des Meereises in der Atka Bucht, Antarktis", von Josef Kipfstuhl

Heft-Nr. 86/1991 – „Die Expedition ANTARKTIS-VIII mit „FS Polarstern" 1989/90. Bericht vom
Fahrtabschnitt ANT-VIII / 5", von Heinz Miller und Hans Oerter

Heft-Nr. 87/1991 –"Scientific cruise reports of Arctic expeditions ARK VI / 1-4 of RV "Polarstern"
in 1989", edited by G. Krause, J. Meincke & H. J. Schwarz

Heft-Nr. 88/1991 – „Zur Lebensgeschichte dominanter Copepodenarten (*Calanus finmarchicus,
C. glacialis, C. hyperboreus, Metridia longa)* in der Framstraße", von Sabine Diel

Heft-Nr. 89/1991 – „Detaillierte seismische Untersuchungen am östlichen Kontinentalrand des Weddell-Meeres vor Kapp Norvegia, Antarktis", von Norbert E. Kaul

Heft-Nr. 90/1991 – „Die Expedition ANTARKTIS-VIII mit FS „Polarstern" 1989/90. Bericht von den Fahrtabschnitten ANT-VIII/6-7", herausgegeben von Dieter Karl Fütterer und Otto Schrems

Heft-Nr. 91/1991 – "Blood physiology and ecological consequences in Weddell Sea fishes (Antarctica)", by Andreas Kunzmann

Heft-Nr. 92/1991 – „Zur sommerlichen Verteilung des Mesozooplanktons im Nansen-Becken, Nordpolarmeer", von Nicolai Mumm

Heft-Nr. 93/1991 – „Die Expedition ARKTIS VII mit FS „Polarstern", 1990. Bericht vom Fahrtabschnitt ARK VII/2", herausgegeben von Gunther Krause

Heft-Nr. 94/1991 – „Die Entwicklung des Phytoplanktons im östlichen Weddellmeer (Antarktis) beim Übergang vom Spätwinter zum Frühjahr", von Renate Scharek

Heft-Nr. 95/1991 – „Radioisotopenstratigraphie, Sedimentologie und Geochemie jungquartärer Sedimente des östlichen Arktischen Ozeans", von Horst Bohrmann

Heft-Nr. 96/1991 – „Holozäne Sedimentationsentwicklung im Scoresby Sund, Ost-Grönland", von Peter Marienfeld

Heft-Nr. 97/1991 – „Strukturelle Entwicklung und Abkühlungsgeschichte der Heimefrontfjella (Westliches Dronning Maud Land/Antarktika)", von Joachim Jacobs

Heft-Nr. 98/1991 – „Zur Besiedlungsgeschichte des antarktischen Schelfes am Beispiel der Isopoda (Crustacea, Malacostraca)", von Angelika Brandt

Heft-Nr. 99/1992 – "The Antarctic ice sheet and environmental change: a three-dimensional modelling study", by Philippe Huybrechts

* **Heft-Nr. 100/1992** – „Die Expeditionen ANTARKTIS IX/1-4 des Forschungsschiffes „Polarstern" 1990/91", herausgegeben von Ulrich Bathmann, Meinhard Schulz-Baldes, Eberhard Fahrbach, Victor Smetacek und Hans-Wolfgang Hubberten

Heft-Nr. 101/1992 – „Wechselbeziehungen zwischen Schwermetallkonzentrationen (Cd, Cu, Pb, Zn) im Meewasser und in Zooplanktonorganismen (Copepoda) der Arktis und des Atlantiks", von Christa Pohl

Heft-Nr. 102/1992 – „Physiologie und Ultrastruktur der antarktischen Grünalge *Prasiola crispa* ssp. *antarctica* unter osmotischem Streß und Austrocknung", von Andreas Jacob

Heft-Nr. 103/1992 – „Zur Ökologie der Fische im Weddelmeer", von Gerd Hubold

Heft-Nr. 104/1992 – „Mehrkanalige adaptive Filter für die Unterdrückung von multiplen Reflexionen in Verbindung mit der freien Oberfläche in marinen Seismogrammen", von Andreas Rosenberger

Heft-Nr. 105/1992 – „Radiation and Eddy Flux Experiment 1991 *(REFLEX I)*", von Jörg Hartmann, Christoph Kottmeier und Christian Wamser

Heft-Nr. 106/1992 – „Ostracoden im Epipelagial vor der Antarktischen Halbinsel - ein Beitrag zur Systematik sowie zur Verbreitung und Populationsstruktur unter Berücksichtigung der Saisonalität", von Rüdiger Kock

Heft-Nr. 107/1992 – „ARCTIC '91: Die Expedition ARK-VIII/3 mit FS „Polarstern" 1991", von Dieter K. Fütterer

Heft-Nr. 108/1992 – „Dehnungsbeben an einer Störungszone im Ekström-Schelfeis nördlich der Georg-von-Neumayer Station, Antarktis. – Eine Untersuchung mit seismologischen und geodätischen Methoden", von Uwe Nixdorf.

Heft-Nr. 109/1992 – „Spätquartäre Sedimentation am Kontinentalrand des südöstlichen Weddellmeeres, Antarktis", von Michael Weber.

Heft-Nr. 110/1992 – „Sedimentfazies und Bodenwasserstrom am Kontinentalhang des nordwestlichen Weddellmeeres", von Isa Brehme.

Heft-Nr. 111/1992 – „Die Lebensbedingungen in den Solekanälchen des antarktischen Meereises", von Jürgen Weissenberger.

Heft-Nr. 112/1992 – „Zur Taxonomie von rezenten benthischen Foraminiferen aus dem Nansen Becken, Arktischer Ozean", von Jutta Wollenburg.

Heft-Nr. 113/1992 – „Die Expedition ARKTIS VIII/1 mit FS "Polarstern" 1991", herausgegeben von Gerhard Kattner.

* **Heft-Nr. 114/1992** – „Die Gründungsphase deutscher Polarforschung, 1865-1875", von Reinhard A. Krause.

Heft-Nr. 115/1992 – „Scientific Cruise Report of the 1991 Arctic Expedition ARK VIII/2 of RV "Polarstern" (EPOS II)", by Eike Rachor.

Heft-Nr. 116/1992 – „The Meteorological Data of the Georg-von-Neumayer-Station (Antarctica) for 1988, 1989, 1990 and 1991", by Gert König-Langlo.

Heft-Nr. 117/1992 – „Petrogenese des metamorphen Grundgebirges der zentralen Heimefrontfjella (westliches Dronning Maud Land / Antarktis)", von Peter Schulze.

Heft-Nr. 118/1993 – „Die mafischen Gänge der Shackleton Range / Antarktika: Petrographie, Geochemie, Isotopengeochemie und Paläomagnetik", von Rüdiger Hotten.

* **Heft-Nr. 119/1993** – „Gefrierschutz bei Fischen der Polarmeere", von Andreas P.A. Wöhrmann.

* **Heft-Nr. 120/1993** – „East Siberian Arctic Region Expedition '92: The Laptev Sea - its Significance for Arctic Sea-Ice Formation and Transpolar Sediment Flux", by D. Dethleff, D. Nürnberg, E. Reimnitz, M. Saarso and Y. P. Sacchenko. – „Expedition to Novaja Zemlja and Franz Josef Land with RV.'Dalnie Zelentsy'", by D. Nürnberg and E. Groth.

* **Heft-Nr. 121/1993** – „Die Expedition ANTARKTIS X/3 mit FS 'Polarstern' 1992", herausgegeben von Michael Spindler, Gerhard Dieckmann und David Thomas.

Heft-Nr. 122/1993 – „Die Beschreibung der Korngestalt mit Hilfe der Fourier-Analyse: Parametrisierung der morphologischen Eigenschaften von Sedimentpartikeln", von Michael Diepenbroek.

* **Heft-Nr. 123/1993** – „Zerstörungsfreie hochauflösende Dichteuntersuchungen mariner Sedimente", von Sebastian Gerland.

Heft-Nr. 124/1993 – „Umsatz und Verteilung von Lipiden in arktischen marinen Organismen unter besonderer Berücksichtigung unterer trophischer Stufen", von Martin Graeve.

Heft-Nr. 125/1993 – „Ökologie und Respiration ausgewählter arktischer Bodenfischarten", von Christian F. von Dorrien.

Heft-Nr. 126/1993 – „Quantitative Bestimmung von Paläoumweltparametern des Antarktischen Oberflächenwassers im Spätquartär anhand von Transferfunktionen mit Diatomeen", von Ulrich Zielinski

Heft-Nr. 127/1993 – „Sedimenttransport durch das arktische Meereis: Die rezente lithogene und biogene Materialfracht", von Ingo Wollenburg.

Heft-Nr. 128/1993 – „Cruise ANTARKTIS X/3 of RV 'Polarstern': CTD-Report", von Marek Zwierz.

Heft-Nr. 129/1993 – „Reproduktion und Lebenszyklen dominanter Copepodenarten aus dem Weddellmeer, Antarktis", von Frank Kurbjeweit

Heft-Nr. 130/1993 – „Untersuchungen zu Temperaturregime und Massenhaushalt des Filchner-Ronne-Schelfeises, Antarktis, unter besonderer Berücksichtigung von Anfrier- und Abschmelzprozessen", von Klaus Grosfeld

Heft-Nr. 131/1993 – „Die Expedition ANTARKTIS X/5 mit FS 'Polarstern' 1992", herausgegeben von Rainer Gersonde

Heft-Nr. 132/1993 – „Bildung und Abgabe kurzkettiger halogenierter Kohlenwasserstoffe durch Makroalgen der Polarregionen", von Frank Laturnus

Heft-Nr. 133/1994 – "Radiation and Eddy Flux Experiment 1993 *(REFLEX II)*", by Christoph Kottmeier, Jörg Hartmann, Christian Wamser, Axel Bochert, Christof Lüpkes, Dietmar Freese and Wolfgang Cohrs

* **Heft-Nr. 134/1994** – "The Expedition ARKTIS-IX/1", edited by Hajo Eicken and Jens Meincke

Heft-Nr. 135/1994 – „Die Expeditionen ANTARKTIS X/6-8", herausgegeben von Ulrich Bathmann, Victor Smetacek, Hein de Baar, Eberhard Fahrbach und Gunter Krause

Heft-Nr. 136/1994 – „Untersuchungen zur Ernährungsökologie von Kaiserpinguinen *(Aptenodytes forsteri)* und Königspinguinen *(Aptenodytes patagonicus)*", von Klemens Pütz

* **Heft-Nr. 137/1994** – „Die känozoische Vereisungsgeschichte der Antarktis", von Werner U. Ehrmann

Heft-Nr. 138/1994 – „Untersuchungen stratosphärischer Aerosole vulkanischen Ursprungs und polarer stratosphärischer Wolken mit einem Mehrwellenlängen-Lidar auf Spitzbergen *(79° N, 12° E)*", von Georg Beyerle

Heft-Nr. 139/1994 – „Charakterisierung der Isopodenfauna (Crustacea, Malacostraca) des Scotia-Bogens aus biogeographischer Sicht: Ein multivariater Ansatz", von Holger Winkler.

Heft-Nr. 140/1994 – „Die Expedition ANTARKTIS X/4 mit FS 'Polarstern' 1992", herausgegeben von Peter Lemke

Heft-Nr. 141/1994 – „Satellitenaltimetrie über Eis – Anwendung des GEOSAT-Altimeters über dem Ekströmisen, Antarktis", von Clemens Heidland

Heft-Nr. 142/1994 – "The 1993 Northeast Water Expedition. Scientific cruise report of RV'Polarstern' Arctic cruises ARK IX/2 and 3, USCG 'Polar Bear' cruise NEWP and the NEWLand expedition", edited by Hans-Jürgen Hirche and Gerhard Kattner

Heft-Nr. 143/1994 – „Detaillierte refraktionsseismische Untersuchungen im inneren Scoresby Sund Ost-Grönland", von Notker Fechner

Heft-Nr. 144/1994 – „Russian-German Cooperation in the Siberian Shelf Seas: Geo-System Laptev Sea", edited by Heidemarie Kassens, Hans-Wolfgang Hubberten, Sergey M. Pryamikov und Rüdiger Stein

* **Heft-Nr. 145/1994** – „The 1993 Northeast Water Expedition. Data Report of RV 'Polarstern' Arctic Cruises IX/2 and 3", edited by Gerhard Kattner and Hans-Jürgen Hirche.

Heft-Nr. 146/1994 – "Radiation Measurements at the German Antarctic Station Neumayer 1982-1992", by Torsten Schmidt and Gert König-Langlo.

Heft-Nr. 147/1994 – „Krustenstrukturen und Verlauf des Kontinentalrandes im Weddell Meer / Antarktis", von Christian Hübscher.

Heft-Nr. 148/1994 – "The expeditions NORILSK/TAYMYR 1993 and BUNGER OASIS 1993/94 of the AWI Research Unit Potsdam", edited by Martin Melles.

** **Heft-Nr. 149/1994** – "Die Expedition ARCTIC' 93. Der Fahrtabschnitt ARK-IX/4 mit FS 'Polarstern' 1993", herausgegeben von Dieter K. Fütterer.

Heft-Nr. 150/1994 – "Der Energiebedarf der Pygoscelis-Pinguine: eine Synopse", von Boris M. Culik.

Heft-Nr. 151/1994 – „Russian-German Cooperation: The Transdrift I Expedition to the Laptev Sea", edited by Heidemarie Kassens and Valeriy Y. Karpiy.

Heft-Nr. 152/1994 – „Die Expedition ANTARKTIS-X mit FS 'Polarstern' 1992. Bericht von den Fahrtabschnitten / ANT-X / 1a und 2", herausgegeben von Heinz Miller.

Heft-Nr. 153/1994 – "Aminosäuren und Huminstoffe im Stickstoffkreislauf polarer Meere", von Ulrike Hubberten.

Heft-Nr. 154/1994 – "Regional und seasonal variability in the vertical distribution of mesozooplankton in the Greenland Sea", by Claudio Richter.

Heft-Nr. 155/1995 – "Benthos in polaren Gewässern", herausgegeben von Christian Wiencke und Wolf Arntz.

Heft-Nr. 156/1995 – "An adjoint model for the determination of the mean oceanic circulation, air-sea fluxes und mixing coefficients", by Reiner Schlitzer.

Heft-Nr. 157/1995 – "Biochemische Untersuchungen zum Lipidstoffwechsel antarktischer Copepoden", von Kirsten Fahl.

** **Heft-Nr. 158/1995** – "Die Deutsche Polarforschung seit der Jahrhundertwende und der Einfluß Erich von Drygalskis", von Cornelia Lüdecke.

Heft-Nr. 159/1995 – The distribution of $\partial^{18}O$ in the Arctic Ocean: Implications for the freshwater balance of the haloclin and the sources of deep and bottom waters", by Dorothea Bauch.

* **Heft-Nr. 160/1995** – "Rekonstruktion der spätquartären Tiefenwasserzirkulation und Produktivität im östlichen Südatlantik anhand von benthischen Foraminiferenvergesellschaftungen", von Gerhard Schmiedl.

Heft-Nr. 161/1995 – "Der Einfluß von Salinität und Lichtintensität auf die Osmolytkonzentrationen, die Zellvolumina und die Wachstumsraten der antarktischen Eisdiatomeen *Chaetoceros* sp. und *Navicula* sp. unter besonderer Berücksichtigung der Aminosäure Prolin", von Jürgen Nothnagel.

Heft-Nr. 162/1995 – "Meereistransportiertes lithogenes Feinmaterial in spätquartären Tiefseesedimenten des zentralen östlichen Arktischen Ozeans und der Framstraße", von Thomas Letzig.

Heft-Nr. 163/1995 – "Die Expedition ANTARKTIS-XI/2 mit FS "Polarstern" 1993/94", herausgegeben von Rainer Gersonde.

Heft-Nr. 164/1995 – "Regionale und altersabhängige Variation gesteinsmagnetischer Parameter in marinen Sedimenten der Arktis", von Thomas Frederichs.

Heft-Nr. 165/1995 – "Vorkommen, Verteilung und Umsatz biogener organischer Spurenstoffe: Sterole in antarktischen Gewässern", von Georg Hanke.

Heft-Nr. 166/1995 – "Vergleichende Untersuchungen eines optimierten dynamisch-thermodynamischen Meereismodel mit Beobachtungen im Weddellmeer", von Holger Fischer.

Heft-Nr. 167/1995 – "Rekonstruktionen von Paläo-Umweltparametern anhand von stabilen Isotopen und Faunen-Vergesellschaftungen planktischer Foraminiferen im Südatlantik", von Hans-Stefan Niebler

Heft-Nr. 168/1995 – "Die Expedition ANTARKTIS XII mit FS 'Polarstern' 1993/94. Bericht von den Fahrtabschnitten ANT XII/1 und 2", herausgegeben von Gerhard Kattner und Dieter Karl Fütterer.

Heft-Nr. 169/1995 – "Medizinische Untersuchung zur Circadianrhythmik und zum Verhalten bei Überwinterern auf eine antarktischen Forschungsstation", von Hans Wortmann.

Heft-Nr. 170/1995 – DFG-Kolloquium: Terrestrische Geowissenschaften - Geologie und Geophysik der Antarktis.

Heft-Nr. 171/1995 – "Strukturentwicklung und Petrogenese des metamorphen Grundgebirges der nördlichen Heimefrontfjella (westliches Dronning Maud Land/Antarktika)", von Wilfried Bauer.

Heft-Nr. 172/1995 – "Die Struktur der Erdkruste im Bereich des Scoresby Sund, Ostgrönland: Ergebnisse refraktionsseismischer und gravimetrischer Untersuchungen", von Holger Mandler.

Heft-Nr. 173/1995 – "Paläozoische Akkretion am paläopazifischen Kontinentalrand der Antarktis in Nordvictorialand – P-T-D-Geschichte und Deformationsmechanismen im Bowers Terrane", von Stefan Matzer.

Heft-Nr. 174/1995 – "The Expedition ARKTIS-X/2 of RV 'Polarstern' in 1994", edited by Hans-W. Hubberten.

Heft-Nr. 175/1995 – "Russian-German Cooperation: The Expedition TAYMYR 1994", edited by Christine Siegert and Dmitry Bolshiyanov.

Heft-Nr. 176/1995 – "Russian-German Cooperation: Laptev Sea System", edited by Heidemarie Kassens, Dieter Piepenburg, Jörn Thiede, Leonid Timokhov, Hans-Wolfgang Hubberten and Sergey M. Priamikov.

Heft-Nr. 177/1995 – "Organischer Kohlenstoff in spätquartären Sedimenten des Arktischen Ozeans: Terrigener Eintrag und marine Produktivität", von Carsten J. Schubert.

Heft-Nr. 178/1995 – "Cruise ANTARKTIS XII/4 of RV 'Polarstern' in 1995: CTD-Report", by Jüri Sildam.

Heft-Nr. 179/1995 – "Benthische Foraminiferenfaunen als Wassermassen-, Produktions- und Eisdriftanzeiger im Arktischen Ozean", von Jutta Wollenburg.

Heft-Nr. 180/1995 – "Biogenopal und biogenes Barium als Indikatoren für spätquartäre Produktivitätsänderungen am antarktischen Kontinentalhang, atlantischer Sektor", von Wolfgang J. Bonn.

Heft-Nr. 181/1995 – "Die Expedition ARKTIS X/1 des Forschungsschiffes ‚Polarstern' 1994", herausgegeben von Eberhard Fahrbach.

Heft-Nr. 182/1995 – "Laptev Sea System: Expeditions in 1994", edited by Heidemarie Kassens.

Heft-Nr. 183/1996 – "Interpretation digitaler Parasound Echolotaufzeichnungen im östlichen Arktischen Ozean auf der Grundlage physikalischer Sedimenteigenschaften", von Uwe Bergmann.

Heft-Nr. 184/1996 – "Distribution and dynamics of inorganic nitrogen compounds in the troposphere of continental, coastal, marine and Arctic areas", by María Dolores Andrés Hernández.

Heft-Nr. 185/1996 – "Verbreitung und Lebensweise der Aphroditiden und Polynoiden (Polychaeta) im östlichen Weddel meer und im Lazarevmeer (Antarktis)", von Michael Stiller.

Heft-Nr. 186/1996 – "Reconstruction of Late Quaternary environmental conditions applying the natural radionuclides ^{230}Th, ^{10}Be, ^{231}Pa and ^{238}U: A study of deep-sea sediments from the eastern sector of the Antrctic Circumpolar Current System", by Martin Frank.

Heft-Nr. 187/1996 – "The Meteorological Data of the Neumayer Station (Antarctica) for 1992, 1993 and 1994", by Gert König-Langlo and Andreas Herber.

Heft-Nr. 188/1996 – "Die Expedition ANTARKTIS-XI/3 mit FS 'Polarstern' 1994", herausgegeben von Heinz Miller und Hannes Grobe.

Heft-Nr. 189/1996 – "Die Expedition ARKTIS-VII/3 mit FS 'Polarstern' 1990", herausgegeben von Heinz Miller und Hannes Grobe.

Heft-Nr. 190/1996 – "Cruise report of the Joint Chilean-German-Italian Magellan 'Victor Hensen' Campaign in 1994", edited by Wolf Arntz and Matthias Gorny.

Heft-Nr. 191/1996 – "Leitfähigkeits- und Dichtemessung an Eisbohrkernen", von Frank Wilhelms.

Heft-Nr. 192/1996 – "Photosynthese-Charakteristika und Lebensstrategie antarktischer Makroalgen", von Gabriele Weykam.

Heft-Nr. 193/1996 – "Heterogene Raktionen von N_2O_5 und HBr und ihr Einfluß auf den Ozonabbau in der polaren Stratosphäre", von Sabine Seisel.

Heft-Nr. 194/1996 – "Ökologie und Populationsdynamik antarktischer Ophiuroiden (Echinodermata)", von Corinna Dahm.

Heft-Nr. 195/1996 – "Die planktische Foraminifere *Neogloboquadrina pachyderma* (Ehrenberg) im Weddellmeer, Antarktis", von Doris Berberich.

Heft-Nr. 196/1996 – "Untersuchungen zum Beitrag chemischer und dynamischer Prozesse zur Variabilität des stratosphärischen Ozons über der Arktis", von Birgit Heese.

Heft-Nr. 197/1996 – "The Expedition ARKTIS-XI/2 of 'Polarstern' in 1995", edited by Gunther Krause.

Heft-Nr. 198/1996 – "Geodynamik des Westantarktischen Riftsystems basierend auf Apatit-Spaltspuranalysen", von Frank Lisker.

Heft-Nr. 199/1996 – "The 1993 Northeast Water Expedition. Data Report on CTD Measurements of RV 'Polarstern' Cruises ARKTIS IX/2 and 3", by Gereon Budéus and Wolfgang Schneider.

Heft-Nr. 200/1996 – "Stability of the Thermohaline Circulation in analytical and numerical models", by Gerrit Lohmann

Heft-Nr. 201/1996 – "Trophische Beziehungen zwischen Makroalgen und Herbivoren in der Potter Cove (King George-Insel, Antarktis)", von Katrin Iken.

Heft-Nr. 202/1996 – "Zur Verbreitung und Respiration ökologisch wichtiger Bodentiere in den Gewässern um Svalbard (Arktis)", von Michael K. Schmid.

Heft-Nr. 203/1996 – "Dynamik, Rauhigkeit und Alter des Meereises in der Arktis - Numerische Untersuchungen mit einem großskaligen Modell", von Markus Harder.

Heft-Nr. 204/1996 – "Zur Parametrisierung der stabilen atmosphärischen Grenzschicht über einem antarktischen Schelfeis", von Dörthe Handorf.

Heft-Nr. 205/1996 – "Textures and fabrics in the GRIP ice core, in relation to climate history and ice deformation", by Thorsteinn Thorsteinsson.

Heft-Nr. 206/1996 – "Der Ozean als Teil des gekoppelten Klimasystems: Versuch der Rekonstruktion der glazialen Zirkulation mit verschieden komplexen Atmosphärenkomponenten", von Kerstin Fieg.

Heft-Nr. 207/1996 – "Lebensstrategien dominanter antarktischer Oithonidae (Cyclopoida, Copepoda) und Oncaeidae (Poecilostomatoida, Copepoda) im Bellingshausenmeer", von Cornelia Metz.

Heft-Nr. 208/1996 – "Atmosphäreneinfluß bei der Fernerkundung von Meereis mit passiven Mikrowellenradiometern", von Christoph Oelke.

Heft-Nr. 209/1996 – "Klassifikation von Radarsatellitendaten zur Meereiserkennung mit Hilfe von Line-Scanner-Messu gen", von Axel Bochert.

Heft-Nr. 210/1996 – "Die mit ausgewählten Schwämmen (Hexactinellida und Demospongiae) aus dem Weddellmeer, Antarktis, vergesellschaftete Fauna", von Kathrin Kunzmann.

Heft-Nr. 211/1996 – "Russian-German Cooperation: The Expediton TAYMYR 1995 and the Expedition KOLYMA 199 by Dima Yu. Bolshiyanov and Hans-W. Hubberten.

Heft-Nr. 212/1996 – "Surface-sediment composition and sedimentary processes in the central Arctic Ocean and alon the Eurasian Continental Margin", by Ruediger Stein, Gennadij I. Ivanov, Michael A. Levitan, and Kirsten Fahl.

Heft-Nr. 213/1996 – "Gonadenentwicklung und Eiproduktion dreier *Calanus*-Arten (Copepoda): Freilandbeobachtung Histologie und Experimente", von Barbara Niehoff.

Heft-Nr. 214/1996 – "Numerische Modellierung der Übergangszone zwischen Eisschild und Eisschelf", von Christoph Mayer.

Heft-Nr. 215/1996 – "Arbeiten der AWI-Forschungsstelle Potsdam in Antarktika, 1994/95", herausgegeben von Ulrich Wand.

Heft-Nr. 216/1996 – "Rekonstruktion quartärer Klimaänderungen im atlantischen Sektor des Südpolarmeeres anhand von Radiolarien", von Uta Brathauer.

Heft-Nr. 217/1996 – "Adaptive Semi-Lagrange-Finite-Elemente-Methode zur Lösung der Flachwassergleichungen: Implementierung und Parallelisierung", von Jörn Behrens.

Heft-Nr. 218/1997 – "Radiation and Eddy Flux Experiment 1995 (REFLEX III)", by Jörg Hartmann, Axel Bochert, Dietmar Freese, Christoph Kottmeier, Dagmar Nagel and Andreas Reuter.

Heft-Nr. 219/1997 – "Die Expedition ANTARKTIS-XII mit FS 'Polarstern' 1995. Bericht vom Fahrtabschnitt ANT-XII/3" herausgegeben von Wilfried Jokat und Hans Oerter.

Heft-Nr. 220/1997 – "Ein Beitrag zum Schwerefeld im Bereich des Weddellmeeres, Antarktis. Nutzung von Altimetermessungen des GEOSAT und ERS-1", von Tilo Schöne.

Heft-Nr. 221/1997 – "Die Expeditionen ANTARKTIS-XIII/1-2 des Forschungsschiffes 'Polarstern' 1995/96", herausgegeben von Ulrich Bathmann, Mike Lucas und Victor Smetacek.

Heft-Nr. 222/1997 – "Tectonic Structures and Glaciomarine Sedimentation in the South-Eastern Weddell Sea from Seismic Reflection Data", by László Oszkó.

Heft-Nr. 223/1997 – "Bestimmung der Meereisdicke mit seismischen und elektromagnetisch-induktiven Verfahren", von Christian Haas.

Heft-Nr. 224/1997 – "Troposphärische Ozonvariationen in Polarregionen", von Silke Wessel.

Heft-Nr. 225/1997 – "Biologische und ökologische Untersuchungen zur kryopelagischen Amphipodenfauna des arktischen Meereises", von Michael Poltermann.

Heft-Nr. 226/1997 – "Scientific Cruise Report of the Arctic Expedition ARK-XI/1 of RV 'Polarstern' in 1995", edited by Eike Rachor.

Heft-Nr. 227/1997 – "Der Einfluß kompatibler Substanzen und Kyroprotektoren auf die Enzyme Malatdehydrogenase (MDH) und Glucose-6-phosphat-Dehydrogenase (G6P-DH) aus Acrosiphonia arcta (Chlorophyta) der Arktis", von Katharina Kück.

Heft-Nr. 228/1997 – "Die Verbreitung epibenthischer Mollusken im chilenischen Beagle-Kanal", von Katrin Linse.

Heft-Nr. 229/1997 – "Das Mesozooplankton im Laptevmeer und östlichen Nansen-Becken - Verteilung und Gemeinschaftsstrukturen im Spätsommer", von Hinrich Hanssen.

Heft-Nr. 230/1997 – "Modell eines adaptierbaren, rechnergestützten, wissenschaftlichen Arbeitsplatzes am Alfred-Wegener-Institut für Polar- und Meeresforschung", von Lutz-Peter Kurdelski.

Heft-Nr. 231/1997 – "Zur Ökologie arktischer und antarktischer Fische: Aktivität, Sinnesleistungen und Verhalten", von Christopher Zimmermann.

Heft-Nr. 232/1997 – "Persistente clororganische Verbindungen in hochantarktischen Fischen", von Stephan Zimmermann.

Heft-Nr. 233/1997 – "Zur Ökologie des Dimethylsulfoniumpropionat (DMSP)-Gehaltes temperierter und polarer Phytoplanktongemeinschaften im Vergleich mit Laborkulturen der Coccolithophoride *Emiliania huxleyi* und derantarktischen Diatomee *Nitzschia lecointei*", von Doris Meyerdierks.

Heft-Nr. 234/1997 – "Die Expedition ARCTIC '96 des FS 'Polarstern' (ARK XII) mit der Arctic Climate System Study (ACSYS)", von Ernst Augstein und den Fahrtteilnehmern.

Heft-Nr. 235/1997 – "Polonium-210 und Blei-219 im Südpolarmeer: Natürliche Tracer für biologische und hydrographische Prozesse im Oberflächenwasser des Antarktischen Zirkumpolarstroms und des Weddellmeeres", von Jana Friedrich.

Heft-Nr. 236/1997 – "Determination of atmospheric trace gas amounts and corresponding natural isotopic rations by means of ground-based FTIR spectroscopy in the high Arctic", by Arndt Meier.

Heft-Nr. 237/1997 – "Russian-German Cooperation: The Expedition TAYMYR / SEVERNAYA ZEMLYA 1996", edited by Martin Melles, Birgit Hagedorn and Dmitri Yu. Bolshiyanow.

Heft-Nr. 238/1997 – "Life strategy and ecophysiology of Antarctic macroalgae", by Iván M. Gómez.

Heft-Nr. 239/1997 – "Die Expedition ANTARKTIS XIII/4-5 des Forschungsschiffes 'Polarstern' 1996", herausgegeben von Eberhard Fahrbach und Dieter Gerdes.

Heft-Nr. 240/1997 – "Untersuchungen zur Chrom-Speziation im Meerwasser, Meereis und Schnee aus ausgewählten Gebieten der Arktis", von Heide Giese.

Heft-Nr. 241/1997 – "Late Quaternary glacial history and paleoceanographic reconstructions along the East Greenland continental margin: Evidence from high-resolution records of stable isotopes and ice-rafted debris", by Seung-Il Nam.

Heft-Nr. 242/1997 – "Thermal, hydrological and geochemical dynamics of the active layer at a continuous site, Taymyr Peninsula, Siberia", by Julia Boike.

Heft-Nr. 243/1997 – "Zur Paläoozeanographie hoher Breiten: Stellvertreterdaten aus Foraminiferen", von Andreas Mackensen.

Heft-Nr. 244/1997 – "The Geophysical Observatory at Neumayer Station, Antarctica. Geomagnetic and seismological observations in 1995 and 1996", by Alfons Eckstaller, Thomas Schmidt, Viola Gaw, Christian Müller and Johannes Rogenhagen.

Heft-Nr. 245/1997 – "Temperaturbedarf und Biogeographie mariner Makroalgen - Anpassung mariner Makroalgen an tiefe Temperaturen", von Bettina Bischoff-Bäsmann.

Heft-Nr. 246/1997 – "Ökologische Untersuchungen zur Fauna des arktischen Meereises", von Christine Friedrich.

Heft-Nr. 247/1997 – "Entstehung und Modifizierung von marinen gelösten organischen Substanzen", von Berit Kirchhoff.

Heft-Nr. 248/1997 – "Laptev Sea System: Expeditions in 1995", edited by Heidemarie Kassens.

Heft-Nr. 249/1997 – "The Expedition ANTARKTIS XIII/3 (EASIZ I) of RV 'Polarstern' to the eastern Weddell Sea in 1996", edited by Wolf Arntz and Julian Gutt.

Heft-Nr. 250/1997 – "Vergleichende Untersuchungen zur Ökologie und Biodiversität des Mega-Epibenthos der Arktis und Antarktis", von Andreas Starmans.

Heft-Nr. 251/1997 – "Zeitliche und räumliche Verteilung von Mineralvergesellschaftungen in spätquartären Sedimenten des Arktischen Ozeans und ihre Nützlichkeit als Klimaindikatoren während der Glazial/Interglazial-Wechsel", von Christoph Vogt.

Heft-Nr. 252/1997 – "Solitäre Ascidien in der Potter Cove (King George Island, Antarktis). Ihre ökologische Bedeutung und Populationsdynamik", von Stephan Kühne.

Heft-Nr. 253/1997 – "Distribution and role of microprotozoa in the Southern Ocean", by Christine Klaas.

Heft-Nr. 254/1997 – "Die spätquartäre Klima- und Umweltgeschichte der Bunger-Oase, Ostantarktis", von Thomas Kulbe.

Heft-Nr. 255/1997 – "Scientific Cruise Report of the Arctic Expedition ARK-XIII/2 of RV 'Polarstern' in 1997", edited by Ruediger Stein and Kirsten Fahl.

Heft-Nr. 256/1998 – "Das Radionuklid Tritium im Ozean: Meßverfahren und Verteilung von Tritium im Südatlantik und im Weddellmeer", von Jürgen Sültenfuß.

Heft-Nr. 257/1998 – "Untersuchungen der Saisonalität von atmosphärischen Dimethylsulfid in der Arktis und Antarktis", von Christoph Kleefeld.

Heft-Nr. 258/1998 – "Bellinghausen- und Amundsenmeer: Entwicklung eines Sedimentationsmodells", von Frank-Oliver Nitsche.

Heft-Nr. 259/1998 – "The Expedition ANTARKTIS-XIV/4 of RV 'Polarstern' in 1997", by Dieter K. Fütterer.

Heft-Nr. 260/1998 – "Die Diatomeen der Laptevsee (Arktischer Ozean): Taxonomie und biogeographische Verbreitung", von Holger Cremer.

Heft-Nr. 261/1998 – "Die Krustenstruktur und Sedimentdecke des Eurasischen Beckens, Arktischer Ozean: Resultate aus seismischen und gravimetrischen Untersuchungen", von Estella Weigelt.

Heft-Nr. 262/1998 – "The Expedition ARKTIS-XIII/3 of RV 'Polarstern' in 1997", by Gunther Krause.

Heft-Nr. 263/1998 – "Thermo-tektonische Entwicklung von Oates Land und der Shackleton Range (Antarktis) basierend auf Spaltspuranalysen", von Thorsten Schäfer.

Heft-Nr. 264/1998 – "Messungen der stratosphärischen Spurengase ClO, HCl, O_3, N_2O, H_2O und OH mittels flugzeuggetragener Submillimeterwellen-Radiometrie", von Joachim Urban.

Heft-Nr. 265/1998 – "Untersuchungen zu Massenhaushalt und Dynamik des Ronne Ice Shelfs, Antarktis", von Astrid Lambrecht.

Heft-Nr. 266/1998 – "Scientific Cruise Report of the Kara Sea Expedition of RV 'Akademik Boris Petrov' in 1997", edited by Jens Matthiessen and Oleg Stepanets.

Heft-Nr. 267/1998 – "Die Expedition ANTARKTIS-XIV mit FS 'Polarstern' 1997. Bericht vom Fahrtabschnitt ANT-XIV/3", herausgegeben von Wilfried Jokat und Hans Oerter.

Heft-Nr. 268/1998 – "Numerische Modellierung der Wechselwirkung zwischen Atmosphäre und Meereis in der arktischen Eisrandzone", von Gerit Birnbaum.

Heft-Nr. 269/1998 – "Katabatic wind and Boundary Layer Front Experiment around Greenland (KABEG '97)", by Günther Heinemann.

Heft-Nr. 270/1998 – "Architecture and evolution of the continental crust of East Greenland from integrated geophysical studies", by Vera Schlindwein.

Heft-Nr. 271/1998 – "Winter Expedition to the Southwestern Kara Sea - Investigations on Formation and Transport of Turbid Sea-Ice", by Dirk Dethleff, Peter Loewe, Dominik Weiel, Hartmut Nies, Gesa Kuhlmann, Christian Bahe and Gennady Tarasov.

Heft-Nr. 272/1998 – "FTIR-Emissionsspektroskopische Untersuchungen der arktischen Atmosphäre", von Edo Becker.

Heft-Nr. 273/1998 – "Sedimentation und Tektonik im Gebiet des Agulhas Rückens und des Agulhas Plateaus ('SETA-RAP')", von Gabriele Uenzelmann-Neben.

Heft-Nr. 274/1998 – "The Expedition ANTARKTIS XIV/2", by Gerhard Kattner.

Heft-Nr. 275/1998 – "Die Auswirkung der 'NorthEastWater'-Polynya auf die Sedimentation vor NO-Grönland und Untersuchungen zur Paläo-Ozeanographie seit dem Mittelwechsel", von Hanne Notholt.

Heft-Nr. 276/1998 – "Interpretation und Analyse von Potentialfelddaten im Weddellmeer, Antarktis: der Zerfall des Superkontinents Gondwana". von Michael Studinger.

Heft-Nr. 277/1998 – "Koordiniertes Programm Antarktisforschung". Berichtskolloquium im Rahmen des Koordinierten Programms "Antarktisforschung mit vergleichenden Untersuchungen in arktischen Eisgebieten", herausgegeben von Hubert Miller.

Heft-Nr. 278/1998 – "Messung stratosphärischer Spurengase über Ny-Ålesund, Spitzbergen, mit Hilfe eines bodengebundenen Mikrowellen-Radiometers", von Uwe Raffalski.

Heft-Nr. 279/1998 – "Arctic Paleo-River Discharge (APARD). A New Research Programme of the Arctic Ocean Science Board (AOSB)", edited by Ruediger Stein.

Heft-Nr. 280/1998 – "Fernerkundungs- und GIS-Studien in Nordostgrönland", von Friedrich Jung-Rothenhäusler.

Heft-Nr. 281/1998 – "Rekonstruktion der Oberflächenwassermassen der östlichen Laptevsee im Holozän anhand aquatischen Palynomorphen", von Martina Kunz-Pirrung.

Heft-Nr. 282/1998 – "Scavenging of ^{231}Pa and ^{230}Th in the South Atlantic: Implications for the use of the $^{231}Pa/^{230}Th$ ratio as a paleoproductivity proxy", by Hans-Jürgen Walter.

Heft-Nr. 283/1998 – "Sedimente im arktischen Meereis - Eintrag, Charakterisierung und Quantifizierung", von Frank Lindemann.

Heft-Nr. 284/1998 – "Langzeitanalyse der antarktischen Meereisbedeckung aus passiven Mikrowellendaten", von Christian H. Thomas.

Heft-Nr. 285/1998 – "Mechanismen und Grenzen der Temperaturanpassung beim Pierwurm *Arenicola marina* (L.)", von Angela Sommer.

Heft-Nr. 286/1998 – "Energieumsätze benthischer Filtrierer der Potter Cove (King George Island, Antarktis)", von Jens Kowalke.

Heft-Nr. 287/1998 – "Scientific Cooperation in the Russian Arctic: Research from the Barents Sea up to the Laptev Sea", edited by Eike Rachor.

Heft-Nr. 288/1998 – "Alfred Wegener. Kommentiertes Verzeichnis der schriftlichen Dokumente seines Lebens und Wirkens", von Ulrich Wutzke.

Heft-Nr. 289/1998 – "Retrieval of Atmospheric Water Vapor Content in Polar Regions Using Spaceborne Microwave Radiometry", by Jungang Miao.

Heft-Nr. 290/1998 – "Strukturelle Entwicklung und Petrogenese des nördlichen Kristallingürtels der Shackleton Range, Antarktis: Proterozoische und Ross-orogene Krustendynamik am Rand des Ostantarktischen Kratons", von Axel Brommer.

Heft-Nr. 291/1998 – "Dynamik des arktischen Meereises - Validierung verschiedener Rheologieansätze für die Anwendung in Klimamodellen", von Martin Kreyscher.

Heft-Nr. 292/1998 – "Anthropogene organische Spurenstoffe im Arktischen Ozean. Untersuchungen chlorierter Biphenyle und Pestizide in der Laptevsee, technische und methodische Entwicklungen zur Probenahme in der Arktis und zur Spurenstoffanalyse", von Sven Utschakowski.

Heft-Nr. 293/1998 – "Rekonstruktion der spätquartären Klima- und Umweltgeschichte der Schirmacher Oase und des Wohlthat Massivs (Ostantarktika)", von Markus Julius Schwab.

Heft-Nr. 294/1998 – "Besiedlungsmuster der benthischen Makrofauna auf dem ostgrönländischen Kontinentalhang", von Klaus Schnack.

Heft-Nr. 295/1998 – "Gehäuseuntersuchungen an planktischen Foraminiferen hoher Breiten: Hinweise auf Umweltveränderungen während der letzten 140.000 Jahre", von Harald Hommers.

Heft-Nr. 296/1998 – "Scientific Cruise Report of the Arctic Expedition ARK-XIII/1 of RV 'Polarstern' in 1997", edited by Michael Spindler, Wilhelm Hagen and Dorothea Stübing.

Heft-Nr. 297/1998 – "Radiometrische Messungen im arktischen Ozean - Vergleich von Theorie und Experiment", von Klaus-Peter Johnsen.

Heft-Nr. 298/1998 – "Patterns and Controls of CO_2 Fluxes in Wet Tundra Types of the Taimyr Peninsula, Siberia - the Contribution of Soils and Mosses", by Martin Sommerkorn.

Heft-Nr. 299/1998 – "The Potter Cove coastal ecosystem, Antarctica. Synopsis of research performed within the frame of the Argentinean-German Cooperation at the Dallmann Laboratory and Jubany Station (King George Island, Antarctica, 1991-1997)", by Christian Wiencke, Gustavo Ferreyra, Wolf Arntz & Carlos Rinaldi.

Heft-Nr. 300/1999 – "The Kara Sea Expedition of RV 'Akademik Boris Petrov' 1997: First results of a Joint Russian-German Pilot Study", edited by Jens Matthiessen, Oleg V. Stepanets, Ruediger Stein, Dieter K. Fütterer, and Eric M. Galimov.

Heft-Nr. 301/1999 – "The Expedition ANTARKTIS XV/3 (EASIZ II)", edited by Wolf E. Arntz and Julian Gutt.

Heft-Nr. 302/1999 – "Sterole im herbstlichen Weddellmeer (Antarktis): Großräumige Verteilung, Vorkommen und Umsatz", von Anneke Mühlebach.

Heft-Nr. 303/1999 – "Polare stratosphärische Wolken: Lidar-Beobachtungen, Charakterisierung von Entstehung und Entwicklung", von Jens Biele.

Heft-Nr. 304/1999 – "Spätquartäre Paläoumweltbedingungen am nördlichen Kontinentalrand der Barents- und Kara-See. Eine Multi-Parameter-Analyse", von Jochen Knies.

Heft-Nr. 305/1999 – "Arctic Radiation and Turbulence Interaction Study (ARTIST)", by Jörg Hartmann, Frank Albers, Stefania Argentini, Axel Borchert, Ubaldo Bonafé, Wolfgang Cohrs, Alessandro Conidi, Dietmar Freese, Teodoro Georgiadis, Alessandro Ippoliti, Lars Kaleschke, Christof Lüpkes, Uwe Maixner, Giangiuseppe Mastrantonio, Fabrizio Ravegnani, Andreas Reuter, Giuliano Trivellone and Abgelo Viola.

Heft-Nr. 306/1999 – "German-Russian Cooperation: Biogeographic and biostratigraphic investigations on selected sediment cores from the Eurasian continental margin and marginal seas to analyze the Late Quternary climatic variability", edited by Robert F. Spielhagen, Max S. Barash, Gennady I. Ivanov, and Jörn Thiede.

Heft-Nr. 307/1999 – "Struktur und Kohlenstoffbedarf des Makrobenthos am Kontinentalhang Ostgrönlands", von Dan Seiler.

Heft-Nr. 308/1999 – "ARCTIC '98: The Expedition ARK-XIV/1a of RV 'Polarstern' in 1998", edited by Wilfried Jokat.

* vergriffen / out of print.
➨ nur noch beim Autor / only from the author.